# Measurement of Human PTH (1-34) and Human PTHrP (1-36) using Liquid-Chromatography Tandem Mass Spectrometry: Application to Therapeutic Studies and Drug Monitoring

**Sulaiman Al Riyami**

Thesis submitted for the degree of Doctor of Philosophy (PhD)

Norwich Medical School

Faculty of Medicine and Health Sciences

University of East Anglia

February 2019

# Abstract

**Background:** Teriparatide, a recombinant human parathyroid hormone (PTH) (1-34), is an osteoanabolic agent for treatment of osteoporosis. The effect on bone decreases the risk of vertebral and non-vertebral fractures and increases bone mineral density (BMD) in post-menopausal women with osteoporosis. PTH (1-34) can also be used as replacement therapy in hypoparathyroidism and to accelerate fracture healing. PTH (1-34) has also been used to assess response to PTH in conditions such as pseudohypoparathyroidism (PHP) (Ellsworth-Howard test (EHT)). Abaloparatide, a synthetic peptide analog of human parathytoid hormone-related peptide (PTHrP) (1-34), is also an osteoanabolic agent recently approved for treatment of osteoporosis by the FDA. The amino acid sequence of abaloparatide is identical to that of PTHrP in the first 21 amino acids, while eight of the remaining amino acids are different to enhance its affinity for PTHR1. PTHrP (1-36) induces beta cell proliferation and improves glucose-stimulated insulin secretion. Ongoing studies are exploring the potential of PTHrP (1-36) to enhance the functional beta cell mass in the setting of diabetes.

**Aims:** To develop a sensitive method for quantification of PTH (1-34) and PTHrP (1-36) using liquid chromatography-tandem mass spectrometry (LC-MS/MS). To develop assays in accordance with published guidelines on bioanalytical method validation. To perform a comparison study on human PTH (1-34) with a commercial immunoassay. To review the use of PTH (1-34) measurements in drug development studies, and in the drug monitoring during diagnosis of patients with PHP.

**Method:** Sample extraction was developed using a Waters (Milford, MA, USA) Oasis® HLB µElution solid phase extraction. Quantification m/z transitions of 589.2>656.1 and 609.5>682.7 were used on Waters/Micromass® Quattro Ultima™ Pt mass spectrometer to measure PTH (1-34) and PTHrP (1-36), respectively, in human plasma using rat PTH (1-34) as internal standard. Validation criteria were carried out against industry standards. hPTH (1-34) results obtained by LC-MS/MS (n=390) were compared against results obtained from an immunoassay (IDS; Boldon Tyne and Wear. UK). Pharmacokinetic (PK) profiles from human subjects given either single subcutaneous (sc) injection of 20 µg Teriparatide (n=10) or 0.69 mg (n=5), 2.07 mg (n=10) oral PTH (1-34) (EnteraBio) were analysed using the validated LC-MS/MS method for hPTH (1-34).

**Results and Discussion:** LC-MS/MS produced a linear calibration curve from 10 to 2000 pg/mL ($r^2$ >0.990). The LLoQ and LLoD for PTH (1-34) were 10 pg/mL and 2.1 pg/mL respectively. The inter-assay precision (CV%) and accuracy (%RE) of the method were <9.8% and <14.9%, respectively, for four QCs (20, 100, 200, and 800 pg/mL). While, the intra-assay precision and accuracy were <7.8% and <6.9%, respectively. The mean recovery of PTH (1-34) was 107.2%. For PTHrP (1-36), LC-MS/MS produced a linear calibration curve from 25 to 2000 pg/mL ($r^2$ >0.96). The LLoQ and LLoD for PTHrP (1-36) were 25 pg/mL and 2.5 pg/mL respectively. The inter- and intra-assay variations of the precision were <11.8% and 12.4%, respectively, while those for accuracy were <9.1 and 10.7%, respectively, at four QC concentrations (50, 100, 200, and 800 pg/mL). The assay showed efficient recovery of hPTHrP (1-36) from plasma with an average recovery of 103.7%. Method comparison between the LC-MS/MS and immunoassay for PTH (1-34) using human

EDTA plasma samples showed a high correlation ($r^2$ = 0.950). A concentration-dependent, negative bias of 35.5% was observed across the range of 0 – 800 pg/mL. The immunoassay showed a 7% cross reactivity to human PTH (1-84) and 44% to rat PTH (1-34), no interference was observed in the LC-MS/MS method. Matrix effect and cross reactivity to human PTH (1-84) in the immunoassay were the likely contributing factors to the bias between the methods. The oxidized form of PTH (1-34) does not interfere with the LC-MS/MS method. PK profiles of oral PTH (1-34) showed a rapid absorption then rapid elimination. In contrast, teriparatide injection showed a slower rate of plasma clearance, possibly due to continuous absorption from the site of administration. $C_{max}$ was proportional to oral dosage given and the 2.07 mg of oral PTH (1-34) produced comparable $C_{max}$ to that produced by 20 ug teriparatide injection.

**Conclusion:** The LC-MS/MS methods for measurement of PTH (1-34) and PTHrP (1-36) demonstrated linearity over the calibration range, good precision and accuracy, excellent analyte recovery, and negligible matrix effects. The methods have a capability of measuring oxidized and non-oxidized forms of PTH (1-34) that may offer new insights into the physiology and pathophysiology of PTH, aid studies in the therapeutic use/efficacy of osteoanabolic agents and may facilitate in the development of combination therapy with other anti-resorptive/anti-remodeling agents.

Word count = 45626

# Table of Contents

# List of Figures

# List of Tables

## Declaration

No portion of the work referred to in the thesis has been submitted in support of an application for another degree or qualification of this or any other university or other institute of learning.

## Ethics statement

All blood samples were collected from consented healthy participants enrolled in stage 3 of a Phase 1 study on an oral PTH (1-34) drug delivery technology. The study was conducted in accordance with Hadassah Medical Centre ethical approval (ethics approval number 032-13-HMO).

## Acknowledgments

I extend my sincere thanks to the following individuals:

Professor William D Fraser for accepting me into his research group and allowing me to complete a qualification of the PhD level and for his encouragement, guidance, support and teaching.

My other supervisors, Dr. Colin Kay, Dr. Gary John and Prof. John Wain for their encouragement and support.

Mr. Jonathan Tang and Mr. John Dutton for their advisory support with Liquid-chromatography tandem mass spectrometry and in all technical aspects of my work.

Mr. Christopher Washbourne and Miss Isabelle Piec and all members of bioanalytical facility for their friendship, help and support during this time.

Lastly, My beloved Mother, wife and children for their love and support. I hope that I have made them proud by doing this.

# Abbreviations

$1,25(OH)_2D$ = 1, 25-dihydroxyvitamin D

AC = Adenylyl cyclase

ACN = Acetonitrile

AP-1 = Activator protein-1

APC = Adenomatous polyposis coli

AR = Androgen receptor

Bad = Bcl-2-associated death promoter

Bcl-2 = B-cell lymphoma-2

BMD = Bone mineral density

BMP = Bone morphogenetic protein

BMU = Basic multiple unit

BSA = Bovine serum albumin

Ca = Calcium

$Ca^{2+}$ = Ionized calcium

cAMP = cyclic Adenosine monophosphate

CaSR = Calcium-sensing receptor

cDNA = Complementary DNA

CID = Collision-induced dissociation

CKD = Chronic kidney disease

CREB = cAMP response element binding protein

CTX = Collagen type-1 C-telopeptide

DAG = diacylglycerol

Dkk-1 = Dickkopf-1

DMSO = Dimethylsulfoxide

DNA= Deoxyribonucleic acid

ECD = Extracellular domain

ECF = Extracellular fluid

EDTA = Ethylenediaminetetraacetic acid

EHT = Ellsworth-Howard test

ELISA = Enzyme-linked immunosorbent assay

ER = Endoplasmic reticulum

FA = Formic Acid

FDA = USA Food and Drugs Administration

FGF23 = Fibroblast growth factor 23

FGFR1c= FGF receptor 1c

GCM = Glial cell missing

GDP = Guanosine diphosphate

GPCR = G protein-coupled receptors

$G_s$ = stimulatory G protein

GSK-3β = Glycogen synthase kinase 3β

GTP = guanosine triphosphate

HHM = Humoral Hypercalcemia of Malignancy

hPTH (1-34) = PTH (1-34) human fragment

hPTH = Human parathyroid hormone

IGF = Insulin-like growth factor

IP3 = Inositol 1,4,5-triphosphate

IPA = Isopropanol

IRMA = Immunoradiometric assay

IS = Internal standard

LC-MS/MS = Liquid-chromatography tandem mass spectrometry

LEF-1 = Lymphoid enhancer binding factor 1

LLoD = Lower limit of detection

LLoQ = Lower limit of quantification

LRP5/LRP6 = Low-density lipoprotein receptor-related protein-5/6

MAH = Malignancy-associated hypercalcemia

MAPK = Mitogen-activated protein kinases

MCP-1 = Monocyte chemoattractant protein-1

M-CSF = Macrophage colony-stimulating factor

MeOH = Methanol

MRM = Multiple-reaction monitoring

mRNA = Messenger ribonucleic acid

NaPi 2a/2c= Sodium-phosphate co-transporters 2a/2c

$NH_4OH$ = Ammonium hydroxide

NLS = Nuclear localization sequence

Nurr1 = Orphan nuclear receptor

OPG = Osteoprotegerin

P1NP = N-terminal propeptide of type 1 collagen

PD = Pharmacodynamics

PHP = Pseudohypoparathyroidism

PHPT = Primary hyperparathyroidism

PIP2 = phosphatidylinositol 4, 5-biphosphate

PK = Pharmacokinetics

PKA = Protein kinase A

PKC = Protein kinase C

PLC = Phospholipase C

PLD = Phospholipase D

PTH = Parathyroid hormone

PTHR1 = Parathyroid hormone type 1 receptor

PTHrP = Parathyroid hormone-related peptide

QC = Quality control

RANK = Receptor activator of nuclear factor-kappa B

RANKL = Receptor activator of nuclear factor-kappa B ligand

rhPTH = Recombinant human parathyroid hormone

RIA = Radioimmunoassay

RP-HPLC = Reverse-phase high-performance liquid chromatography

rPTH (1-34) = PTH (1-34) rat fragment

Runx = Runt-related transcription factor

sFRP = Soluble frizzled-related protein 1

Sost = Sclerostin

SPE = Solid-phase extraction

SRM = Single-reaction monitoring

TFA = Triflouroacetic acid

TIO= Tumour-induced osteomalacia

TIP39 = Tuberoinfundibular peptide of 39 residues

TMD = Transmembrane domain

TUNEL = Transferase–mediated Nick End Labelling

UK NEQAS = UK National External Quality Assessment Service

UTR = Untranslated region

VD3 1A hydroxylase = 25-hydroxyvitamin D3 1-α-hydroxylase

VDR = Vitamin D receptor

Wnt = Wingless-type mouse mammary tumor virus (MMTV) interaction site

XLHR= X-linked hypophosphatemic rickets

# 1. Chapter 1 – An Introduction

Parathyroid hormone (PTH) and PTH-related peptide (PTHrP) share some homology at their N-terminal amino acid sequences. This homology allows both hormones to act through binding to the same receptor, the G protein-coupled PTH/PTHrP type-1 receptor (PTHR1), yet they have different biological functions. PTH is primarily produced in the parathyroid chief cells and is the major regulator of blood calcium. PTH is released from the parathyroid glands in response to low calcium in blood and then functions to increase the concentration of blood calcium. When the concentration of blood calcium increases, PTH secretion is suppressed by a classic endocrine feedback loop and maintains blood calcium concentration within a narrow range (2). PTHrP, by contrast, is expressed in most tissues of the human body and acts locally as paracrine/autocrine factor (Figure 1-1).

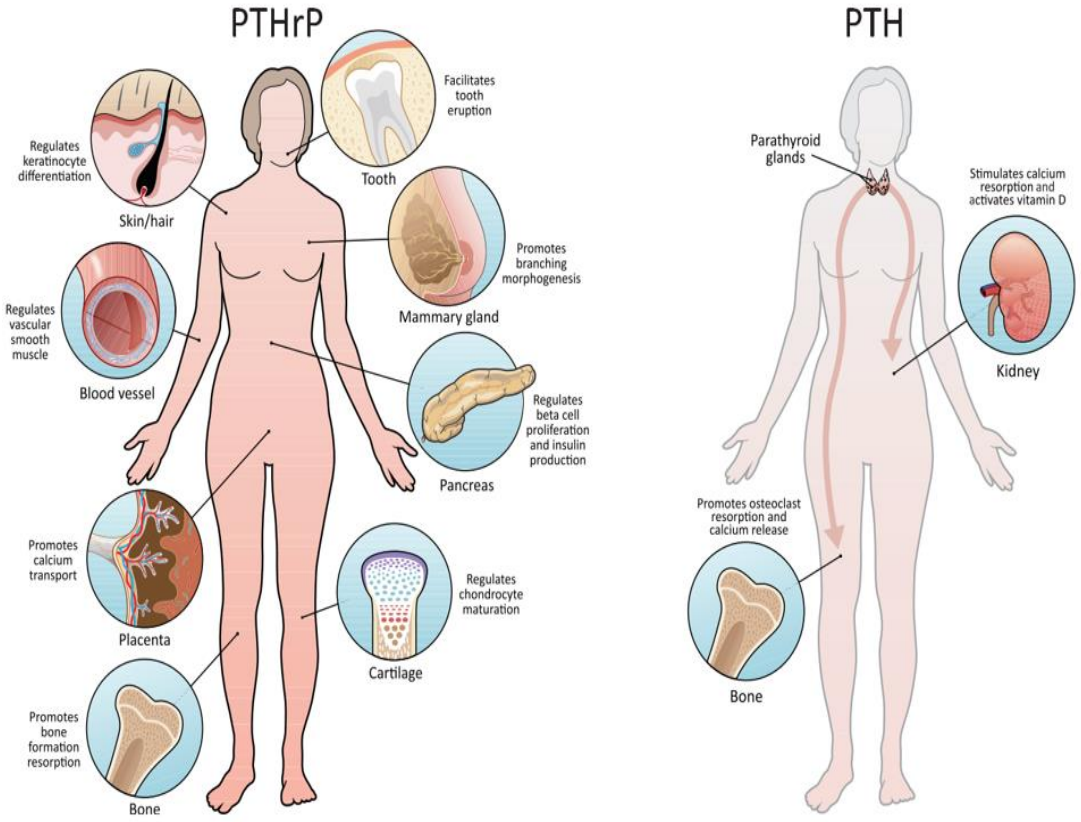


**Figure 1-1 PTH and PTHrP actions in humans.** *PTHrP has numerous paracrine/autocrine actions, including roles in keratinocytes/hair follicles, cartilage, vascular smooth muscle, bone, mammary gland development, tooth eruption and pancreas. In comparison, PTH acts mainly on bone and kidney via its endocrine mode of operation. Figure taken from reference (3).*

During fetal development and during lactation, PTHrP also acts as a hormone and regulates calcium homeostasis (3). PTHrP was originally identified as a causal factor associated with the humoral hypercalcemia of malignancy syndrome (HHM). HHM is characterized by hypercalcemia and hypophosphatemia, biochemical features that are usually indicative of over secretion of PTH (4).

## 1.1 Parathyroid Hormone

### 1.1.1 PTH Gene structure

The human PTH gene is located on the small arm of chromosome 11 (11p15.2) and covers about 4 kb of genomic DNA. It consists of three exons and two interrupting introns (Figure 1-2). Exon 1 encodes most of the 5' untranslated region (UTR). Exon 2 encodes six nucleotides of the 5' UTR, the entire signal peptide (pre-sequence) of 25 amino acids, and part of the pro-sequence (the first three of a total of six amino acids and two nucleotides of the fourth amino acid). Exon 3 encodes the remainder of the pro-sequence (the last nucleotide of the fourth amino acid and the last two amino acids, lysine-Arginine), the entire full-length PTH (1-84) and the 3' UTR containing the canonical AATAAA polyadenylation signal (2).

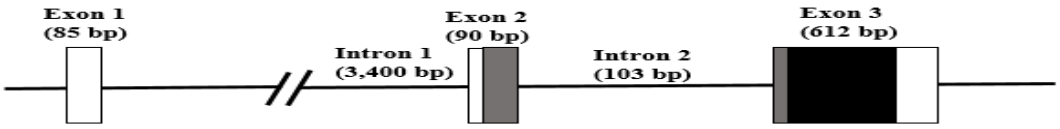


**Figure 1-2 Diagrammatic structure of the human PTH gene**. *Exons with length indicated. Non-coding exon in white, prepro-sequence in gray, coding sequence in black box (Figure reproduced from Reference (2)).*

### 1.1.2 PTH Protein structure

The complete primary 84 amino acid sequence of PTH was first published in 1970. Mature mammalian PTH is a single-chain 84 amino acid polypeptide hormone that is expressed in the chief cells of the parathyroid gland. The primary translational product of parathyroid mRNA is the precursor molecule prepro-PTH [115 amino acids] that includes a 25 amino acid pre-sequence, a 6 amino acid pro-sequence, and an 84 amino acid mature PTH sequence (5). The pre-sequence functions as a signal sequence that directs the precursor polypeptide to the machinery that transports it across the endoplasmic reticulum (ER), where the pre-sequence is cleaved. Pro-

sequence seems to be of importance for efficient ER transport of the polypeptide and may play a role in subsequent events such as protein folding (6).

Upon synthesis on polysomes attached to ER, prepro-PTH crosses the ER membrane co-translationally into the ER lumen. The signal peptide is cleaved, and pro-PTH is transported to the Golgi network. During the transit through the Golgi apparatus, the pro-sequence is cleaved, and the 84-amino acid mature PTH is packed into secretory granules. Figure 1-3 shows the process of PTH synthesis. PTH is then released into the blood stream in response to certain stimuli such as $Ca^{2+}$, 1,25-dihydroxy vitamin D ($1,25(OH)_2D$), plasma phosphate, and fibroblast growth factor 23 (FGF23). The mature hormone can be secreted through a classical exocytotic mechanism or it may be cleaved by calcium-sensitive proteases present within secretory vesicles, resulting in the production and secretion of truncated fragments of PTH (1-84) that lack the amino-terminal domain and are thus inactive with respect to response mediated by the PTHR1 (7).

In addition, there is evidence that small amounts of PTH mRNA and protein are also produced in the hypothalamus (8, 9) and in the thymus (10-12). The certain function of hypothalamic and thymic PTH is unknown. Gunther et al. (11) proposed thymic PTH as an auxiliary mechanism for the regulation of calcium in the absence of parathyroid glands. Liu *et al.* (12) argued that the thymus does not serve as an auxiliary source of either serum PTH and parathyroid function, rather they demonstrated that the normal process of parathyroid organogenesis in both mice and humans leads to the generation of multiple small parathyroid clusters in addition to the main parathyroid glands, that are the likely source of physiologically relevant "thymic PTH".

### 1.1.3 Regulation of PTH gene transcription

Parathyroid cells respond to various external stimuli by promoting secretion of preformed PTH from secretory granules, transcription of the PTH gene, and an increase in the size of parathyroid glands. The extent of each response differs according to whether it is stimulatory or inhibitory and the length of interaction.

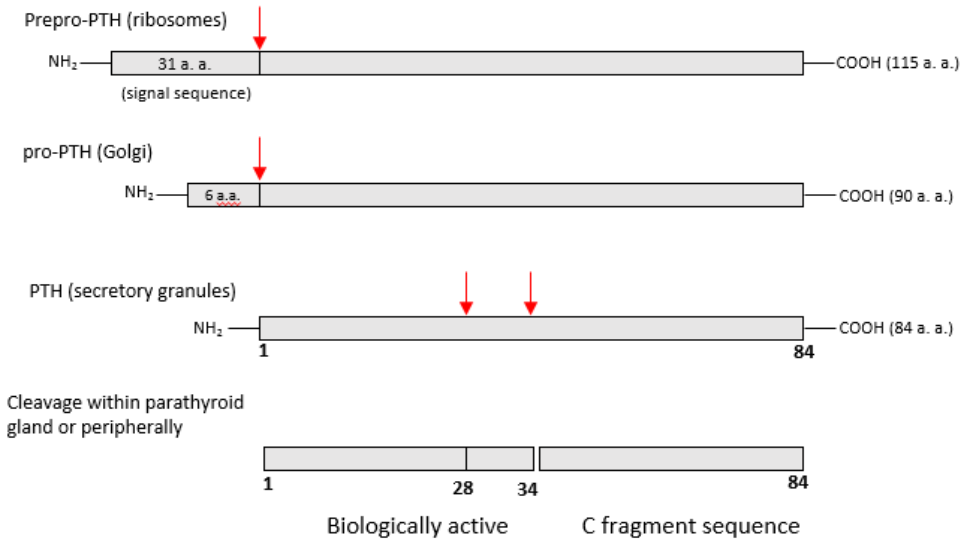


**Figure 1-3 Schematic diagram illustration of PTH synthesis**. *PTH initially synthesized as a prepro hormone (115 a.a.), which is cleaved in ribosome to proPTH (90 a.a.). The proPTH is then transferred to Golgi network, where it further cleaved to mature PTH hormone (84 a.a.) and packed into secretory granules to be released in response to stimulation. Red arrows represent potential sites of cleavage. PTH fragments lack N-terminus part cannot initiate responses mediated by PTHR1.*

#### *1.1.3.1 Regulation of PTH by extracellular calcium*

Several studies have investigated the role of calcium in regulation of the parathyroid gene expression. *In vivo*, hypocalcemia leads to a marked increase in PTH mRNA. PTH mRNA levels in the parathyroid glands of rats kept on a low calcium (0.02%) diet for three weeks increased five-fold compared to a normal calcium diet (0.4%). In contrast, a high calcium diet (2%) did not change the PTH mRNA levels (13). A number of *in vitro* studies show the mechanism by which calcium can supress PTH gene transcription. This mechanism involves the post-transcriptional regulation of PTH mRNA through the regulation of mRNA stability, which is controlled by binding of proteins to the mRNA's 3' UTR. Parathyroid glands from rats fed a low calcium diet for 2-3 weeks were shown to contain a five- to 10-fold increase in steady-state PTH mRNA , as compared to parathyroid glands from rats on control diet (14). A low calcium diet resulted in significant protection of PTH mRNA from degradation (transcripts were mainly intact after 180 min as compared to 40 min when using a control diet) (15).

#### *1.1.3.2 Regulation of PTH by 1,25 $(OH)_2$ D*

Vitamin D deficiency is linked to excessive production of PTH, which is caused by reduced suppression of PTH secretion by extracellular calcium and by 1,25$(OH)_2$D. The role of vitamin D metabolites in regulating the synthesis of PTH has been studied and the findings suggest that vitamin D metabolites play an important role in regulating the production of PTH by inhibiting the transcription of prepro PTH mRNA with 1,25$(OH)_2$D effect being the most significant (16). This seems to involve 1,25$(OH)_2$D-induced binding of the vitamin D receptor (VDR) to negative regulatory elements in the PTH gene promoter (17).

#### *1.1.3.3 Regulation of PTH by plasma phosphate and FGF 23*

PTH regulates phosphate concentration through its actions at several organs, and elevated serum phosphate concentration in turn stimulates PTH secretion, presumably by lowering extracellular calcium and increasing stability of the PTH mRNA (14, 15, 18, 19).

For a long time, PTH and 1,25$(OH)_2$D have been known to be major regulators of blood phosphate. The discovery of FGF23, has expanded the understanding of phosphate homeostasis and established the PTH-vitamin D-FGF23 regulation axis. Serum phosphate concentration is determined by the balance between intestinal absorption of phosphate from the diet, storage of phosphate in the skeleton plus muscles, and excretion of phosphate through the urine. It is estimated that 80-85% of filtered phosphate is reabsorbed in the proximal tubules via sodium-phosphate co-transporters (NaPi) 2a and 2c (20). *In vitro* experiments with proximal renal tubular cells have confirmed that FGF23 directly down-regulates transcription, translation, and translocation of NaPi 2a and 2c transporters leading to reduced renal phosphate reabsorption. FGF23 also directly down-regulates renal 1-α hydroxylase, which decreases the production of active 1,25$(OH)_2$D (20-22) and consequently, decreases intestinal phosphate and calcium absorption. This effect of FGF23 is mediated by a specific receptor system composed of the transmembrane protein α-Klotho (Klotho) and certain subtypes of FGF receptors (FGFR1c). FGF23 has low affinity for FGF receptors. However, co-expression of α-Klotho turns the FGFR1c into a specific receptor for FGF23 by increasing the affinity of the receptor complex and serves as a non-enzymatic scaffold that simultaneously bond FGFR1c and FGF23 to implement FGF 23-FGFR1c proximity and hence stability (23-25).

FGF23 and PTH mutually regulate each other in a negative feedback loop, where PTH stimulates FGF23 production and FGF23 in turn suppresses PTH synthesis. Animals and *in vitro* studies have shown that FGF23 is a negative regulator of PTH mRNA expression and secretion (26, 27). Using both rats and in vitro rat parathyroid cultures, Ben-Dov *et al.* (26) showed that full-length FGF23 harbouring ADHR mutations (FGF $23^{R176Q/R179Q}$), which inhibit proteolytic inactivation of FGF23 and increase its half-life suppresses both PTH secretion and (27) PTH gene expression and increases parathyroid Klotho protein. Krajisnik *et al.* reported the same findings in cultured bovine parathyroid cells. Ben-Dov *et al.* (26) also demonstrated that FGF23 acts directly on the parathyroid through the mitogen-activated protein kinases (MAPK) pathway, where the FGF23-induced decrease in PTH secretion was prevented by a MAPK inhibitor. PTH increases FGF23 mRNA and protein levels *in vitro* and *in vivo* rat parathyroid cells (28-30). The effect of PTH to increase FGF23 transcription is mediated by the orphan nuclear receptor (Nurr1) (29).

In contrast, evidence is lacking to support the inhibitory effect of FGF23 on PTH secretion in informative clinical states, where elevated PTH secretion was reported in a patient with a translocation that resulted in increased α-klotho production and elevated FGF23 (31). Also, disorders resulting in FGF23 excess, such as tumour-induced osteomalacia (TIO) and X-linked hypophosphatemic rickets (XLHR) do not demonstrate inhibition of PTH synthesis and secretion in the setting of markedly elevated FGF23 (32).

### 1.1.4 Structure of PTH receptor type 1

PTH plays a key role in regulation of calcium and phosphate metabolism by acting in two main target tissues, namely bone and kidney. In bone, PTH acts directly through osteoblastic cells (that express PTHR1) and indirectly on osteoclasts (lack PTHR1) to induce the release of calcium from bone mineral compartment. In kidney, PTH acts on distal tubule cells to increase the rate of calcium reabsorption from the filtrate, and on the proximal tubule cells to decrease the rate of phosphate reabsorption. Whereas the majority of renal calcium recovery occurs in proximal tubules, the PTH regulation of calcium absorption is restricted to distal tubules, where PTH stimulates active calcium absorption through a cellular transport mechanism (2). Renal phosphate transport is essentially restricted to proximal

tubules, where two sodium-coupled transporters NaPi2a and NaPi2c mediate uptake of phosphate from luminal fluid. PTH inhibits renal phosphate transport by metabolic down-regulation of brush border NaPi2a, and to a lesser extent, NaPi2c and by reducing NaPi2a mRNA stability (2). In addition, PTH acts in renal proximal tubule cells to stimulate the rate of transcription of the CYP27B1 gene, which encodes the 25-hydroxyvitamin D3 1-α-hydroxylase (VD3 1A hydroxylase), and thus increase the blood concentrations of active 1,25 $(OH)_2$ D and provides for a further hormonal line of defence that helps to maintain calcium and phosphate homeostasis (2). The actions of PTH on its target tissues is mediated by PTHR1, which is expressed on the surface of bone osteoblasts and osteocytes, and renal proximal and distal tubule cells, but it is not expressed on osteoclasts. PTHR1 was successively cloned in 1991 using COS-7 cells transfected with opossum kidney cell complementary DNA (cDNA) library (33). The cDNA encoded a 585-amino acid PTHR1 with seven transmembrane domains. PTHR1 was found to bind PTH and PTHrP with equal affinity (33). Because PTHR1 lacks the homology with other G protein-coupled receptors (GPCR), known at the time, and shares striking homology with newly identified receptors for calcitonin and secretin PTHR1 was categorised in a distinct GPCR subgroup called the family B GPCR, which comprise in addition to PTHR1, receptors of calcitonin, secretin, glucagon, glucagon-like peptide-1, corticotrophin-releasing factor, and several other hormones (2).

In humans, the gene encoding the PTHR1 is located on chromosome 3p and consists of 14 coding exons. The mature mRNA encodes a protein of 593 amino acids, including 22 amino acids N-terminal signal peptide that is removed during intracellular processing. PTHR1 consists of a relatively large N-terminal extracellular domain (ECD) of ≈ 165 amino acids, a transmembrane domain (TMD) region containing the seven membrane spanning helices and interconnecting loops, and a C-terminal tail of about 130 amino acids (2) (Figure 1-4).

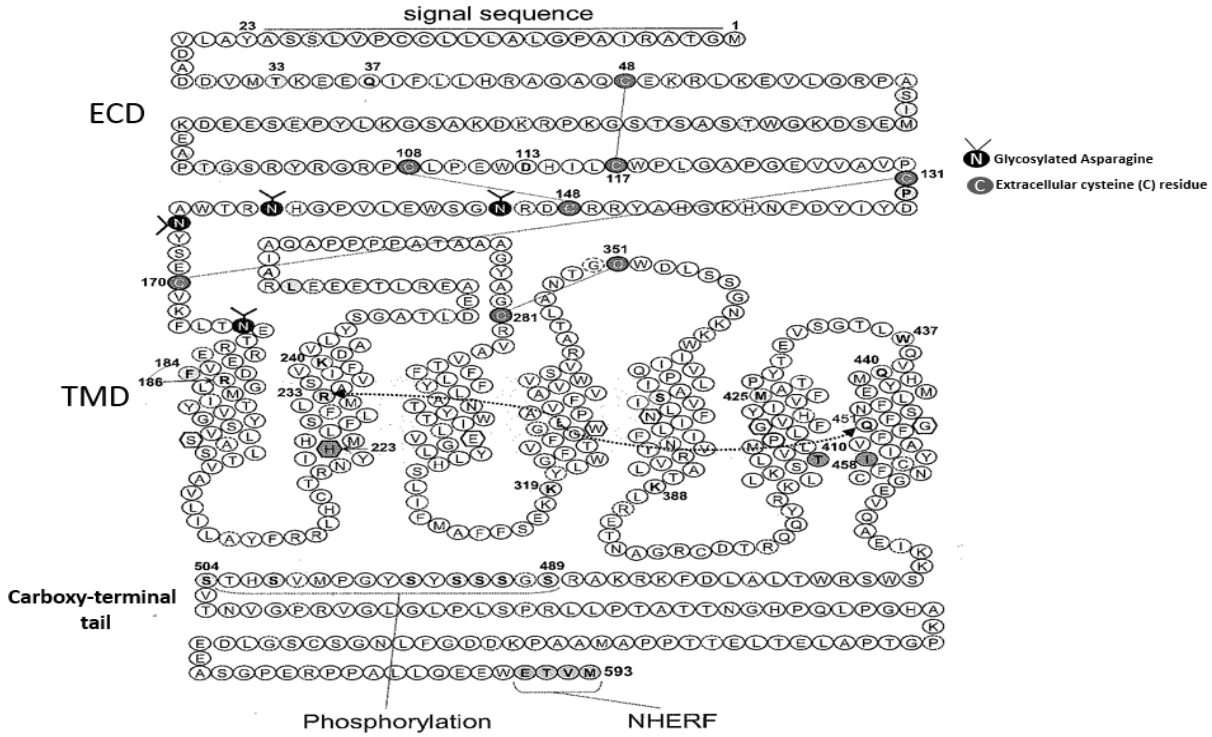


**Figure 1-4 Schematic representation of the human PTHR1**.*The receptor has a relatively large extracellular domain (ECD) that mediates initial ligand binding; a transmembrane domain (TMD) region comprises of the seven membrane-spanning helices and connecting intracellular and extracellular loops, that mediates agonist-induced receptor activation and signal transduction; and C-terminal tail that contains sites involved in ligand-induced receptor internalization and signal termination, including the seven serine (S) residues that are phosphorylated upon agonist activation and mediate recruitment of β-arrestine, and the C-terminal ETVM sequence that mediates interaction with the sodium-hydrogen exchanger regulating factor (NHERF) family of proteins. Other specific amino acids shown include the four pairs of extracellular cysteine (C) residues that form the stabilizing disulphide bond network, four glycosylated asparagine (N) residues in the ECD, Arginine 233 and Glutamine 451, which participate in an inter-helical interaction network (dashed connector) (Reproduced from Reference (2)).*

### 1.1.5 Interaction of PTH with receptor and signalling

The N-terminal domain of PTH binds PTHR1 and induces conformational change in the receptor that promotes coupling with heterotrimeric G protein (Gαβγ), and stimulates the α-subunit of G protein to exchange its bound guanosine diphosphate (GDP) for guanosine triphosphate (GTP). This exchange triggers conformational changes of the α-subunit that lead to its dissociation from βγ dimer. The stimulated α-subunit of G protein ($G_{s\alpha}$) activates adenylyl cyclase (AC), which synthesises cAMP from ATP and activates protein kinase A (PKA) Activation of PKA phosphorylates cAMP response element binding (CREB) proteins in the nucleus,

which bind cAMP response element in the regulatory region of target genes and activate transcription. PTHR1 can also couple to several other G protein subclasses, including $G_q$/11, and G12/13, which results in the activation of many pathways, such as $G_{\alpha q}$- phospholipase Cβ (PLCβ)/inositol triphosphate (IP3)/intracellular calcium/protein kinase C (PKC) pathway; the $G_\alpha$12/13-phospholipase D (PLD)/Ras homolog gene family, member A (RhoA) pathway (34); and the MAPK (extracellular signal-regulated kinase 1 and 2 (ERK1/2) signaling cascade(35). However, the best studied are the AC and PLCβ pathways. Gαq and $G_\alpha$11, of $G_q$ and G11, respectively, activate PLC, which cleaves phosphatidylinositol 4, 5-biphosphate (PIP2) into diacylglycerol (DAG) and inositol 1,4,5-triphosphate (IP3). IP3 then diffuses through the cytoplasm and activates IP3-gated $Ca^{2+}$ channel in the membranes of the ER, causing the release of stored $Ca^{2+}$ into the cytoplasm. The increase in the cytosolic $Ca^{2+}$ promotes protein kinase C (PKC) translocation to the plasma membrane and then activation by DAG. The activated PKC elicits cellular responses.

### 1.1.6 Determinants of PTH biological activity

In 1970, the complete PTH primary amino acid sequence was reported. This was 84 residues in length, and led, a year later, to the synthesis of the N-terminal 1-34 peptide of the native PTH molecule (36). The synthetic PTH (1-34) peptide was found to be as potent as the intact native PTH at inducing biological responses in animal models and cells in culture (36). Much research has been conducted since then that has analysed the structural features of PTH that determine its function. It has been shown that the first two N-terminal residues are necessary for PTH to elicit biological activity (37, 38). Tregear *et al.* (37) reported that deletion of the first N-terminal residue (alanine) resulted in marked decrease in PTH (1-34) activity and removal of the second residue (valine) at the N-terminus completely suppressed activity *in vitro* using a rat kidney adenylyl cyclase assay and an *in vivo* chick hypercalcemia assay. They also reported that peptide 1-27 was active in the rat kidney adenylyl cyclase assay, while the deletion of residue 27 turned it inactive (37). PTH (3-34) peptide was found to lack the ability to stimulate signalling activity and yet could effectively bind to the PTHR1 and inhibited the activity of the PTH (1-84) and PTH (1-34) (39, 40). The structural confirmation of stepwise N-terminal truncated PTH peptide in solution was studied using circular dichroism

spectroscopy, two-dimensional nuclear magnetic resonance spectroscopy, and restrained molecular dynamic calculation. Human PTH (2-37), PTH (3-37) and PTH (4-37) were compared to PTH (1-37). All peptides showed stable helical structures and hydrophobic interaction in approximately the region 15-34, whereas the N-terminal portion was found to be more random and showed only a relatively minor tendency for α-helical structure (41, 42). Figure 1-5 illustrates the bioactive domains of the PTH (1-34) ligand.

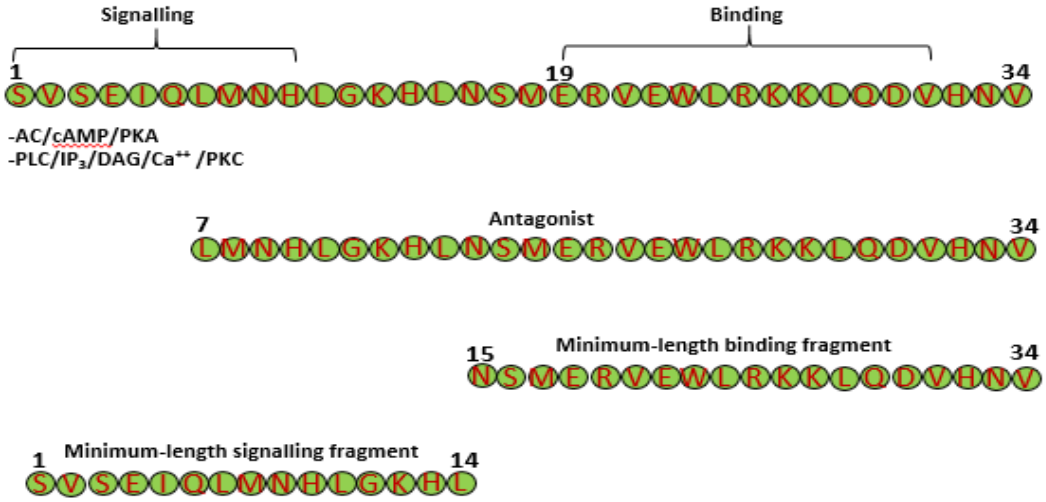


**Figure 1-5 The bioactive domains of the PTH (1-34) ligand.** *Shown is the sequence of bioactive PTH (1-34). The determinants for activating signalling pathways resides in the N-terminal portion of the ligand particularly in the 1-9 segment and the first two amino acids being the key important residues for signalling. Receptor binding determinant resides in the C-terminal portion of the PTH (1-34) fragment, particularly in the 19-31 segment. PTH (7-37) is a potent antagonist, the PTH (15-34) fragment is the shortest length peptide of native sequence that exhibits detectable binding to the PTH receptor, and the PTH (1-14) peptide is the shortest length N-terminal peptide that exhibits detectable cAMP signalling activity.*

### 1.1.7 Regulation of Extracellular Calcium Homeostasis by PTH

Calcium plays crucial roles in cell biology. It is an important element in many physiological functions, such as cell proliferation, cellular secretion, neural transmission, neuromuscular function, muscle contraction (including cardiac muscle), the stability and permeability of cell membranes, blood clotting, and the mineralization of bone (43). PTH acts as the key endocrine regulator to modulate physiological actions in the bone, kidney and the intestine to maintain the homeostasis of $Ca^{2+}$ concentration in the extracellular fluid (ECF). The reference

range of total and free plasma calcium is 2.2–2.6 mmol/L and 1.1-1.3 mmol/L respectively (43). The tight control of plasma calcium concentration is maintained by a classic feedback loop with $Ca^{2+}$ acting on the calcium-sensing receptor (CaSR) located on the surface of the parathyroid gland chief cells. CaSR represents the molecular mechanism by which parathyroid cells detect changes in serum $Ca^{2+}$ concentration and stimulate PTH secretion and synthesis to maintain calcium level within a narrow physiological range. Rapid PTH release from secretory granules in hypocalcemia state is enhanced by binding of $Ca^{2+}$ to CaSR on chief cells. PTH functions to increase $Ca^{2+}$ by acting directly on kidneys and bones and indirectly on intestine. In the kidneys, PTH increase renal calcium reabsorption and phosphate excretion. In the renal proximal tubules, PTH activates the enzyme 1-hydroxylase, which converts 25-hydroxyvitamin D (25-(OH) D) to its most active metabolite, $1,25(OH)_2D$. $1,25(OH)_2D$ then promotes intestinal absorption of the dietary calcium and phosphate. PTH promotes bone resorption and consequently increases the release of calcium and phosphate into ECF. Hypocalcemia also increase the protection of PTH protein and PTH mRNA from degradation, thus making more PTH available for release (14, 15) and increases parathyroid cell proliferation possibly through the action of CaSR (44). $1,25(OH)_2D$ may have an indirect effect on PTH release by increasing the expression of CaSR, where vitamin D response elements (VDREs) have been identified in promoter elements that regulate the expression of the CaSR (44, 45)

Feedback inhibition of PTH release occurs primarily by direct effect of elevated $Ca^{2+}$ on parathyroid glands. $Ca^{2+}$ acting through negative regulatory elements located upstream from the gene for prepro-PTH decreases gene transcription, hormone synthesis and effect PTH mRNA stability. These effects are mediated by CaSR (44, 45). $1,25(OH)_2D$ may have inhibitory effect on the parathyroid glands as well, where increased $Ca^{2+}$ inhibits $1,25(OH)_2D$ and consequently effects the expression of CaSR(44, 45) Figure 1-6 illustrates calcium homeostasis mechanism and key physiological regulators.

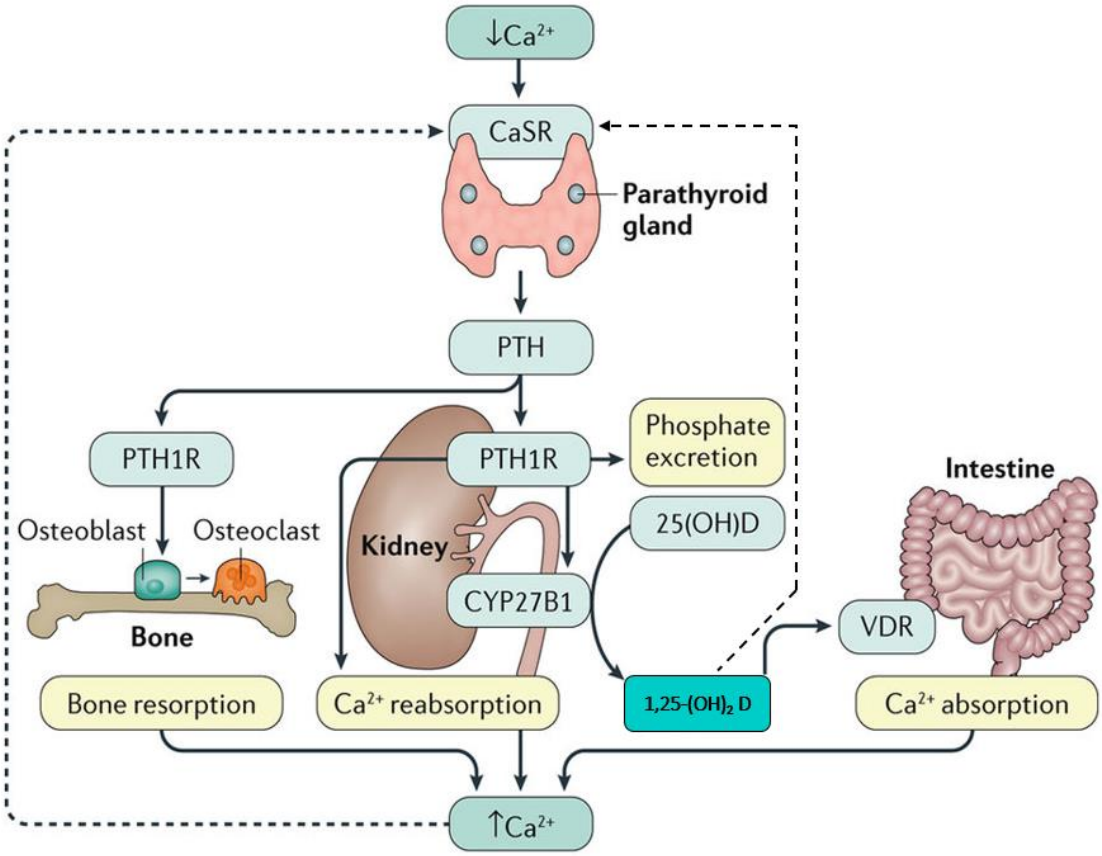


**Figure 1-6 Calcium Homeostasis.** *Low ECF $Ca^{2+}$ sensed by CaSR and then stimulates parathyroid glands to synthesise and release PTH. PTH acts on the PTHR1 in the kidney and bone. In bone, PTHR1 activation in osteoblasts and osteocytes results in the release of cytokines that stimulate osteoclasts activity, thereby enhancing bone resorption and release of calcium and phosphate from skeleton. In the kidney, PTH increases tubular calcium reabsorption, phosphate excretion and activates the enzyme 1-hydroxylase that converts 25-(OH) D to 1,25-$(OH)_2$ D. 1,25-$(OH)_2$ D acts on the intestine to increase the absorption of dietary calcium via the vitamin D receptor (VDR). The increase in calcium and 1,25-$(OH)_2$ D concentration mediated by PTH act on parathyroid glands via CaSR to induce feedback inhibition of further PTH secretion. (Figure taken from reference (46))*

### 1.1.8 Cellular actions of PTH

PTH has direct effects on osteoblasts and osteocytes as well as indirect effects on osteoclast through its action on osteoblasts and osteocytes. The combination of these PTH actions on bone cells promotes both bone formation and bone resorption. The final effect, either anabolic or catabolic, will depend on the dose and periodicity of the PTH signal. Continuous exposure to a high level of PTH, as seen in primary hyperparathyroidism (PHPT), causes bone loss. On the other hand, the anabolic

properties of PTH are much more clearly seen when PTH is given intermittently (47, 48). The advances in elucidating the direct and indirect effect of PTH on various bone cells has led to a better understanding of the overall effects of PTH.

#### *1.1.8.1 PTH action on Osteoblasts*

PTHR1 is expressed in pre-osteoblasts, osteoblasts, lining cells, and osteocytes (2). Several pre-clinical and clinical studies showed that intermittent PTH administration can stimulate bone formation (47-55). Histological studies in animals and humans have shown that intermittent PTH rapidly increases the mineralizing surface and mineral apposition rate in cancellous bone, indicating that PTH has a stimulatory effect on osteoblast numbers or function (56-58). Jilka *et al.* (59) suggested that the increases in osteoblasts number upon intermittent administration of PTH may explain why this therapy reverses bone loss. This osteoanabolic effect relies on the ability of PTH to increase ostoblastogenesis, decrease osteoblast apoptosis, enhance the differentiation of lining cells into active osteoblasts, or a combination of all these effect (60).

#### *1.1.8.2 PTH action on Osteoclasts*

PTH induces bone resorption and releases calcium from bone surfaces via activating osteoclasts. A considerable amount of evidences indicates that osteoclasts do not express PTHR1 (2). PTH acts indirectly on osteoclasts through its action on osteoblasts and osteocytes. PTH stimulates the differentiation of osteoclast precursors to osteoclasts and enhances the survival and activity of fully formed osteoclasts. This action is mediated by a number of factors such as the receptor activator of nuclear factor-kappa B ligand (RANKL), osteoprotegerin (OPG), and the monocyte chemoattractant protein-1 (MCP-1). In osteoblasts, the binding of PTH to PTHR1 activates AC and PLC with the formation of cAMP and a subsequent increase in intracellular calcium concentration as well as activating PKC through PLC-dependent and –independent pathways. These pathways stimulate formation of osteoclasts by production of RANKL and macrophage colony-stimulating factor (M-CSF) that are required for osteoclast formation and activation of bone resorption. OPG production is also induced in osteoblasts. OPG acts as a decoy receptor, as it binds to RANKL and prevents binding of RANKL to RANK on osteoclast precursors. This subsequently inhibits osteoclast formation and activation, thus

regulating bone resorption (60). Figure 1-7 shows osteoclastogenesis and bone resorption.

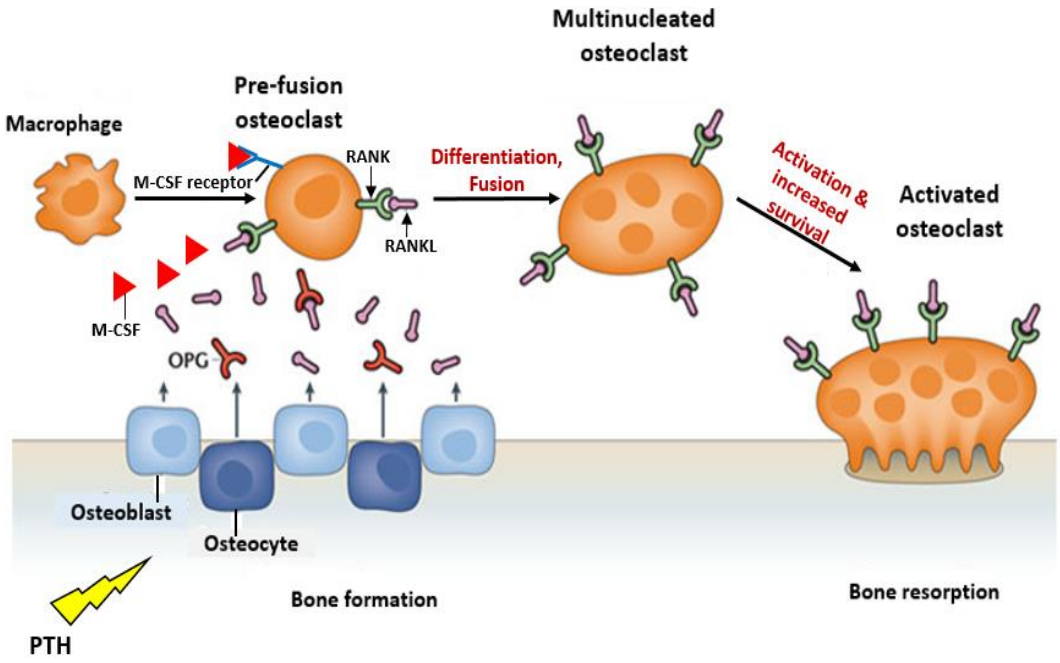


**Figure 1-7 Schematic diagram representation of osteoclastogenesis and bone resorption.** *Binding of PTH to PTHR1 on osteoblasts stimulates formation of RANKL and M-CSF, which bind to RANK and M-CSF receptor on osteoclast precursors and enhancing their fusion to form multi-cellular mature osteoclast. Activated osteoclasts initiate bone resorption. OPG acts as a decoy receptor, binds to RANKL and consequently prevents RANK-RANKL interaction on osteoclast precursors, inhibits osteoclast formation and activation (Figure modified from reference (61)).*

### 1.1.9 PTH secretion and Metabolism

Studies have reported the existence of different PTH fragments in the circulation, which may arise either by direct secretion from the parathyroid glands, or by peripheral metabolism of the hormone (62-67). D'Amour *et al.* (66) reported the presence of Non-(1-84) PTH fragments alongside the intact PTH (1-84) in serum and parathyroid cells supernatant obtained from patients with primary and secondary hyperparathyroidism. The non-(1-84) PTH fragments constitute a family of fragments which have an N-structure starting at position 4,7,8,10, and 15 (66).

#### *1.1.9.1 Sources of circulating C-terminal PTH fragments*

a. Secretion by the parathyroid gland

Chromatographic analyses of normal and adenomatous parathyroid gland extracts and electrophoretic analyses of parathyroid gland immunoextracts revealed at least

four PTH species, each with a distinct pattern of cross-reactivity in the sequence-specific RIAs (64). Analysis of parathyroid venous effluent sera fractionated using high resolution gel filtration system (Bio-Gel P-150 column) from PHPT patients using N- and C-terminal specific RIAs demonstrated the presence of Non-(1-84) PTH fragments that are biologically inactive (65). Studies of cultured or perfused bovine parathyroid tissue showed that C-terminal PTH fragments are present in parathyroid cells and are secreted directly from the glands (68). All these findings indicate that parathyroid cells are a source of non-PTH (1-84) fragments.

b. Hepatic proteolysis of intact PTH

Data from several laboratories indicate that hepatic mechanisms may have a distinctive role in the metabolism of intact parathyroid hormone after secretion (69-71). Serge *et al.* (69) studied the proteolysis of intact PTH by isolated rat kupffer cells and hepatocytes, where kupffer cells and hepatocytes were incubated with unlabelled and $^{125}$I-labelled bovine PTH. Analysis of fragments resulting from incubation of labelled and unlabelled bovine PTH with kupffer cells with sequence-specific RIAs revealed PTH fragments that lack a N-terminal fragment, which have an immunochemical appearance indistinguishable from, and chemically identical with those found in plasma when intact PTH is injected intravenously. In contrast, hepatocytes did not hydrolyse the hormone (69). Pillai and Zull (71) reported that iodinated PTH labelled at position 43 was cleaved into two radioactive fragments when incubated with isolated rat kupffer cells, which were shown by Edman degradation to have residues 35 and 38 as their N-termini. In addition, using reverse-phase high-performance liquid chromatographic (RP-HPLC) techniques, Bringhurst *et al.* (70) reported that [$^{3}$H]tyrosine-labelled bovine PTH metabolized by isolated rat kupffer cells yielded multiple C-terminal fragments that are chemically identical with those found in plasma. These results suggest that kupffer cells contribute substantially to the metabolism and clearance of circulating intact PTH.

#### *1.1.9.2 Clearance of PTH and PTH fragments*

The Kidney plays a crucial role in clearance of both intact and C-terminal PTH fragments from blood (72-74). Both glomerular filtration and peritubular uptake are important mechanisms for renal PTH uptake (67, 72, 73). Renal uptake of C-terminal fragments of PTH is dependent exclusively upon glomerular filtration and tubular reabsorption, whereas peritubular uptake can only be demonstrated for biologically

active PTH (1-84) and synthetic PTH (1-34) (73). It is well established that PTH immunoreactivity disappears more slowly from blood in humans with renal insufficiency and in nephrotic animals (67), which partly explains increased C-terminal PTH fragments in individuals with renal failure.

### 1.1.10 Clinical uses of the biologically active PTH (1-34) Fragment

#### *1.1.10.1 PTH (1-34) in treatment of osteoporosis*

The prevalence of osteoporosis in postmenopausal women continues to increase with the growing elderly population. According to data from World Population Ageing report, every country in the world is experiencing growth in the number and proportion of older persons in their population and this growth is projected to accelerate in the coming decades. The report pointed out that the numbers of people aged 60 years or over have risen from 607 million in 2000 to 901 million in 2015 (75). Postmenopausal osteoporosis is a bone disorder mainly characterized by bone resorption that exceeds bone formation and consequently reduced bone strength and increased risk of fractures. It is estimated to affect 200 million women worldwide (76). Many FDA-approved anti-resorptive drugs are available for the treatment of osteoporosis (e.g. Bisphosphonate, Raloxifene, Estrogen, and Calcitonin). These drugs mainly act by reducing bone turnover by inhibiting osteoclast activity (77, 78). Another therapeutic approach for osteoporosis acts by enhancing bone formation. An example of an osteoanabolic drug is teriparatide, an FDA approved recombinant human PTH (1-34) (Forsteo, E. Lilly, Indianapolis, USA) used for treating patients (men and women) with osteoporosis who are at high risk for future fracture (48, 52, 79).

PTH (1-34) decreases the risk of vertebral and non-vertebral fractures and increases bone mineral density (BMD) in postmenopausal women with osteoporosis. Neer *et al.* (48) studied the efficacy of teriparatide in prevention of future fracture in postmenopausal women with prior vertebral fracture (n=1637), where they subjected subjects to daily teriparatide (20 or 40 µg) or placebo injections for an average period of 18 months. A 65% reduction in risk of new vertebral fractures ($p<0.001$), and a 35% reduction in risk of non-vertebral fractures ($p=0.04$) were observed in subjects who received 20 µg dose as well as a 9% increase in BMD of lumbar spine ($P<0.001$) compared to placebo. The authors stated the 40 µg dose increased BMD of lumbar spine more than the 20 µg dose but had similar effect on risk of fractures

(48). These results have been supported by several other clinical trials. A meta-analysis of eight randomised controlled trials (n= 2388) that used teriparatide to treat postmenopausal osteoporosis found that the treatment was associated with an increase in BMD of 8.14% (95% confidence interval (CI), 6.72% - 9.55%) in lumbar spine and of 2.48% (95% CI, 1.67% - 3.29%) in hip. In trials that reported fracture data, the treatment was associated with a 70% reduction in risk of vertebral fracture and a 38% decrease in risk of non-vertebral fracture compared to placebo group (80). It has also been found that teriparatide treatment of postmenopausal women with osteoporosis significantly increased cancellous bone volume and connectivity, improved trabecular morphology with a shift toward a more plate-like structure, and increased cortical bone thickness. These changes in cancellous and cortical bone morphology should improve biomechanical competence and are consistent with the reduced incidences of vertebral and non-vertebral fracture during administration of teriparatide (57).

#### *1.1.10.2 PTH (1-34) in treatment of Hypoparathyroidism*

Individuals with hypoparathyroidism are characterized by deficient or no circulating PTH and low serum calcium, typically associated with hyperphosphatemia, hypercalciuria, and reduced concentration of 1,25-$(OH)_2D$ (81, 82). The clinical presentation may include muscle cramping, spasms, or tetany and, rarely, life threatening events such as seizure or laryngospasm (83). Hypothyroidism is most commonly caused by surgical removal of, or damage to, the parathyroid glands during thyroid, parathyroid, or other neck surgery. It also can be caused by autoimmune destruction of parathyroid cells and rare genetic diseases such as DiGeorge syndrome (81, 82). Hypoparathyroidism, regardless of the etiology, is treated with oral calcium and vitamin D/analog supplementation (81, 82). This treatment can cause hypercalciuria, which consequently may cause irreversible renal damage and renal failure (81-83). To reduce this risk, the vitamin D/analog and calcium dosages are often reduced to maintain serum calcium at the lowest tolerable level (without causing symptoms), which in turn results in varying degrees of hypocalcemia in most hypoparathyroid patients treated this way (83).

Synthetic PTH (1-34) has been investigated as an alternative treatment of chronic hypoparathyroidism in adults and children (83-90). The studies have shown that PTH (1-34) provides better control of serum calcium levels along with reduced needs

for calcium and vitamin D/analog supplementation when compared with calcium and vitamin D/analog supplementation alone (84-88). Notably, treatment with twice-daily hPTH (1-34) reduced the variation in serum calcium and normalised urine calcium at a lower daily PTH dose compared to once-daily dosing (81, 84-88). Winer *et al.* (83) published a 6-month, open-label crossover trial of PTH (1-34) delivered continuously via pump versus twice-daily subcutaneous injection. Eight subjects were studied, aged 36–54 years, all with post-surgical hypoparathyroidism. Pump delivery of PTH (1-34) produced a significant decrease in urine calcium excretion and a 65% reduction in the daily PTH (1-34) dose needed to maintain eucalcemia compared with twice-daily injections (83). The study demonstrated that pump therapy restored bone turnover to normal levels compared to twice-daily injection, which produce chronic elevation of bone markers (83). The investigators noted no significant difference in the incidence of adverse events between the two groups and no treatment-related incidence of hypercalcaemia was reported (83). The overall findings of pump therapy look promising as a replacement hormone therapy for chronic hypoparathyroidism. However, a long-term study on pump therapy is needed to confirm these findings.

#### *1.1.10.3 PTH (1-34) to Accelerating Fracture Healing*

PTH (1-34) has been shown to promote bone healing in several animal and human studies. In a randomized double-blind study, Aspenberg *et al.* (91) investigated the potential benefit of PTH (1-34) in postmenopausal women who had sustained a dorsally angulated distal radial fracture in need of closed reduction without surgery. Within 10 days of fracture, the women were randomly assigned to once daily injections of placebo or PTH (1-34) at doses of 20 µg or 40 µg for a total treatment period of 8 weeks. All patients, regardless of randomization group, received supplements of 1000 mg /day of elemental calcium and 800 IU/day of vitamin D throughout the study period. The results demonstrated that time to healing, at 7.4 weeks, was significantly shorter in the treatment group receiving 20 µg of PTH (1-34). Time to healing was 9.1 weeks in the placebo and 8.8 weeks in the treatment group receiving 40 µg PTH (1-34). Aspenberg and Johansson (92) reported improved early callus formation in postmenopausal women with distal radius fracture treated with PTH (1-34) at doses of both 20 and 40 µg in comparison to placebo. Warden *et al.* (93) studied the combination of low-intensity pulsed

ultrasound (LIPUS) and PTH (1-34) on fracture healing in bilateral midshaft femur fractures created in rats. LIPUS was found to primarily increase total callus volume without influencing bone mineral content, and PTH (1-34) have the opposite effect of increasing bone mineral content without influencing total callus volume. As a consequence of the effect of LIPUS on total callus volume but not bone mineral content, it decreased volumetric bone mineral density resulting in a less mature callus. In contrast, the effect of PTH on callus bone mineral content but not total volume resulted in increased callus volumetric bone mineral density and a more mature callus. This resulted in PTH increasing fracture site mechanical strength and stiffness. These data suggest that PTH may be more useful in treatment of acute bone fracture. PTH (1-34) was combined with mechanical loading, a known stimulus towards fracture healing, in the study of tibial fracture healing in 25-week-old ovariecotomized female rats (94). In this study, mechanical loading was achieved by an external loading device and PTH (1-34) was administered once daily via subcutaneous injection at a dose of 20 μg/kg/day. The results showed that unloading reduced callus area significantly, whereas no effects of PTH (1-34) on callus area were seen in neither normally nor unloaded animals. PTH (1-34) increased callus bone mineral density and bone mineral content significantly, whereas unloading decreased callus bone mineral density and bone mineral content significantly. PTH (1-34) treatment increased bone volume of the callus in both unloaded and control animals. These results suggested a synergetic effect of PTH (1-34) and mechanical loading and confirmed the stimulatory effect of PTH (1-34) on fracture healing (94).

### 1.1.11 Mechanisms for the bone anabolic effect of PTH treatment

The intermittent administration of low-dose PTH (1-34) results in anabolic effects on the skeleton. This aspect of PTH is quite interesting and complex at the same time, as how can a “bad” hormone for bones become a useful treatment for osteoporosis? However, the keys to understanding the net anabolic effect of intermittent PTH is to understand that the process is not purely anabolic as it concomitantly stimulates osteoclastic bone resorption plus osteoblast bone formation and that osteoclasts do not express PTHR1 and they only are activated indirectly through binding of PTH to PTHR1 on osteoblasts. So, due to the short half-life of intermittent PTH in the circulation, osteoblasts anabolic activity precedes catabolic activity of osteoclasts creating the so-called ‘anabolic window’, which means that there is a time frame of a

number of months (6-18 months) in which bone formation is in excess over bone resorption as measured by serum bone turnover markers (see figure 1-8) (60, 78). The cellular and molecular mechanisms of this anabolic window are not yet fully understood and cannot be explained by one single hypotheses. Following is a summary of hypothesized mechanisms for the anabolic actions of PTH in bone.

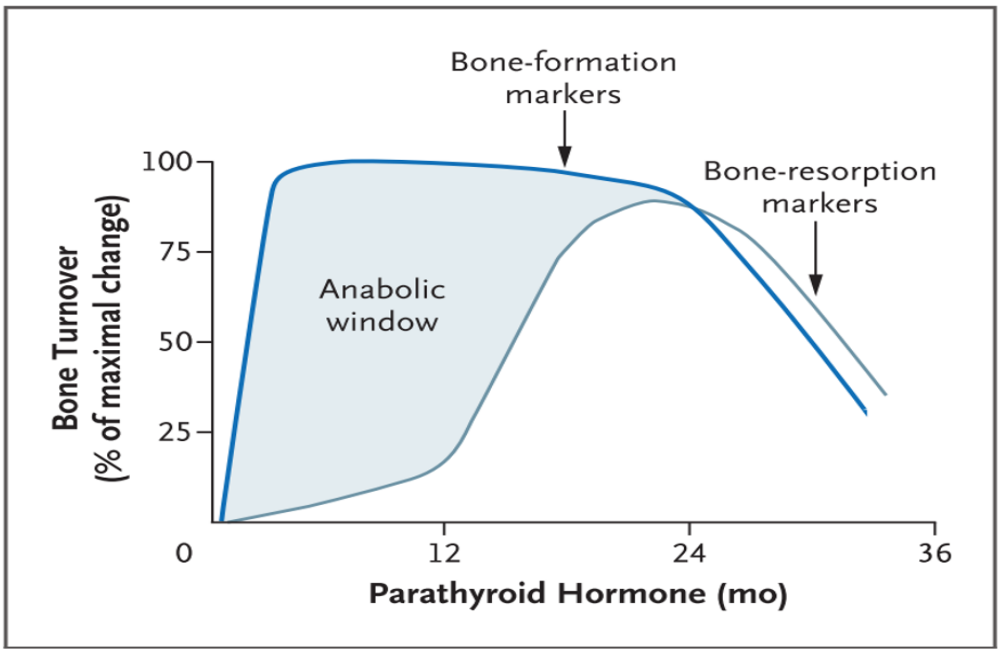


**Figure 1-8 The anabolic Window.** *PTH stimulates the processes associated with bone formation before there is a subsequent stimulation of the process associated with bone resorption. The 'window' between the effects of PTH on these actions is variable, but is thought to represent the period when PTH is maximally anabolic for bone. (Taken from reference (78) )*

#### *1.1.11.1 PTH reduces sclerostin expression*

The Wnt-β-catenin signalling pathway is important for bone and cartilage formation as well as for bone homeostasis (60, 95, 96) and β-catenin deficiency associated with low bone mass in mice (60, 97, 98). Bellido *et al.* (1) demonstrated that PTH decreases *Sost*/sclerostin expression in osteocytes *via* increasing the proteasomal degradation of Runx2. Down-regulation of sclerostin accounts for the anabolic action of PTH (Figure 1-9).

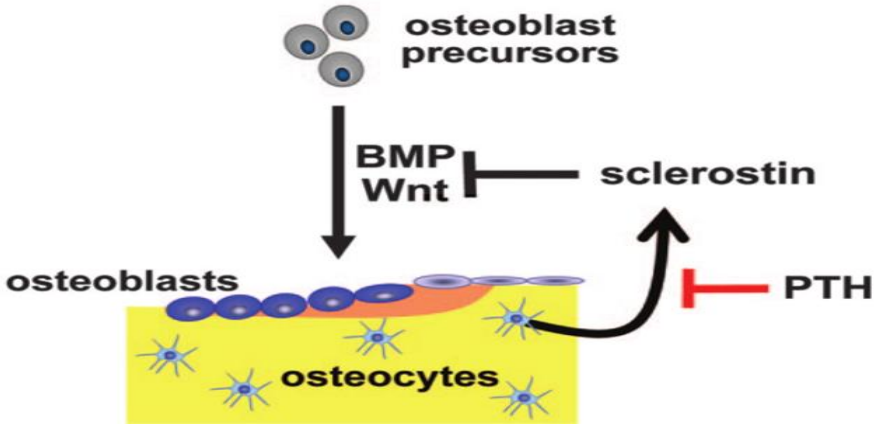


Figure 1-9 **Regulation of osteoblastogenesis via actions of PTH on osteocytes.** *The model depicts the sclerostin-mediated negative feedback loop by which osteocytes suppress bone formation (black lines) and the inhibitory effect of PTH on sclerostin secretion by osteocytes (red line) which unleashes the prodifferentiating actions of BMP and Wnt signalling on osteoblast progenitors*

In skeletal cells, Wnt uses the canonical Wnt-β-catenin signalling pathway. Wnt binds to specific receptors, called frizzled, and to low-density lipoprotein receptor-related proteins 5 and 6 (LRP5 and LRP6). These interactions lead to the stabilization of β-catenin, which translocate to the nucleus and regulate gene expression (Figure 1-10). The importance of Wnt- β-catenin signalling in osteogenesis is confirmed by studies of the effects of mutations in this pathway. Activating mutations of Wnt co-receptors result in increased bone mass, whereas inhibition of this pathway leads to reduced bone mass (78). Wnt antagonists like sclerostin and Dickkopf-1 (Dkk-1), which are both expressed by osteoblasts and osteocytes prevent Wnt signaling by interacting with Wnt co-receptors (Figure 1-10).

#### *1.1.11.2 PTH induces bone cell survival by exerting an anti-apoptotic effect*

Bellido *et al.* (99) demonstrated that daily intermittent injection of as little as 30 ng/g of PTH (1-34) in mice for 28 days increased hindlimb and spine BMD. These changes were associated with a reduction in osteoblasts apoptosis at both sites as well as an increase in the level of serum osteocalcin, a biochemical index of osteoblast number. At the same dose that PTH inhibited osteoblasts apoptosis, it also increased osteoblast number, bone formation rate, and the amount of cancellous bone in the distal femur, but the number of osteoclasts was not affected at any dose examined. The prevalence of osteoblasts apoptosis was inversely correlated with

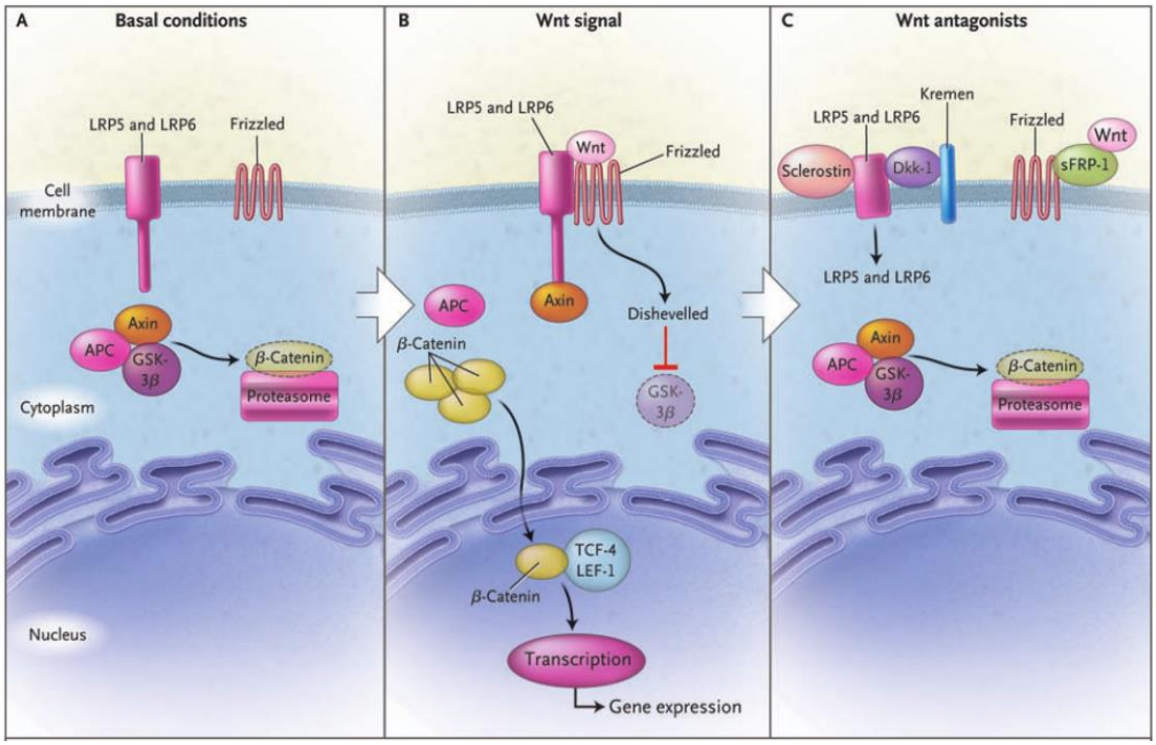


**Figure 1-10 The Canonical Wnt–β-Catenin Signaling Pathway Used in Osteoblasts.** *Panel A shows that under basal conditions, β-catenin is phosphorylated by glycogen synthase kinase 3β (GSK-3β), axin, and adenomatous polyposis coli (APC) tumor-suppressor protein and degraded in the proteasome. Panel B shows that after Wnt binding to its receptor (frizzled) and co-receptors (low-density lipoprotein receptor–related proteins 5 and 6 [LRP5 and LRP6]), dishevelled, an intracellular protein, is induced to degrade GSK-3β. In addition, the cytoplasmic tails of LRP5 and LRP6 bind and anchor axin. These two events lead to the stabilization of β-catenin and its translocation to the nucleus, where it binds to T-cell factor 4 (TCF-4) or lymphoid enhancer binding factor 1 (LEF-1) to regulate transcription. Panel C shows that the extracellular Wnt antagonists prevent Wnt signaling. Dickkopf-1(Dkk-1) in association with Kremen and sclerostin bind LRP5 and LRP6. Soluble frizzled-related protein 1 (sFRP-1) binds Wnt and prevents its interaction with frizzled. (Figure taken from reference (78)).*

three independent measures of bone formation, serum osteocalcin, bone formation rate, and osteoblast number. The authors argued that attenuation of osteoblast apoptosis by daily injections of PTH in mice accounts, at least in part, for the increased number of osteoblasts and, thereby, the increased bone formation produced by this regimen (99). The same research group has studied the effect of daily subcutaneous injection of 400 ng/g of hPTH (1-34) over a 4-week period in two strains of adult mice, mice with normal bone mass (SAMR1) and mice with osteopenia due to impaired osteoblastogenesis and decreased bone formation (SAMP6) (100). Daily PTH injection caused progressive increase in BMD of

hindlimb and spine in adult mice, though it was greater in the hindlimb than in the spine. Remarkably, the increase in BMD was similar in the two strains, even though the baseline values were different (100). The authors reported an equivalent anabolic response of normal SMAR1 and SAMP6 mice with defective osteoblastogenesis to daily injections of hPTH (1-34), and the number of osteoblast progenitors obtained from the marrow of PTH-treated animals of either strains was similar to that obtained from the marrow of vehicle-treated animals, which indicates that PTH does not have a stimulatory effect on the number of osteoblast progenitors (100). They also showed that the proportion of osteoblast undergoing apoptosis, as determined by transferase–mediated nick end labelling (TUNEL), was greatly decreased in animals of either strain receiving PTH (100). Accordingly, the authors suggested that intermittent PTH treatment increases osteoblast survival by suppressing/inhibiting osteoblast apoptosis, which results in an increase in osteoblast numbers and thereby bone formation (100). Bellido *et al. (99)* also studied the effects of sustained (140 ng/h) versus intermittent (230 ng/g/day) PTH (1-84) elevation on the prevalence of osteoblast apoptosis and on the number of osteoblasts and osteoclasts 2, 4, and 6 days. Sustained elevation of PTH caused an increase in the number of osteoclasts at day 2 and was followed by an increase in osteoblasts number at day 4. Sustained elevation of PTH had no effect on the prevalence of osteoblast apoptosis at any time during the experiment, whereas daily injection of PTH (1-84) reduced osteoblast apoptosis and increased osteoblast number beginning on day 2. The increase in osteoblast number seen with daily injections was significantly greater and occurred earlier than that caused by sustained infusion of PTH (99). Why then did continuous PTH administration, in contrast to intermittent administration, not affect the prevalence of osteoblast apoptosis? The PTH anti-apoptotic pathway involves cAMP-mediated PKA signalling. PKA phosphorylates the apoptotic protein, Bad and thereby inactivates its pro-apoptotic function by facilitating interaction with 14-3-3, a protein that sequesters proteins containing phosphoserine. Inactivation of Bad consequently stimulates the transcription of the anti-apoptotic gene Bcl-2 (Figure 1-11). These effects combine to increase the ratio of the amount of anti- to pro-apoptotic members of the Bcl-2 family, which is known to determine the ability of the cell to resist death signals. Other survival gene(s) could be involved to increase transcription of the anti-apoptotic Bcl-2 gene in response to PTH requires at least two transcription factors, CREB and the osteoblast-specific transcription factor

Runx2. However, PTH also decreases the concentration of Runx2 by promoting its proteasomal degradation in a process involving the ligase Smurf1. In turn, reduction of Runx2 levels below a critical threshold terminates the ability of PTH to maintain its anti-apoptotic signal by removing this critical factor on which the transcription of the pro-survival genes by PTH depends. This provides for a negative feedback loop that shortens the duration of the anti-apoptotic effect of the hormone. In other words, the decline in Runx2 is the critical event limiting survival signaling, as transcription of survival genes is maintained when the level of Runx2 is kept above a critical level. Bellido *et al.* (99) demonstrated that when Runx2 degradation is abrogated or when Runx2 is overexpressed, phospho-Bad and CREB are no longer needed, and the comparatively high level of Runx2 is sufficient for prolonged anti-apoptotic effect of PTH (99).

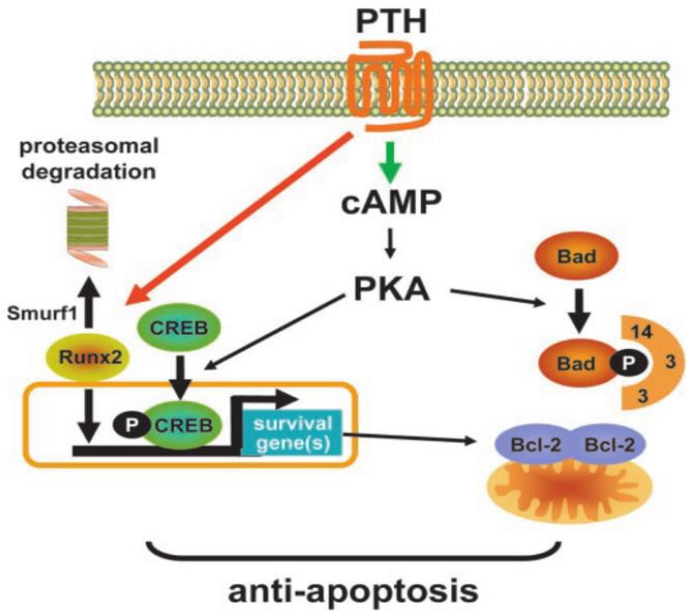


**Figure 1-11 Self-limited anti-apoptotic signalling pathways induced by PTH in osteoblasts.** *PTH induces PKA-mediated phosphorylation and inactivation of the pro-apoptotic protein Bad as well as transcription of survival genes Bcl-2 mediated by CREB and Runx2. PTH also increases proteasomal proteolysis of Runx2 via a process involving Smurf1.The anti-apoptotic effect of PTH is prolonged by inhibition of proteasomal activity or by overexpressing Runx2 itself. Sustained PTH concentration increases Runx2 degradation by Smurf1. Reduction of Runx2 below a critical threshold terminates the anti-apoptotic effect of PTH. (Figure taken from reference (99))*

#### *1.1.11.3 IGFs are essential for anabolic effect of PTH*

Insulin-like growth factors (IGFs) are known to exert anabolic actions on bone (60, 78, 101). Gazzerro and Canalis (101) reported that IGF-I increases the function of the differentiated osteoblasts in bone tissue and mediates selected anabolic actions of PTH. IGF-I and PTH are co-dependent on each other as IGF-I synthesis in bone cells is primarily dependent on PTH and is required, in turn, for the anabolic actions of PTH in rodent bone (78). *In vivo*, two experimental models confirm the anabolic effect of IGF-I. Overexpression of IGF-I increases the volume of cancellous bone by increasing bone formation (102). On other hand, targeted deletions of the *IGFI* receptor gene or deletions of the insulin-IGF-I signaling molecules, insulin-receptor substrate (IRS) 1 and 2, causes osteopenia due to impaired bone formation (103, 104). These observations indicated a role for IGF-I as a regulator of bone mass.

### 1.1.12 PTH (1-34) in Diagnosis of Pseudohypoparathyroidism

Hypoparathyroidism is indicated by the presence of hypocalcaemia along with normo- or hyperphosphatemia with normal renal function and low or undetectable PTH (1-84). The first step of differential diagnosis of hypoparathyroidism is the measurement of serum PTH (1-84) (105). Low or undetectable serum concentration of PTH (1-84) (<30 pg/mL) means decreased secretion of PTH, which is most often associated with post-surgical or idiopathic hypoparathyroidism, and hypomagnesemia. Serum PTH (1-84) values of ≥ 30 pg/mL suggested possible pseudohypoparathyroidism (PHP) (105). PHP is a group of heterogeneous rare metabolic disorders whose common feature is resistance to PTH and other hormones that activate cAMP-dependent pathways via $G_s\alpha$ protein (106). The resistance is caused by defects in the *GNAS* gene, which encodes the $G_s\alpha$ protein that stimulate cAMP formation (106). All forms of PHP are characterized by a defect in the response of the proximal renal tubule to PTH and associated with hypocalcaemia, hyperphosphatemia, and elevated circulating concentrations of PTH in the absence of vitamin D or Mg deficiency (106). The Ellsworth-Howard test (EHT) or PTH loading test has been used traditionally to confirm PHP. Because the PTH receptor is coupled to the stimulatory G protein ($G_s$), thereby activating cAMP formation, measurement of serum and urinary cAMP concentrations after the injection of exogenous PTH permitted the differentiation of PHP type 1 (PHP1), in which a blunted cAMP response is observed, from PHP type 2 (PHP2) in which the cAMP

response to PTH is normal or elevated but the phosphaturic response is deficient (106). Figure 1-12 shows the plasma cAMP response of healthy individuals after subcutaneous injection of teriparatide (top) and EHT results of suspected PHP patient after teriparatide injection (bottom).

The effect of the synthetic hPTH (1-34) fragment on plasma cAMP in human subjects and the diagnostic criteria for the plasma cAMP response in EHT were studied (107, 108). Sohn *et al.* (107) reported that plasma cAMP increased to over 100 nmol/L within 5 or 10 min after the end of infusion of 20 or 30 µg of hPTH (1-34) in all patients with idiopathic hypoparathyroidism and normal subjects. The mean values for maximum plasma cAMP concentrations were (170.0 ± 43.6) nmol/L with 20 µg (n=4), (211.0 ± 71.4) nmol/L with 30 µg (n=30) in patients with idiopathic hypoparathyroidism, and (204.8 ± 59.5) nmol/L with 30 µg (n=5) in normal subjects. In 5 patients with PHP plasma cAMP did not increase above 44.4 nmol/L after infusion of 20 or 30 µg of hPTH (1-34), and these low responses were not improved during treatment with Vitamin $D_2$ or Vitamin D metabolites (107). Figure 1-13 shows plasma cAMP profiles after infusion of hPTH (1-34) in normal, idiopathic hypoparathyroidism and pseudohypoparathyroidism subjects before and during treatment with vitamin D (107).

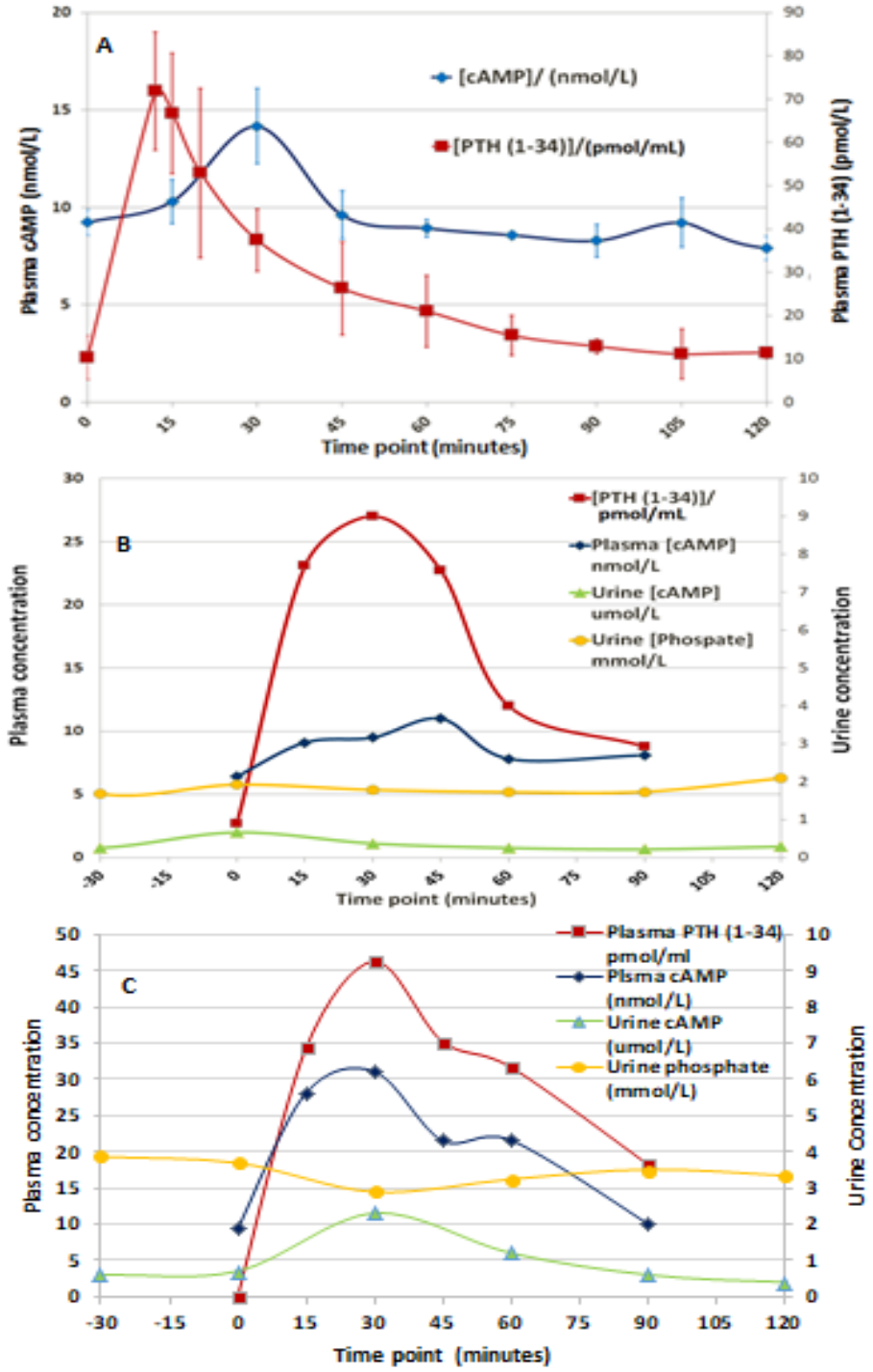


**Figure 1-12 Ellsworth-Howard test.** *Top panel (A): Changes in plasma cAMP (mean± SEM) and PTH (1-34) (mean ± SEM) of healthy subjects after subcutaneous injection of teriparatide. No Urine cAMP and phosphate were provided. Middle panel (B): EHT results on a PHP type-1 patient after subcutaneous injection of teriparatide. Note the blunt plasma cAMP and deficient urinary cAMP and phosphate response to elevated plasma PTH (1-34) levels. Bottom panel (C): EHT results on a PHP type-2 patient after subcutaneous injection of teriparatide. Note the deficient urine phosphate despite normal plasma and urinary cAMP response. Figures taken from reference (109)*

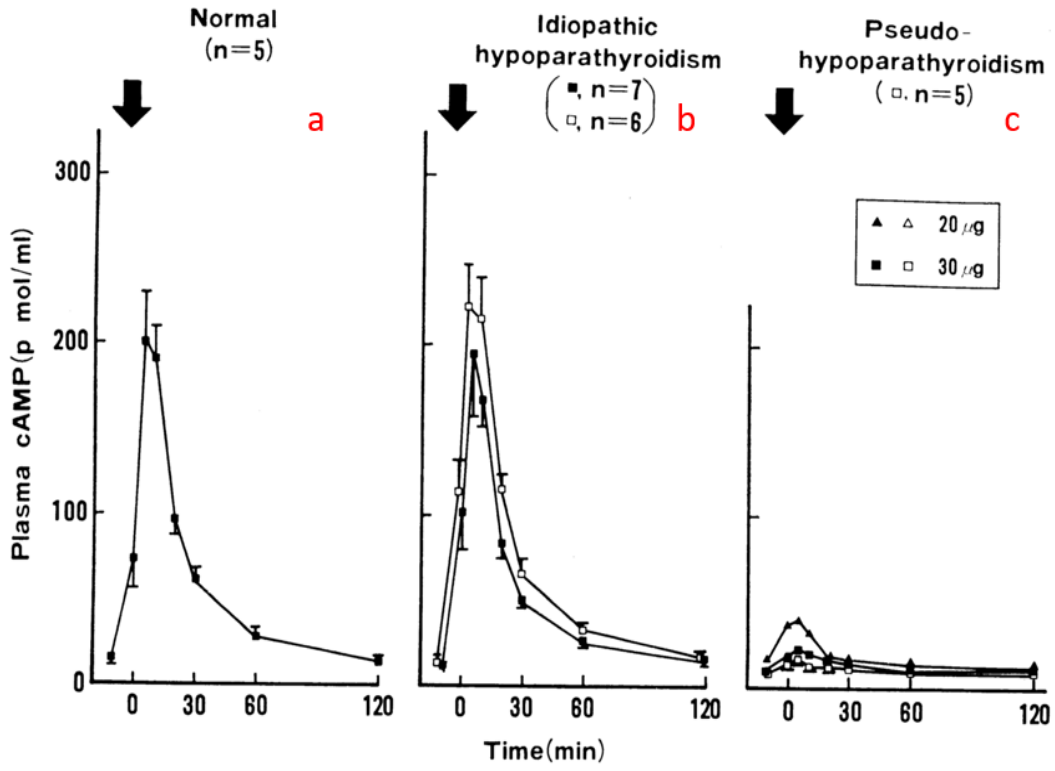


**Figure 1-13 Change in plasma cAMP (mean ± SEM) concentration in an EHT performed with hPTH (1-34).** *The arrows indicate intravenous hormone administration over 5 min. closed symbols (■,▲) represent the results obtained before treatment and open symbols (□, Δ) during maintenance treatment with Vitamin D. (a) Normal control subject (n=5) treated with 30 µg hPTH (1-34), (b) idiopathic hypoparathyroidism patients treated with 30 µg hPTH (1-34) only (n=7) and during treatment with vitamin D (n=6) and (c) pseudohypoparathyroidism patients treated with 30 µg (n=3) or 20 µg hPTH (1-34) only (n=2) and during treatment with vitamin D all the 5 pseudohypoparathyroidism patients were given 30 µg hPTH (1-34) (Figure taken from reference (107).*

### 1.1.13 Measurement of PTH (1-34)

#### *1.1.13.1 Why do we need to replace immunoassay by LC-MS/MS?*

Immunological assays such as enzyme-linked immunosorbent assay (ELISA) and immunoradiometric assay (IRMA) are today the most common quantitative assays for proteins, and protein-/peptide-based therapeutic drugs. They are very sensitive, and protein concentrations in the pg/mL range can be detected with good specificity and linearity, if antibodies with the desired performance are available. These assays are, mostly, non-competitive or sandwich assays in which two antibodies bind different epitopes of the analyte. However, despite a long history of application of

immunoassays in diagnostic and research laboratories, its variability has always been a substantial and critical issue and has been questioned by many researchers (110-114). Massart *et al.* (113) reported high inter-method variability in three porcine thyroid receptor antibody (TRAb) assays results in untreated Grave disease patients despite the use of the same reference standards for calibration and emphasised the necessity for assay standardisation for correct interpretation in the follow-up of Graves opthalmopathy. Similarly, the variation in PTH immunoassay results is very well studied and documented and the lack of comparability of PTH results has been convincingly demonstrated by method comparison studies in which PTH concentrations have been determined for similar specimens (individuals and/or pooled patient samples) using different commercially available immunoassays (112, 115-120). In one study, PTH concentrations were measured with 15 commercial immunoassays in 47 serum pools from dialysis patients, using the Nichols Allegro® intact PTH IRMA (Nichols Institute, San Clemente, CA, USA) as the reference. The median bias between the tested assays and Allegro intact PTH assay ranged from -44.9 to 123.0% (4-fold variation). When the PTH concentrations were 150 or 300 ng/L with the Allegro intact PTH assay, they ranged with other assays from 83 to 323 ng/L and from 160 to 638 ng/L, respectively. Also, a 2.5-fold variation in intact PTH results were reported by Cantor *et al.* (115) where PTH results from stage 5 chronic kidney disease (CKD) patients (n=46) obtained using seven commercial immunoassays were compared against Nichols Allegro® intact PTH IRMA. PTH results for lyophilized pools of plasma from patients with CKD distributed by the UK National External Quality Assessment Service (UK NEQAS) typically vary by at least 2-fold for six commonly used methods (119). Similar variability in results has been reported in an independent study of 99 single dialysis patient plasma specimens assayed using the same six methods (120).

The reproducibility of results is a crucial element in making the appropriate clinical decisions and therefore inter-method variability seen with many immunoassays has been a primary challenge in patient management and calls for assay standardisation. However, there are many reasons that make the standardisation of immunoassays difficult. The main one is that each immunoassay uses in-house or commercial biological reagents that possess inherent different biological specificity. This causes differential biological responses, since they are

susceptible to cross-reaction and disruption with metabolised fragments, endogenous analogous peptides/proteins, and circulating components of the biological matrix (121). For instance, changing a key reagent component such as the antibody lot used, or implementing an inter-laboratory comparison program changes reproducibility of results.

Liquid chromatography coupled to mass spectrometry (LC-MS) is of proven sensitivity and specificity, especially for low-molecular-weight drugs where it is considered as the reference technique by regulatory agencies (121). For peptide detection, LC-MS usually employs triple quadrupoles operated in the multiple reaction monitoring (MRM) mode, which is appropriate for quantification in complex matrices because of its high specificity and sensitivity. In the MRM mode, only parent/product ion pairs of interest are detected while all others are excluded, which allows the specific quantification of the target peptide. Any modification of the peptide/protein primary structure during *in vivo* metabolism would be unlikely to be detected by LC-MS, which clearly illustrates the potential use of LC-MS as an alternative bioanalytical method to immunoassays for quantification of peptides/proteins. The target peptide mass is selected, based on its mass-to-charge ratio, in the first quadrupole for subsequent fragmentation in the collision cell. Then, the products of interest are selected in the third quadrupole and finally detected.

In the same context, non-specific interaction between assay antibodies and other compounds, typically other endogenous antibodies (heterophilic antibodies) could be a source of errors in immunoassays (122). In addition saturation (Hook-effect) and limited dynamic range are also limiting factors for immunoassays (123). LC-MS/MS with its multiplex (detection of many metabolites in a single run) capability is a good option to replace/supplement immunoassay. However, the use of LC-MS/MS in clinical setting is relatively new application. One of the significant barriers hampering the transition of LC-MS/MS from the research labs into a clinical setting is the uncertainty of how successfully develop and validate a method that meets guidelines for clinical applications and lack of LC-MS/MS expertise make this transition more slow. Furthermore, the cost of LC-MS/MS machine is big (approximately £150,000) and the maintenance of the machine could be very costly.

#### *1.1.13.2 Current status of PTH (1-34) measurement*

Several commercial immunoassays are available for measurement of PTH (1-34) and have been used for pharmacokinetic studies with a low detection limit of 10 pg/mL or less (53, 124). However, one major challenge affecting the measurement of PTH (1-34) is reactivity of the immunoassays to other molecular forms of PTH including the intact molecule and various truncated forms (e.g. PTH (7-84). Satterwhite *et al*. (53) reported significant cross-reactivity of their PTH (1-34) immunoassay with PTH (1-84) as well as with some smaller N-terminus and C-terminus PTH fragments. Because PTH (1-34) contains two Methionine residues in its structure at position 8 and 18, it is susceptible to oxidation by peroxides, which is the major degradation pathway of therapeutic proteins (125-129). Three oxidized PTH (1-34) products have been isolated, namely Met 8 sulfoxide alone, Met 18 Sulfoxide alone, and both positions having Met Sulfoxide (127, 130-132). All oxidized forms of PTH (1-34) possess reduced biological activity, which consequently is reflected in the potency of PTH treatment (130, 131, 133-135). This effect of oxidation necessitates development of an assay that is able to discriminate between oxidized and non-oxidized forms of PTH.

LC-MS/MS is regarded as a method for assaying peptides by maintaining specificity without compromising sensitivity. Recently, a number of LC-MS/MS assays for measurement of PTH (1-34) have been developed by different research groups (136-138). MacNeill *et al.* (137) developed a LC-MS/MS method for PTH (1-34) with LLoQ of 1.0 ng/mL, which is not sensitive enough to detect sub ng/mL changes in concentrations. Chambers *et al.* (136) also described a LC-MS/MS method with a dynamic range of 15 – 500 pg/mL with good precision and accuracy, but poor robustness, especially at low concentrations, represented by a concave quadratic fit calibration curve rather than linear regression, which may be an indication of severe loss in analytical sensitivity, especially at lower concentrations. Kay *et al.* (138) reported a LC-MS/MS method for PTH (1-34) analysis in porcine plasma. The method had a dynamic range of 10 - 1000 pg/mL with LLOQ of 15 pg/mL and good precision and accuracy (138). However, the specificity of Kay's method is questioned as a relatively large peak persistently observed for PTH (1-34) in blank extracted samples and zero samples. The peak area obtained for PTH (1-34) in the zero sample was 86. The presence of interfering compound co-eluted with

PTH (1-34) can also be extrapolated from PTH (1-34) appearance, where split peak observed in blank and zero samples chromatogram and broad peak with shoulder and front tail observed in LLOQ sample (138). Shoulder peaks and split peaks often result due to presence of two closely unresolved compounds, which is likely to be the case given that protein crash was the only clean-up method used prior injecting sample into LC-MS/MS. None of the above mentioned studies had conducted a method comparison study or addressed measurement of oxidized forms of PTH (1-34).

## 1.2 Parathyroid Hormone-Related Protein

PTHrP was first identified in 1987 when several research groups successfully purified it from a human lung cancer cell line (139), a breast cancer cell line (140), and renal cancer cell line (141) . As the name implies, PTHrP and PTH are ancestrally related. The cloning of PTHrP cDNA showed that eight of the first 13 residues of PTHrP were identical to those of PTH (142, 143) and the structural requirements for full biological activity of PTHrP were contained within the first 34 amino acids, just like PTH (139, 142, 144, 145). It was not surprising that PTHrP acts through the binding and activation of PTHR1 on PTH classical target organs. Although PTHrP was originally identified as a tumour derived factor, in the past two decades information on its structure, regulation and function have dramatically expanded the knowledge of its role in normal physiology and in pathologic conditions such as cancer and skeletal metastasis. Thus, PTHrP is increasingly represented as a poly-hormone with an impressive breadth of biologic actions.

### 1.2.1 PTHrP gene (*pthlp)* structure

The human *pthlp* (mapped to the short arm of chromosome 12) and the *pth* (short arm of chromosome 11) belong to the same gene family, which includes the gene encoding for tuberoinfundibular peptide of 39 residues (TIP39) (146). Compared to *pth*, *pthlp* is more complex containing nine exons spanning 15 kilobases of DNA and three promoters (P1, P2, and P3) located on the 5'-end of the gene (147-150). P1 and P3 are TATA-containing promoters located upstream of exons 1 and 4, respectively, while P2 is a GC-rich regulatory region located upstream of exon 3 (149). Exons 1-4 encode the 5'- UTR in the mature mRNA, exon 5 encodes the translational start site and the “prepro” region, and exon 6 encodes the majority of

the coding region (149). The 3'-end of the gene contains three exons, 7, 8, and 9, which may be alternatively spliced to yield three distinct PTHrP protein isoforms of 139, 141, or 173 amino acids (151, 152), which are identical through amino acid 139 but each has a unique C-terminus (149, 153). Figure 1-14 illustrates *pthlp* structure and shows the complexity of *pthlp* in comparison with *pth.* The presence of several promoters in the human PTHrP gene suggests the potential use of different promotor regions, which may result in tissue-specific expression of PTHrP (148). It has also been suggested that normal and tumour tissues, which express PTHrP may contain all three transcripts, but some tissues appear to express one of them preferentially (151, 154, 155).

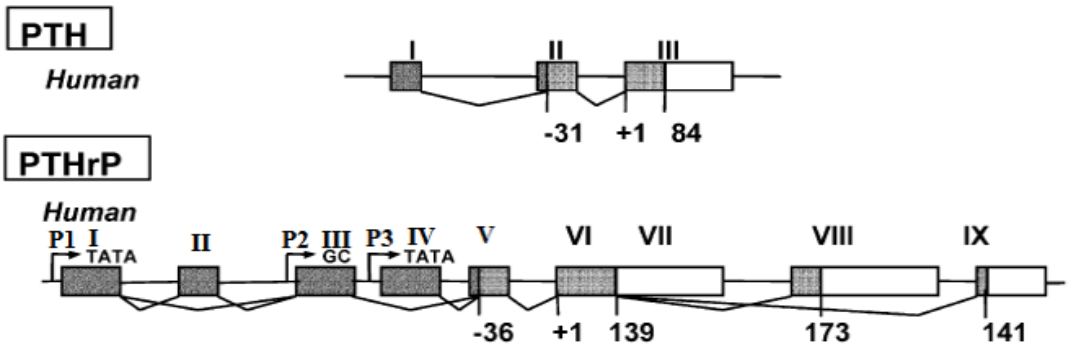


**Figure 1-14 Structure of human PTHrP gene.** *The Panel shows the human PTHrP gene structure complexity compared to PTH gene. 5' untranslated exons are represented as dark solid shaded boxes, Coding exons as light solid shaded boxes, and 3' untranslated exons as white boxes. Introns represented by a line. The PTHrP gene promoters (P1, P2, and P3) are represented by arrows above the sequences. Potential alternative splicing combinations are represented as bent lines connecting the exons. Following 5' and 3' alternative splicing and the use of the different promoters, three PTHrP mRNA isoform are generated. These isoforms are translated into three PTHrP proteins containing 139, 141, and 173 amino acids in humans depending on the cell or tissue type. (Figure taken from reference (156))*

### 1.2.2 PTHrP protein structure, biosynthesis and processing

The Nature of PTHrP secretion and its circulating forms are not yet fully known. The PTHrP gene gives rise to three PTHrP mRNA species through alternative splicing, which encode three mature PTHrP products with lengths of 139, 141, and 173 amino acids. Some cells, like keratinocytes are found to produce all the three mature PTHrP species (157). The primary translation product of PTHrP can undergo a variety of

post-translational processing events resulting in overlapping series of biological peptides (Figure 1-15) (158). *In vitro* studies in human renal carcinoma cell line and rat insulinoma cell lines transfected with a cDNA encoding PTHrP (1-141) demonstrated the presence of several immunoreactive fragments including PTHrP (1-36), PTHrP (38-94), PTHrP (1-74), and a mid-region fragment of 7 kD, likely PTHrP (38-101)(153). Rabbani *et al.* (159) examined the biosynthesis and processing of endogenous [$^{3}$H]Ile-labelled PTHrP in cultured rat H-500 Leydig tumour cells. The analysis of cell extracts and culture media by affinity chromatography employing an antibody directed against the bioactive N-terminal region, PTHrP (1-34), followed by gel-permeation or reversed-phase HPLC revealed the presence of three bioactive fragments including PTHrP (1-36), PTHrP (1-86) and PTHrP (1-141). Growing evidence suggest that PTHrP processing is cell-specific. Though, details of PTHrP processing and the biological significance of the different PTHrP peptides are not entirely clear and more investigation is required.

Based on the primary amino acid sequence, PTHrP can be divided into distinct regions. The first 36 amino acids (-36 to -1) code for the intracellular "prepro" and "pro" precursors of the mature peptide, which acts as signaling sequence and facilitates the transport and secretion of the precursor polypeptide. The next functional region is the PTH-like N-terminal fragment or PTHrP (1-36), which is the region showing the highest degree of primary sequence homology with PTH. Eight of the first 13 residues are identical to that of PTH. This amino acid sequence of PTHrP is necessary for interaction with PTHR1. The 14-36 amino acid sequence of PTHrP has almost no homology with that of PTH, yet it is critical for the binding of PTHrP to PTHR1 and for subsequent activation (160). Based on competitive binding assays, investigators have shown that PTH (1-34) and PTHrP (1-36) bind PTHR1 with approximately equal affinity, while shorter N-terminal fragments of either PTH or PTHrP do not (161). The renal tubule and skeletal osteoblast are regarded as the "classical" target tissues for the action of PTH, and studies indicate that synthetic N-terminal PTHrP interact with the PTHR1 in these "classical" tissues. PTH also induces functional responses in a variety of "non-classical" target tissues, such vascular smooth muscle. Administration of PTHrP (1-36) into rats leads to an immediate, short-term decrease in blood pressure (162). PTHrP relaxes smooth muscle vasculature, in addition to increasing contractility,

heart rate, and coronary blood flow. The effects of PTHrP on vascular smooth muscle could be mimicked with PTH (1-34), indicating that the PTHR1 likely mediates signaling in this tissue (162).

The secretion of mid-region including amino acids 38-94, 38-95, and 38-101 has also been described (153, 158). The biology of these specific secretory forms is not yet clear, but the mid-region of PTHrP stimulates placental calcium transport and modulates renal bicarbonate handling. This portion of the molecule contains nuclear localization signals (NLS), which typically consist of one or more short sequences of positively charge lysine or arginine molecules exposed in the protein surface that facilitate the import of protein into the cell nucleus by nuclear transport (163, 164). PTHrP (107-139) and (109-139) fragments is known as osteostatin and was shown to have anti-osteoclastic activity *in vitro* and to stimulate osteoblast proliferation and function (158, 163), perhaps by down-regulation of sclerostin (165). The final C-terminal region of PTHrP, from amino acid 141 to 173, is encoded by only one of the three isoforms of human PTHrP mRNA (156).

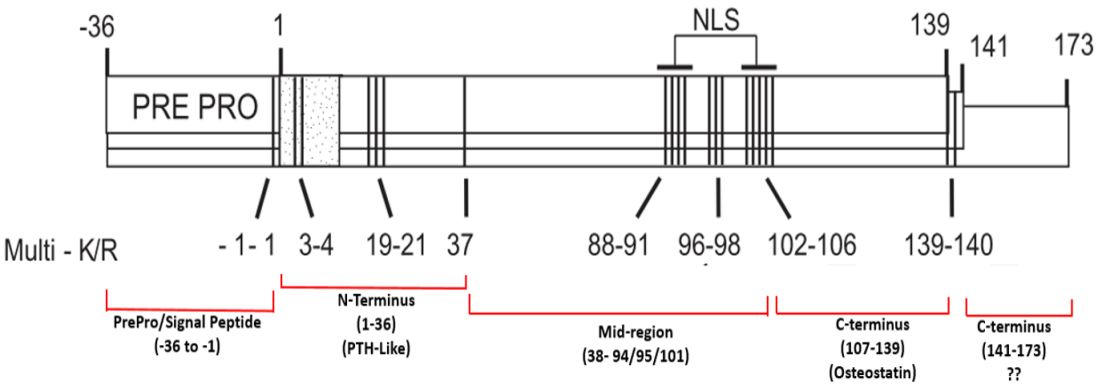


**Figure 1-15 Post-translational isoforms of PTHrP and their biologic properties.** *The three human PTHrP isoforms produced by translation are outlined, one atop other, of 139, 141, and 173 amino acid in length. The numbers under the isoforms outlines indicate multibasic amino acids (Arginine/Lysine) that serve as prohormone convertase sites or NLS. The NLS overlap with the mid-region of PTHrP. Posttranslational processing at the multibasic endoproteolytic sites may leads to multiple secretory forms of the peptide, including full-length, PTH-like N-terminal form, mid-region form, and C-terminal peptides. The prepro region acts as a signaling peptide to facilitate secretion of the molecule outside the cell. (Figure taken with adjustment from reference (156))*

### 1.2.3 Circulating forms of PTHrP

The nature of the circulating PTHrP is not yet fully understood. Studies in patients with malignancy-associated hypercalcemia (MAH) and PHPT indicated the presence

of heterogeneous PTHrP fragments in the circulation. Using a two-site IRMA directed toward PTHrP amino acid sequence 1 to 74 and a radiometric immunoassay (RIA) directed toward PTHrP amino acid sequence 109 to 138, Burtis *et al.* (166) characterized PTHrP in a variety of cancer conditions with and without hypercalcemia. The sensitivity of the IRMA and the RIA was 1.0 pmol/L and 2.0 pmol/L respectively. Burtis *et al.* (166) indicated that sixty normal volunteers had low or undetectable plasma PTHrP (1-74) with a mean of (1.9 pmol/L) and undetectable plasma PTHrP (109-138) concentrations (<2.0 pmol/L). Patients with renal failure (n=15), whom were all on hemodialysis, had plasma PTHrP (1-74) concentrations similar to those in normal individuals, but their plasma PTHrP (109-138) concentrations were elevated with a mean of (29.6 pmo/L). Patients with HHM (n=30) had elevated plasma concentrations of both PTHrP (1-74) (mean, 20.9 pmol/L) and PTHrP (109-138) (mean, 23.9 pmol/L). The concentration of both peptides were normal in patients with hyperparathyroidism (n=13) and those with hypercalcemia with miscellaneous causes other than malignancies (n=4). Another two-site IRMA, recognizing an N-terminal fragment of at least 86 amino acids, was developed by Ratcliffe *et al.* (167). The assay sensitivity was 0.23 pmol/L. Concentrations of PTHrP (1-86) were undetectable (<0.23 pmol/L) in all normal individuals (n=30) and in patients with PHPT (n=19), and were significantly increased in HHM patients with mean of 6.1 pmol/L. Ratcliffe *et al.* (167) have also developed two direct RIAs for PTHrP (1-34) and PTHrP (37-67). The two assays, in general, detected higher concentrations of PTHrP than the IRMA, especially when plasma was assayed directly without affinity purification. The RIA of PTHrP (1-34) used polyclonal antibody specific for region 9-18. PTHrP (1-34) concentrations assayed with the direct N-terminal PTHrP RIA ranged from 13 to 760 pmol/L with a mean of 140 pmol/L in normal individuals, from 32 to 1530 pmol/L with a mean of 360 pmol/L in PHPT patients and from 21 to 1110 pmol/L with a mean of 190 pmol/L in HHM patients. The difference in mean plasma PTHrP (1-34) concentrations in the three study groups were found insignificant using the direct RIA. In contrast, plasma PTHrP (1-34) concentrations obtained with RIA of affinity-extracted plasma with monoclonal antibodies ranged from 0.35 to 5.7 pmol/L with a mean of 2.9 pmol/L in normal individuals, from 0.65 to 4.0 pmol/L with a mean of 1.7 pmol/L in patients with PHPT and from 2.7 to 41.3 pmol/L with a mean of 10.7 pmol/L in HHM patients. Mean plasma PTHrP (1-34) concentrations in HHM

patients were significantly higher than in normal subjects or in patients with PHPT (167). Fraser *et al.* (168) published an evaluation of another commercial two-site IRMA for PTHrP from Nichols Institute. The assay was very sensitive with a detection limit of 0.7 pmol/L. The assay utilizes two affinity-purified populations of antibodies raised in two different species. One population of antibodies is directed toward the 60-72 amino acid sequence (goat) and the other is specific for the 1-40 amino acid sequence (sheep), so only peptides that can bridge the two antibodies can be quantified, e.g., PTHrP (1-86) and PTHrP (1-74). 60 normal volunteers, 20 patients with PHPT and 95 MAH patients were studied. PTHrP exceeded the detection limit of 0.7 pmol/L in 78% of the normal subjects and a reference range of <0.7 – 2.6 pmol/L was then established. PTHrP was increased in a high percentage of patients with solid tumours associated with hypercalcemia. Interestingly, inappropriate or increased Nephrotic cAMP (NcAMP) was detected in a subgroup of patients with low PTHrP and low or undetectable PTH (1-84). Authors suggested that either a fragment of PTHrP or PTH that was not detected by the immunoassays was present or that another uncharacterized molecule was being produced that has a hypercalcemic action and can stimulate NcAMP production (168).

A number of LC-MS/MS methods for PTHrP have been also reported. Lu *et al.* (169) developed a LC-MS/MS assay with a LLoQ of 62 nmol/L, which is insufficient for diagnostic applications. Washam *et al.* (170) developed a qualitative surface-enhanced laser desorption/ionization Time-of-flight mass spectrometry (SELDI-TOF MS) method for detection of PTHrP (12-48) fragment in plasma of patients with breast cancer. The sensitivity of the assay was not specified nor were the levels in normal volunteers. Kushnir *et al.* (171) recently reported 2-dimentional LC-MS/MS method to quantify PTHrP-specific tryptic digested peptide. Prior to digestion with trypsin, PTHrP was enriched from plasma sample with rabbit polyclonal antibody conjugated to magnetic beads. The assay was very sensitive with a detection limit of 0.6 pmol/L and a dynamic range from 0.6 – 600 pmol/L. The LC-MS/MS showed poor agreement with a commercial PTHrP RIA kit (Immunotech). Reference ranges established for PTHrP with this method were 0.6 – 3.3 pmol/L and 0.6 – 2.2 pmol/L in adult women and men, respectively. However, the LC-MS/MS method analysed PTHrP by quantifying PTHrP-specific peptide released during tryptic digestion. The peptide (102 YLTQETNK 110) is in the C-terminus of the

PTHrP sequence and its concentration does not represent the concentration of bioactive PTHrP.

Because of the lack of information on the molecular forms of PTHrP in plasma, synthetic fragments of PTHrP have been used to produce region-specific antibodies for the immunoassays reported to date. However, there is increasing evidence that the metabolism of PTHrP is complex and the exact circulating peptide forms of PTHrP remain to be established.

### 1.2.4 PTHrP signalling pathways

Like other peptide hormones, PTHrP is secreted from source cells. PTHrP has paracrine/autocrine and endocrine actions by acting, respectively, on adjacent or distant target cells that express the PTHR1 on their surface. Binding of PTHrP to PTHR1 prompts the ligand bound receptor to be internalized and elicits signaling pathways. PTHrP can also act in autocrine fashion through NLS in the med-region, through which PTHrP avoids the secretion pathway, remains within the cytoplasm of the source cell, and is then transported into the nucleus or nucleolus. Nucleolar localization of PTHrP in chondrocytes and other cell types may enhances their survival and influences their growth/differentiation (172).

#### *1.2.4.1* cAMP-dependent signaling pathway

Most evidence suggest that PTHrP binds and activates PTHR1, which is associated with a G-protein. This binding stimulates conformational changes in the G-protein and transforms it to the stimulatory form (Gs). The activated α-subunit of Gs (Gsα) binds AC, which converts ATP into cAMP and subsequently activates protein kinase A (PKA). This allows the catalytic subunit of PKA to dissociate and phosphorylates targets in both the cytoplasm and nuclear transcription factors (173, 174). One target of phosphorylation by PKA in the nucleus is the cAMP response element binding protein (CREB) family. CREB proteins bind cAMP response elements in the regulatory regions of target genes, and serve as major cellular activators of transcription. Phosphorylation by PKA also activates RUNX2 and the activator protein-1 (AP-1) family of transcription factors, both of which increase target gene transcription (174). PKA signaling also activates downstream signaling pathways, such as the MAPK pathway, that ultimately serve to increase cellular proliferation and decrease differentiation in target tissues (175). Activation of the cAMP/PKA

pathway typically elicits a robust cellular response and is considered the prototypical second messenger pathway downstream of PTHR1 activation (176).

#### *1.2.4.2 Intracellular Calcium-dependent signaling pathway*

Alternatively, binding of PTHrP to PTHR1-coupled G-protein can also initiate another common signaling pathway that utilizes intracellular calcium as a second messenger. The G-protein in this signaling pathway is called Gq. The activated α-subunit of Gq (Gqα) activates PLC. This enzyme acts on the molecule phosphatidylinositol 4,5-bisphosphate (PIP2) to generate inositol triphosphate (IP3) and diacylglycerol (DAG). The accumulation of DAG on the plasma membrane leads to the recruitment of protein kinase C (PKC), which upon binding $Ca^{++}$ in the cytoplasm becomes activated and elicits a host of cellular responses (176). While the data is inconsistent, activation of the PLC/PKC pathway by PTHR1 signaling seems to be partially dependent upon cell-type, cell-cycle, and receptor density (173). Some evidence also suggests that activation of PLC/PKC signaling by the PTHR1 functions as an "alternative" pathway to oppose the cellular response induced by PKA signaling, namely, decrease proliferation and promote differentiation (175).

In addition to Gsα and Gqα, activated PTHR1 can also couple to pertussis toxin sensitive Gi-proteins that inhibit adenylyl cyclase activity (67). Treatment of COS-7 cells with pertussis toxin increased PTHR1-mediated cAMP accumulation in cells with wild type receptor, but failed to do so in cells with a truncated C-terminal receptor (177). Coupling of the PTHR1 to multiple G-proteins has also been studied in rat osteoblast-like cells (ROS 17/2.8) and in PTHR1-transfected human embryonic kidney (HEK) cells (178). Gi-mediated signaling was reported after using a nonhydrolyzable photo-reactive GTP analogue [alpha-P32] GTP-gamma-azidoanilide (GTP-AA) and peptide antisera raised against multiple G-proteins. The intracellular tail of the receptor seems to be responsible for signaling through the Gi-mediated pathway (177).

#### *1.2.4.3 Intracrine signaling pathway*

PTHrP can also signal as an intracrine factor. PTHrP can enter the nucleus under the direction of its NLS, which is composed of multibasic amino acids in the 88-106 region of the peptide (179). PTHrP can only gain access to the nucleus with the help of importin-β, a nuclear targeting protein (180). The mechanism by which PTHrP gets into the cytoplasm for subsequent targeting to the nucleus and the precise role of

nuclear PTHrP is still unclear, although it appears to be a potent mitogenic signal in certain cell types (181). In rat vascular smooth muscle cells, transfection of the PTHrP gene resulted in increased cellular proliferation (181). PTHrP transfection of MCF-7 breast cancer cells also lead to an increase in cell proliferation, a response opposite to the one elicited upon treatment of these same cells with N-terminal PTHrP fragments. Additionally, intracrine PTHrP appears to promote survival in both chondrocytes and MCF-7 breast cancer cells grown in serum-free conditions (172, 182). Furthermore, intracrine PTHrP is associated with increased proliferation in vascular smooth muscle cells, whereas autocrine/paracrine PTHrP signaling through the PTHR1 inhibits proliferation (183). More recently, mid-region PTHrP (38-94/95/101) was shown to promote increased tumour cell growth in MCF-7 and MDAMB- 231 breast cancer cells, and the presence of an intact NLS was necessary for this function (184). Fluorescent-labelling of mid-region PTHrP peptides confirmed the presence of PTHrP(67-101) in the nucleus, while fragments lacking an intact NLS were excluded (184). It has also been reported that mid-region PTHrP (38-94) can enter the nucleus and bind chromatin of MDA-MB-231 breast cancer cells, suggesting a potential role of intracrine PTHrP as a nuclear transcription factor (185).

### 1.2.5 PTHrP in Health

Although PTHrP was originally described as a humoral factor contributing to malignancy-associated hypercalcemia, studies on animal models increasingly indicate that PTHrP plays important physiological roles in the growth and development of many tissues and revealed an amazing breadth of actions in health and disease.

#### *1.2.5.1 Action of PTHrP in bone development*

Bone formation during embryonic development is established either by intramembranous or endochondral ossification. Intramembranous ossification is responsible primarily for the formation of the flat bones of the skull and part of jawbone and collarbone, and occurs by differentiation of mesenchymal precursors directly into osteoblasts. All the long bones of the axial skeleton (vertebrae and ribs) and of the appendicular skeleton (limbs) originate from cartilage templates by endochondral ossification, where mineralized bone is formed through the deposition of bone matrix by differentiated osteoblasts on top of scaffolding cartilage mold first synthesised by chondrocytes (186-188). The process of bone development and

growth is tightly regulated by a huge number of local signaling molecules, the best characterized being PTHrP and Indian hedgehog (Ihh), BMPs, and FGFs (186, 187). In the growth plates of bone forming through endochondral ossification, the PTHrP/Ihh pathway provides a negative feedback regulation of chondrocyte maturation. Chondrocytes located close to the articular end of the bone secrete PTHrP. PTHrP acts upon its receptor PTHR1, which is expressed at low levels by columnar proliferating chondrocytes and at high levels by pre-hypertrophic chondrocytes. As a result of this PTHrP signaling, the chondrocytes are kept in the proliferative state and their further differentiation to hypertrophic cells is delayed. This ensures that the chondrocytes divided sufficiently prior to their exit of the cell cycle and continuation towards terminal differentiation and turnover. However, when the cells escape the PTHrP-mediated differentiation block and become (pre-) hypertrophic chondrocytes. Pre-hypertrophic and early hypertrophic chondrocytes of the growth cartilage produce Ihh, a member of the conserved family of hedgehog proteins that also contains Sonic hedgehog (Shh) and Desert hedgehog (Dhh). Ihh signals back to chondrocytes located near the articular ends of the bone and acts directly on these cells to stimulate the expression of PTHrP. The mechanisms that mediate the relay of the Ihh signal are not fully clarified, but involve signaling through a receptor complex consisting of Patched (Pct) and Smoothened (Smo). Ptc is also a downstream target of Ihh signaling and is expressed in domains adjacent to the domain of Ihh expression, including in cells of the perichondrium, proliferative chondrocytes, and osteoblasts. Since increased Ihh production results in increased PTHrP signaling, further differentiation of chondrocytes to become Ihh-producing cells will consequently be slowed down; this well, in turn, lower the production of PTHrP. Thus, PTHrP and Ihh regulate each other via a negative feedback signaling pathway that controls the kinetics of cellular differentiation in the growth plate (figure 1-16) (189-192).

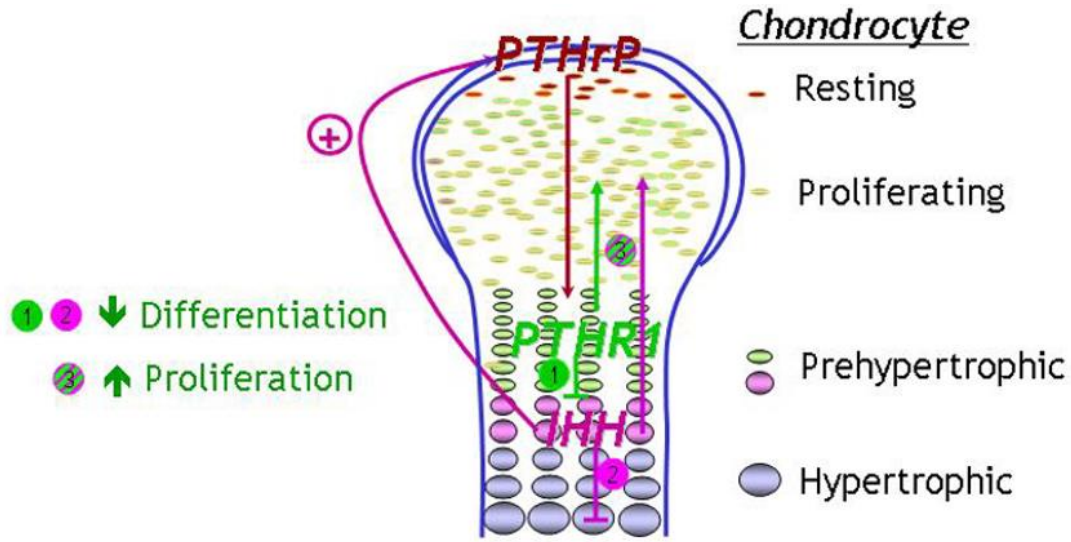


**Figure 1-16 Importance of IHH and PTHrP signaling in the modulation of chondrocyte proliferation and differentiation during endochondral bone formation**. *PTHrP is synthesized by chondrocytes and perichondrial cells in the periarticular growth plate. PTHrP diffuses toward the pre-hypertrohic zone where it binds to and activates its receptor, the PTHR1, and thereby maintains chondrocyte proliferation and delays chondrocyte differentiation into pre-hypertrophic and hypertrophic chondrocytes. After chondrocytes stop proliferating at the transition from a proliferating into a hypertrophic phenotype, they synthesize IHH. IHH acts to indirectly increase the synthesis of PTHrP. IHH and PTHrP thus participate in a negative feed-back loop that serves to regulate the rate and synchrony of growth plate chondrocytes. Besides increasing PTHrP synthesis, IHH also stimulates, both directly and indirectly, chondrocyte proliferation and inhibits their terminal differentiation. (Figure taken from Ref (192).*

Disruption of *pthlp* lead to widespread morphologic bone defects. PTHrP-null mice died immediately after birth due to respiratory failure, secondary to defective rib cage formation (193). They exhibited severely reduced growth and impaired development of all bones formed by endochondral bone formation. Specifically, a reduced zone of proliferating cells and accelerated onset of hypertrophic chondrocyte maturation characterized the growth plate of $PTHrP^{-/-}$ mice (193). Targeted disruption of the gene encoding PTHR1 in mice resulted in an even more severe phenotype than loss of PTHrP, yet showing striking similarities in the fetal growth plate. PTHR1-null mice died earlier, during gestation, showing a dwarfed phenotype with complete absence of a proliferating chondrocyte zone in the growth plate and an accelerated onset of hypertrophic maturation of chondrocytes, eventually leading to excessive bone formation (194). In human, mutations in

PTHR1 have been found to cause severe human dwarfing conditions, such as Jansen-type metaphyseal chondrodysplasia (195) and Blomstrand chondrodysplasia (196). Mutations in PTHR1 can also cause Ollier disease or enchondromatosis, which is characterized by a proliferated and randomly distributed enchondromas. Affected bones in Ollier disease are often shortened and deformed. These bone shortening are often associated with bone bending and curving (192).

#### *1.2.5.2 Action of PTHrP on mammary gland*

PTHrP plays a critical role in the epithelial-mesenchymal communications that guide the initial round of branching morphogenesis that occurs during the embryonic development of the mammary gland. True PTHrP-knockout mice die shortly after birth, but mice expressing the type II collagen promoter-PTHrP transgene ("rescued knockout" mice) are viable and only express PTHrP in cartilage. These PTHrP-rescued knockout mice fail to develop embryonic mammary epithelial ducts, resulting from impaired epithelial mesenchymal interactions in the embryonic development of the mammary gland (197). PTHrP appears to be an epithelial signal that is necessary to direct the mammary mesenchyme during branching morphogenesis, and without PTHrP, the mammary epithelial cells revert to an epidermal fate, no mammary ducts are formed and the nipple does not form (198). Consistent with this observation is the finding that PTHR1-knockout mice exhibit similar defects in mammary gland development as PTHrP-knockout mice, which indicated that mammary development require that PTHrP be expressed and PTHR1 present (198). PTHrP also plays a role in sexual dimorphism during the embryonic development of the mammary gland. In males, under the influence of newly-produced androgens from the embryonic testes, the mammary bud is destroyed. In the absence of PTHrP, androgens fail to activate the androgen receptor (AR) in the mammary mesenchyme, and apoptosis of the mammary bud is impaired (199). PTHrP appears to induce mesenchymal AR gene expression, which is essential for sexual dimorphism during embryonic mammary development (199). During lactation, PTHrP is secreted into the circulation by mammary epithelial cells and induces bone resorption and participates in systemic calcium homeostasis to withstand the large demand of calcium that is transferred to offspring via milk (200). PTHrP production and calcium transport in the lactating mammary is regulated by the calcium-sensing receptor (CaSR) (201).

#### *1.2.5.3 Action of PTHrP on Placenta and Amnion*

Both PTHrP mRNA and PTHrP protein have been detected in rat and human placenta in cytotrophoblasts and syncytiotrophoblasts (202-204). The cubidal cells of the amniotic membranes also express PTHrP at higher concentrations than in either cytotrophoblasts or syncytiotrophoblasts. PTHrP concentrations were higher in the amniotic membrane covering the placenta compared to the reflected amnion. Cells within the amnion are likely the source of the PTHrP found in the amniotic fluid. Studies have demonstrated that PTHrP concentrations increase within the amnion and amniotic fluid as pregnancy advances but decline with the onset of labour and rupture of the fetal membrane (202-204). It has been reported that PTHrP production in culture human cytotrophoblast was regulated by CaSR (203). PTHR1 mRNA has been demonstrated in rat (205), mouse (206), and human placenta (207).

The best-studied aspect of PTHrP in the placenta is its involvement in calcium transport. Nearly all of the calcium, and a large proportion of the inorganic phosphate (85%) and magnesium (70%) transferred from the mother to the foetus is associated with development and mineralization of the fetal skeleton (208, 209). The majority of this calcium is transported across the placenta during a relatively short interval in late pregnancy. Both total and ionized calcium concentrations are higher in the developing foetus than in the mother to support fetal skeletal development (158). This gradient is eliminated in the absence of PTHrP, suggesting a likely role for PTHrP in regulating the transport of calcium across the placenta (164). Kovacs *et al*. (164) demonstrated that the deletion of *pthlp* in transgenic mice causes loss of the fetal-to-maternal serum calcium gradient. The bioactivity of PTHrP for placental calcium transport is mediated by NLS sequence in the mid-molecular region that does not use the PTHR1 receptor (164, 210).

#### *1.2.5.4 Action of PTHrP on teeth*

PTHrP is ordinarily expressed in the enamel epithelium which covers the top portion of developing teeth, while the PTHR1 is expressed in the dental mesenchyme and alveolar bone (211). Philbrick et al. (211) demonstrated that survived rescued PTHrP-knockout mice have smaller stature and displayed a number of developmental defects, including a failure of tooth eruption. Teeth appear to develop normally but become trapped by the surrounding bone and undergo progressive

impaction. The replacement of PTHrP expression in the enamel epithelium of PTHrP-knockout mice with a keratin 14-driven transgene corrects the defect in bone resorption and restores the normal program of tooth eruption (211). PTHrP therefore represents an essential signal in the formation of the tooth eruption pathway.

#### *1.2.5.5 Action of PTHrP on pancreas*

PTHrP is produced by the pancreatic islet. It also has receptors on islet cells, suggesting it may serve a paracrine or autocrine role within the islet (212, 213). Studies have documented that PTHrP stimulates the proliferation of mouse and human pancreatic β cells during development and in the adult pancreas (213-216). Vasavada and colleagues generated transgenic mice that overexpress PTHrP under the control of the rat insulin-II promoter (RIP) (213, 217). RIP-PTHrP mice display striking degree of islet hyperplasia and an increase in islet number, as well as the size of individual islets as compared to their control littermates. This increased islet mass is associated with hyperinsulinemia and hypoglycaemia. Interestingly, RIP-PTHrP mice are also resistant to the diabetogenic effect of the β-cell toxin, streptozotocin. Following the administration of streptozotocin, normal mice readily, develop diabetic, but RIP-PTHrP mice either fail to become diabetic or develop only mild hyperglycemia (217). The increased β-cell mass in these mice is the result of increased proliferation and decreased apoptosis (215, 216). Acute treatment with PTHrP (1-36) was noted to induce beta cell proliferation and improve glucose-stimulated insulin secretion in cultured human β cells (218) and in a mouse model of partial pancreatectomy (219).

#### *1.2.5.6 Action of PTHrP on skin and hair follicles*

Human keratinocytes in culture were the first normal cells found to secret PTHrP (220). Subsequently, multiple studies confirmed that cultured rodent and human keratinocytes express and secrete bioactive PTHrP (158). PTHrP implicated in the regulation of keratinocyte proliferation and/or differentiation. Data from in vitro studies have suggested that PTHrP promotes the differentiation of keratinocytes (158), but studies in vivo have suggested that PTHrP inhibits keratinocytes differentiation (221). A careful comparison of the histology of PTHrP-null and PTHrP-overexpressing skin demonstrated reciprocal changes. In the absence of PTHrP, it appeared that keratinocyte differentiation was accelerated, whereas in skin exposed to PTHrP overexpression, keratinocyte differentiation appeared to be

retarded (221). Therefore, in the physiologic context, PTHrP appears to slow the rate of keratinocyte differentiation and to preserve the proliferative, basal compartment. Remarkably, these changes in the rate of keratinocytes differentiation are exactly analogous to those noted for chondrocyte differentiation in the growth plates of mice overexpressing PTHrP as compared to PTHrP- and PTHR1-null mice (189, 222, 223). Two research groups generated transgenic mice that produce truncated forms of PTHrP (1-84 and 1-66) lacking the NLS and C-terminal regions (224, 225). Turibio and colleagues, who generated the PTHrP (1-66) knock-in mouse, reported that loss of nuclear trafficking of PTHrP caused skin hyperkeratosis, perhaps also reflecting abnormalities in in keratinocytes differentiations (225). The regulation of keratinocyte proliferation and differentiation by PTHrP appear to be complex and that PTHrP participates either through autocrine/paracrine or intracrine pathways in keratinocyte growth.

Several studies suggest that PTHrP involved in the regulation of hair growth. In embryonic skin, the PTHrP gene is expressed most prominently in developing hair follicles, and overexpression of PTHrP in the basal keratinocytes of skin in transgenic mice leads to a severe inhibition of ventral hair follicle morphogenesis during fetal development (226). This appears to be the result of interactions between PTHrP, BMP, and Wnt signaling pathways that normally regulate the patterning of the mammary mesenchyme and cause lateral inhibition of hair follicle development around the nipple (227, 228). However, it is unlikely that PTHrP is critical to hair follicle morphogenesis elsewhere because disruption of the PTHrP gene or PTHR1 gene does not seem to affect hair follicle formation or patterning in mice except for the vicinity of the nipple (189, 222, 228). Systemic or topical administration of PTHR1 antagonists to mice appear to perturb the hair cycle by prematurely terminating telogen, prolonging anagen growth, and inhibiting catagen (229, 230). In a reciprocal fashion, mice overexpressing PTHrP in basal keratinocytes (K14-PTHrP mice) demonstrate a delayed emergence of dorsal hair, have shorter hair and their hair follicles enter catagen approximately 2 days early (231). These findings were associated with a lower proliferation rate in the hair matrix and a less well-developed perifollicular vasculature during anagen. Together, these studies imply that PTHrP may regulate follicle growth by pushing growing hair follicles into the growth-arrested or catagen/telogen phase of the hair cycle. Surprisingly, in PTHrP knock-out

mice, the hair cycle appear normal (221). In fact, rather than a promotion of hair growth, these mice demonstrate a thinning of their coat over time. These conflicting results are difficult to concile at this point, but suggest that while PTHrP may contribute to the regulation of the hair cycle, it is unlikely to be necessary for this process to unfold normally.

#### *1.2.5.7 Action of PTHrP on vascular smooth muscle cell*

PTHrP is produced by vascular smooth muscle cell (VSMC), up-regulated in the arterial media by vascular injury, and essential for normal VSMC proliferation (232-234). PTHrP mediates VSCM proliferation via intracrine action by entering the nucleus using NLS. PTHrP containing NLS derives VSCM proliferation, whereas PTHrP engineered to lack an NLS markedly inhibits VSMC proliferation (181, 183, 235). *In vitro* VSMC as well as *in* vivo studies on rat carotid have shown that PTHrP regulates VSMC proliferation via p27. Fiaschi-Taesch et al. (235) demonstrated that adenoviraly delivered PTHrP markedly enhances development of the neointima after carotid angioplasty. Overexpression of PTHrP in VSMC leads to marked increases in retinoblastoma protein phosphorylation, cdk2 kinase activity, and cell cycle progression, all resulting from a specific and marked PTHrP-induced loss of p27, mostly through increased proteasomal degradation (235, 236). Conversely, overexpression of an NLS-deleted form of PTHrP decreases cdk2 kinase activity and inhibits cell cycle progression via increased p27. Sicari et al. (237) determine the molecular mechanisms through which PTHrP targets p27 proteosomal degradation. S-phase kinase-associated protein 2 (skp2) and c-myc, two critical regulators of p27 expression and stability, and neointima formation were up-regulated in PTHrP overexpression in VSMC. Normalisation of skp2 or c-myc using small interfering RNA (si-RNA) restores normal cell cycle and p27 expression in PTHrP overexpression in VSMC, which indicates that skp2 and c-myc mediate p27 loss and proliferation induced by PTHrP (237).

PTH and PTHrP have been regarded to have positive inotropic effects on the heart as well as positive chronotropic and vasodilator effects. Ogino et al. (238) demonstrated that the inotropic effects of PTH and PTHrP are results of their influence on coronary flow and heart rate, but not by any direct effect on contractile elements in the heart. Schluter and colleagues identified that coronary endothelial cells produce PTHrP under ischemic conditions and enhance myocardial inotropy

(contraction velocity) and lusitropy (relaxation velocity) (239, 240). PTHrP has also been proposed as a local modulator of myogenic tone, where VSMC mechanical stretch acts together with angiotensin II to regulate the expression of vasodilator PTHrP (241, 242). Clemens and colleagues first established that augmenting local PTHrP/PTHR1 signaling could impact blood pressure and vascular contractility; implementing novel vascular smooth muscle cell-specific transgenic mice expressing either PTHrP or PTHR1, these investigators elicited sustained reduction in blood pressure and increases in volume-dependent renal tissue perfusion (243). Moreover, pressor response to angiotensin II were significantly reduced by VSMC PTHR1 activation. Given that wild-type PTHR1 activation is ligand dependent, these data strongly suggested that endogenous paracrine PTHrP production modulated by mechanical, inflammatory, and endocrine stimuli helps to locally regulate vasodilation and sustain tissue perfusion (243).

### 1.2.6 PTHrP in Cancer

#### *1.2.6.1 Breast Cancer*

Differential expression of PTHrP was detected at different tumour sites in breast cancer. Linforth et al. (244) reported that 68% of cases of early breast cancer expressed PTHrP while 50% of them expressed PTHR1. 100% and 81% of cases of bone metastasis showed PTHrP and PTHR1 expression respectively and the expression of either PTHrP or PTHR1 correlated with poor survival, while co-expression of both PTHrP and receptor predicted a worse clinical outcome at 5 years, with higher mortality rate (244). Many researchers have indicated that PTHrP expression and localization in primary breast tumours was associated with increased incidence of bone metastases and skeletal morbidity in patients (245-248). Genome-wide association studies (GWAS) have recently reported that PTHrP was up-regulated in breast cancer and identified *pthlp* as a novel breast cancer susceptibility gene, providing convincing evidence that PTHrP may play a role in primary breast tumourogenesis as well as in bone metastasis from breast cancer (249).

#### *1.2.6.2 Prostate cancer*

Iwamura et al. (250) reported the localizations of PTHrP in the cell cytoplasm of prostatectomy specimens of primary prostate tumours and the intensity of the immunohistochemical staining was correlated with tumour grade. Another study showed that expression of PTHrP was associated with progression of prostate

carcinoma (251). The receptor for PTHrP, the PTHR1 has also been reported to be highly expressed in bone metastasis from prostate cancer (252).

#### *1.2.6.3 Lung cancer*

PTHrP expression is common in all major lung cancer cell types (253). More than 50% of human lung tumours express PTHrP (253-255). Iguchi et al. (256) found that the likelihood of bone metastasis development in human lung squamous cell carcinoma-derived cells is proportional to their PTHrP expression and the treatment of these carcinoma cells with neutralizing anti-PTHrP antibody reduces this likelihood.

#### *1.2.6.4 Colorectal cancer and gastric adenocarcinoma*

Nishihara et al. (257) reported that PTHrP was expressed in 85 out of 90 (~95%) colorectal adenocarcinomas and its expression was significantly correlated with differentiation, depth of invasion, lymphatic invasion, lymph node metastasis, and hepatic metastasis. PTHrP was suggested to be involved in carcinogenesis, tumour growth, differentiation, and progression, and might have prognostic value by determining the behaviour of human colorectal adenocarcinoma (258).

#### *1.2.6.5 Renal Carcinoma*

Elevated serum PTHrP has been detected in many renal cell carcinoma (RCC) patients with hypercalcemia. An immunohistochemical study performed by Iwamura et al. (259) showed PTHrP (109-141) expression is present in the majority of RCCs. The authors demonstrated that the results of their study indicate PTHrP(109-141) may be a possible marker of cellular differentiation and may be useful for predicting recurrence free survival in RCC patients after radical nephrectomy (259).

#### *1.2.6.6 Oral squamous cell carcinoma*

Lv et al. (260) demonstrated that PTHrP mRNA and PTHrP protein were upregulated in 89% of oral squamous cell carcinoma (OSCC) tissues and in all nine OSCC cell lines studied. The authors noted that high PTHrP expression was positively correlated with pathological differentiation and associated with an overall poor prognosis and significantly low survival rate of patients (260). Conversely, they observed that cell growth and colony formation were inhibited by downregulation of PTHrP, suggesting a growth factor role of PTHrP (260).

### 1.2.7 PTHrP (1-36) as osteoanabolic agent for treatment of osteoporosis

PTHrP is homologous with PTH, as they share striking similarity in eight of the first 13 amino acids of their N-terminal sequence. PTHrP also acts on PTH classical targets (i.e. bone and kidney) via binding to PTHR1. Intermittent administration of native PTHrP (1-36) has been found to increase bone formation and BMD in mice and humans (261-263). In short-term small-scale studies, a daily injection of PTHrP (1-36) in doses as high as 750 µg appeared to act as a pure anabolic agent in postmenopausal osteoporosis (263, 264). In contrast to PTH, high-dose (400 µg) PTHrP (1-36) daily injection for three months was not associated with hypercalcemia and did not activate bone resorption markers (263). The PrOP study compared 3-month daily subcutaneous injections of (400 and 600 µg) PTHrP (1-36) against the standard injection (20 µg) of teriparatide (PTH (1-34)) in postmenopausal women with osteoporosis. The PTH (1-34) group showed two- to four-fold greater increase in N-terminal propeptide of type 1 collagen (P1NP) than in both PTHrP (1-36) 600 or 400 µg/day doses, respectively. PTHrP (1-36) treatment groups produced minimal change in collagen type-1 C-telopeptide (CTX) compared to the PTH (1-34) group, which was 3-fold higher than in PTHrP (1-36) groups. By the end of the study, PTHrP and PTH treatment groups showed equivalent increase in lumbar spine BMD, but only PTHrP treatment groups showed significant increase in total hip and femoral neck BMD (262). Studies on the potential use of PTHrP (1-36) in treatment of osteoporosis indicated that intermittent administration of high-dose PTHrP (1-36) increases bone formation without concomitant stimulation of bone resorption (262-264). This may be due, at least partly, to a greater selectivity to RG receptor conformation exhibited by PTHrP (1-36) and lower $R^0$ affinity, which is associated with more transient cAMP signaling responses compared with the responses induced by PTH (1-34) (265, 266).

Abaloparatide is a synthetic peptide analog of human PTHrP (1-34) developed and recently approved by the FDA for the treatment of osteoporosis. The amino acid sequence of Abaloparatide is identical to that of PTHrP in the first 21 amino acids, while eight of the remaining amino acids are different (Figure 1-16) (265). Abaloparatide was designed to retain potent anabolic activity with decreased bone resorption, less calcium-mobilization potential, and improved room-temperature stability (267). It is prescribed as an 80 µg daily subcutaneous injection

for an 18 month period for treatment of postmenopausal osteoporotic patients with high risk of future vertebral and non-vertebral fractures.


**Figure 1-17 Amino-acid sequence of teriparatide, human PTHrP (1-36) and abaloparatide.** *Green residues in abaloparatide represent homology with teriparatide and those coloured black are homologues residues with the native hPTHrP. Abaloparatide is different from PTHrP as shown in those red residues inserted into the linear sequence of the PTHrP molecule to develop a molecule that seems to have preferential affinity for transient state of PTHR1. That transient state is thought to be the more anabolic state.*

Preclinical animal studies have shown that Abaloparatide [BA058] increases bone formation markers without change in bone resorption markers, and increases BMD at spine and femoral neck, as well as improving trabecular architecture (268). Clinical human trials have also shown that Abaloparatide was as potent as teriparatide in increasing BMD at the lumbar spine over an 18 months period. However, the increases in BMD at the total hip and femoral neck were significantly higher and more rapid in Abaloparatide treatment group compared to teriparatide treatment group at all time-points (268, 269). Abaloparatide also significantly increased bone turn over markers P1NP and CTX, but the increase was less than that in the teriparatide-treated group (268, 269). The incidence of hypercalcemia was significantly lower in the Abaloparatide group (3.4%) than in the teriparatide group (6.4%) for all time-points (268, 269). Compared to placebo group, abaloparatide reduced vertebral fractures by 86% and non-vertebral fractures by 43%, whereas teriparatide reduced vertebral fractures and non-vertebral fractures by 80% and 28% respectively (268, 269). Abaloparatide does not contain methionine residues in its amino acid sequence. Therefore, it is not subjected to oxidation like teriparatide (Figure 1-16).

The findings from preclinical and clinical trials show that abaloparatide is an important option for the anabolic treatment of postmenopausal osteoporosis, especially in total hip and femoral neck, and in reduction of non-vertebral fractures.

## 1.3 Aims and Objectives

Our laboratory has run PTH (1-34) assay since 2012 using a fully automated commercial immunoassay kit, IDS-iSYS PTH (1-34), from Immunodiagnostic systems (Boldon Tyne and Wear, UK). The immunoassay has been primarily used for preclinical and clinical studies on an oral PTH (1-34) drug delivery technology. It has also been used to measure hPTH (1-34) as a part of EHT for differential diagnosis and confirmation of PHP after loading of exogenous hPTH (1-34) confirming a suitable circulating concentration of hPTH(1-34) has been achieved during the EHT. The immunoassay analytical range claimed by the manufacturer is 4 – 1000 pg/mL. The assay performance has been reliable. However, some issues around the lower limit of quantification (LLoQ) have become a concern lately, where inappropriate >4.0 pg/mL PTH (1-34) concentrations are obtained for samples which should have undetectable PTH (1-34).

Part of the initial aims of this thesis were to develop a sensitive LC-MS/MS method for measurement of hPTH (1-34), validate the method and compare the LC-MS/MS with the currently used commercial immunoassay kit.

The subsequent aims were:

- To utilize the validated LC-MS/MS method to conduct a pharmacokinetic analysis study on participants that have been treated with subcutaneous and oral hPTH (1-34).
- To explore the ability of the LC-MS/MS method to measure oxidized PTH (1-34) forms alongside non-oxidized PTH (1-34).
- To test the feasibility of measuring PTHrP (1-36) in human plasma using the same SPE procedure, LC gradient, and MS conditions developed for measurement of hPTH (1-34).
- To perform a validation procedure for hPTHrP (1-36) assay in accordance with published bioanalytical method validation guidelines.

# 2. Chapter 2 – Materials and Methods

## 2.1 Development and validation of a LC-MS/MS assay for quantification of PTH (1-34) in human plasma

There are no reference standard materials commercially available to use for calibration of LC-MS/MS assay for hPTH (1-34) quantification. Also, there is no isotopically-labelled hPTH (1-34) that can be used as an internal standard (IS) for the assay. Therefore, all calibration standards and quality control (QC) materials used in the development of the assay described herein were prepared in our laboratory. To ensure high quality of our in-house standards and QCs, high purity (>98.0%) recombinant hPTH (1-34) was used to prepare calibration standards and quality controls. Positive-dispense pipettes have always been used to prepare solutions and making diluents.

Due to the lack of commercially available isotopically-labelled hPTH (1-34), rat PTH (rPTH) (1-34) fragment was used as an IS in our assay. rPTH (1-34) amino acid sequence shows a great deal of homology with that of hPTH (1-34) (Figure 2-1). Both peptides also have similar chemical and physical characteristics (Table 2-1).

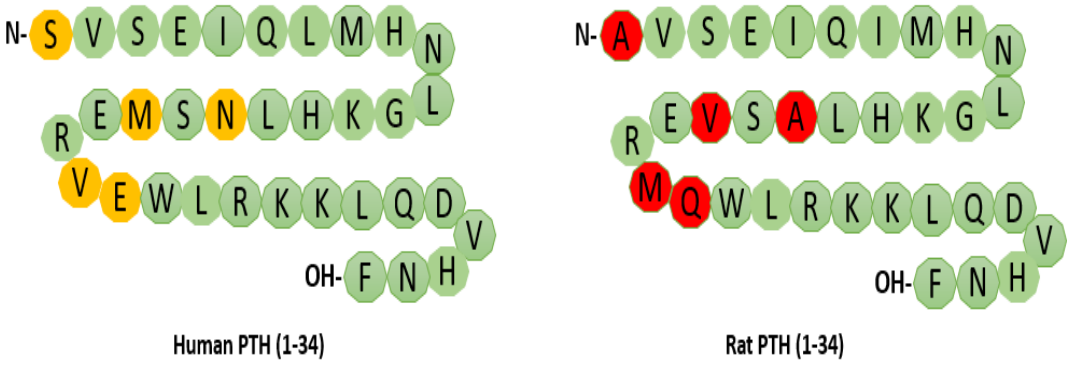


**Figure 2-1 Primary amino acids sequence of hPTH (1-34) and rPTH (1-34) fragments.** *Highlights (yellow and red) are dissimilar amino acids.*

**Table 2.1 Chemical and physical characteristics of human and rat PTH (1-34)**

| Characteristic | hPTH (1-34) | Rat PTH (1-34) |
|---|---|---|
| Average mass | 4,117.8 D | 4,057.8 D |
| Monoisotopic mass | 4,115.1 D | 4,055.2 D |
| pI | 9.1 | 10.1 |
| Hydrophobicity index | -0.65 | -0.42 |
| Acidic residues | 12% | 9% |
| Basic residues | 15% | 15% |
| Aromatic residues | 6% | 6% |

### 2.1.1 Chemicals and Reagents

Lyophilized recombinant hPTH (1-34) was supplied by PROSPEC (NJ, USA) and rPTH (1-34) by Sigma-Aldrich (Dorset, UK). Acetonitrile (ACN), Methanol (MeOH), Isopropanol (IPA), Formic Acid (FA), Water ($H_2O$), Triflouroacetic acid (TFA), and ammonium hydroxide ($NH_4OH$) were all of MS-grade (Fisher Scientific, Loughborough, UK). Bovine serum albumin (BSA) was supplied by Fisher Scientific UK Ltd. Hydrogen peroxide solution (30% w/w), fetal bovine Serum (calf serum) and dimethylsulfoxide (DMSO) were supplied by Thermo Scientific (Cramlington, UK). IDS-iSYS PTH (1-34) immunoassay kit was supplied by Immunodiagnostic Systems (Boldon Tyne and Wear, UK).

### 2.1.2 Standard Solutions

Primary Stock solutions of human and rat PTH (1-34) were prepared gravimetrically in 80:20:0.1:0.1 (v:v:v:w) ($H_2O$: MeOH: FA: BSA), each to a concentration of 0.1 mg/mL and stored in small aliquots at -20 $^{o}$C. Plasma calibration standards were prepared by spiking the primary standards into charcoal-stripped human ethylenediaminetetraacetic acid (EDTA) plasma at concentrations of 10, 25, 50, 250, 500, 1000, and 2000 pg/mL. Quality controls (QC) (20, 100, 200, and 800 pg/mL) were prepared in human charcoal-stripped EDTA plasma. Low surface adhesion receptacles were used in order to minimize non-specific binding (NSB) of PTH (1-34) peptide to plastic surfaces.

### 2.1.3 Oxidation of hPTH (1-34)

In order to specify multiple reaction monitoring (MRM) transitions to measure oxidized forms of hPTH (1-34), 1 mL of 1 µg/mL hPTH (1-34) was incubated with 20 µL of 98 mM $H_2O_2$ (final concentration of $H_2O_2$ was 1.9 mM) for 40 minutes at room temperature. Then, the oxidized sample solution was directly infused into the

MS and precursor ions and product ions scan were performed. Precursor to product ion transitions specific for every oxidized PTH (1-34) form was then designated.

### 2.1.4 Sample Collection

Blood samples were collected from consented healthy participants enrolled in stage 3 of a Phase 1 study on an oral PTH (1-34) drug delivery technology. The study was carried out at the Hadassah clinical research centre at the Hebrew University in Jerusalem. The study was conducted in accordance with Hadassah Medical Centre ethical approval (ethics approval number (032-13-HMO)). The age range of the participants was 18-50 years. Participants received either a single 20 µg subcutaneous (sc) injection of teriparatide (n=10), or 0.69 mg (n=5) or 2.07 mg (n=10) oral PTH (1-34) (EnteraBio, Jerusalem, Israel). Blood samples were collected in EDTA BD vacutainers at baseline immediately before drug administration, and then post-dose at 15 minute intervals for up to two hours then hourly intervals for up to three hours (time course 0-300 min). Blood samples were separated by centrifugation at 4,000 x g for 10 minutes within 30 min of blood collection, plasma was stored at -20°C until analysis. Prior to analysis, plasma aliquots were allowed to defrost at room temperature, then homogenised and spun at 4,000 x g for 5 minutes.

### 2.1.5 Sample preparation

All plasma samples, calibrators and QCs were prepared using the following preparation method:

**Pre-treatment:** 200 µL of samples, calibration standards, and QCs were pipetted into 96-well sample rack. 20 µL of IS (2000 pg/mL) was added to every sample, calibrator, and QC and briefly mixed using an orbital mixer. The final IS concentration was 200 pg/mL. Then, samples, calibration standards and QCs were mixed with 500 µL of 95:5 (v:v) $H_2O$: $NH_4OH$.

**Solid-phase extraction (SPE)**: The SPE of hPTH (1-34) and IS was carried out on Waters Oasis® HLB (Hydrophilic-Lipophilic Balance) sorbent (bed mass/particle size 2mg/30µm) 96-well µElution plates for reversed-phase SPE (part# 186001828BA). Wells of the SPE plate were initially conditioned with 200 µL MeOH and equilibrated with 200 µL 95:5 (v:v) ($H_2O$: $NH_4OH$). The entire diluted sample (720 µL) was loaded into the SPE well. The well was then washed with 200 µL of 60:40 (v:v) ($H_2O$:MeOH). hPTH (1-34) and the IS were eluted in two steps

using 25 µL (2 x 25 µL) of 70:30:0.2 (v:v:v) (ACN:$H_2O$:FA) each time. Finally, the eluate was diluted with 50 µL $H_2O$ and 30 µL was injected into the LC-MS/MS.

### 2.1.6 Systematic SPE Method Development

Before the sample preparation method described in 2.5 was adopted, all the process steps were thoroughly evaluated. In this study, two different phase chemistries were tested: Oasis® HLB C18 and Oasis® mixed-mode anion-exchange (MAX) µElution 96-well plates. Using standards and buffered/organically modified solutions, key variable (pH and percent organic modifier) affecting analyte retention and elution were systematically profiled to determine analyte behaviour relative to changing extraction conditions. The systematic approach used to develop the sample preparation method generated valuable data adopted for a more effective sample clean-up method.

#### *2.1.6.1 Phase chemistry selection, load optimization and establishment of optimal wash solvent*

- A stock of aqueous hPTH (1-34) standard (1000 pg/mL) was prepared in 90:10:0.1:0.01 (v:v:v:w) $H_2O$:ACN:FA:BSA.
- Then, the stock solution was divided into two groups.
- Each group was further divided into two sub-groups of 10 vials containing 200 µL each.
- Samples from group 1 were alkalinised with 500 µL 95:5 (v:v) $H_2O$: $NH_4OH$ (pH≈11).
- Samples from group 2 were acidified by adding 500 µL 98:2 (v:v) $H_2O$: FA (pH≈2).
- For wash, 10 solvents with different organic ratios ranging from 5-90% methanol were prepared.
- Then, samples from each group were taken through the whole SPE process using either Waters Oasis® HLB µElution 96-well plates for reversed-phase SPE or Waters Oasis® MAX µElution 96-well plates for reversed-phase and anion-exchange SPE separately.
- Load flow-through eluate was analysed for premature hPTH (1-34) breakthrough.
- Wash/elute eluates were analysed for hPTH (1-34) breakthrough.

Figure 2-2 illustrates our approach towards optimizing wash solvent, sample load and sorbent chemistry selection.

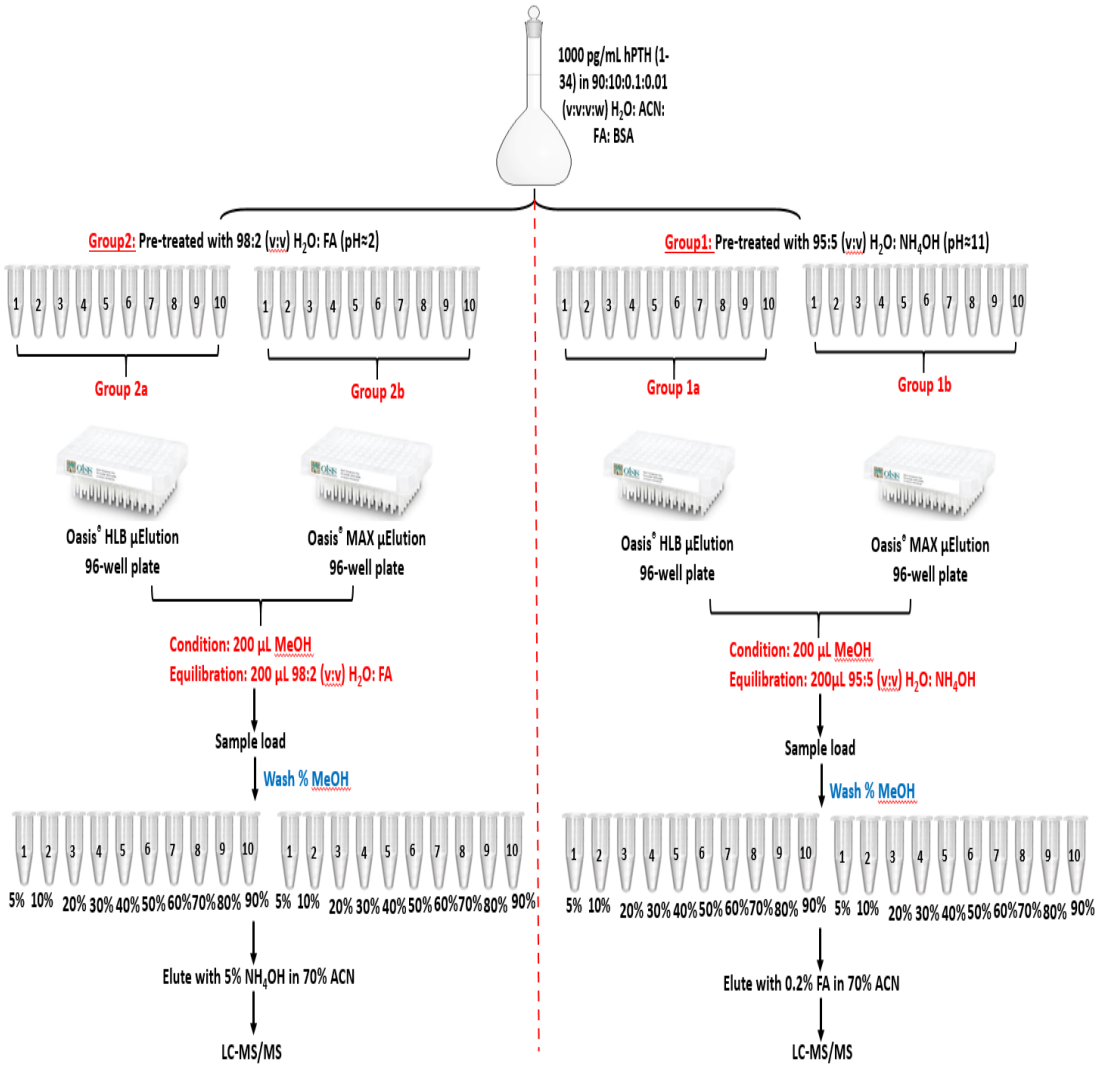


**Figure 2-2 The Approach toward phase chemistry selection, load optimization and establishment of optimal wash solvent**

### *2.1.6.2 Establishment of optimal elution solvent*

In order to establish an optimum elution solvent that gave best recovery, solvents ranging from 30-90% acetonitrile in 0.2% FA were used, while maintaining the rest of the SPE process fixed based on results obtained from experiments described in 2.6.1.

The following steps and figure 2-3 describe the approach used for the optimization of elution solvent:

- A stock of neat aqueous standard of 1000 pg/mL of hPTH (1-34) was prepared in 90:10:0.1:0.01 (v:v:v:w) $H_2O$: ACN: FA: BSA.
- Then, the stock hPTH (1-34) solution was divided into seven tubes, each contained 200 µL and pre-treated with 500 µL 95:5 (v:v) $H_2O$: $NH_4OH$ (pH≈11).
- Using Oasis® HLB µElution 96-well plate, SPE steps were the same for all seven samples except the elution step, where solvents ranging from 30-90% acetonitrile in 0.2% FA were used to elute respective wells.
- Load flow-through, wash and elute eluates were analysed for compound breakthrough.

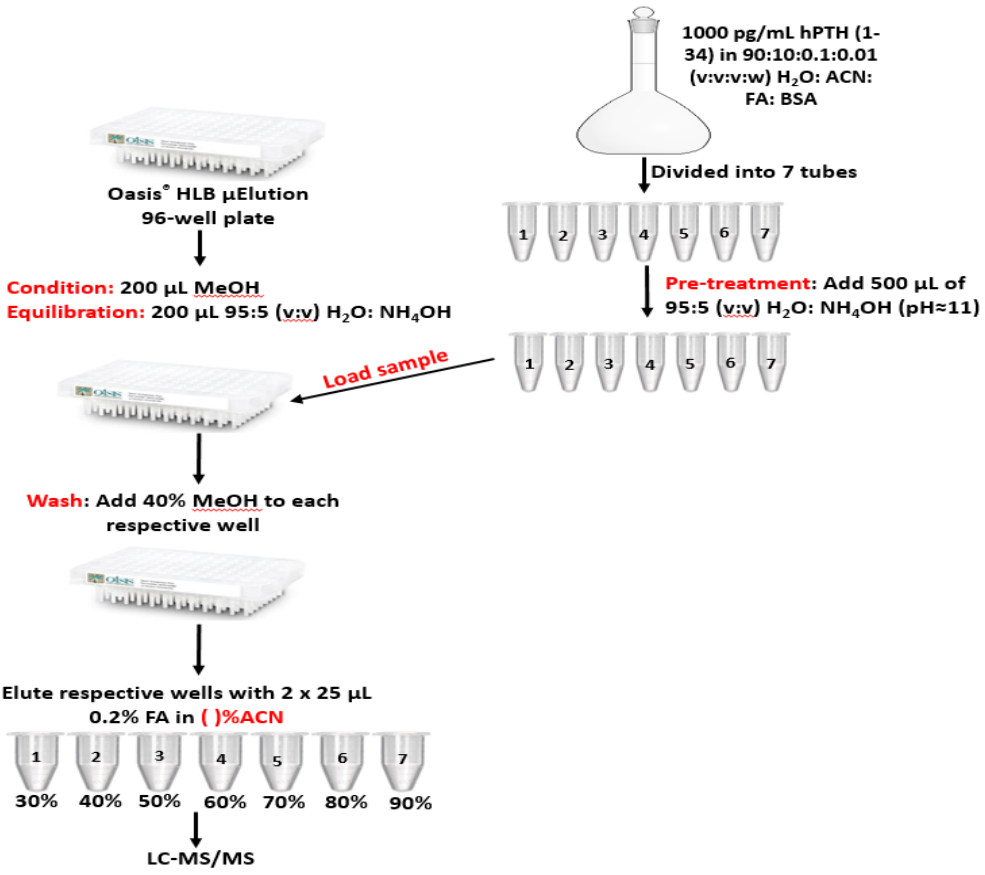


**Figure 2-3 The approach toward establishing optimum elution solvent**

### *2.1.6.3 Further optimization of sample pre-treatment*

Simple dilution of plasma sample with 5%$NH_4OH$ at ratio 1:2.5 (sample:5%$NH_4OH$) was compared against a procedure that involved the following steps: (1) Precipitation of abundant large protein (PPT) with ACN at ratio 1:1

followed by centrifugation of sample at 4000 rpm for 5 min and then the supernatant transferred to a fresh tube. (2) 1 mL of 5%$NH_4OH$ was added to the supernatant. Samples of both pre-treatment method groups were then taken through the whole SPE procedure and response yield (mean ± SEM) were compared. The experiment was carried out using a stock sample of human plasma spiked with hPTH (1-34) at final concentration 1000 pg/mL), which then was divided into two groups of 6 samples each. Figure 2-4 describes the comparison approach between the two pre-treatment procedures.

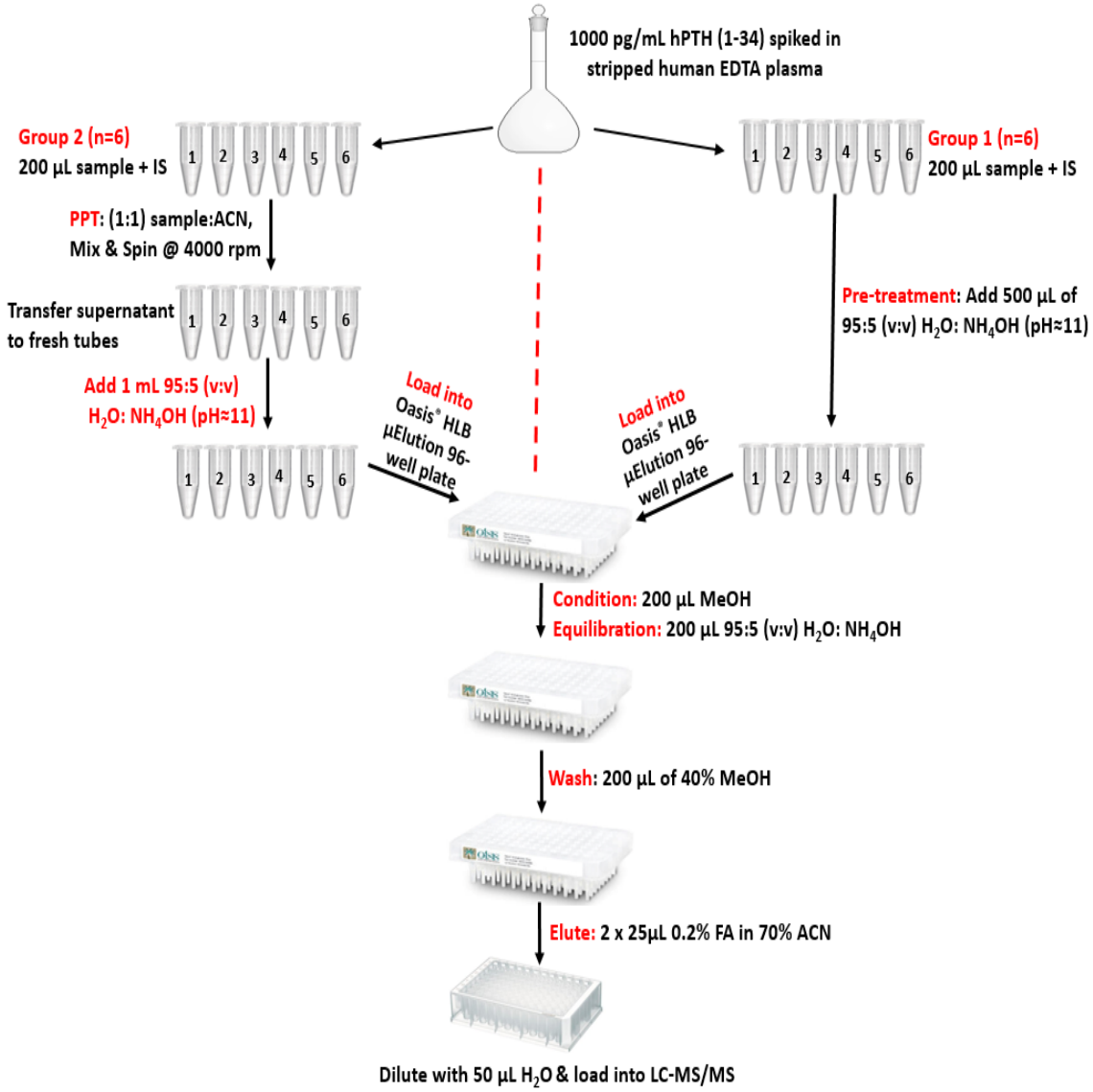


**Figure 2-4 Flow diagram describing the approach in evaluating two different pre-treatment methods: (1) simple dilution with 5%$NH_4OH$ and (2) a method that involves protein precipitation using 1:1 sample: ACN ratio.**

### 2.1.7 LC Instrumentation and Chromatographic Conditions

The chromatographic separation of PTH (1-34) was performed using a Rheos Allegro UHPLC Pump (Flux Instruments, Switzerland). A Waters AQUITY UPLC® Peptide CSH™ C18 column 130 Å (1.7 µm, 2.1 x 50 mm) was used to selectively separate the PTH (1-34) peptide. Beside AQUITY UPLC® Peptide CSH™ C18 column, several analytical columns from different manufacturers with different packing materials and chemistries were evaluated and compared according to their ability to produce hPTH (1-34) peaks with good shapes and intensity (table 2.2).

***Table 2.2 Analytical LC Columns have been tested in LC method development for PTH (1-34)***

| Column | Chemistry | Specification |
|---|---|---|
| Sunfire™ | C18 | 3.5 µm, 100Å, (2.1 x 50 mm) |
| Kinetex | C18 | 2.6 µm, 100Å, (2.1 x 50 mm) |
| Kinetex | Biphenyl | 2.6 µm, 100Å, (2.1 x 50 mm) |
| Cortecs™ | C18 | 2.7 µm, 100Å, (2.1 x 50 mm) |
| Viva | C4 | 5 µm, (2.1 x 50 mm) |
| Agilent | XDB-C8 | 1.8 µm, (2.1 x 50 mm) |
| Accucore | C18 | 2.6 µm, (2.1 x 50 mm) |
| AQUITY UPLC® BEH | C18 | 1.7 µm, 300Å, (2.1 x 50 mm) |

Mobile phase A consisted of 0.2% FA in water and mobile phase B consisted of 0.2% FA in ACN. The flow rate was set at 400 µL/min during the entire chromatography process, and 30 µL of sample was injected through a 50 µL loop. Initially, the mobile phase composition began with 10 % B and then gradually increased from 20% to 30% B over 2.5 minutes to elute hPTH (1-34) and the IS peaks, the composition of mobile phase B was then ramped from 30% to 80% in 0.2 minutes, then further increased to 100% over 1.5 min where it was held for 2.0 minutes to clean the column. Finally, the column was equilibrated at the initial condition. The total run time was 7.0 minutes. Column temperature was maintained at 60$^{o}$C and the autosampler tray temperature was maintained at 10$^{o}$C (±2°C). A weak wash 85:15 (v:v) ($H_2O$: ACN) and strong wash solutions 0.1% DMSO in 25:25:25:25 (v:v:v:v) ($H_2O$: ACN: MeOH: IPA) were used to clean the sampler needle and tubing.

### 2.1.8 Tandem mass spectrometry analysis

Waters/Micromass® Quattro Ultima™ Pt mass spectrometer (MS) (Manchester, UK) with a Z-shape electrospray Ionization (ESI) source was operated in positive

ionization mode ($ESI^+$). The Capillary voltage, source temperature, desolvation temperature, nebulizer nitrogen flow rate and desolvation nitrogen flow rate were set at 3.0 kV, 150 °C, 350 °C, 200 L/h, and 1000 L/h respectively. Sample cone voltage was 35 V, collision energies for non-oxidized hPTH (1-34), oxidized hPTH (1-34) were 10 eV and 16 eV for IS. Argon was used as collision gas. Sample analysis was performed in multiple reaction monitoring (MRM) mode with dwell time of 0.1 second. The precursor to product ion transition for non-oxidized hPTH (1-34), single-oxidized hPTH (1-34), double-oxidized hPTH (1-34) and IS were 589.2>656.1, 591.4>658.8, 593.7>661.5 and 677.1>777.9 respectively. MassLynx version 4.1 and Quanlynx software (Waters Corp., Milford, MA, USA) were used for system control, data acquisition, peak area integration, and sample quantification.

### 2.1.9 Method Validation

Method validation was carried out in accordance with the FDA guidance (270) and the EMA guidelines (271).

#### *2.1.9.1 Calibration Curve/Linearity*

Dynamic range, assay accuracy and precision were determined using calibration standards and quality control samples were prepared as described previously in section 2.2. The calibration curve was constructed by plotting the ratio of the analyte peak area to internal standard peak area against the concentration of their respective standards. Calibration standard concentrations ranged from 10 to 2000 pg/mL. Using a $\frac{1}{x}$ weighting, the calibration curves were accepted as linear if correlation coefficient ($r^2$) of regression analysis was >0.90 and each standard value within 15% of the nominal value. The $\frac{1}{x}$ weighting factor was selected based on the linear relationship between standard deviation (σ) and instrument response compared to linear relationship between variance ($\sigma^2$) and instrument response (272). LC-MS/MS responses for hPTH (1-34) of calibration standards and QCs in six analytical runs were plotted against standard deviation (σ) and variance ($\sigma^2$) of assay responses (figure 3-21).

#### *2.1.9.2 Carry-over*

Carry over was assessed by analysis of sample containing 2000 pg/mL hPTH (1-34) immediately followed by three blank plasma samples.

#### *2.1.9.3 Matrix effect assessment*

Two methods were used to assess the effect of sample matrix. In the first methods we compared the slopes of linear calibration curves generated by analysing calibrators (9 concentrations) spiked in neat aqueous solution (90:10:0.1:0.01) (v:v:v:w) ($H_2O$: ACN: FA: BSA) and in charcoal-stripped human EDTA plasma. Then, the aqueous calibrators were divided into two sets, one set was taken through the whole extraction process exactly the same as spiked plasma standards. The second set of the aqueous calibrators was not extracted. Calibration curves from non-extracted aqueous standards, extracted aqueous standards, and spiked plasma standards were generated by plotting the ratio of the analyte peak area to internal standard peak area (response) against the concentration of the respective standards.

The second method used to evaluate matrix effects was by analysing standard solutions at two different concentration (100 and 1000 pg/mL) prepared either in solvent (90:10: 0.1: 0.01) (v:v:v:w) ($H_2O$: ACN: FA: BSA) (Sample A), or spiked in extracted blank human EDTA plasma at the final step of extraction after evaporating the eluent (sample B). Five replicates of each sample standard groups were analysed. A fixed amount of internal standard was used in all replicates. The percentage of matrix effect was calculated using the following formula:

$$\%Matrix\ effect = \left(\frac{Response\ of\ sample\ B}{Response\ of\ sample\ A} - 1\right) x100 \qquad \textit{(Equation 1)}$$

#### *2.1.9.4 Precision and Accuracy*

To assess intra-assay precision and accuracy, four levels of QCs (20, 100, 200, and 800 pg/mL) were analysed 10 times within a single run, whilst inter-assay precision and accuracy were generated by repeated measurement (n=10) of all QCs over a period of one month. The precision of an analytical method describes the closeness between measurement values of the analyte when multiple aliquots of a single homogeneous sample are measured exactly the same way repeatedly. Coefficient of variation (CV) serves as a measure of assay/method precision. Accuracy describes the closeness of measurement values obtained by the method to the actual value of the analyte. Relative error (RE), which is the deviation of the measured value from the actual/nominal value serves as the measure of accuracy. The acceptance criteria defined that the inter- and intra-assay precision determined at each concentration should not exceed 15% of the coefficient of variation (%CV) and the measured value

at each concentration should be within 15% of the true value (%RE) (270, 271). %RE is calculated as shown below:

$$\%Relative\ error\ (RE) = \frac{(Actual\ value - measured\ value)}{Actual\ value} \times 100$$

#### *2.1.9.5 Ion suppression*

Ion suppression was examined by post column infusion of constant flow of a neat aqueous standard of hPTH (1-34) at a concentration of 100 ng/mL via a T-junction at a flow rate 20 µL/min (1.2 mL/h) directly into the MS/MS source. A blank human plasma sample and a sample containing PTH (1-34) were extracted with and without IS, then injected into the column at 400 µL/min.

#### *2.1.9.6 Recovery efficiency*

Recovery efficiency was assessed by analysing three human plasma samples at low, medium and high concentrations of endogenous PTH (1-34), each spiked with 20 and 800 pg/mL rhPTH (1-34). Three replicates of each spiked plasma samples were analysed in the same run. Recovery was calculated by dividing the measured hPTH (1-34) by the expected value (endogenous + spiked).

#### *2.1.9.7 Lower limit of quantification and detection*

Lower limit of quantification (LLoQ) was determined by the lowest concentration quantifiable for which intra-assay precision %CV and %RE do not exceed 20% and minimum peak signal-to-noise (S/N) ratio of 10:1 (270, 271). Lower limit of detection (LLoD) was determined by the lowest concentration that produced a peak area of five times the response produced by the blank (S/N = 5) (270, 271).

#### *2.1.9.8 Method comparison*

hPTH (1-34) measurements obtained by LC-MS/MS from human samples (n=390) were compared against those obtained using the commercial IDS-iSYS PTH (1-34) immunoassay. Samples collected from participants enrolled in stage 1, 2, and 3 of a phase 1 study on an oral PTH (1-34) drug delivery technology as described in section 2.4 were batched into treatments groups (i.e. 20 µg sc teriparatide injection, 0.69 mg oral PTH (1-34) and 2.07 mg oral PTH (1-34). Samples used in method comparison were randomly selected from these three treatment groups' batches. All samples were stored at -80$^{o}$C. The immunoassay is based on chemiluminescence technology, where PTH (1-34) peptide is captured by two antibodies, namely anti-PTH polyclonal antibody labelled with acridinium ester derivative and anti-PTH

polyclonal antibody labelled with biotin. The selectivity of the assay has not been published by the manufacturer. According to the manufacturer, the LLoD and LLoQ of the assay is 2.0 pg/mL and 4.0 pg/mL respectively with an average recovery of 111% in EDTA-plasma and 95% in serum. The manufacturer also declared a 4% cross-reactivity of the assay to PTH (1-84) and <0% cross-reactivity to PTH (7-84).

#### *2.1.9.9 Cross-reactivity testing*

Cross-reactivity of the immunoassay and LC-MS/MS method to hPTH (1-84), hPTHrP (1-86), hPTHrP (1-36), hPTH (13-34), and rat PTH (1-34) was assessed using charcoal-stripped EDTA plasma spiked with three different concentrations of each peptide. The concentrations used were 20 ng/mL, 2 ng/mL and 396 pg/mL. Blank EDTA plasma was analysed in the same run. The cross-reactivity percentage was calculated by dividing the measured value by actual amount spiked in plasma multiplied by 100.

Oxidized PTH (1-34) was also tested. For this experiment, five plasma aliquots each containing 500 pg/mL of hPTH (1-34) were prepared. Four aliquots were treated with 1.9 mM $H_2O_2$ for 10, 20, 40, and 60 minutes respectively and then quenched with Methionine, whilst one aliquot was left untreated. All samples were then analysed simultaneously using LC-MS/MS and the immunoassay.

### 2.1.10 Pharmacokinetic (PK) analysis

Pharmacokinetic (PK) profiles (time-course 0-300 min) from human subjects given either a single subcutaneous (sc) injection of 20 ug Teriparatide (n=10) or a single oral PTH (1-34) dose of either 0.69 mg (n=5) or 2.07 mg (n=10) were analysed using the LC-MS/MS method. Concentrations below the limit of quantification were set to zero for the calculation of pharmacokinetic parameters. The PK parameters used were: $C_{max}$ (maximum concentration achieved), $T_{max}$ (time to reach $C_{max}$), and $AUC_{0\text{-}last}$ (the area under PK curve calculated as a sum of AUCs using the linear trapezoidal summation from 0 to the last measurable data point) were determined for each treatment group. Additionally, $T_{1/2}$ (apparent terminal elimination half-life time (minutes), defined as 0.696 divided by first order elimination constant ($\lambda_z$) was also determined. $\lambda_z$ was calculated using log-linear regression of the terminal portions of the plasma concentration-versus-time curves.

### 2.1.11 Statistical analysis

Linear regression analysis and Bland-Altman plots were constructed and analysed by Statistical Package for the Social Science (SPSS) version 23 (IBM, NY, USA). SPSS version 23 was also used to perform descriptive statistical analysis of PK parameters of the PTH (1-34) treatment groups. One-way ANOVA was used to compare $C_{max}$, AUC, $T_{max}$ , and $T_{1/2}$ in Forsteo and oral hPTH (1-34) treatment groups. Significance was defined as $p$ <0.05.

## 2.2 Development and validation of a LC-MS/MS assay for quantification of PTHrP (1-36) in human plasma

### 2.2.1 Chemicals and Reagents

Lyophilized recombinant human PTHrP (hPTHrP) (1-36) (MW= 4266 Da) was purchased from Creative BioMart (NY, USA). rPTH (1-34) was purchased from Sigma-Aldrich was used as an internal standard. Acetonitrile (ACN), Methanol (MeOH), Isopropanol (IPA), Formic Acid (FA), Water ($H_2O$), Triflouroacetic acid (TFA), and ammonium hydroxide ($NH_4OH$) were all of MS-grade (Fisher Scientific, Loughborough, UK). Bovine serum albumin (BSA) was purchased from Fisher Scientific UK Ltd. Hydrogen peroxide solution (30% w/w), fetal bovine Serum (calf serum) and dimethylsulfoxide (DMSO) were purchased from Thermo Scientific (Cramlington, UK). The amino acid sequence of hPTHrP (1-36) is shown in (figure 2-5).

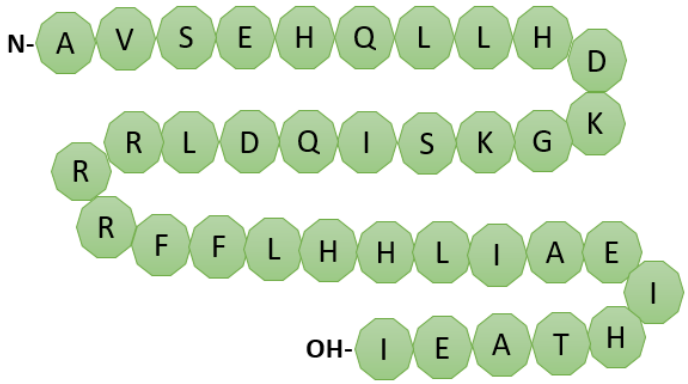


**Figure 2-5 Amino acid sequence of recombinant hPTHrP (1-36).**

### 2.2.2 Standard Solutions

No reference materials are commercially available for PTHrP (1-36). Calibrators and controls were prepared in our laboratory using high purity (>98.0%) recombinant

human PTHrP (1-36). Primary stock solutions of human PTHrP (1-36) were prepared gravimetrically in 80:20:0.1:0.1 (v:v:v:w) ($H_2O$: MeOH: FA: BSA), to a concentration of 0.1 mg/mL and stored at -20 $^oC$. Plasma calibration standards were prepared by spiking the primary standards into charcoal-stripped human EDTA plasma into concentrations of 25, 250, 500, 1000, and 2000 pg/mL. Quality controls (QC) (50, 100, 200, and 800 pg/mL) were also prepared in charcoal-stripped EDTA plasma and analysed in each batch with calibration standards. Low surface adhesion receptacles were used in order to minimize non-specific binding of PTHrP (1-36) peptides to plastic surfaces.

### 2.2.3 Sample Preparation

Sample preparation for hPTHrP (1-36) analysis by LC-MS/MS was guided by the results from the hPTH (1-34) experiments.

#### *2.2.3.1 Sample pre-treatment*

Prior to SPE, 200 µL of calibration standards, and QCs were pipetted into a 2mL deep 96-well plate. 20 µL of 2000 pg/mL rat PTH (rPTH) (1-34) (IS) was added into each well and mixed using orbital mixer for 30 s. Then, 500 µL of 95:5 (v:v) ($H_2O$:$NH_4OH$) was added to every sample and mixed.

#### *2.2.3.2 Solid phase extraction*

SPE procedure was conducted as described in section 2.7. The entire SPE process and sample pre-treatment was carried out using the Extrahera automated SPE processor.

### 2.2.4 Chromatographic conditions and mass spectrometry analysis

LC conditions and mass spectrometry parameters used to process PTHrP (1-36) were as described in sections 2.8 and 2.9 respectively.

### 2.2.5 Method Validation

Method validation was carried out in accordance with the FDA guides (270) and EMA guidelines (271).

#### *2.2.5.1 Calibration curve/Linearity*

Dynamic range was determined using calibration standards prepared as described in 5.2.2. The calibration curve was constructed by plotting the ratio of the analyte peak area to internal standard peak area against the concentration of the respective standards. Calibration standards concentrations ranged from 25 to 2000 pg/mL.

Using a 1/x weighting, the calibration curves were accepted as linear if correlation coefficient ($r^2$) of regression analysis was >0.90.

#### *2.2.5.2 Carry over*

Carry over was assessed by running blank plasma samples immediately after a sample containing 2000 pg/mL hPTHrP (1-36).

#### *2.2.5.3 Matrix effect assessment*

To assess the effect of sample matrix, hPTHrP (1-36) standard solutions at two different concentration (100 and 1000 pg/mL) were prepared in either aqueous solution of (90:10: 0.1: 0.01) (v:v:v:w) ($H_2O$: ACN: FA: BSA) (Sample A), or spiked into extracted blank human EDTA plasma at the final step of extraction after evaporating the eluent (sample B). Four replicates of each sample standards groups were analysed. Fixed amount of internal standard was used in all replicates. The percentage of matrix effect was calculated using equation 1.

#### *2.2.5.4 Precision and Accuracy*

Precision and accuracy of the hPTHrP (1-36) assay was accessed by analysing stock of in-house prepared QCs formulated by spiking hPTHrP (1-36) in charcoal-stripped EDTA plasma. To assess intra-assay precision and accuracy, four levels of QCs (50, 100, 200, and 800 pg/mL) were analysed 10 times within a single run, whilst inter-assay precision and accuracy were generated by repeated measurement (n=10) of all QCs over a period of a month. The acceptance criteria defined that the inter- and intra-assay precision determined at each concentration should not exceed 15% of the coefficient of variation (%CV) and the measured value at each concentration should be within 15% of the true value (%RE) (270, 271).

#### *2.2.5.5 Ion suppression*

Ion suppression was examined by post column infusion of constant flow of a neat aqueous standard of hPTHrP (1-36) at concentration 100 ng/mL via a T-junction at a flow rate 20 µL/min directly into the MS/MS source. A blank human plasma sample and a sample containing hPTHrP (1-36) were extracted and injected into the column at 400 µL/min.

#### *2.2.5.6 Recovery efficiency*

Three hPTHrP (1-36) standards were prepared in charcoal-stripped human EDTA plasma at low (50 pg/mL), medium (400 pg/mL) and high (800 pg/mL) concentrations, each spiked with 50 and 500 pg/mL rhPTH (1-34). Four replicates of

each of spiked plasma samples were assayed in the same run. Recovery was calculated by dividing the measured hPTHrP (1-36) by the expected value (endogenous + spiked).

# 3. Chapter 3 – Results

## 3.1 Development and validation of a LC-MS/MS Method for Quantification of hPTH (1-34)

### 3.1.1 MS Method Development for non-oxidized and oxidized hPTH (1-34)

Full scan spectra of the precursor ions from a standard solution of hPTH (1-34) showed several multiple-charged peaks; the most abundant were found to be the $[M+7H]^{7+}$ and $[M+6]^{6+}$ ions at *m/z* 589.2 and 687.1, respectively (Figure 3-1).

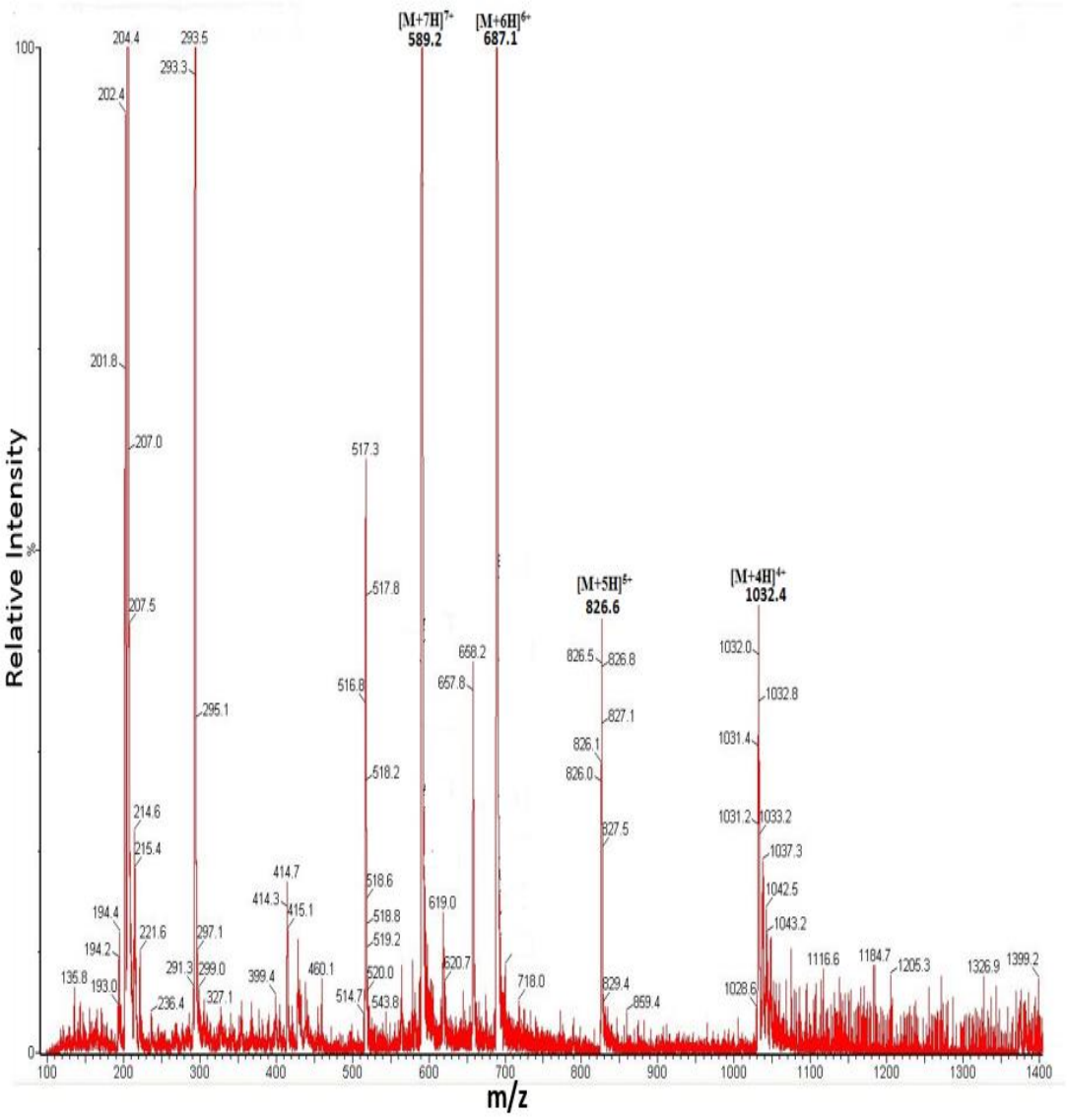


**Figure 3-1 Precursor Ions spectrum of hPTH (1-34) obtained using Waters/Micromass® Quattro Ultima™ Pt mass spectrometer at cone voltage of 35 V.** *$[M+6H]^{6+}$ and $[M+7H]^{7+}$ charge states have similar intensities.*

Fragmentation of the m/z 589 and 687 precursor ions produced two product ions at *m/z* 656.1 (Figure 3-2) and 787.1 (Figure 3-3) respectively.

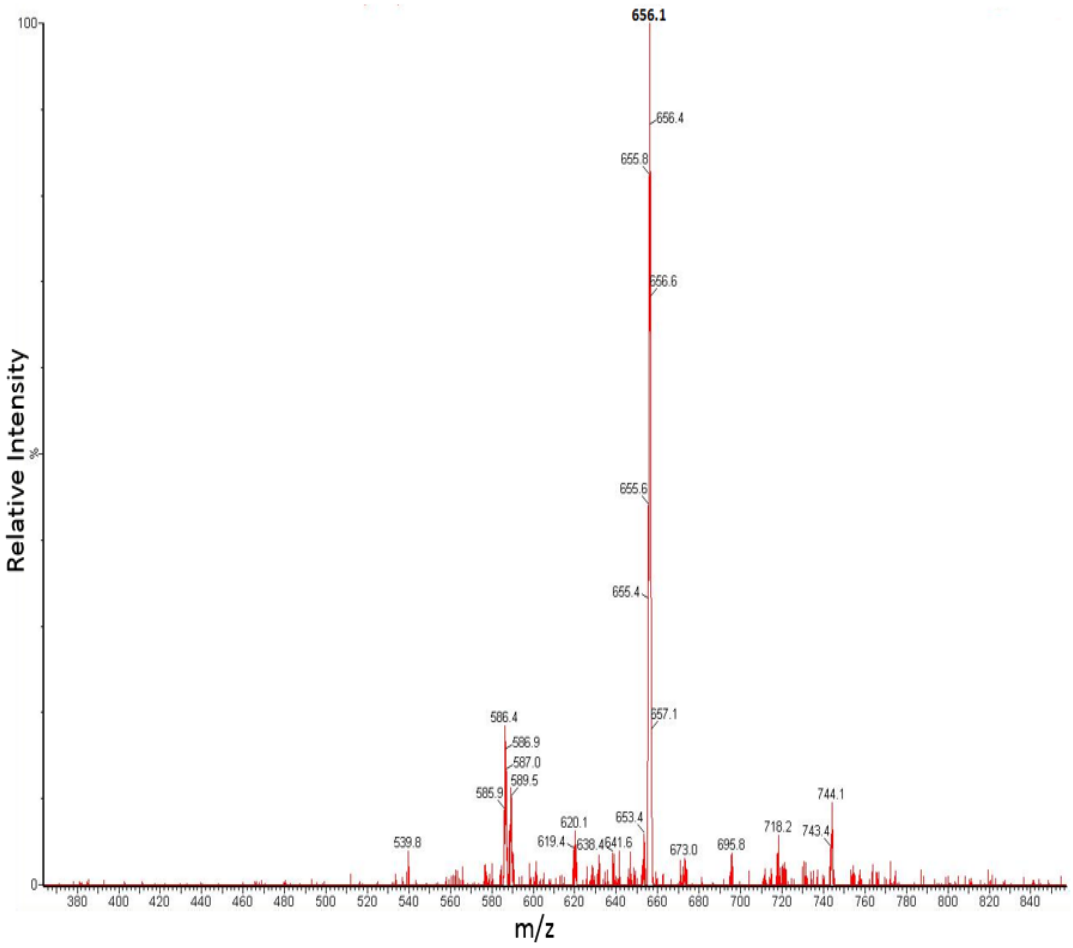


**Figure 3-2 Product ion spectrum from hPTH (1-34) at m/z 589.2.** *High intensity product ion at m/z 656.1 is shown using cone voltage of 35 V and collision energy of 10 eV.*

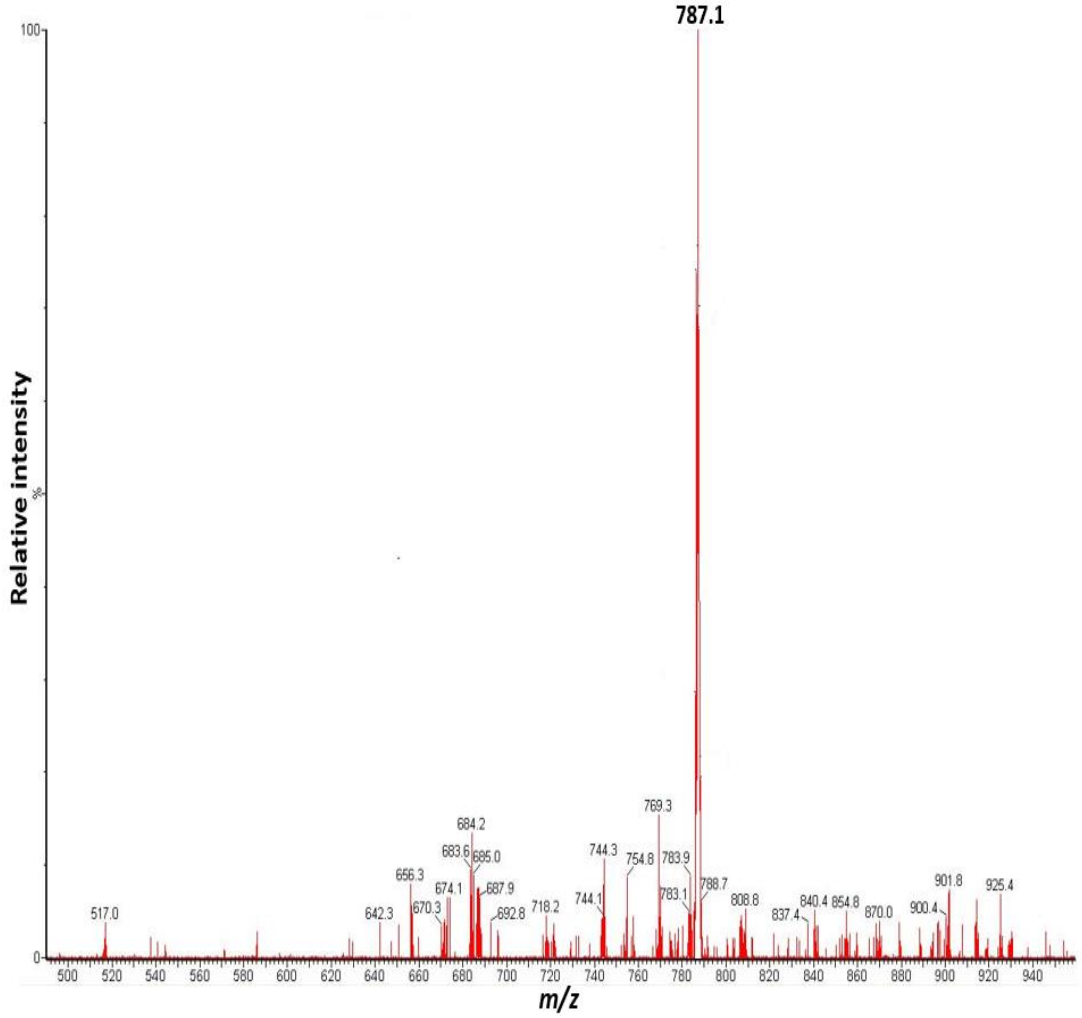


**Figure 3-3 Product ion spectrum from hPTH (1-34) at m/z 687.1.** *High intensity product ion at m/z 787.1 is shown using cone voltage of 35 V and collision energy of 16 eV.*

The mass spectra of rPTH (1-34) fragment (IS) showed prominent precursor ion peaks at *m/z* 677.1 $[M+6H]^{6+}$ and 580.7 $[M+7H]^{7+}$ (Figure 3-4) and produced fragments at *m/z* 777.9 (Figure 3-5) and 649.1, respectively.

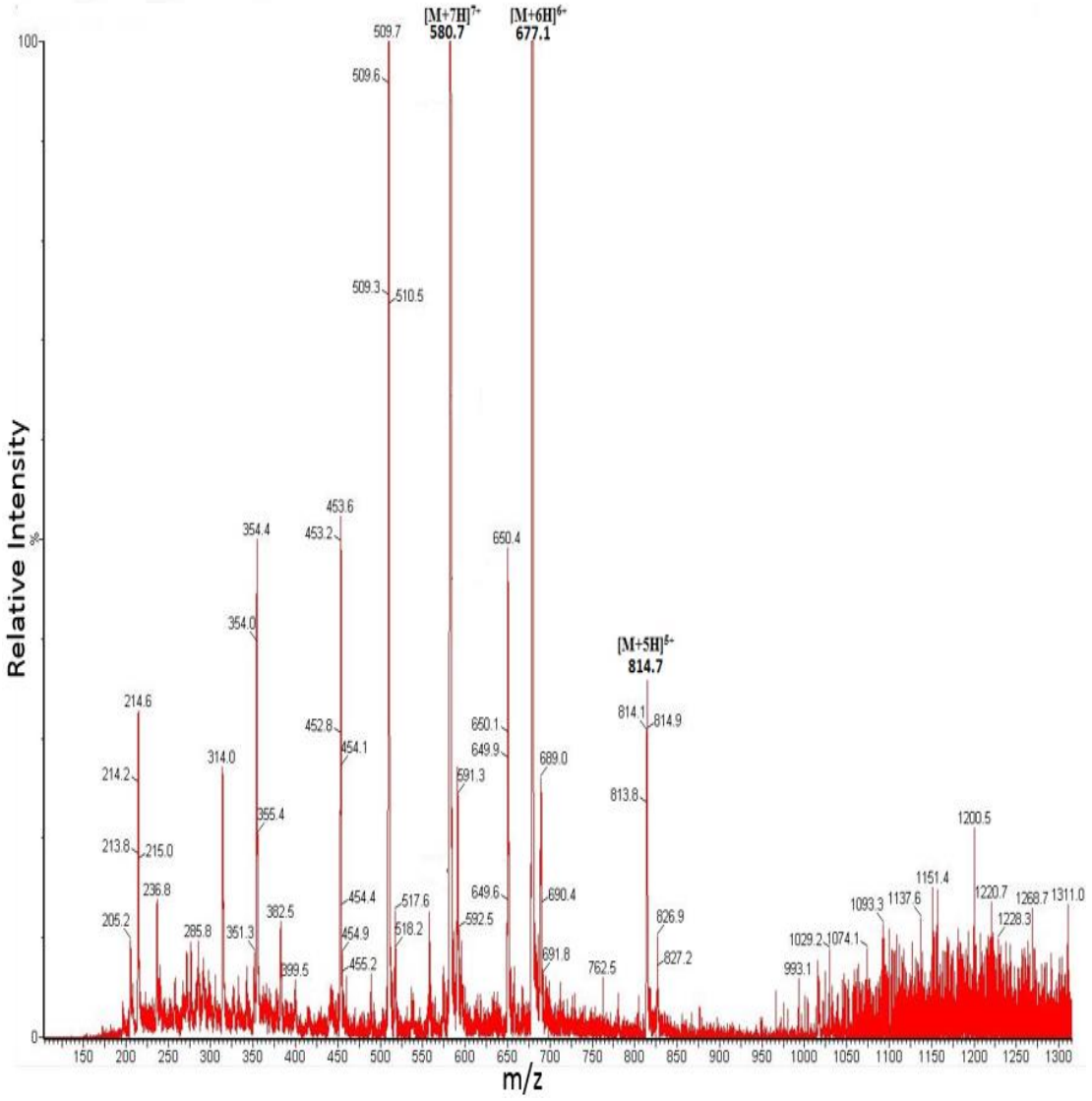


**Figure 3-4 Precursor ions spectrum of rPTH (1-34), the IS, at cone voltage of 35 V.** *$[M+6H]^{6+}$ and $[M+7H]^{7+}$ charge states have similar intensities as demonstrated with hPTH (1-34)*

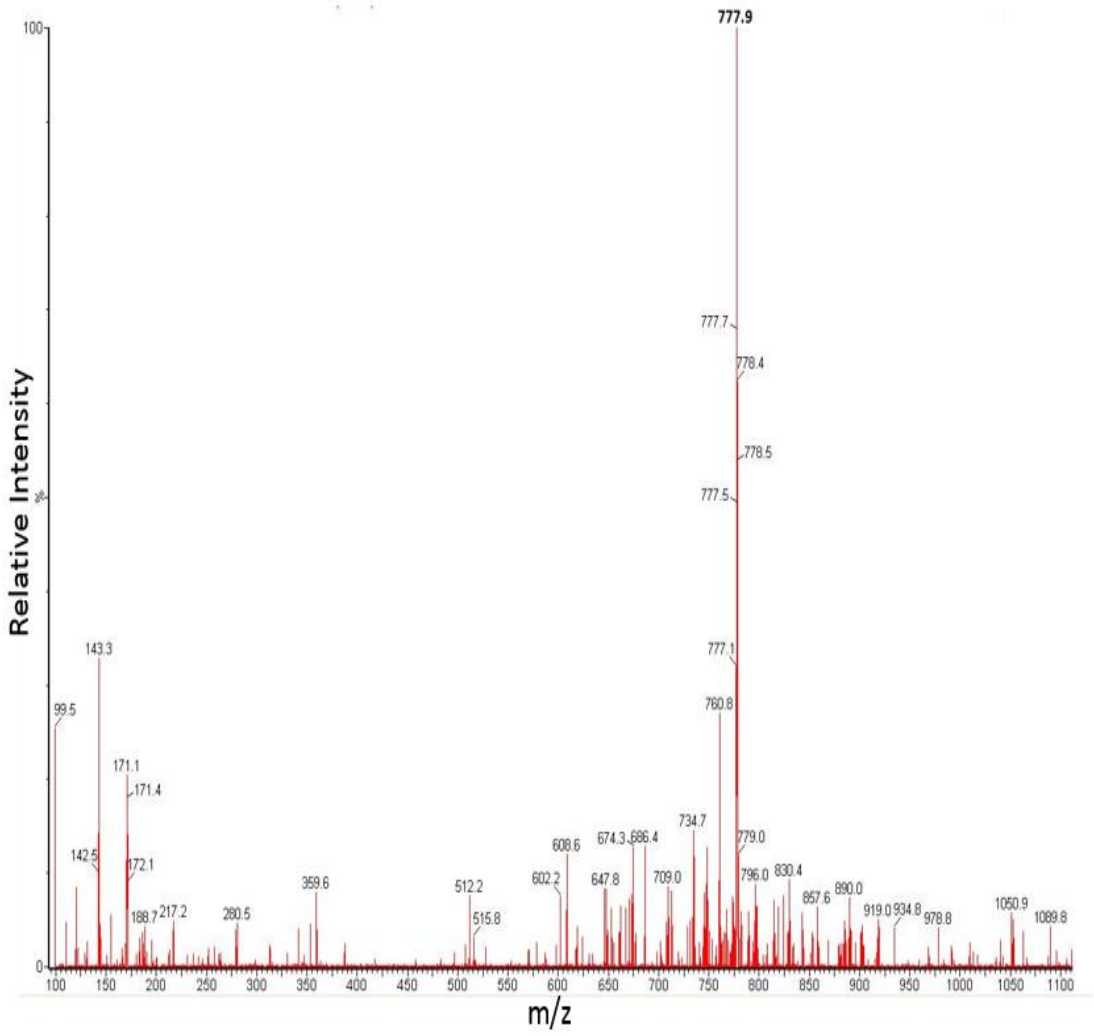


**Figure 3-5 Product ion spectrum from rPTH (1-34) at m/z 677.1.** *Product ion at m/z 777.9 was of the highest intensity obtained using cone voltage of 35 V and collision energy of 16 eV.*

Oxidation of hPTH (1-34) with 1.9 mM $H_2O_2$ has led to emergence of two new peaks beside each charge-state ion peaks in addition to those found for non-oxidized PTH (1-34). The two additional peaks representing hPTH (1-34) oxidized at either Met 8 or Met 18, where 16 mass units are added to molecular weight of hPTH (1-34)) or at both Met 8 and Met 18, where 32 mass units are added to molecular weight of hPTH (1-34)). However, ionization and fragmentation of oxidized hPTH (1-34) occurred the same way as that for non-oxidized hPTH (1-34) (Figure 3-6).

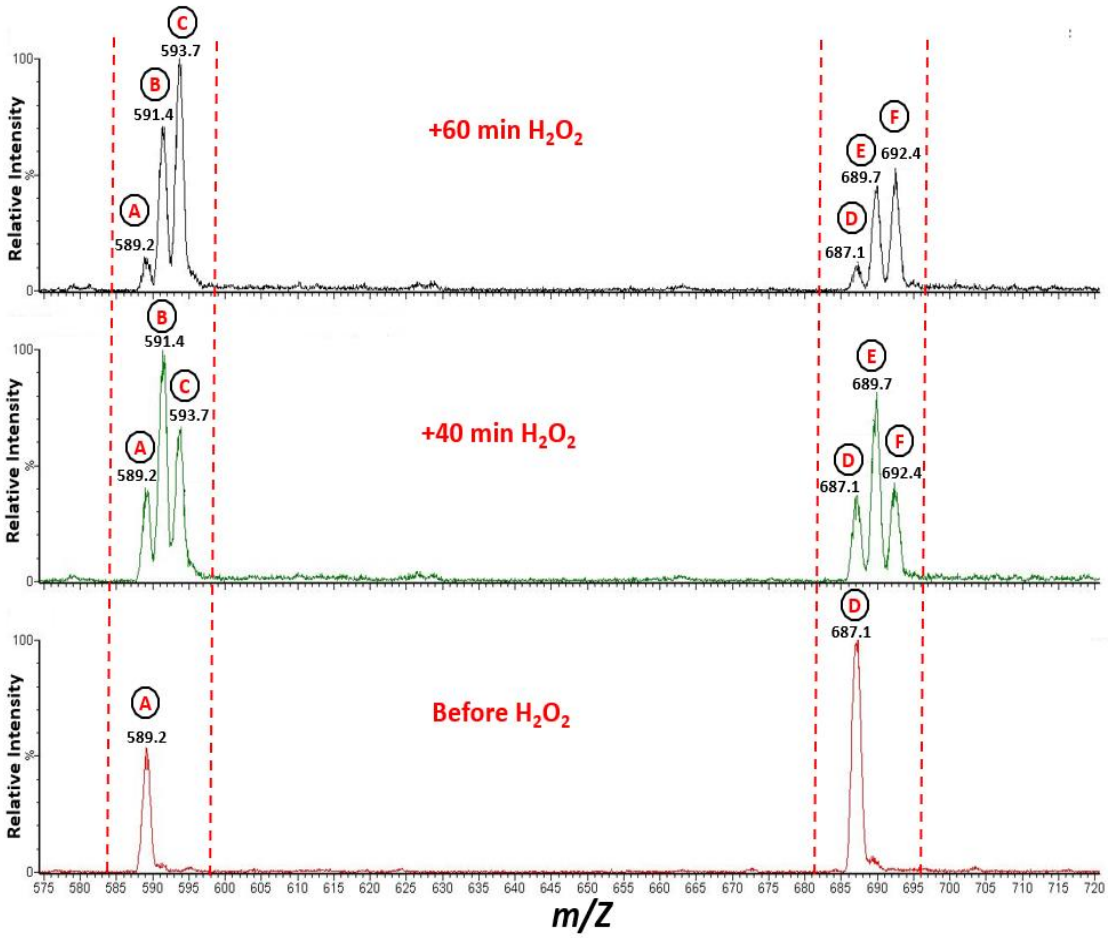


**Figure 3-6 MS spectrum of hPTH (1-34) (MW = 4117.8 D) before and after 40 and 60 min oxidation with $H_2O_2$.** *A & D represent +7 and +6 charged state of non-oxidized hPTH (1-34) respectively. B & E represent +6 and +7 charged state of hPTH (1-34) oxidized at Met 8 or Met 18 respectively (single-oxidized form with a mass shift of 16 units). C & F represent +6 and +7 charged state of hPTH (1-34) oxidized at both Met 8 and Met 18 respectively (double-oxidized form with a mass shift of 32 units). Note the change by time post-oxidation in the intensity of non-oxidized and oxidized hPTH (1-34) forms.*

**Table 3.1 MRM transitions, cone voltages, and collision energies for non-oxidized, single oxidized, double oxidized hPTH 1-34, and rPTH1-34 (internal standard IS)**

| | MRM Transition | Cone Voltage (V) | Collision Energy (eV) |
|---|---|---|---|
| Non-oxidized hPTH (1-34) | 589.2>656.1 | 35 | 10 |
| | 687.1>787.1 | 35 | 16 |
| Single oxidised Met8 or Met18 hPTH (1-34) | 591.4>658.8 | 35 | 10 |
| | 689.7>790.3 | 35 | 16 |
| Double oxidised Met8 & Met18 hPTH (1-34) | 593.7>661.5 | 35 | 10 |
| | 692.4>793.5 | 35 | 16 |
| rPTH (1-34) (IS) | 580.7>649.1 | 35 | 10 |
| | 677.1>777.9 | 35 | 16 |

### 3.1.2 Liquid-chromatography method development

The LC method development for non-oxidized/oxidized PTH (1-34) showed that both peptide forms eluted off the column between 22% and 25% mobile phase B (Figure 3-7 and 3-8). Most of the C18 columns that have been evaluated during LC method development produced low intensity PTH (1-34) peaks which look inappropriately broad with front tailing. AQUITY UPLC® BEH C18 column works the best among all evaluated columns listed in table 2.2 in terms of peak intensity. However, peak broadness and tailing were not rectified by the use of the BEH C18 column. The use of an AQUITY UPLC® Peptide CSH™ C18 column attenuates the broad PTH (1-34) peak and produces symmetric PTH (1-34) peaks with higher intensity compared to the BEH C18 column (Figure 3-9). As it is shown in figure 3-8, all peaks are resolved, except the two single-oxidized hPTH (1-34) due to similarity in their molecular mass.

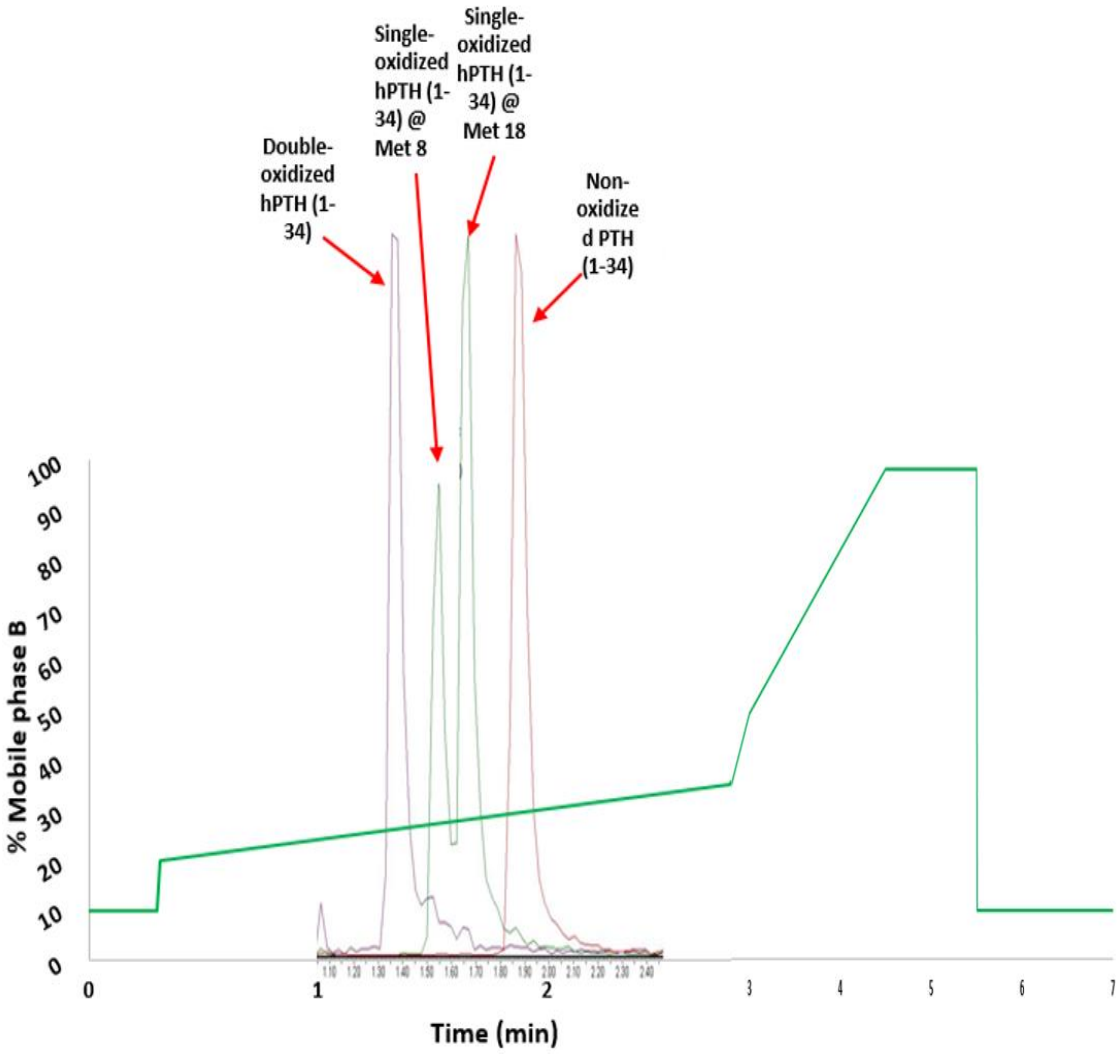


**Figure 3-7 LC gradient for PTH (1-34).** *The gradient started at 10% B. Gradient from 20% to 30% B eluted off non-oxidizedt/oxidized hPTH (1-34) as well as rPTH (1-34) (IS)*

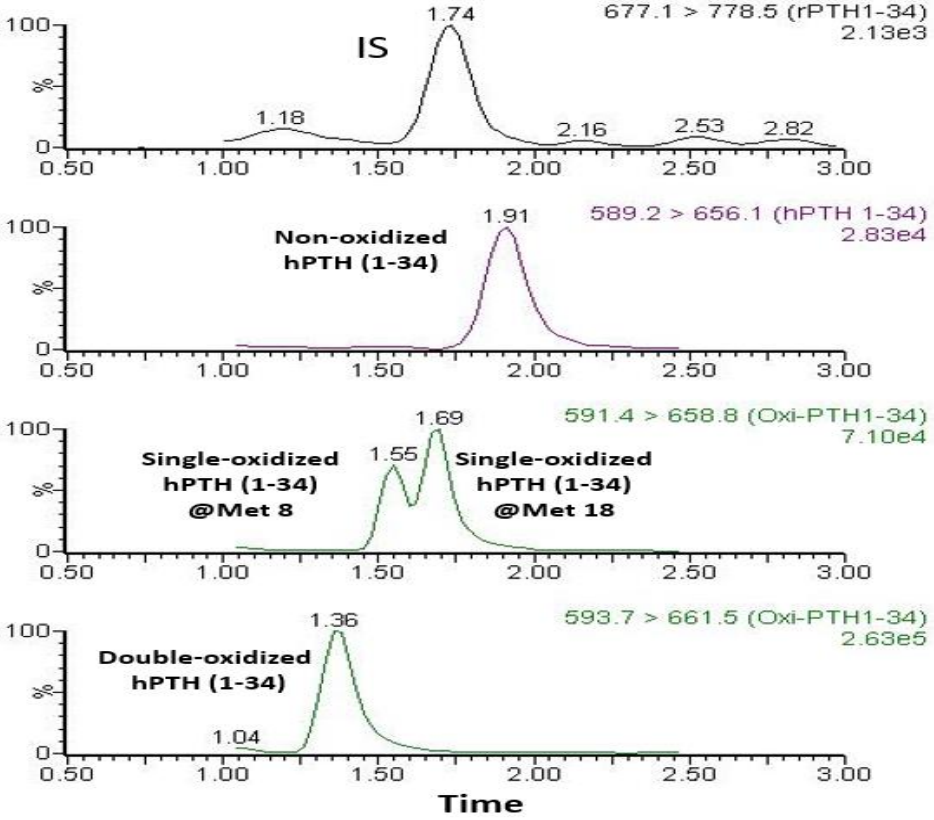


**Figure 3-8 Chromatograms showing elution time of non-oxidized, oxidized hPTH (1-34) and the IS.**

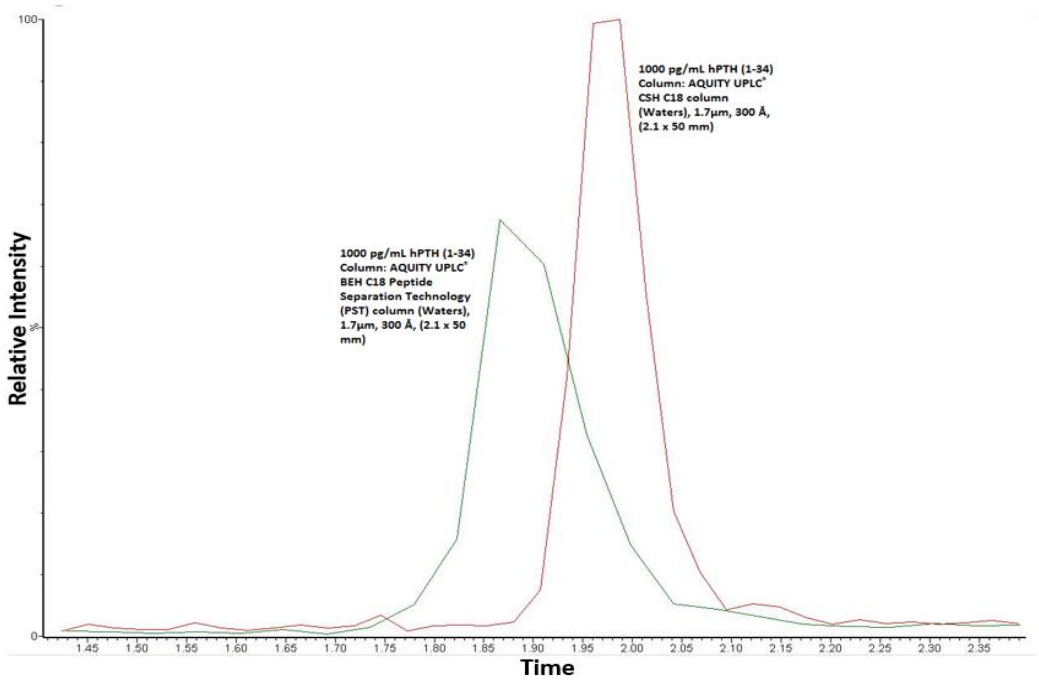


**Figure 3-9 Neat aqueous hPTH 1-34 standard peak run using UPLC BEH column (green), and UPLC CSH column (red). Note the difference in the peak width and height. *CSH column gives better peak shape and improve the intensity compared to BEH column.***

It was observed that adding a small amount of carrier proteins (e.g. calf serum, rat plasma, or BSA) to the solvent used to prepare aqueous peptide calibration standards is important when developing an LC method for peptides. Adding 0.01% of carrier protein to hPTH (1-34) aqueous standard increases the intensity 2-fold compared to that not containing carrier protein (Figure 3-10).

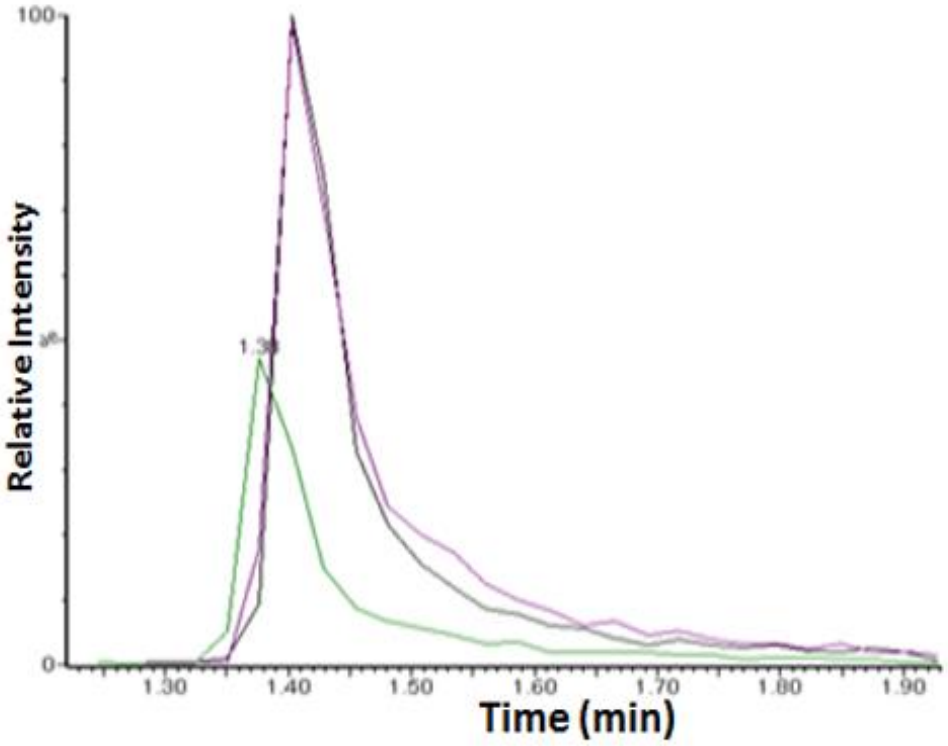


**Figure 3-10 Effect of adding carrier protein in hPTH (1-34) peak intensity.** *Neat hPTH (1-34) standard in water: acetonitrile: formic acid (green peak), Water: acetonitrile: formic acid: calf serum (purple peak), water: acetonitrile: formic acid: BSA (**black**) using AQUITY UPLC® BEH C18 Peptide Separation Technology (PST) column (Waters), 1.7µm, 300 Å, (2.1 x 50 mm). Note the 2-fold increase in peak intensity when small amount carrier protein was added.*

### 3.1.3 Sample preparation method development

NSB of PTH (1-34) peptide to surfaces was a concern. So, in an attempt to minimise NSB during sample preparation, the need to dry-down eluates was avoided. Therefore, the µElution SPE plate was selected for extraction method development. The advantage of µElution SPE plate is that no evaporation and reconstitution is necessary due to small elution volumes required (as low as 25 µL) and it is ideal for analyte enrichment.

### *3.1.3.1 SPE method development*

#### 3.1.3.1.1 Phase chemistry selection, load optimization and establishment of optimal wash solvent

When a reverse-phase (RP)-C18 Oasis® HLB µElution 96-well plate was used, pre-treatment of hPTH (1-34) with high pH solvent (5% $NH_4OH$) yielded the best recovered peak area count in eluate compared to acidified samples (pre-treated with low pH solvent 2%FA) (figure 3-11). hPTH (1-34) appeared more strongly retained by RP SPE under high pH, where a stronger solvent could be used during the wash step. Up to 40% MeOH could be used as a wash solvent on the HLB (C18) SPE before premature elution occurred (Figure 3-12). Premature elution occurred with lower MeOH percentage (20% MeOH) under low pH (figure 3-12). hPTH (1-34) breakthrough was observed under low pH conditions, where signals were detected in load flow-through eluate of samples pre-treated with 2% FA solvent, whereas signals were absent in load flow-through eluate of samples pre-treated with 5% $NH_4OH$. One elution cycle (2 x 25 µL 0.2%FA in 70% ACN) was sufficient to elute off all hPTH (1-34) from the HLB (C18) SPE plate as no signals were seen in the second elution cycle.

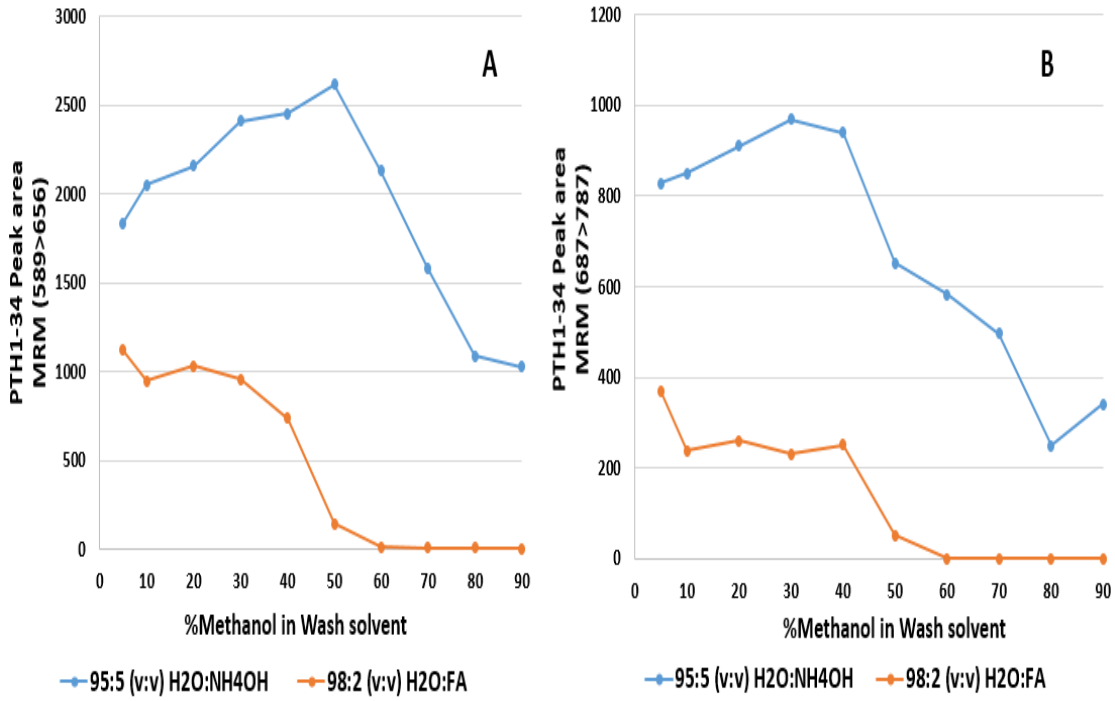


**Figure 3-11 hPTH (1-34) peak area plot against MeOH ratio in wash solvent measured in eluate (1st cycle) using Waters Oasis® HLB µElution 96-well plate.** *hPTH (1-34) peak area signals for MRM 589>656. (B) hPTH (1-34) peak area signals for MRM 687>787.*

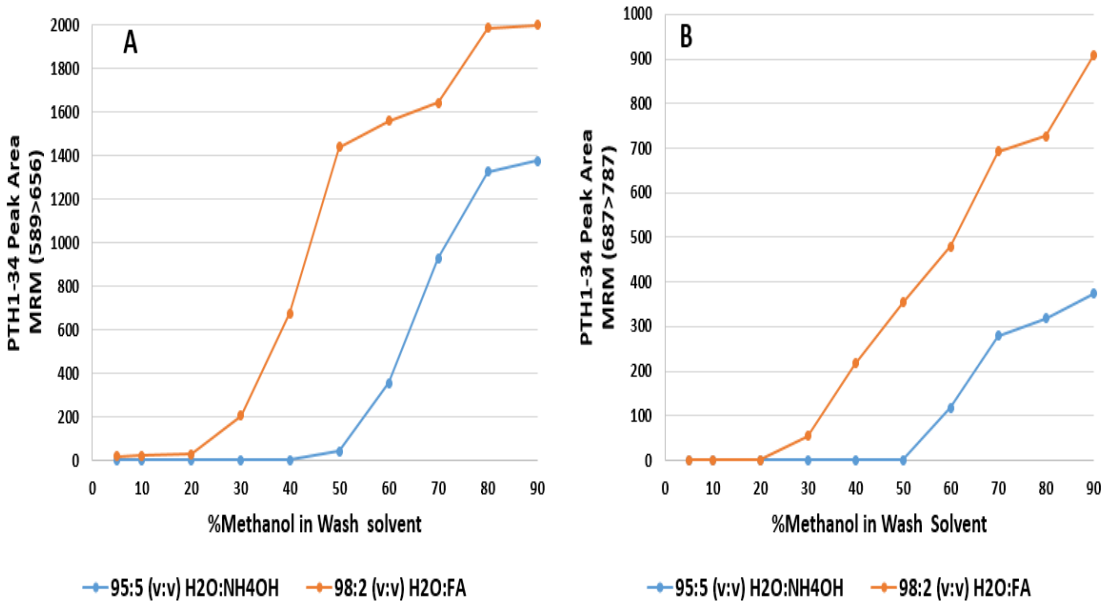


**Figure 3-12 hPTH (1-34) peak area plot against MeOH ratio in wash solvent measured in wash elute using Waters Oasis® HLB µElution 96-well plate.** *(A) hPTH (1-34) peak area signals for MRM 589>656. (B) hPTH (1-34) peak area signals for MRM 687>787. A trace peak area signal count was detected in wash solution collection when 50% MeOH wash solution was used.*

When an Oasis® MAX µElution 96-well plate that comprises both RP and anion-exchange modes of interaction was used for SPE, hPTH (1-34) pre-treated with high pH solvent (5%$NH_4OH$) showed the same behaviour as with RP HLB plate. The MAX retained hPTH (1-34) much stronger than the HLB. In contrast to the HLB, extraction with the MAX yielded lower hPTH (1-34) peak area in the first elution cycle (figure 3-13) and signals were still seen in the second elution cycle (figure 3-14). There was no breakthrough or premature elution observed with the MAX under high pH conditions. hPTH (1-34) was completely unretained by the MAX under low pH conditions (pre-treated with 2%FA) as signals were not detected in eluate (figure 3-13 and 3-14), whereas very high signals were detected in load flow-through eluate (Figure 3-15) and in wash elute (figure 3-16).

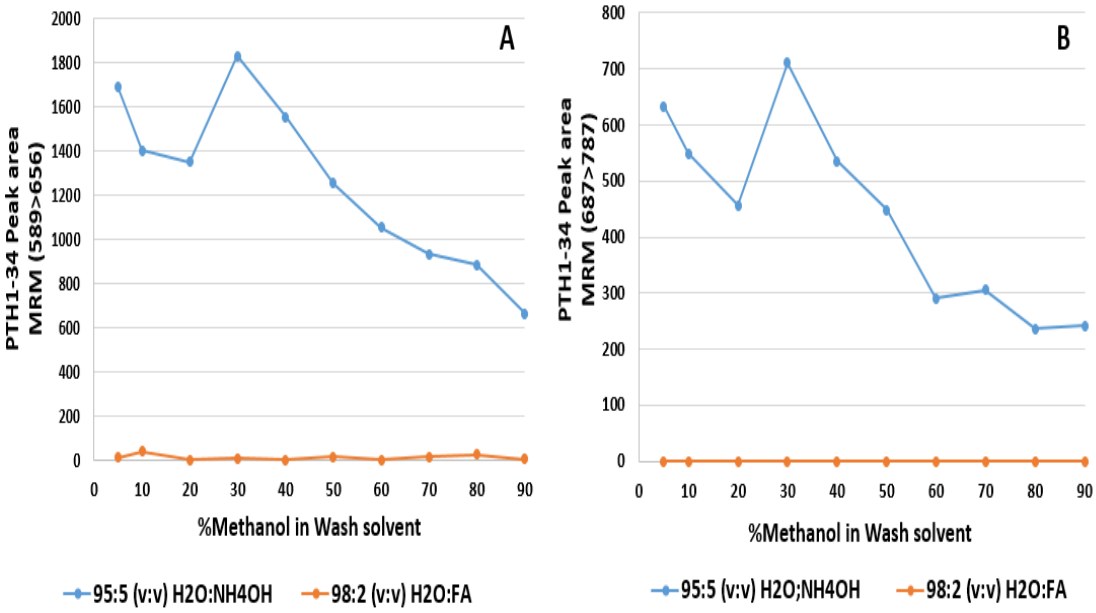


**Figure 3-13 hPTH (1-34) peak area plot against MeOH ratio in wash solvent measured in elute eluate (1st cycle) using Waters Oasis® MAX µElution 96-well plate.** *(A) hPTH (1-34) peak area signals for MRM 589>656. (B) hPTH (1-34) peak area signals for MRM 687>787.*

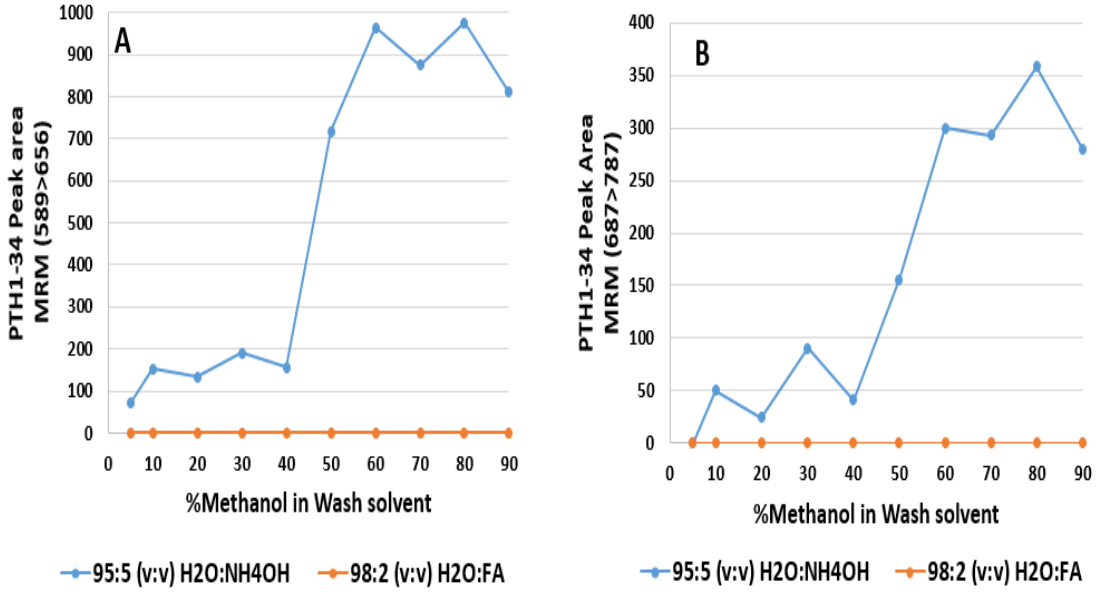


**Figure 3-14 hPTH (1-34) peak area plot against MeOH ratio in wash solvent measured in elute eluate (2nd cycle) using Waters Oasis® MAX µElution 96-well plate.** *(A) hPTH (1-34) peak area signals for MRM 589>656. (B) hPTH (1-34) peak area signals for MRM 687>787.*

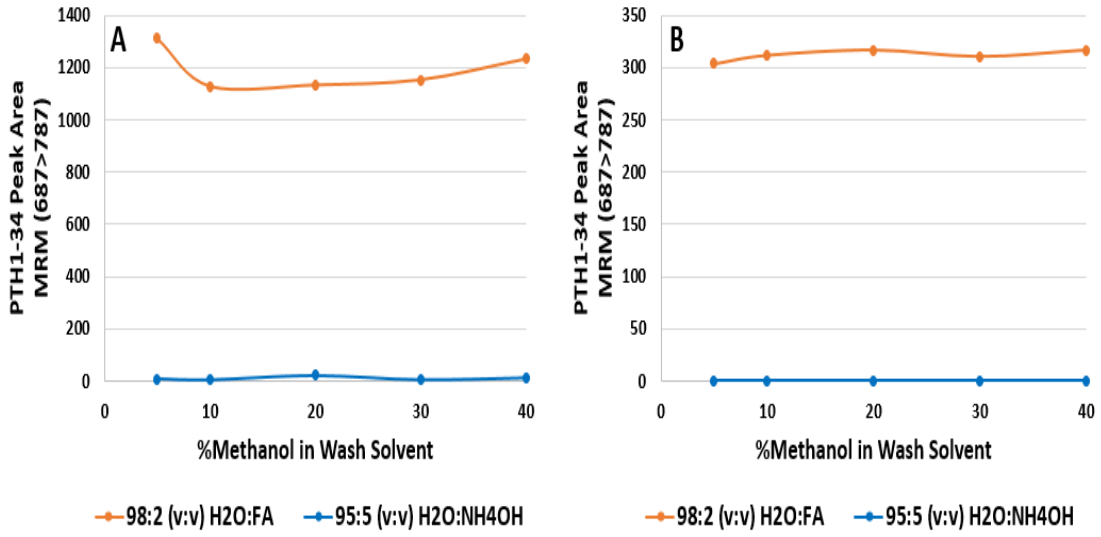


**Figure 3-15 hPTH (1-34) peak area plot against MeOH ratio in wash solvent measured in load flow-through eluate using Waters Oasis® MAX µElution 96-well plate.** *(A) hPTH (1-34) peak area signals for MRM 589>656. (B) hPTH (1-34) peak area signals for MRM 687>787.*

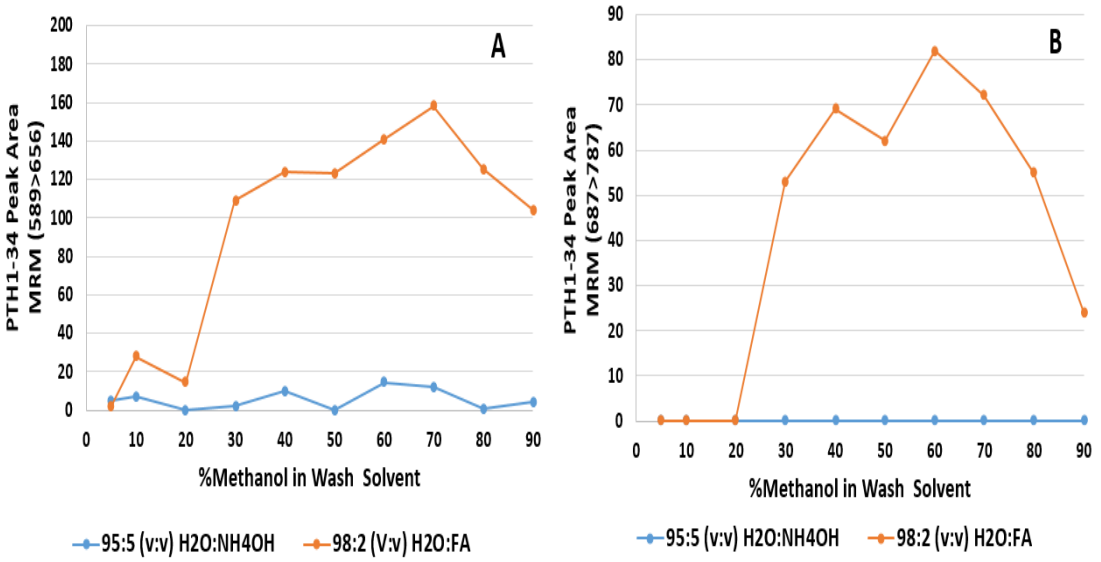


**Figure 3-16 hPTH (1-34) peak area plot against MeOH ratio in wash solvent measured in wash eluate using Waters Oasis® MAX µElution 96-well plate.** *(A) hPTH (1-34) peak area signals for MRM 589>656. (B) hPTH (1-34) peak area signals for MRM 687>787.*

#### 3.1.3.1.2 Optimal Elution solvent

At this stage, decisions were made on the best SPE plate to be used, the most appropriate pre-treatment procedure and what optimum methanol ratio in wash

solvent. To optimize organic ratio in eluting solution, the same approach used in wash step optimization was followed. A stock of hPTH (1-34) aqueous standard (1000 pg/mL) was prepared and divided in seven tubes. Eluting solutions varying in organic content ratio (30 – 90%) were used. 0.2% FA was added to the eluting solution to maintain the orthogonality of extraction procedure. Data showed that the optimum acetonitrile ratio required to elute PTH (1-34) from Oasis® HLB µElution is 70% of the eluting solution (Figure 3-17 and 3-18).

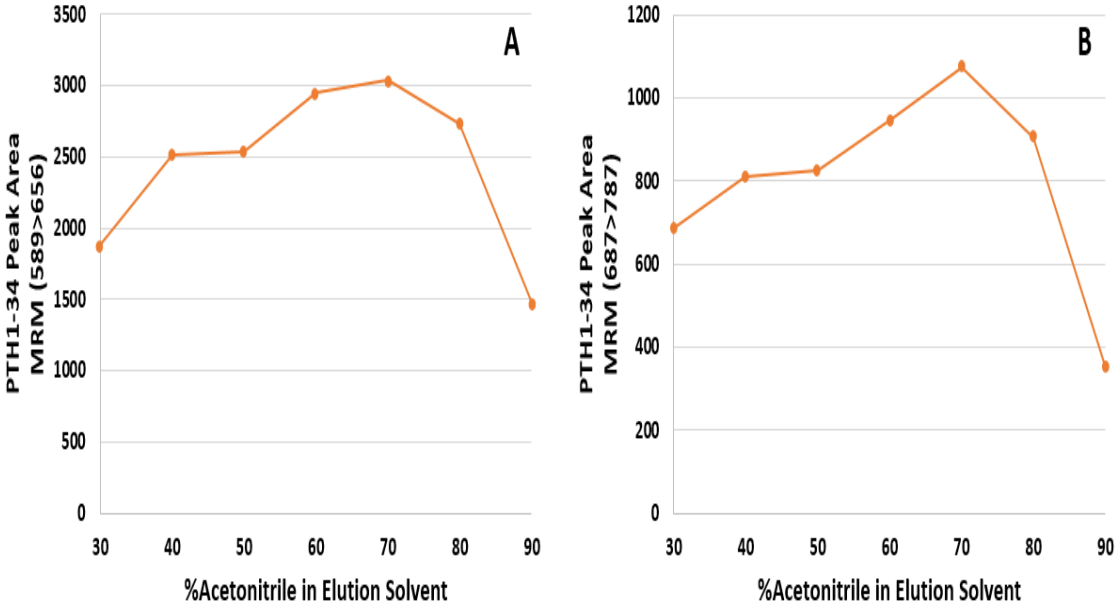


**Figure 3-17 PTH (1-34) Peak Area Plot against acetonitrile ratio in elution solvent measured in elute eluate (1st cycle) using Oasis HLB SPE plate.** *(A) hPTH (1-34) peak area count for MRM 589>656. (B) hPTH (1-34) peak area count for MRM 687>787.*

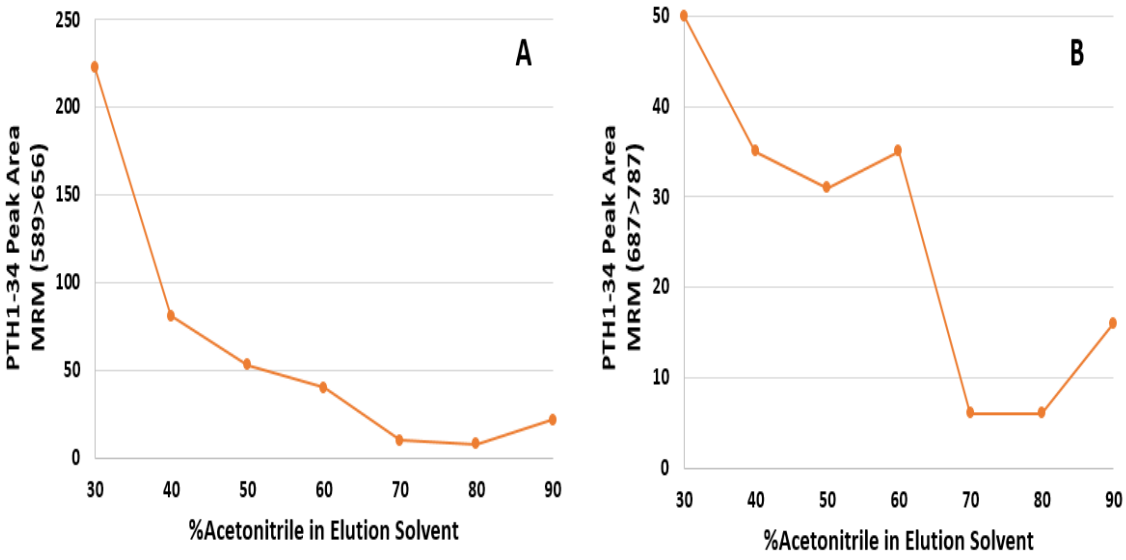


**Figure 3-18 hPTH (1-34) Peak Area Plot against acetonitrile ratio in elution solvent measured in elute eluate (2nd cycle) using Oasis HLB SPE plate.** *(A) hPTH (1-34) peak area count for MRM 589>656. (B) hPTH (1-34) peak area count for MRM 687>787.*

#### 3.1.3.1.3 Sample pre-treatment optimisation

The following bar graph (Figure 3-19) demonstrates the response yield (mean ± SEM) at both quantitative transition (589>656) and qualitative transition (687>787) of 1000 pg/mL hPTH (1-34) in human plasma, which was prepared as a stock and divided in two groups of 6 samples. Samples in group 1 were pre-treated by simple dilution with 0.5 mL 5%$NH_4OH$ only. While samples in group 2 were first crashed with acetonitrile (1:1 plasma: ACN) followed by dilution of supernatant with 1 mL 5%$NH_4OH$. Response yield of group 1 samples is approximately 2-fold higher than that of group 2 samples.

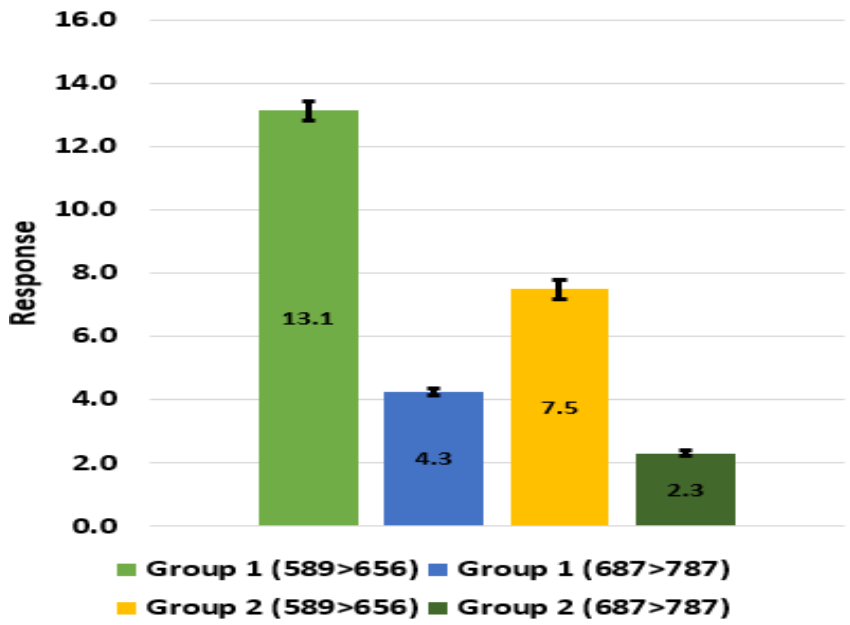


**Figure 3-19 Bar graph illustrates response yield of samples (n=6) pre-treated by simple dilution with 5% $NH_4OH$ (Group 1) and of samples (n=6) which were firstly precipitated by acetonitrile and then the supernatant diluted with 1 mL $NH_4OH$ (Group 2).** *Values in the middle of the bars represent the mean response and the error bar represent SEM.*

### 3.1.4 Method Validation

#### *3.1.4.1 Calibration Curve/Linearity*

The calibration curve was linear across a range from 10 to 2000 pg/mL. Using a 1/x weighting, the $r^2$ values for all curves were consistently >0.990. Figure 3-20 illustrates the typical calibration curve and linearity was evidenced across the calibration range.

Table 3.2 and the line chart in figure 3-21 show the LC-MS/MS response of hPTH (1-34) calibrators (10, 25, 50, 250, 500, 1000, 2000 pg/mL) and QCs (20, 100, 200, 800 pg/mL) in charcoal-stripped human plasma in six analytical runs. Plots of σ vs instrument responses and $\sigma^2$ vs instrument responses of calibration standards and QCs in six analytical runs showed that the relationship between σ and response, and between $\sigma^2$ and response followed the same linear trend. In most of the standard curve range (10 to 1000 pg/mL), the concave upward quadratic curvature between $\sigma^2$ and concentration was not obvious, and was not substantial therafter. This indicates that $\frac{1}{x}$ wighting factors has helped to maintain calibration curve stability.

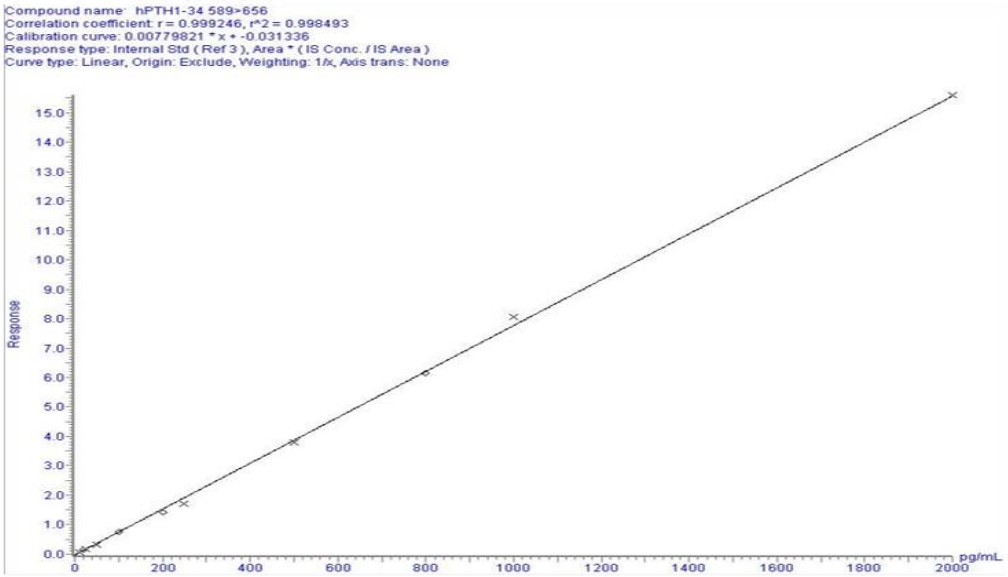


**Figure 3-20 Typical calibration curve for hPTH (1-34) spiked into charcoal-stripped human EDTA plasma.** *$R^2$ value is 0.998. Crosses represent calibration standards and dots represent QCs.*

**Table 3.2 Standard deviation (σ) and variance ($\sigma^2$) of LC-MS/MS responses of hPTH (1-34) calibrators and QCs in charcoal-stripped human EDTA plasma in six analytical runs.**

| Calibrator/QC (pg/ml) | LC-MS/MS response for hPTH (1-34) | | | | | | | |
|---|---|---|---|---|---|---|---|---|
| | Run1 | Run2 | Run3 | Run4 | Run5 | Run6 | Σ | $\sigma^2$ |
| 10 | 0.061 | 0.070 | 0.061 | 0.068 | 0.028 | 0.059 | 0.0153 | 0.0002 |
| 20 | 0.080 | 0.155 | 0.112 | 0.106 | 0.154 | 0.138 | 0.0299 | 0.0009 |
| 25 | 0.128 | 0.134 | 0.164 | 0.112 | 0.218 | 0.175 | 0.0386 | 0.0015 |
| 50 | 0.558 | 0.228 | 0.258 | 0.283 | 0.413 | 0.309 | 0.1235 | 0.0153 |
| 100 | 0.932 | 0.763 | 0.782 | 0.677 | 0.933 | 0.738 | 0.1055 | 0.0111 |
| 200 | 1.640 | 1.672 | 1.350 | 1.358 | 1.780 | 1.422 | 0.1834 | 0.0336 |
| 250 | 2.571 | 2.700 | 2.085 | 2.771 | 2.669 | 2.716 | 0.2539 | 0.0644 |
| 500 | 4.443 | 4.526 | 4.110 | 4.730 | 5.160 | 3.784 | 0.4790 | 0.2294 |
| 800 | 7.028 | 6.014 | 6.815 | 6.553 | 7.634 | 6.136 | 0.6006 | 0.3607 |
| 1000 | 8.387 | 7.231 | 8.202 | 6.970 | 8.882 | 8.046 | 0.7224 | 0.5219 |
| 2000 | 17.590 | 15.113 | 16.808 | 14.178 | 17.480 | 15.598 | 1.3814 | 1.9083 |

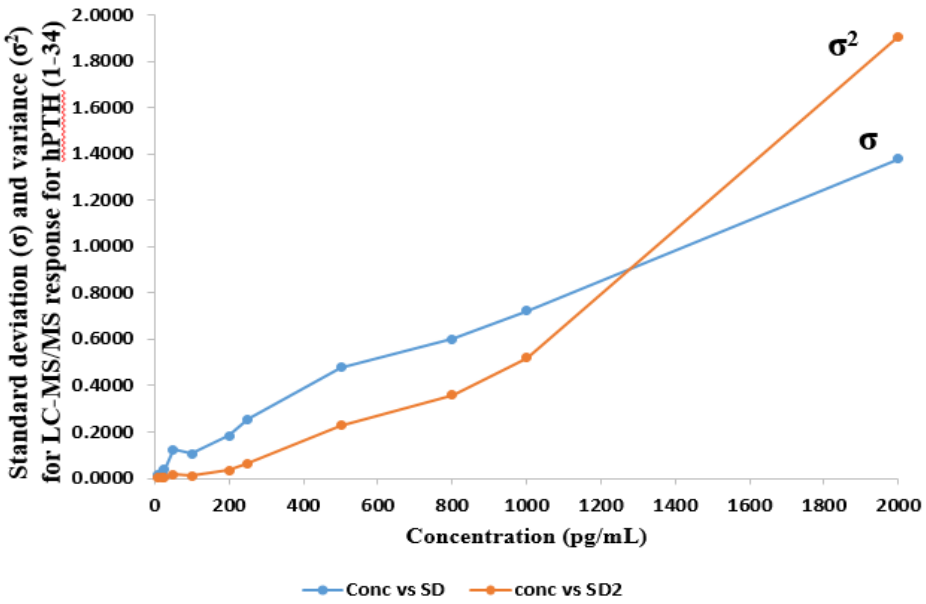


**Figure 3-21 Standard deviation (σ) and variance ($\sigma^2$) for instrument responses of Calibration standards and QCs in six analytical runs for hPTH (1-34) in charcoal-stripped human EDTA plasma. Calibrator concentration range: 10 – 2000 pg/mL**

### *3.1.4.2 Carry over*

No carryover signal of hPTH (1-34) was detected in blank plasma samples analysed immediately after a sample containing 2000 pg/mL hPTH (1-34).

### *3.1.4.3 Matrix effect assessment*

The two approaches followed to evaluate the matrix effect indicated that matrix effects were reduced to a minimum and did not contribute significantly to the quantification of hPTH (1-34). Comparison of slopes of the three calibration curves generated from matrix effect assessment experiments shows that the matrix effect was negligible. The slope of the calibration curve constructed by analysing neat calibration standards that have not been extracted, neat calibration standards that have been extracted, and extracted charcoal-stripped plasma was 0.0066, 0.0077 and 0.0072 respectively (Figure 3-22). The average percentage matrix effect for 100 pg/mL and 1000 pg/mL standard concentrations was 6.1% and 4.0% (Calculated using equation 1) respectively. Table 3.3 shows the response values obtained for each of the five determination runs for each of the two concentrations of sample A (in solvent) and sample B (in matrix).

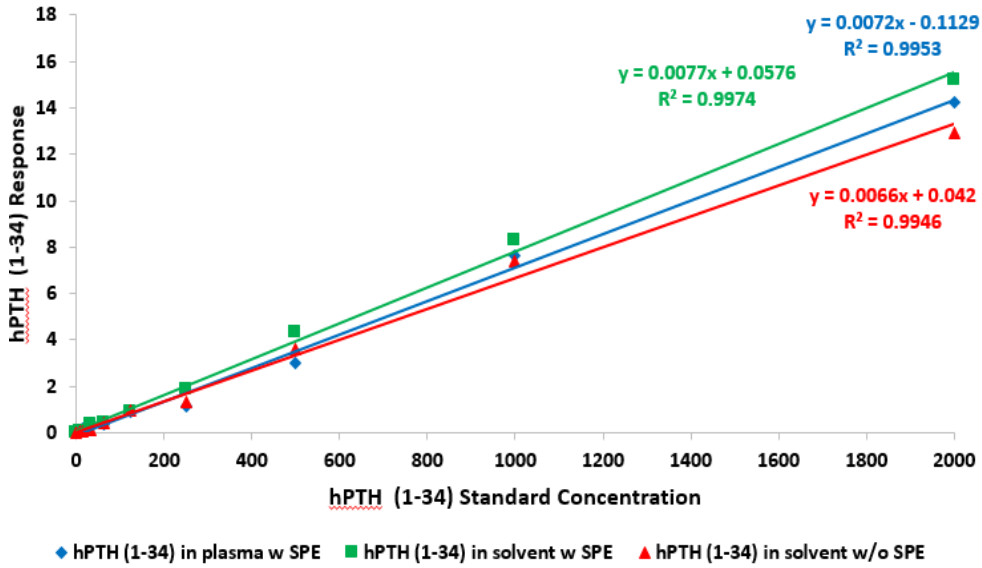


**Figure 3-22 Calibration curve plots for hPTH (1-34) measured in extracted plasma (blue), and in solvent (90:10:0.1:0.01) (v:v:v:w) H2O:ACN:FA:BSA with (green) and without (red) SPE extraction. The figure demonstrates the similarity in curve slopes, which revealed minor matrix effects on hPTH (1-34) assay.**

**Table 3.3 hPTH (1-34) response obtained for five determinations of each of the two concentrations of sample A and B.**

| | Low Concentration (100 pg/mL hPTH (1-34) | | High Concentration (1000 pg/mL hPTH (1-34) | |
|---|---|---|---|---|
| Aliquot # | Sample A (in solvent) | Sample B (in matrix) | Sample A (in solvent) | Sample B (in matrix) |
| 1 | 1.00 | 0.79 | 9.55 | 8.04 |
| 2 | 0.84 | 0.92 | 7.95 | 8.18 |
| 3 | 0.90 | 0.71 | 7.74 | 8.57 |
| 4 | 0.77 | 0.98 | 8.89 | 9.28 |
| 5 | 0.61 | 0.94 | 8.09 | 9.81 |
| Average Response | 0.82 | 0.87 | 8.44 | 8.78 |
| SD | 0.15 | 0.11 | 0.76 | 0.75 |
| %Matrix effect | 6.1% | | 4.0% | |

### *3.1.4.4 Precision and Accuracy*

The inter-assay precision (%CV) and accuracy (%RE) were <9.8% and <14.9% respectively, for four QCs (20, 100, 200, and 800 pg/mL). The intra-assay precision and accuracy for these QCs over a period of a month were <7.8 and <6.9

respectively, for four QCs (20, 100, 200, and 800 pg/mL). Table (3.4) demonstrates inter- and intra-assay precesion and accuracy results. The inter-assay and intra-assay precision and accuracy data indicate that the method is accurate and reproducible.

**Table 3.4 Inter- and intra-assay precision and accuracy of LC-MS/MS hPTH (1-34) assay.**

| | QC1 (20 pg/mL) | QC2 (100 pg/mL) | QC3 (200 pg/mL) | QC4 (800 pg/mL) |
|---|---|---|---|---|
| Inter-assay | | | | |
| Mean | 24.4 | 108.5 | 212.8 | 828.0 |
| SD | 2.4 | 8.9 | 13.8 | 42.4 |
| SE | 0.8 | 2.8 | 4.4 | 13.4 |
| %CV | 9.8 | 8.2 | 6.5 | 5.1 |
| %RE | 14.9 | 9.8 | 7.7 | 4.9 |
| Intra-assay | | | | |
| Mean | 20.8 | 102.1 | 201.9 | 816.2 |
| SD | 1.6 | 7.1 | 14.7 | 19.0 |
| SE | 0.5 | 2.2 | 4.7 | 6.0 |
| %CV | 7.8 | 6.9 | 7.3 | 2.3 |
| %RE | 6.9 | 4.9 | 6.4 | 2.6 |

### *3.1.4.5 Ion suppression*

The susceptibility of the method to ion suppression by infusion of constant flow of a neat aqueous standard of hPTH (1-34) at concentration 100 ng/mL via a T-junction at a flow rate 20 µL/min directly into the MS/MS source was investigated. A sample of extracted blank EDTA human plasma with and without IS, as well as extracted hPTH (1-34) sample were injected into the column at 400 µL/min. Figure 3-23 shows that hPTH (1-34) and the internal standard do not co-elute with ion suppression/enhancement-causing species.

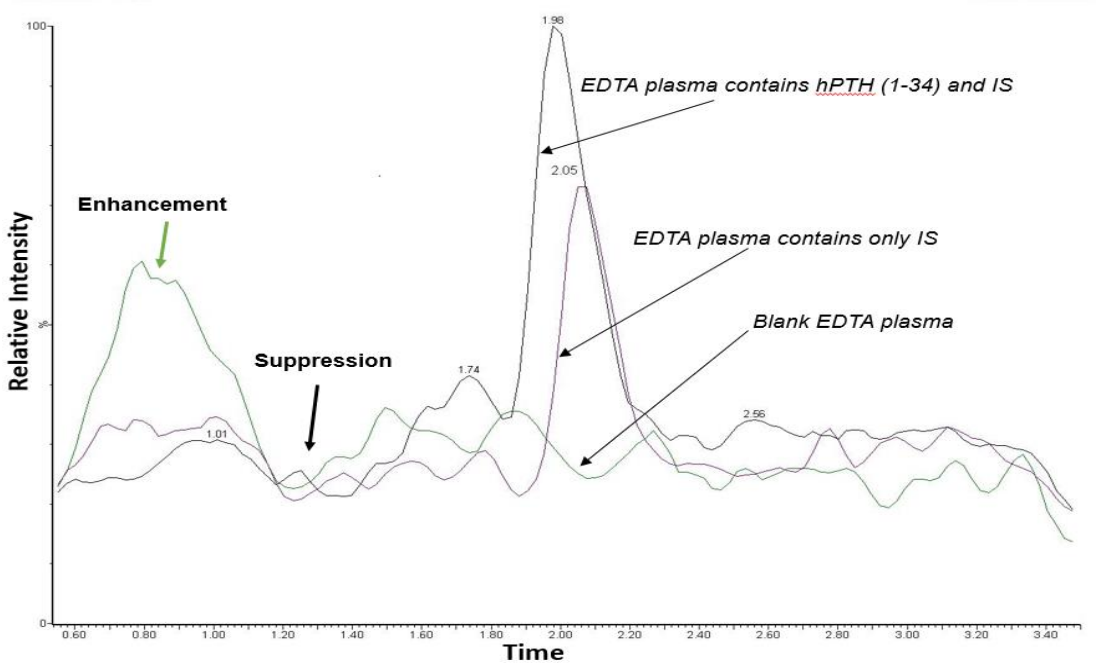


**Figure 3-23 Ion suppression from direct infusion.** *Suppression in baseline signals was observed during co-injection of extracted human plasma sample and post column infusion of PTH (1-34). The elution of hPTH (1-34) and the IS do not co-elute with suppression and enhancement ion species.*

### *3.1.4.6 Recovery efficiency*

The mean recovery of hPTH (1-34) was 107.2% (range 98.6-112.9%) (Table 3.5) The recovery data shows that the extraction method is able to efficiently recover hPTH (1-34) from human plasma.

**Table 3.5 Recovery data of hPTH (1-34) from human EDTA plasma.**

| Endogenous PTH(1-34) (pg/mL) | Spiked (pg/mL) | n | Expected concentration (endogenous + spiked), pg/mL | Mean (±SD) measured hPTH (1-34) (pg/mL) | %Recovery mean (%CV) |
|---|---|---|---|---|---|
| 8.4 | 20 | 3 | 28.4 | 28.0 (±1.0) | 98.6 (3.6) |
| 8.4 | 800 | 3 | 808.4 | 883.4 (±31.4) | 109.3 (3.6) |
| 77.5 | 20 | 3 | 97.5 | 101.9 (±2.0) | 104.5 (1.9) |
| 77.5 | 800 | 3 | 877.5 | 990.3 (±11.8) | 112.9 (1.2) |
| 602.7 | 20 | 3 | 622.7 | 665.0 (±14.8) | 106.8 (2.2) |
| 602.7 | 800 | 3 | 1402.7 | 1560.8 (±111.3) | 111.3 (7.1) |

### *3.1.4.7 LLoQ and LLoD*

A precision and accuracy assessment of LLoQ of hPTH (1-34) was performed at 10 pg/mL and demonstrated a %CV of 16.2% and %RE of 19.5%. The LLoD for the hPTH (1-34) assay was 2.1 pg/mL with a signal to noise ratio (S/N) value of ≈5 required for an LC-MS/MS assay (270, 271). A S/N value of 5 is good enough to differentiate between a true signal and instrument background noise.

### *3.1.4.8 Cross-reactivity testing*

Analysis of different lots of blank EDTA plasma samples from different sources using the LC-MS/MS assay showed no interfering peaks at the retention time of hPTH (1-34) on both m/z transitions as well as the IS and the response was below the LLoD, which indicates high assay selectivity.

The immunoassay showed an average of 6.5% cross reactivity to human PTH (1-84), 44.2% to rat PTH (1-34) and 0.65% to hPTHrP (1-36) while no reactivity was observed to hPTHrP (1-86) and hPTH (13-34) fragments. No interference was observed in the LC-MS/MS method with any of the peptides tested. Details are shown in table 3.6.

**Table 3.6 Cross-reactivity testing. Cross-reactivity of immunoassay to hPTH (1-84), rPTH (1-34), hPTHrP (1-86), hPTHrP (1-36), and hPTH (13-34).** Upper limit of quantification of the immunoassay is 1000 pg/mL.

| Analyte | Actual added amount (pg/mL) | Measure value (pg/mL) | Individual %Cross-reactivity | Average %Cross-reactivity |
|---|---|---|---|---|
| Blank plasma | | 5.3 | | |
| Human PTH (1-84) | 20,000 | >1000 | incalculable | 6.5 |
| | 2000 | 133.5 | 6.7 | |
| | 396 | 24.9 | 6.3 | |
| Rat PTH (1-34) | 20,000 | >1000 | incalculable | 44.2 |
| | 2000 | 871.9 | 43.6 | |
| | 396 | 177.0 | 44.7 | |
| Human PTH (13-34) | 20,000 | <4 | <0 | <0 |
| | 2000 | <4 | <0 | |
| | 396 | <4 | <0 | |
| Human PTHrP (1-86) | 20,000 | <4 | <0 | <0 |
| | 2000 | <4 | <0 | |
| | 396 | <4 | <0 | |
| Human PTHrP (1-36) | 20,000 | 6.1 | 0.2 | 0.65 |
| | 2000 | <4 | <0 | |
| | 396 | 4.5 | 1.1 | |

### 3.1.5 Method comparison

Method comparison between LC-MS/MS and the IDS immunoassay are illustrated by Passing-Bablok regression and Bland-Altman plots (figure 3-24 and 3-25). The Passing-Bablok analysis shows high correlation between the two methods with a Pearson coefficient of 0.973. The line of best fit generated a slope of 0.64 ($r^2$ = 0.95) for hPTH (1-34) (Figure 3-24). The LC-MS/MS method demonstrated a mean negative bias of -35.5 pg/mL with respect to the mean value of both methods (1.96 SD, 53.9 to -124.9 pg/mL) ($r$ = 0.883, $p$<0.001) (Figure 3-25). The negative bias appeared to be proportional or concentration-dependent ($p$<0.001) across the concentration range of (0 – 800) pg/mL.

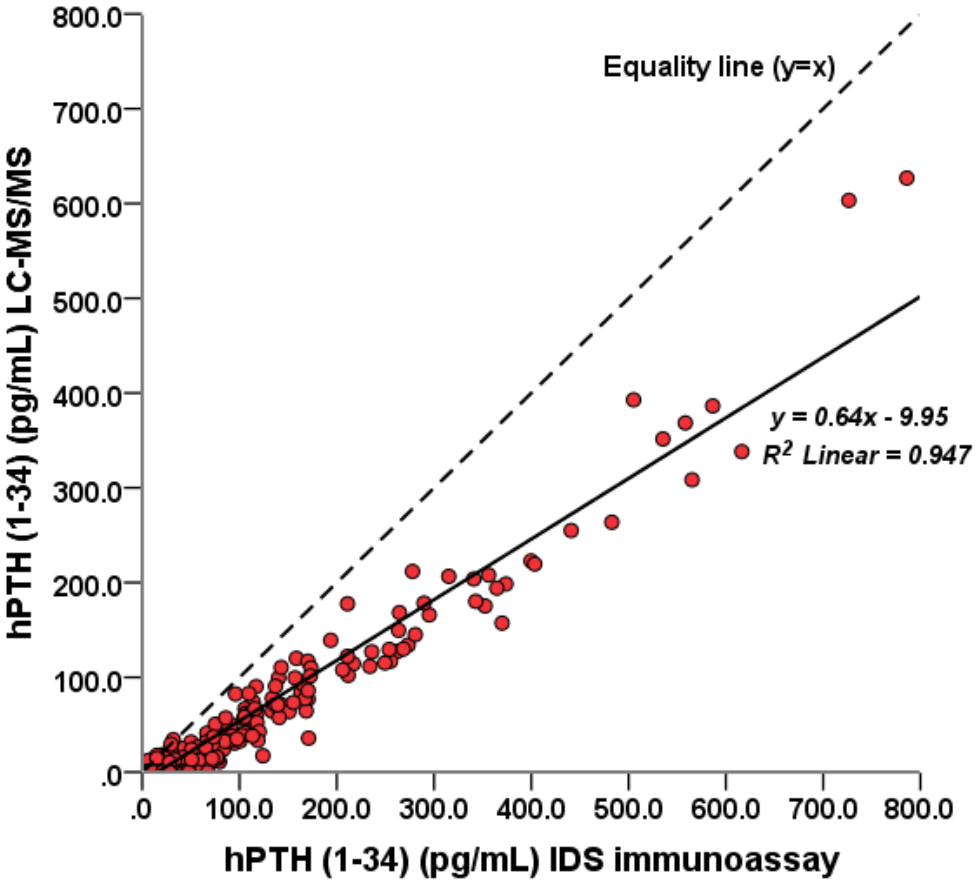


**Figure 3-24 Method comparison of the LC-MS/MS method with IDS immunoassay for hPTH (1-34) by Passing-Bablok regression analysis (n=390).** *Solid line in the graph represents the fitted regression line; dotted line is the line of equality/identity.*

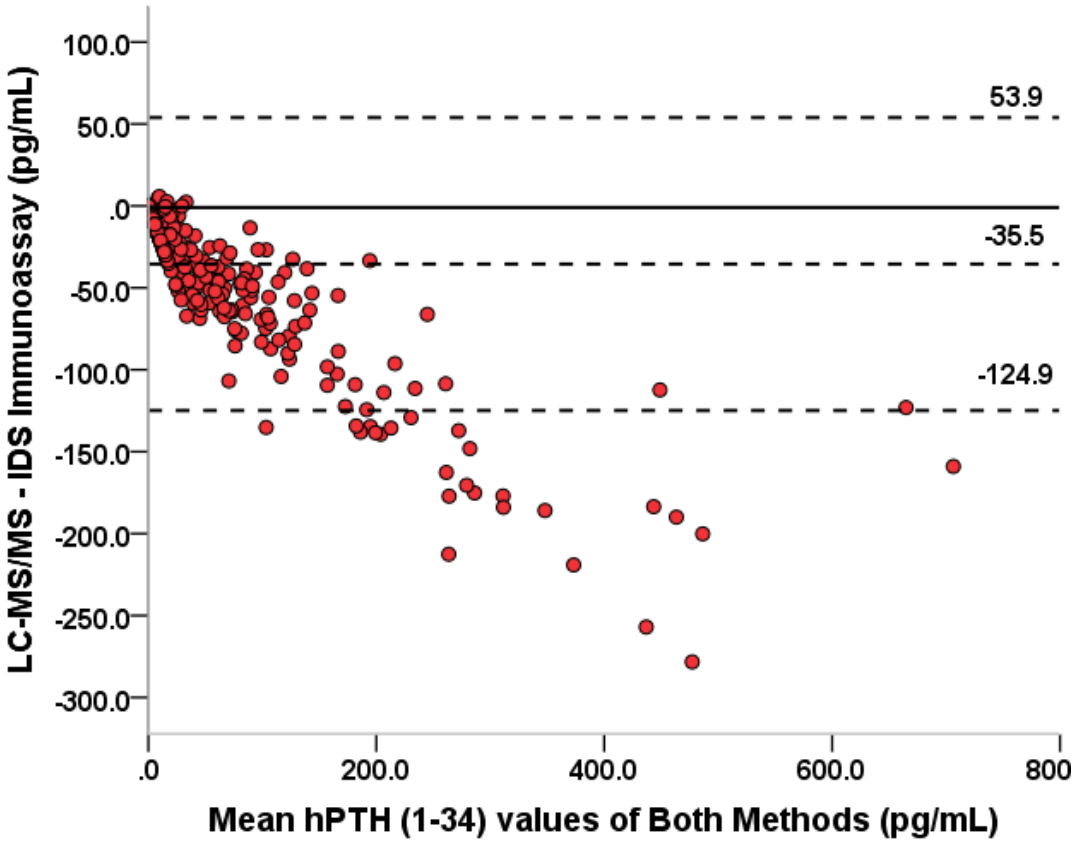


**Figure 3-25 Bland-Altman plots showing the bias of LC-MS/MS assay against the mean hPTH (1-34) values of both LC-MS/MS and IDS methods.** *Bias is shown in pg/mL. The minus sign indicates negative bias. The dashed lines represent average bias and the 95% limits of agreement, while solid line represents zero bias. Bias is proportional to the mean hPTH (1-34) concentration of both methods* ($p<0.001$).

In one experiment, hPTH (1-34) calibration standards (10-2000 pg/mL) were prepared in two different matrices, namely human EDTA plasma and fetal bovine serum. A fixed amount of hPTH (1-84) at a final concentration of 1000 pg/mL was added to all calibration standards. Then, standards were run in parallel on IDS-iSYS immunoassay and LC-MS/MS method and results plotted as shown in the graph below (Figure 3-26). LC-MS/MS assay results were not interfered by hPTH (1-84) and hPTH (1-34) standards results on both matrices were similar (slopes of EDTA plasma and fetal bovine serum curve were 0.99 and 1.00 respectively). In contrast, PTH (1-84) interferes with the immunoassay and results were highly affected by

matrix type, which is clearly indicated by the slopes of hPTH (1-34) calibration curve on human EDTA plasma (1.41) and fetal bovine serum (0.56). This experiment may suggest that the negative bias in the previous method comparison was actually correct measurement by LC-MS/MS and positive bias by the immunoassay.

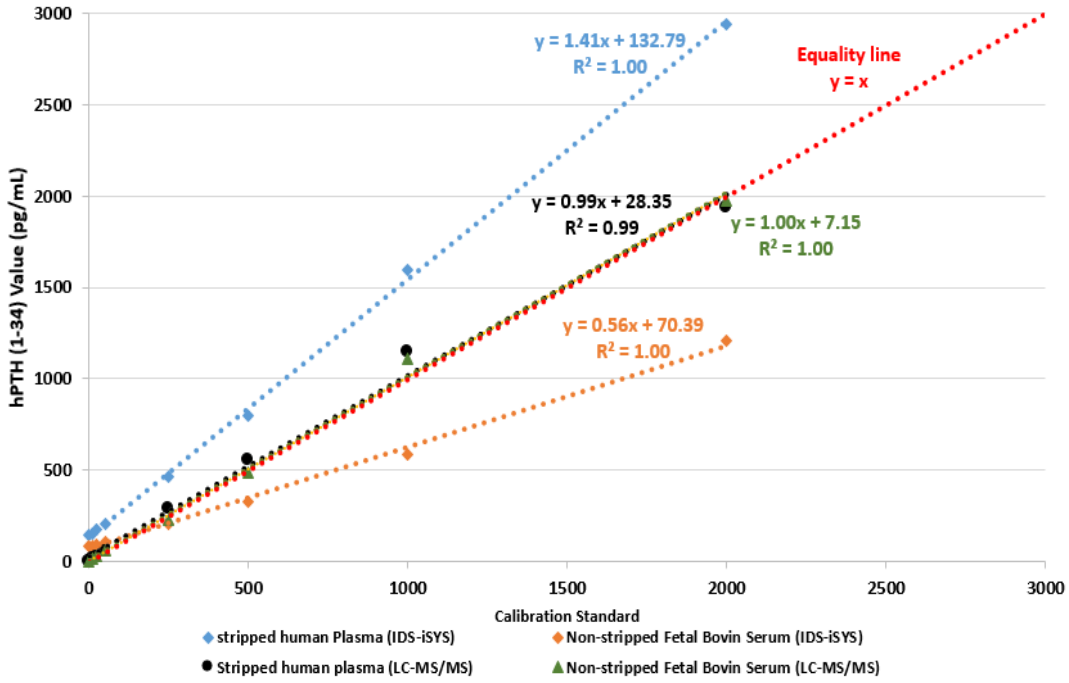


**Figure 3-26 Evaluation of matrix effect and cross-reactivity of LC-MS/MS assay and IDS-iSYS immunoassay to hPTH (1-84).** *Blue and orange dotted lines represent calibration curves for hPTH (1-34) spiked in charcoal-stripped human plasma and non-stripped fetal bovine serum respectively measured using iSYS immunoassay. hPTH (1-34) in charcoal-stripped-human plasma is approximately 2.5-fold higher than that in non-stripped fetal bovine serum when measured using the immunoassay. Black and green dotted lines represent calibration curves for hPTH (1-34) spiked in charcoal-stripped human plasma and non-stripped fetal bovine serum respectively measured on LC-MS/MS. The two curves are perfectly matched with each other and with the equality line.*

To confirm the effect of matrix type on the performance of the immunoassay, analysis of calibration standards was repeated, where hPTH (1-34) standards (range 1-500) were prepared in charcoal-stripped human plasma and charcoal-stripped fetal bovine calf serum. Calibration curves plots are shown in figure 3-27. hPTH (1-34) spiked in human plasma gives 1.4-fold higher concentration values compared to those spiked in fetal bovine serum.

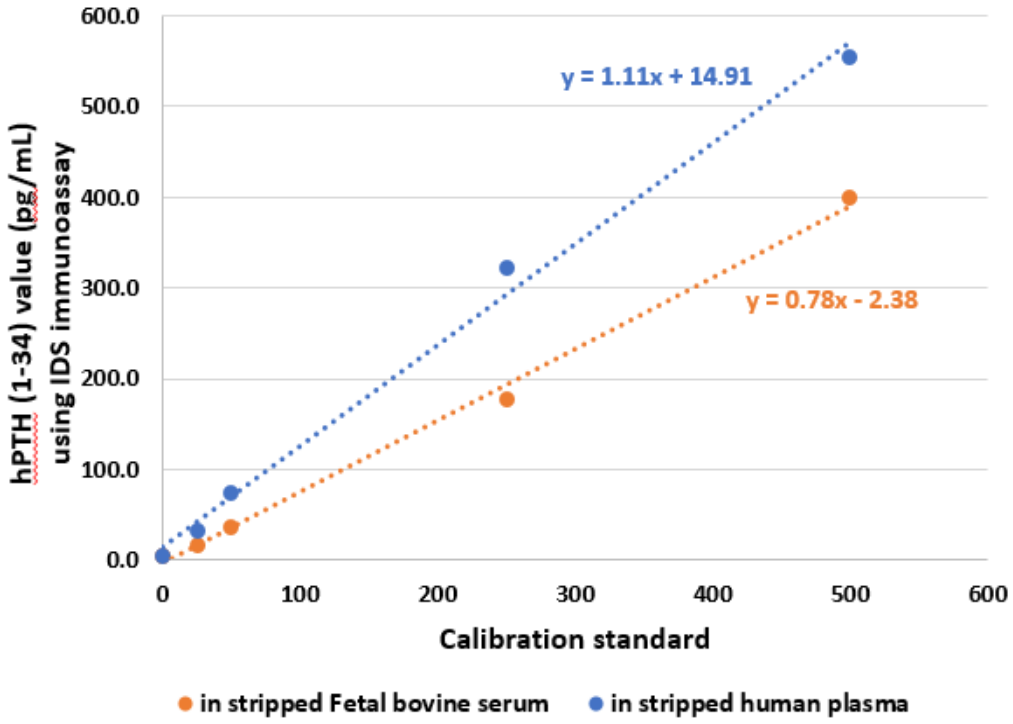


**Figure 3-27 Matrix effect on IDS-iSYS immunoassay.** *Shown calibration curves of hPTH (1-34) spiked in charcoal-stripped human EDTA plasma (Blue curve) and in charcoal-stripped fetal bovine serum. Note that hPTH (1-34) calibrator values are higher in human plasma than in bovine serum.*

After allocating MRMs for oxidized forms of hPTH (1-34), pooled rat plasma from animals that have been given oral PTH (1-34) was examined. All oxidized forms were presented in the analysed plasma. Figure 3-28 shows a real-time chromatogram run of the pooled rat plasma using the LC-MS/MS method. The chromatogram illustrates the presence of naturally occurring oxidized forms of hPTH (1-34).

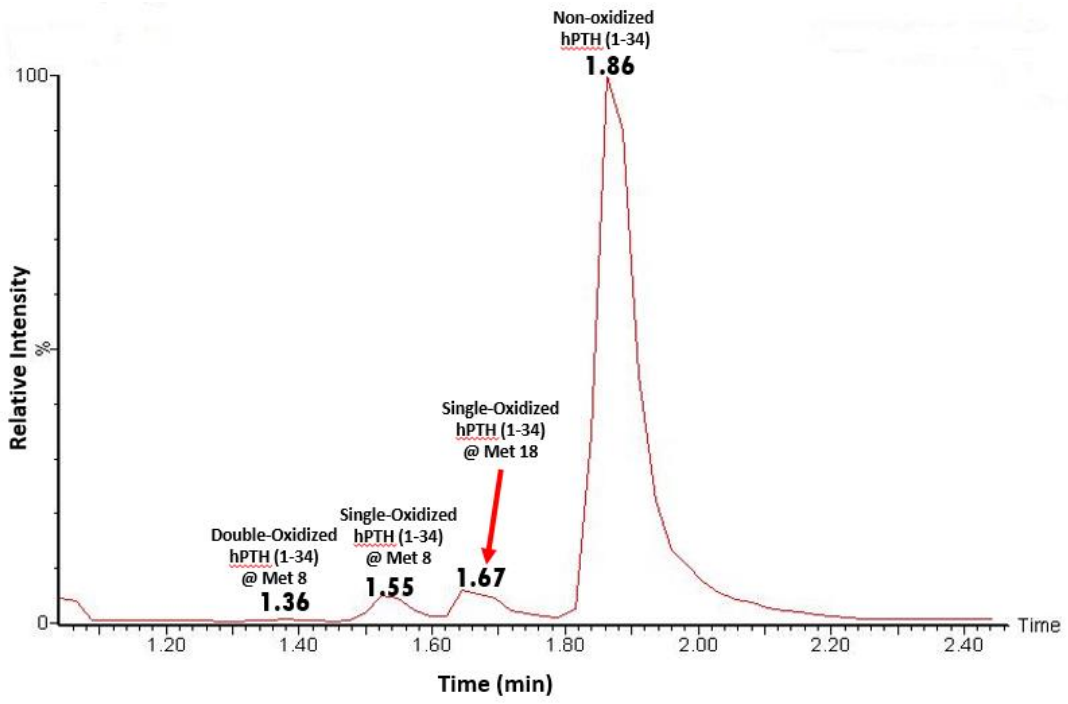


**Figure 3-28 Real-time chromatogram of a pooled rat plasma obtained following administration of an oral hPTH (1-34).** *Note the presence of all oxidized-hPTH (1-34) forms.*

Cross-reactivity of the immunoassay and the LC-MS/MS to the oxidized forms of hPTH (1-34) was also examined. Timed oxidation of hPTH (1-34) samples treated with $H_2O_2$ was analysed using both methods and results obtained are plotted in the following graph (Figure 3-29). A hPTH (1-34) standard at 500 pg/mL was prepared in charcoal-stripped human EDTA plasma. The 500 pg/mL hPTH (1-34) standard was then divided into two groups contain four tubes each. Oxidation was carried out exactly same way in both groups for 10, 20, 40, and 60 min with 1.9 mM $H_2O_2$ before the oxidation reaction was terminated with methionine. It is clearly shown that the immunoassay does not distinguish between oxidized and non-oxidized hPTH (1-34) forms, where results obtained for hPTH (1-34) were similar (difference was within the inter-assay precision range of the assay %CV= 4.2%) throughout oxidation period. The LC-MS/MS method was capable of detecting oxidized forms of hPTH (1-34). The change in non-oxidized hPTH (1-34) throughout oxidation time is plotted in below figure (Figure 3-29)

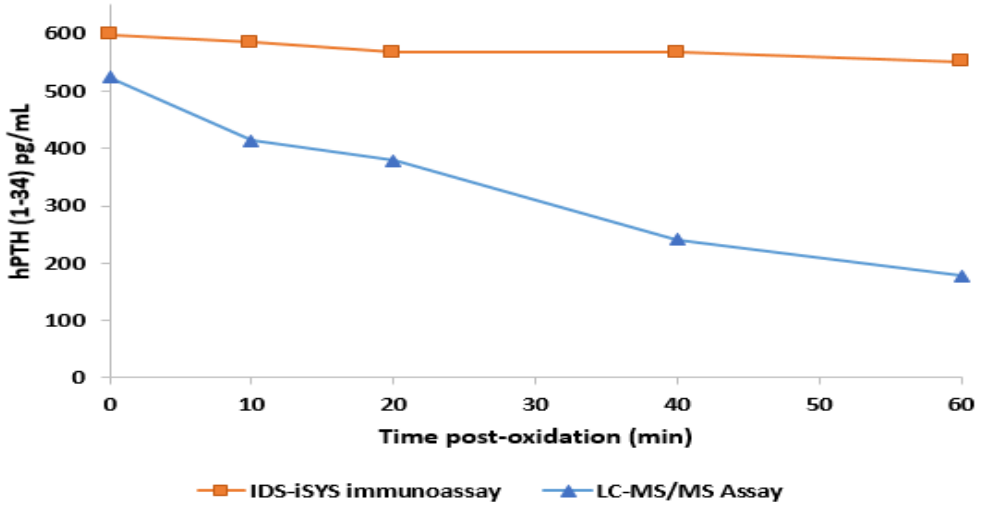


**Figure 3-29 Time-point curve of non-oxidized hPTH (1-34) obtained by immunoassay and LC-MS/MS method.** *Non-oxidized hPTH (1-34) concentration obtained by immunoassay remains constant all through the oxidation time, while it declines by time in LC-MS/MS.*

The decline in non-oxidized hPTH (1-34) concentration obtained by LC-MS/MS method was associated with concurrent increase in single-oxidized hPTH (1-34) concentration, which then decreased indicating its metabolism to double-oxidized hPTH (1-34) (Figure 3-30)

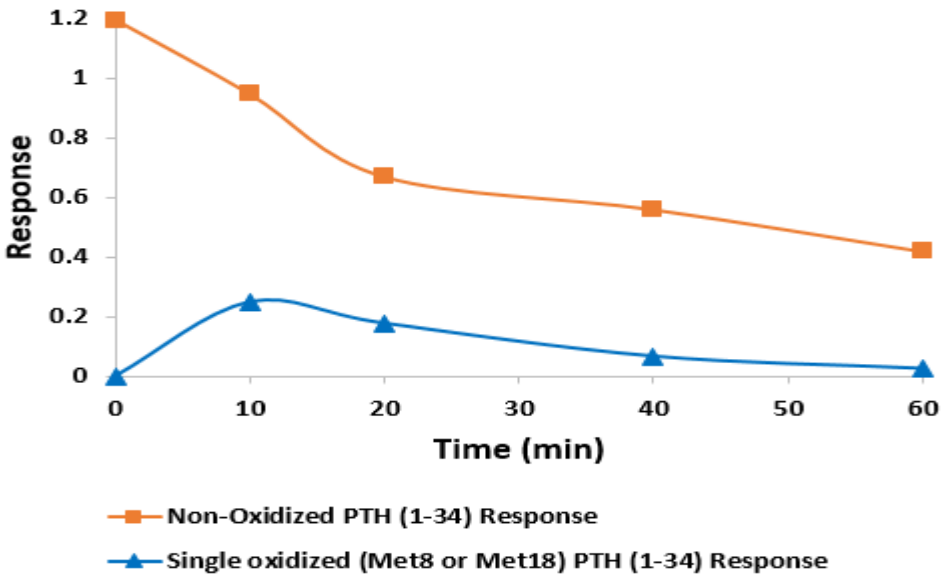


**Figure 3-30 A time-point plot of non-oxidized (orange curve) and single-oxidized (blue cure) hPTH (1-34) response.** *At 10 min oxidation, the sum response (Non-oxidized + single-oxidized hPTH (1-34)) recover the baseline hPTH (1-34) response.*

Four human plasma samples spiked with 20, 100, 200, and 800 pg/mL hPTH (1-34) were prepared. The baseline response of non-oxidized and oxidized-hPTH (1-34) forms was measured in each of them before they were treated with 1.9 mM $H_2O_2$ and incubated at 37 $^{o}$C for 60 minutes. The oxidation reaction was then quenched with methionine and post-oxidation response of hPTH (1-34) forms was measured using the LC-MS/MS method. Table 3.7 summarises pre- and post-oxidation response of non-oxidized and oxidized hPTH (1-34) forms in all sample tested. Oxidized-hPTH (1-34) forms were undetectable in all samples at 0 time. Although, oxidation reaction occurred and response of non-oxidized hPTH (1-34) massively decreased, oxidized hPTH (1-34) forms were undetectable in 20, 100, 200 pg/mL hPTH (1-34) samples after one hour of oxidation with $H_2O_2$. However, both single- and double-oxidized forms were detectable in the 800 pg/mL sample. This experiment shows that oxidized hPTH (1-34) forms were undetectable 60 min after oxidation with $H_2O_2$ not because they were not present, but likely because they were dispersed into various forms with very little concentrations beyond the sensitivity of the LC-MS/MS method.

**Table 3.7 Summary of pre- and post-oxidation response of non-oxidized and oxidized hPTH (1-34) forms in samples spiked with different hPTH (1-34) concentrations.**

| Sample (#) amount of PTH (1-34) spiked in sample | 0 min (Baseline) Response | | | 60 min post-oxidation Response | | |
|---|---|---|---|---|---|---|
| | Non-oxidized PTH (1-34) | Single-oxidized PTH (1-34) | Double-oxidized PTH (1-34) | Non-oxidized PTH (1-34) | Single-oxidized PTH (1-34) | Double-oxidized PTH (1-34) |
| (1) 20 pg/mL | 0.056 | undetectable | undetectable | undetectable | undetectable | undetectable |
| (2) 100 pg/mL | 0.339 | undetectable | undetectable | undetectable | undetectable | undetectable |
| (3) 200 pg/mL | 0.591 | undetectable | undetectable | 0.126 | undetectable | undetectable |
| (4) 800 pg/mL | 3.043 | undetectable | undetectable | 1.207 | 0.56 | 0.13 |

### 3.1.6 Pharmacokinetic analysis results

Pharmacokinetic (PK) profiles (time-course 0-300 min) from human subjects given either a single subcutaneous (sc) injection of 20 ug Teriparatide (n=10) or a single oral PTH (1-34) dose of either 0.69 mg (n=5) or 2.07 mg (n=10) were analysed using the LC-MS/MS method. The overall mean concentration-time profiles and PK parameters of different doses of oral PTH (1-34) and Forsteo® are presented in figure 3-31 and table 3.8 respectively. hPTH (1-34) was undetectable in all pre-dose blood samples. Rapid absorption of PTH (1-34) was observed after oral administration of PTH (1-34) and subcutaneous injection of Forsteo® with maximum concentrations being observed at (Mean ±SEM) (17.5 ± 2.5), (15.0 ± 1.4), and (21.0 ± 1.0) min for Forsteo®, 0.69 mg oral PTH (1-34), and 2.07 mg oral PTH (1-34) respectively. In general, hPTH (1-34)declined/ was eliminated faster from the circulation after oral administration with $T_{1/2}$ (mean ±SEM) of (14.0 ± 4.8) and (12.6 ± 2.6) min for 0.69 mg and 2.07 mg oral PTH (1-34) treatment respectively compared to (33.5 ± 6.8) min for Forsteo® treatment. Treatment with 2.07 mg oral hPTH (1-34) resulted in $C_{max}$ significantly higher than that produced by 0.69 mg oral hPTH (1-34) (*p =0.003)* and sc Forsteo ($p$ = 0.009). Despite the significantly higher $C_{max}$ (mean ± SEM) achieved after oral administration of 2.07 mg PTH (1-34) (289 ± 43.0) pg/mL in comparison to (138.9 ± 21.3) pg/mL after Forsteo® injection , both treatments were found to have similar systemic exposure as approximated by $AUC_{0\text{-last}}$ (*P= 0.87)* AUC (mean ± SEM) of (6444.8 ± 560.3) and (7034.7 ± 1149.6) for Forsteo® and oral 2.07 mg PTH (1-34), respectively. Both Forsteo® and 2.07 mg oral hPTH (1-34) treatment produces significantly higher $AUC_{0\text{-last}}$ than 0.69 mg oral hPTH (1-34) treatment with $p$ value of 0.003 and 0.001, respectively. $C_{max}$ and $AUC_{0\text{-last}}$ values of oral PTH (1-34) appeared to be proportional to dose, where both values increase when oral PTH (1-34) dose increased. Figures 3-32 and 3-33 illustrate the proportionality of $C_{max}$ and $AUC_{0\text{-last}}$ to oral PTH (1-34) dose, respectively. It is clearly shown in PK profile plots of Forsteo® and oral PTH (1-34) doses (figure 3-31) that $C_{max}$ of Forsteo® located in the middle and bracketed between $C_{max}$ of the oral doses.

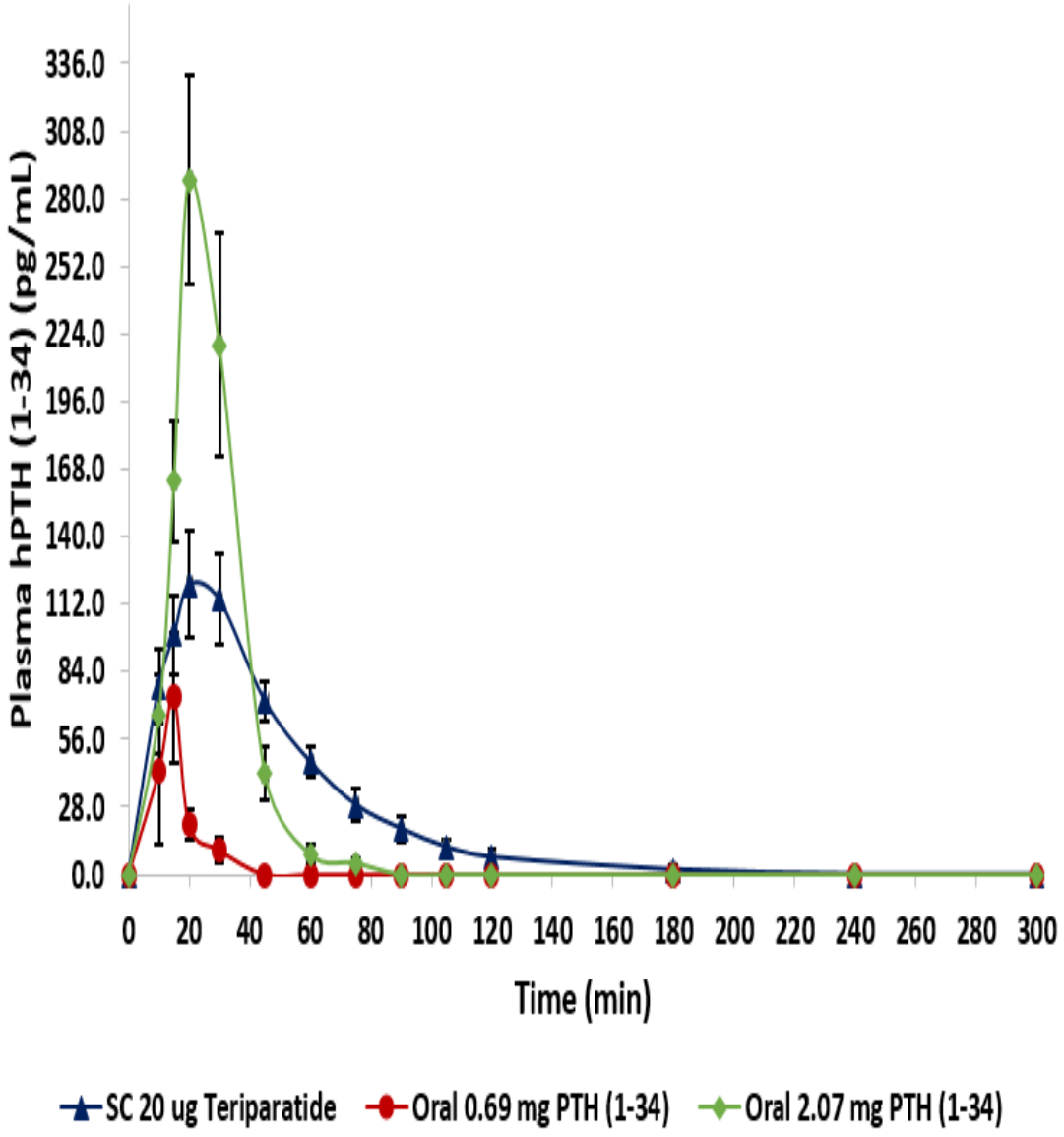


**Figure 3-31 Concentration-time profile of patients treated with 20 µg Forsteo®, and oral hPTH (1-34) (0.69 and 2.07 mg).** *Time course of sample collection was 0-300 minutes. Each point represents (mean ± SEM) of plasma hPTH (1-34) concentration.*

**Table 3.8 Pharmacokinetic parameters for hPTH (1-34) of 20 µg subcutaneous Forsteo® injection and oral (0.69 and 2.07 mg) administration.**

| Statistical Parameter | $C_{max}$ (pg/mL) | $T_{max}$ (min) | $AUC_{0\text{-last}}$ (pg.min/mL) | $T_{1/2}$ (min) |
|---|---|---|---|---|
| **Sc 20 µg Forsteo®** | | | | |
| n | 10 | 10 | 10 | 10 |
| Median | 125.0 | 17.5 | 6771.9 | 35.7 |
| Mean | 138.9 | 17.5 | 6444.8 | 33.5 |
| SD | 67.4 | 7.9 | 1771.8 | 21.6 |
| SEM | 21.3 | 2.5 | 560.3 | 6.8 |
| Minimum | 57.2 | 10 | 2938.0 | 8.8 |
| Maximum | 259.3 | 30 | 8546.5 | 88.8 |
| **Oral 0.69 mg hPTH (1-34)** | | | | |
| n | 5 | 5 | 5 | 5 |
| Median | 42.7 | 15.0 | 592.4 | 13.3 |
| Mean | 78.3 | 15.0 | 972.6 | 14.0 |
| SD | 68.6 | 3.5 | 999.0 | 9.7 |
| SEM | 30.7 | 1.6 | 446.7 | 4.8 |
| Minimum | 24.2 | 10 | 241.8 | 4.8 |
| Maximum | 177.8 | 20 | 2729.8 | 24.7 |
| **Oral 2.07 mg hPTH (1-34)** | | | | |
| n | 10 | 10 | 10 | 10 |
| Median | 238.9 | 20.0 | 6329.7 | 14.1 |
| Mean | 289.0 | 21.0 | 7034.7 | 12.6 |
| SD | 135.9 | 3.2 | 3635.3 | 8.2 |
| SEM | 43.0 | 1.0 | 1149.6 | 2.6 |
| Minimum | 184.0 | 20.0 | 3155.5 | 4.9 |
| Maximum | 629.9 | 30.0 | 16695.8 | 32.8 |

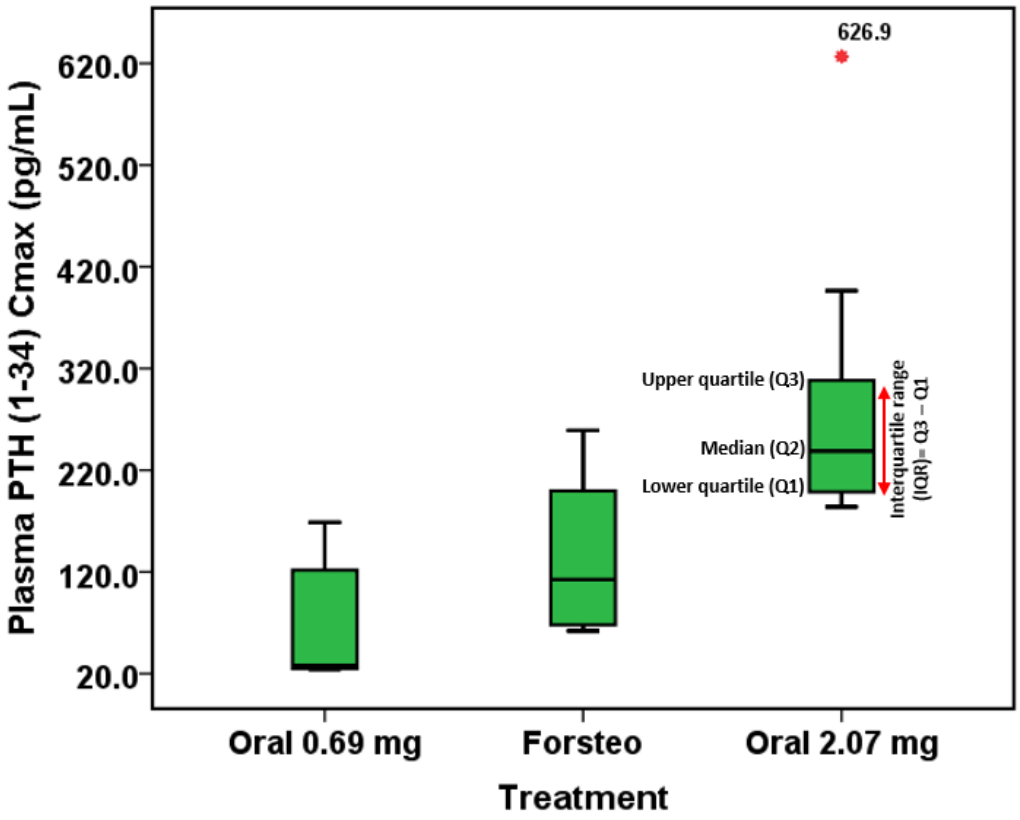


**Figure 3-32 Box and Whisker plot representation of hPTH (1-34) $C_{max}$ in plasma of patients have been given sc Forsteo (n=10), oral doses of hPTH (1-34) (0.69 mg (n=5) and 2.07 mg (n=10)).** *Asterisk represents an extreme outlier that was removed from statistical analysis. Outliers are defined as values less than Q1 by 1.5 IQR or more than Q3 by 1.5 IQR. ANOVA analysis showed that the 2.07 mg oral PTH (1-34) dose gives significantly higher $C_{max}$ compared to 0.69 mg oral PTH (1-34) dose and sc Forsteo®. $C_{max}$ appears to be proportional to dosage of oral PTH (1-34).*

The 2.07 mg oral hPTH (1-34) treatment yielded similar AUC obtained for Forsteo® treatment, which means similar systemic exposure to hPTH (1-34). Figure 3-33 shows box and Whisker plot representation of $AUC_{0\text{-last}}$ for all treatment groups.

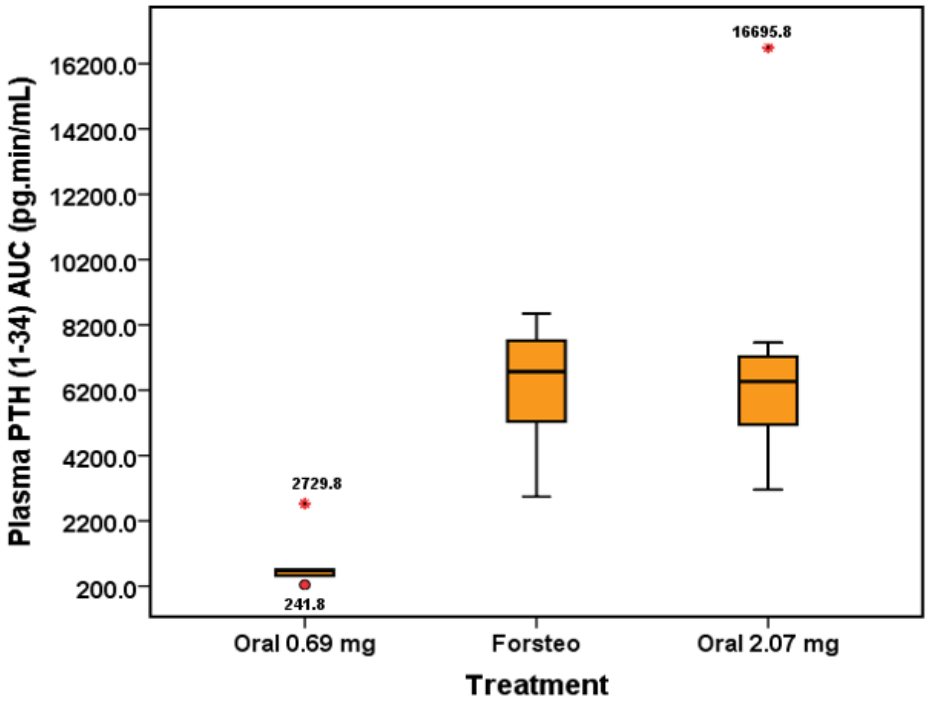


**Figure 3-33 Box and Whisker plot representation of $AUC_{0\text{-last}}$ obtained for sc Forsteo (n=10), oral doses of hPTH (1-34) (0.69 mg (n=5) and 2.07 mg (n=10)).** *mg oral treatment. Asterisk represents an extreme outlier that was removed from statistical analysis and circle represents mild outlier. Outliers are defined as values less than Q1 by 1.5 IQR or more than Q3 by 1.5 IQR. ANOVA analysis showed that the 2.07 mg oral PTH (1-34) treatment produces similar AUC to sc Forsteo® and both of them yield significantly higher AUC than 0.69 mg oral PTH (1-34) treatment. AUC appears to be proportional to dosage of oral PTH (1-34).*

## 3.2 Development and validation of a LC-MS/MS method for quantification of PTHrP (1-36)

### 3.2.1 MRM transitions

A full MS scan analysis was performed to identify hPTHrP (1-36) precursor ions (Figure 3-34). hPTHrP (1-36) demonstrates charge state distribution similar to that given by human and rat PTH (1-34) with m/z 711.1, 609.5, and 853.1 being the most intense precursor ions.

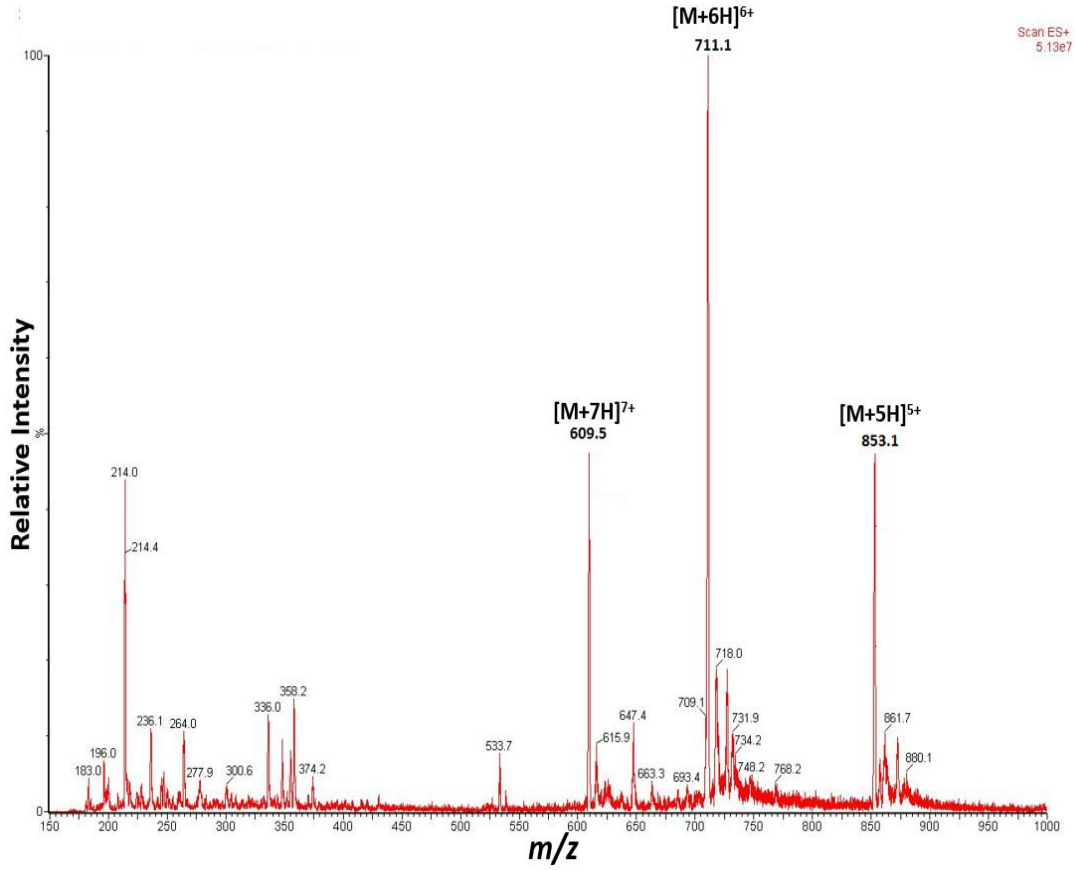


**Figure 3-34 Precursor ions spectrum of hPTHrP (1-36)**

Product ion scans were performed on the two most abundant precursor ions, and it was found that the 7+ charge state generated two useful product ions (Figure 3-35), whereas the 6+ and the 5+ charge state did not generate usable product ions. Figure 3-36 shows the product ion scan on precursor ion at m/z 711.1.

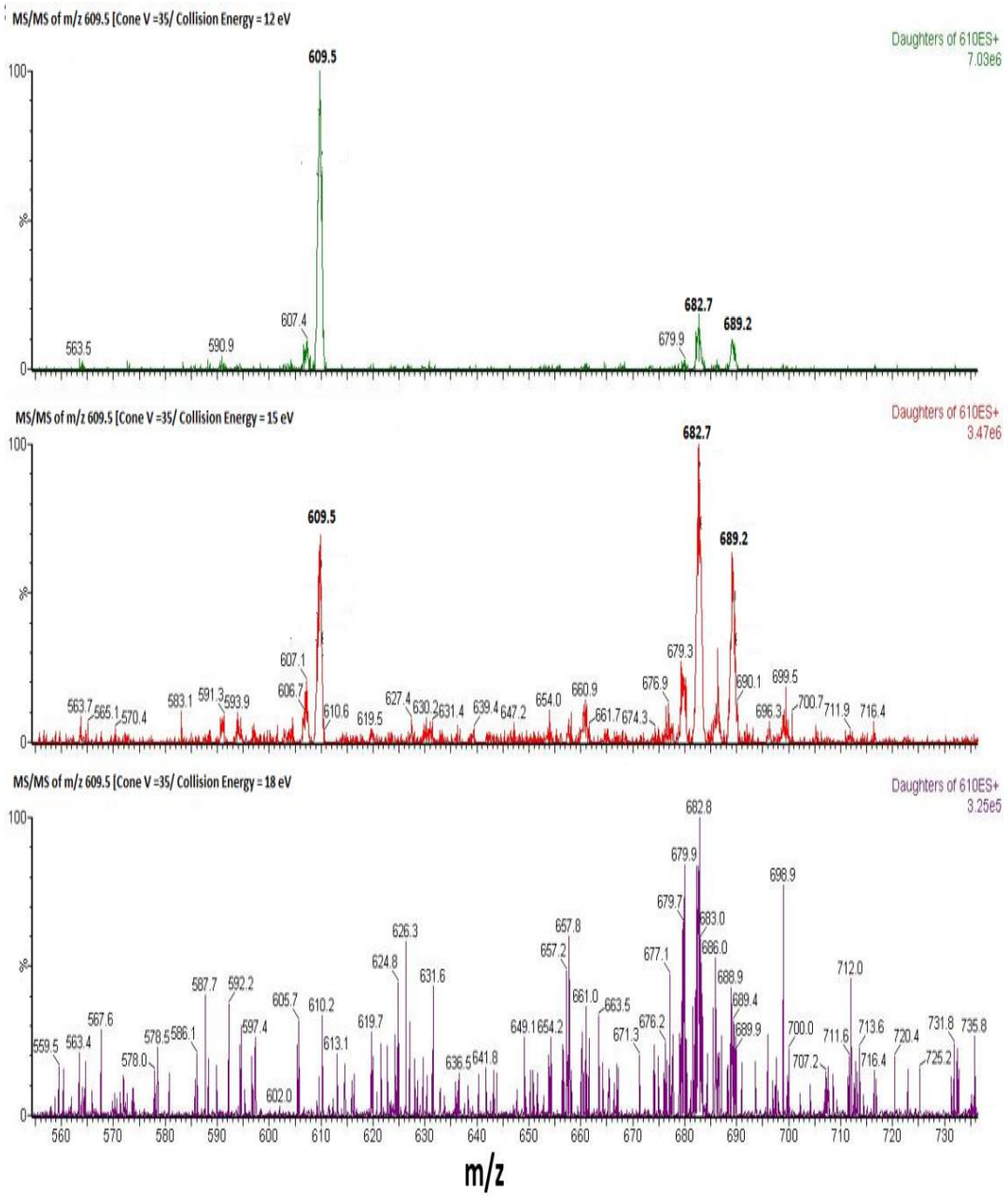


**Figure 3-35 Product ion spectrum from hPTHrP (1-36) at m/z 609.5.** Usable product ions at m/z 682.7 and 689.2 are shown using cone voltage of 35 V and collision energy of 15 eV.

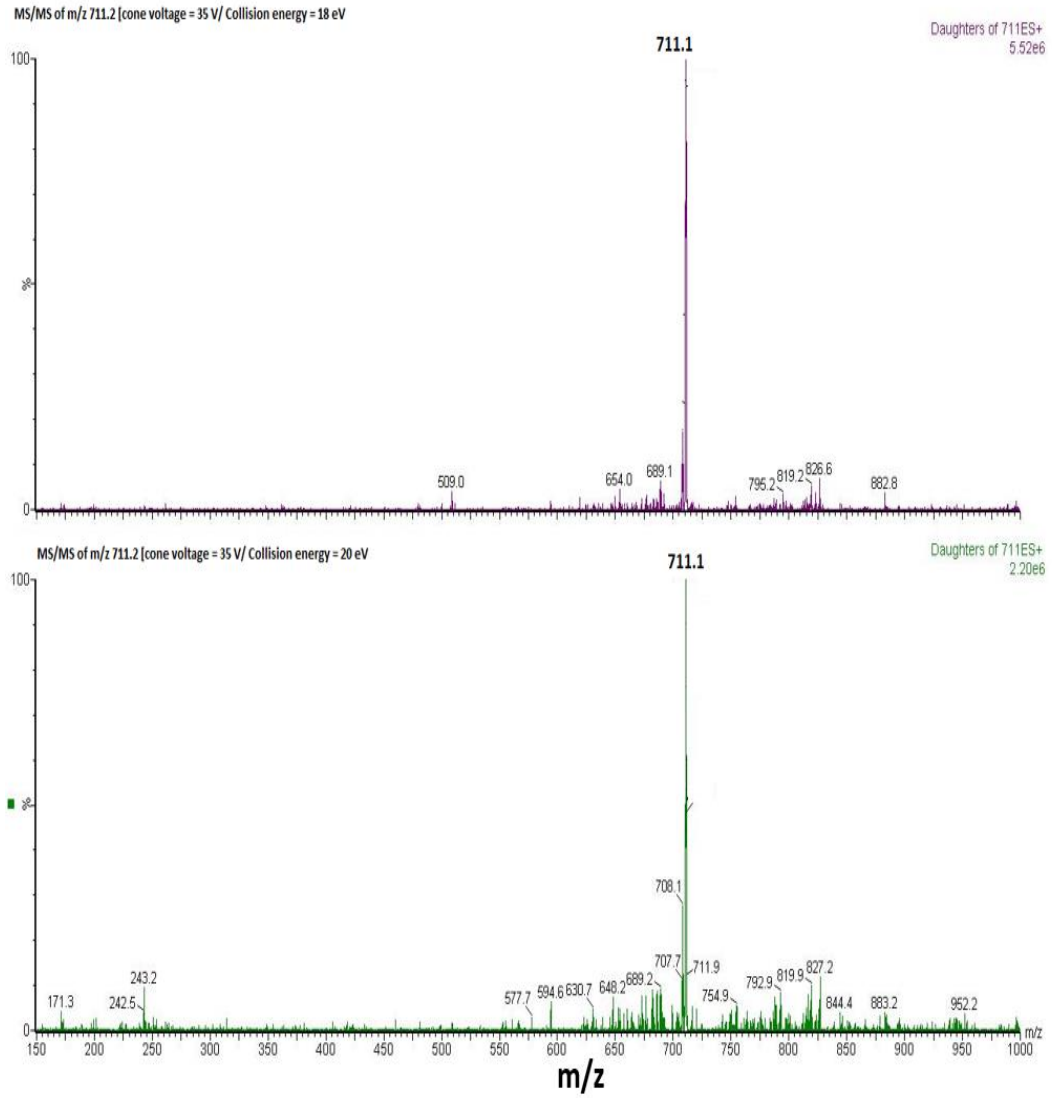


**Figure 3-36 Product ion spectrum at m/z 711.1.** No useful product ion generated even though high collision energies were used.

hPTHrP (1-36) is not oxidized by $H_2O_2$, as MS scan of precursor ions of 1 and 2 hours post-oxidation hPTHrP (1-36) yielded the same spectrum to non-oxidized hPTHrP (1-36). Figure 3-37 demonstrates MS scan of non-oxidized (top), 1 h (middle) and 2 h post oxidation hPTHrP (1-36) (bottom).

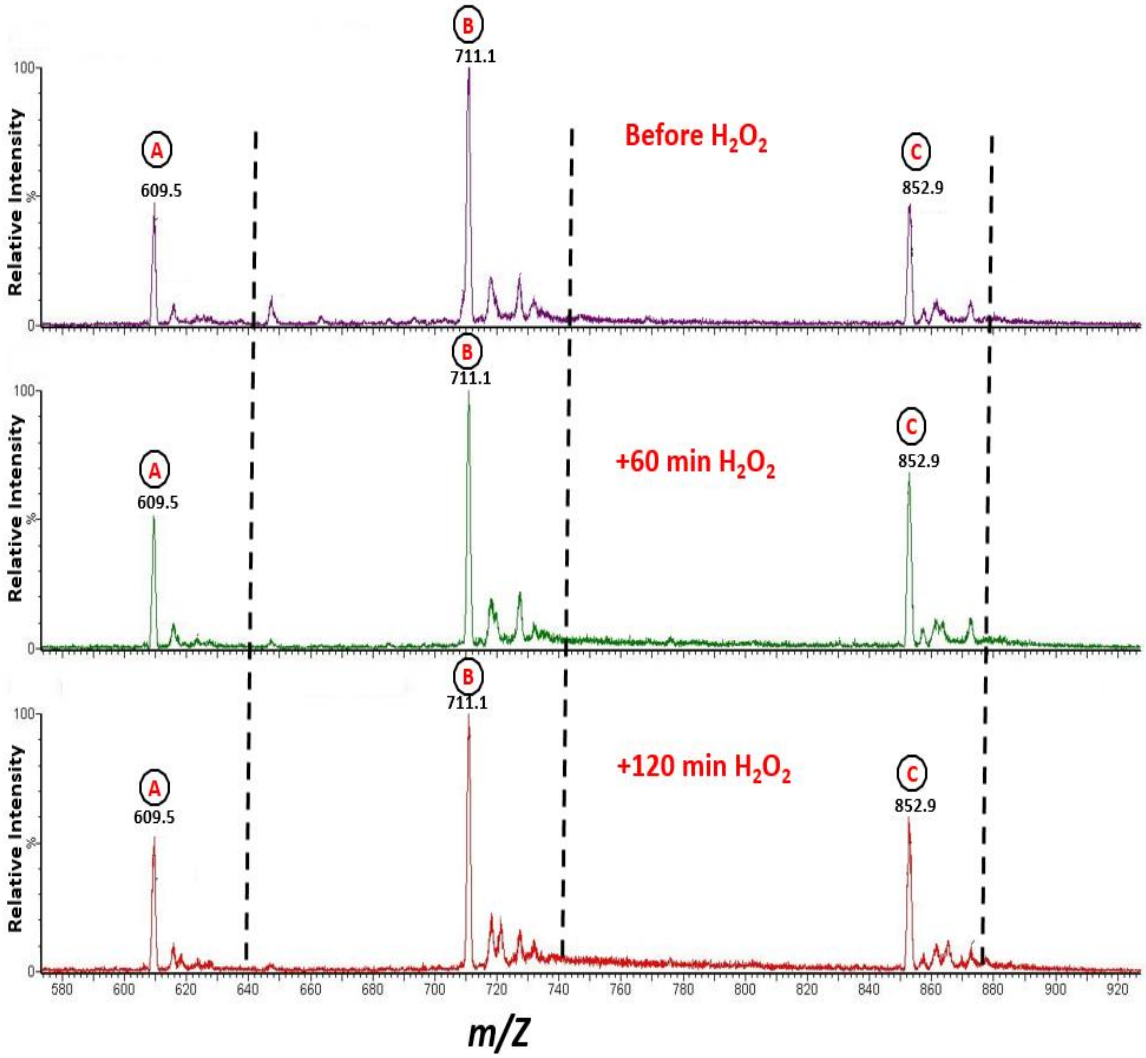


**Figure 3-37 Full MS scan of hPTHrP (1-36) before oxidation, 60 and 120 min after oxidation with H2O2.** It appears that hPTHrP (1-36) is not oxidized by H2O2.

### 3.2.2 Method Validation results

#### *3.2.2.1 Calibration Curve/Linearity*

Using precursor to product mass transition 609>682 to quantify hPTHrP (1-36), the calibration curve of the assay was linear across a range from 25 to 2000 pg/mL. Using a 1/x weighting, the $r^2$ values for all curves were consistently >0.90. Figure 3-

38 illustrates the typical calibration curve of hPTHrP (1-36) assay and linearity was evidenced across the calibration range.

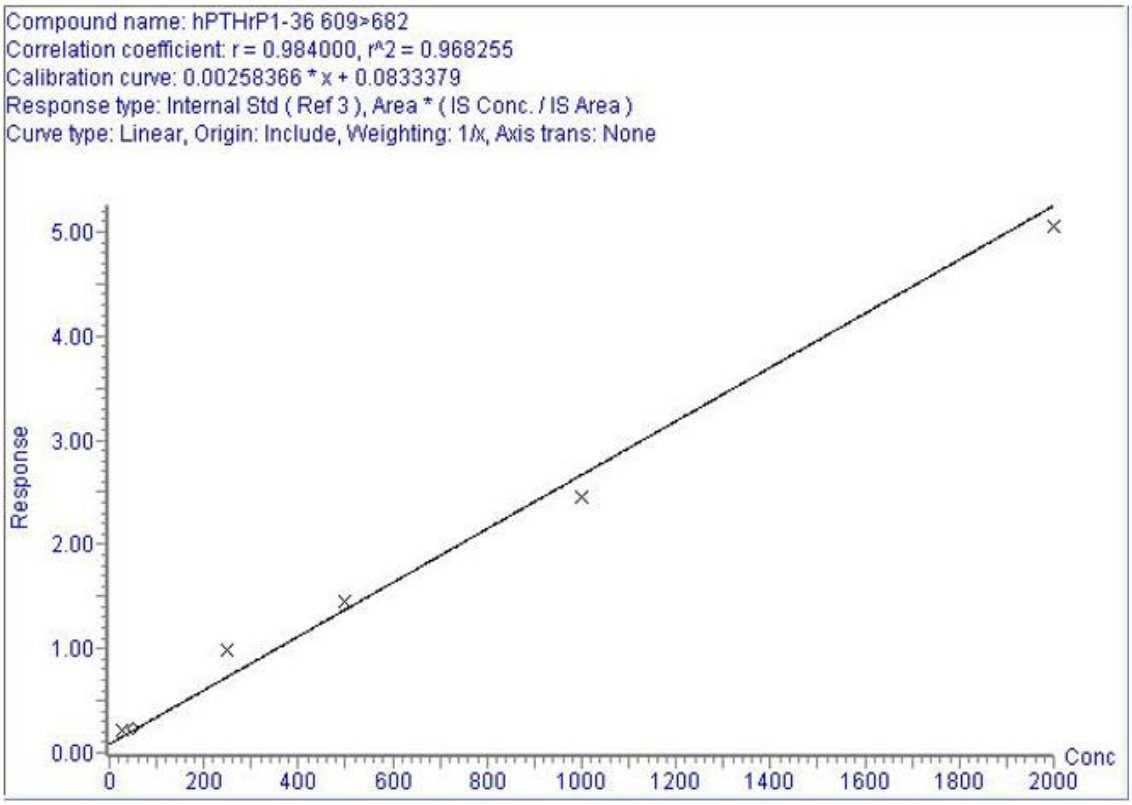


**Figure 3-38 Typical calibration curve for hPTHrP (1-36) spiked into charcoal-stripped human EDTA plasma. R2 value is 0.97**

### *3.2.2.2 Carry over*

No carryover was detected immediately after a sample containing 2000 pg/mL hPTHrP (1-36).

### *3.2.2.3 Matrix effect*

The average percentage matrix effect for 100 pg/mL and 1000 pg/mL standards concentration was 14.4% and 1.7%, respectively. Table 3.9 shows the response values obtained for every replicate measurement at the two tested concentrations of sample A (in solvent) and sample B (in matrix).

**Table 3.9 hPTHrP (1-36) response obtained for four duplicate determinations of each of the two concentrations of sample A and B.**

| | Low Concentration (100 pg/mL hPTHrP (1-36) | | High Concentration (1000 pg/mL hPTHrP (1-36) | |
|---|---|---|---|---|
| Duplicate # | Sample A (in solvent) | Sample B (in matrix) | Sample A (in solvent) | Sample B (in matrix) |
| 1 | 0.83 | 1.08 | 7.17 | 9.34 |
| 2 | 0.95 | 1.02 | 6.78 | 8.85 |
| 3 | 0.85 | 1.00 | 8.25 | 5.85 |
| 4 | 0.97 | 1.00 | 6.62 | 5.24 |
| Average Response | 0.90 | 1.03 | 7.20 | 7.32 |
| SD | 0.07 | 0.03 | 0.73 | 2.07 |
| %Matrix effect | 14.4% | | 1.7% | |

### *3.2.2.4 Precision and Accuracy*

A precision and accuracy assessment of hPTHrP (1-36) assay was assessed at QC concentrations spiked in charcoal-stripped human EDTA plasma. %CV represents assay precision, while accuracy is represented by a percentage of relative error (%RE). As it shown in table 3.10, the inter-assay precision and accuracy were <11.8% and <9.1% respectively. Whereas, the intra-assay precision and accuracy were <12.4% and 10.7% respectively.

**Table 3.10 Inter and intra-assay precision and accuracy of LC-MS/MS hPTHrP (1-36) assay.**

| | QC1 (50 pg/mL) | QC2 (100 pg/mL) | QC3 (200 pg/mL) | QC4 (800 pg/mL) |
|---|---|---|---|---|
| Inter-assay | | | | |
| Mean | 51.9 | 97.5 | 211.9 | 803.9 |
| SD | 5.6 | 11.5 | 16.8 | 47.4 |
| SE | 0.6 | 1.2 | 1.7 | 4.7 |
| %CV | 10.8 | 11.8 | 7.9 | 5.9 |
| %RE | 9.1 | 8.6 | 8.3 | 4.8 |
| Intra-assay | | | | |
| Mean | 52.5 | 101.5 | 203.5 | 822.5 |
| SD | 6.5 | 10.0 | 15.6 | 57.3 |
| SE | 0.7 | 1.0 | 1.6 | 5.7 |
| %CV | 12.4 | 9.9 | 7.7 | 7.0 |
| %RE | 10.7 | 7.7 | 6.5 | 5.6 |

### *3.2.2.5 Ion suppression*

There was no suppression or enhancement signals detected at the elution time of hPTHrP (1-36), which indicates that there is no Ion suppressor or enhancer species co-elute with hPTHrP (1-36) (Figure 3-39).

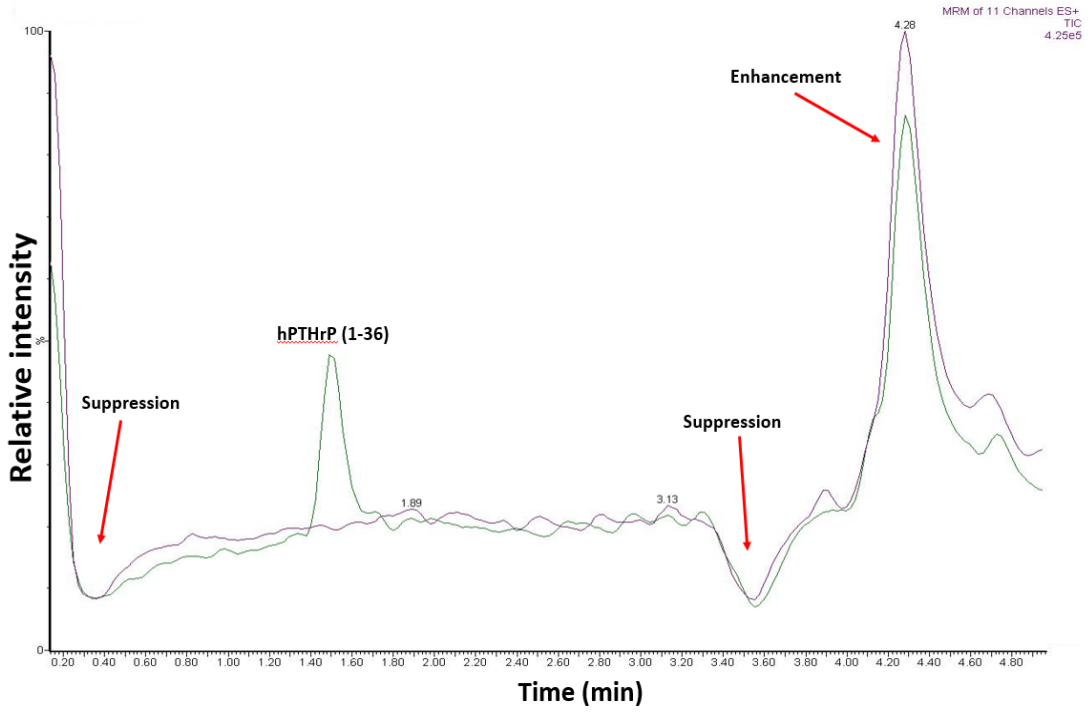


**Figure 3-39 Ion suppression from direct infusion.** *Suppression in baseline signals was observed during co-injection of extracted human plasma sample and post column infusion of PTHrP (1-34). The elution of hPTHrP (1-36) occurs away from suppression and enhancement elution time. Purple spectrum represents blank human plasma, while green spectrum for human plasma containing hPTHrP (1-36) only.*

### *3.2.2.6 Recovery efficiency*

Extraction recovery was evaluated by determining the amount of hPTHrP (1-36) recovered from the amount spiked into plasma prior to extraction. With the use of an internal standard, mean recovery for hPTHrP (1-36) was 103.7% (range 96.7-113.7) (Table 3.11). The data indicate that the SPE procedure was able to extract hPTHrP (1-36) efficiently from human plasma.

**Table 3.11 Recovery of hPTHrP (1-36) from human EDTA plasma**

| Endogenous PTHrP(1-36) (pg/mL) | Spiked (pg/mL) | n | Expected concentration (endogenous + spiked), pg/mL | Mean (±SD) measured hPTHrP (1-36) (pg/mL) | %Recovery mean (%CV) |
|---|---|---|---|---|---|
| 50 | 50 | 4 | 100 | 113.7 (±30.8) | 113.7 (±27.1) |
| 50 | 500 | 4 | 550 | 567.4 (±20.5) | 103.2 (±3.6) |
| 400 | 50 | 4 | 450 | 435.3 (±39.3) | 96.7 (±9.0) |
| 400 | 500 | 4 | 900 | 951.5 (±62.0) | 105.7 (±6.5) |
| 800 | 50 | 4 | 850 | 877.4 (±89.6) | 103.2 (±10.2) |
| 800 | 500 | 4 | 1300 | 1297.1 (±82.5) | 99.8 (±6.4) |

#### *3.2.2.7 LLoQ and LLoD*

A precision and accuracy assessment of LLoQ of hPTHrP (1-36) was performed at 25 pg/mL and demonstrated a precision of 13.0% and accuracy (%RE) of 11.7%. The S/N at the LLoQ was ≥10. The LLoD for the hPTHrP (1-36) assay was 2.5 pg/mL with a S/N value of ≈5 required for a regulated LC-MS/MS assay (270, 271).

# 4. Chapter 4- Discussion

## 4.1 LC-MS/MS method for quantification of PTH (1-34)

### 4.1.1 LC-MS/MS Method and Sample Preparation Method Development

Development of a bioanalytical LC-MS/MS method has to recognise the importance of three main interdependent elements that together form a robust and reliable LC-MS/MS assay. The three elements are: sample preparation, liquid chromatography separation and mass spectrometry detection. Chapter two and three of the thesis have described the development and validation of a high-sensitive and selective electrospray ionization (ESI) - LC-MS/MS method for measurement of PTH (1-34) peptide (MW = 4117.8 Da) in human plasma. ESI-LC-MS/MS has advantages as well as disadvantages. One advantage of ESI-LC-MS/MS is its ability to handle analytes with large masses. Another advantage is that ESI is one of the softest ionization methods available, therefore it has the ability to promote non-destructive vaporization/ ionization of peptides with relatively large masses such as hPTH (1-34). Finally, ESI-MS instrument has an impressive sensitivity useful for accurate quantitative measurement. The major disadvantages are that this technique cannot analyse complex mixtures very well and the multiple charges that are attached to the molecular ions - which is something inevitable in the case of hPTH (1-34) - can make for confusing spectral data. This confusion is further fuelled by use of a mixed/complex sample. Intensive clean-up of samples must be maintained to obtain reliable results. The assay described was validated against published acceptance criteria for clinical and research use. Beside its ability to measure low pg/mL concentrations of hPTH (1-34), the assay was designed to measure oxidized forms of hPTH (1-34) alongside the non-oxidized PTH (1-34). Non-oxidized and oxidized hPTH (1-34) are different in term of bioactivity, where the former is bioactive and the latter is inactive or has reduced activity. This means that the LC-MS/MS assay measures the true biologically active form of hPTH (1-34).

Several LC-MS/MS assays with variable sensitivity have been developed for quantification of PTH (1-34) in the last five years (136-138). However, none of the published assays has addressed oxidation of the hPTH (1-34) peptide. Oxidation of peptides at their sulphur-containing amino acid residues, such as methionine, by

peroxidases in biological systems is one of the major degradation process of these peptides. The biological properties of oxidized and non-oxidized PTH are substantially different. Oxidized PTH loses its PTH receptor-stimulating properties, whereas non-oxidized PTH is a full agonist of the receptor (273). hPTH (1-34) peptide contains two methionine residues in its primary amino acid structure. Studies of porcine PTH, which has only one methionine (residue 8), indicated that oxidation at this single position is sufficient for inactivation, establishing that Met 8 is of key importance in the biological activity of PTH (274, 275). While methionine at position 8 in PTH is conserved from different species, methionine at position 18 is not strictly conserved but is always substituted with another hydrophobic residue, which likely indicates that oxidation of methionine 18 may also affect biological activity (274). Oxidation of methionine residues in PTH (1-34), especially Met 8, markedly effects its biological activity and reduces its potency as a drug (130, 131, 133-135). Therefore, all these findings reassert the importance of a sensitive bioanalytical assay with ability to perform differential measurement of oxidized and non-oxidized PTH (1-34).

Several multiply protonated precursor ions were observed for non-oxidized hPTH (1-34) and for the rat PTH (1-34) fragment (IS) under positive ESI. The septuple (7+) protonated molecule $[M+7H]^{7+}$ and sextuple (6+) protonated molecule $[M+6H]^{6+}$ of non-oxidized hPTH (1-34) at *m/z* 589.2 and 687.1, respectively, were found to be the most intense. This finding is consistent with what have been reported previously (136-138). Full scan spectra of IS showed exactly same multiple-charged ionization pattern as that obtained for hPTH (1-34). The 7+ and 6+ charged states at *m/z* 580.7 and 677.1, respectively, being the most intense precursor ions for IS, which is in agreement with findings reported by MacNeill *et al.* (137). Fragmentation of *m/z* 589.2 and 687.1 yielded selective product ions at *m/z* 656.1 and 787.1 respectively. Precursor-to-product mass transition 589.2>656.1 was observed to give higher peak area count for hPTH (1-34) compared to 687.1>787.1. Therefore, 589.2 > 656.1 was chosen as the primary transition used for quantitative analysis, whilst 687.1 > 787.1 was allocated as the qualitative transition to confirm quantitative peak. This finding contrasts with Chambers *et al.* (136), where it was stated that fragmentation of the 7+ precursor ion did not yield a usable fragment. However, the current results support the finding of Kay et al. (138). The reasons why

two transitions were allocated to quantify non-oxidized hPTH (1-34) in this assay are firstly, because the various charge states of the peptide may fragment differently, and secondly to ensure the specificity of the peak obtained for the quantitative transition.

With regard to IS, fragmentation of precursor ions at *m/z* 677.1 and 580.7 produced product ions at *m/z* 777.9 and 649.1 respectively. 677.1>777.9 was used for quantification of IS as it gave slightly higher signal yield compared to 580.7 > 649.1.

The N-terminal PTH (1-34) interacts with PTHR1 and produces biological effect equivalent to that of full-length PTH (1-84) hormone and has been demonstrated in humans that it enhances bone growth, particularly when administered intermittently in low subcutaneous doses. Because it is a peptide and thus far more labile than the traditionally small molecular weight drugs, the formulation of PTH (1-34) presents a challenge not commonly encountered by the pharmaceutical industry. Like other protein/peptides that have been formulated successfully, PTH (full-length and PTH (1-34)) is particularly sensitive to oxidation, deamination, and hydrolysis, and requires that its N-terminal and C-terminal sequences remain intact in order to preserve bioactivity. Development of a formulation that is acceptable in terms of storage stability is one of the major challenges facing commercial exploitation of PTH-based drugs. Also development of more convenient, non-invasive administration of drug (e.g. oral or nasal) is another important area of research. Exploring the possibility of detecting/quantifying oxidized forms of PTH (1-34) side by side with non-oxidized form, will be helpful for drug development studies.

To specify MRM transitions for oxidized hPTH (1-34), hPTH (1-34) peptide in solvent treated with $H_2O_2$ was scanned and then the precursor and product ions allocated. Full ion scan of oxidized PTH (1-34) solution revealed two more peaks at each charge state in addition to the one observed with non-oxidized hPTH (1-34) form, which reflects location of the oxidized methionine residue on hPTH (1-34) structure. MRM chromatography of the oxidized hPTH (1-34) shows four different peaks representing the non-oxidized hPTH (1-34), the single-oxidized hPTH (1-34) at Met8 and at Met18 and the double- oxidized hPTH (1-34) at both methionine residues. Peaks for non-oxidized, single-oxidized and double-oxidized hPTH (1-34) are nicely resolved from each other. The peaks for the two single-oxidized hPTH (1-

34) are not completely resolved due to similarity in molecular mass. However, they can be separated by increasing the run time. These peaks are corresponding to intact, single oxidized at Met 8, single oxidized at Met 18, and double oxidized at both methionine residues hPTH (1-34) (figure 3-7 and 3-8). This finding is consistent with those HPLC chromatography results previously reported (132, 276). 591.4 > 658.8 and 593.7 > 661.5 were designated as quantitative MRMs, while 689.7 > 790.3 and 692.4 > 793.5 were designated as qualitative/confirmatory MRMs for single- and double-oxidized PTH (1-34) respectively.

hPTH (1-34) is a hydrophobic molecule with hydrophobicity index and isoelectric point (pI) of -0.65 and 9.1 respectively. This was reflected in its LC behaviour in RP C18 column where experiments have shown that it is eluted off between 22 and 25% in low pH mobile phase (MP)-B (0.2% FA in ACN). A shallow LC gradient was used that starts with 10% MP-B changed to 20% soon (0.3 min) after loading on the column and increased to 30% over 2.5 min. This allowed reduction in the ion suppression from material eluting before the peptide and gave better MS response for the PTH (1-34) peptide. Further precautions that were taken in order to reduce ion suppression include, eluent injection time was set up between 1 to 2.5 min so that most of the ion suppression materials diverted to waste rather than injected into the MS. The common observation with all RP C18 analytical columns, including the BEH column, was broad PTH (1-34) peaks with severe tailing, which impacted on resolution and consequently on the consistency of results. This could be caused by the strong secondary interaction between PTH (1-34) peptide and the free silanol groups in all silica-based reversed-phase columns (277, 278). The ACQUITY UPLC CSH C18 column with a controlled, low-level positive surface charge produces a neat symmetrical peak and enhances peak intensity under formic acid conditions. hPTH (1-34) is positively charged under low pH mobile phase employed (0.2% FA in ACN), has a reduced secondary interaction with the positively charged stationary phase surface of CSH column, which resulted in improved peak shape and intensity. The use of a column packed with smaller particle size (1.7 µm) and wider pore size (170 – 300 Å) contributes to improved resolution and intensity. It is well documented that resolution and peak height increase markedly as particle diameter decreases and large pore sorbent gives higher recoveries for large peptides because size exclusion effects will be excluded (277). It

was noted that adding 0.01% of carrier protein (e.g. BSA, calf serum, rat plasma) to aqueous solvent has given a 2-fold increase in peak intensity. A possible explanation for this might be that carrier proteins help to reduce adsorption of the peptide to surfaces (i.e. vial, tube, column) and facilitate its elution and improve its recovery (136).

Microelution solid-phase extraction (SPE) 96-well plate format was the preferred method for sample preparation and clean-up in this thesis. Many advantages were achieved with the use of µElution SPE plates with their small sorbent bed mass (2 mg). Firstly, analyte could be eluted off with a small volume of solution (25 µL), so no dry down/evaporation of solvent was required, which consequently minimized the possibility of NSB of peptide that is likely to occur during this step. Secondly, this SPE sorbent format allowed concentration of eluted analyte and yielded x4 enrichment of hPTH (1-34). Concentration of analyte in a smaller volume prior loading into LC-MS/MS is important to achieve quantification at low picomolar concentrations. All components of the SPE method for hPTH (1-34) extraction were systematically evaluated and studied in order to establish optimum SPE sorbent chemistry, sample loading volume, wash solution, and eluting solution. The overall result of this thesis shows that hPTH (1-34) is better recovered on either HLB or MAX under high pH conditions and analyte recovery on HLB was superior to that on MAX. Both human and rat PTH (1-34) are composed of a sequence of acidic, basic and aromatic amino acid residues (table 2.1). Figure 4-1 explains the behaviour of acidic and basic residues under certain pH conditions. Acidic residues tend to be in ionized form under high pH, while they are in a neutral state under low pH. In contrast basic residues tend to be in an ionized state under low pH and in neutral state under high pH. Under high pH conditions, basic residues become neutral (unionized) and acidic residues become negatively charged (ionized). Neutral state of basic residues promotes hydrophobic/RP interaction. Negatively-charged residues enhances ionic interaction in mixed-mode sorbent. So, while the interaction between PTH (1-34) and HLB sorbent is hydrophobic only, PTH (1-34) molecules interacts ionically and hydrophobically with MAX sorbent, which explains the need for a second elution cycle to elute off the entire PTH (1-34) from MAX. This observation is in agreement with Chambers *et al.* (136) who stated that

precipitation with base-modified ACN gave higher recovery than acid modified ACN on both HLB and MAX SPE plates.

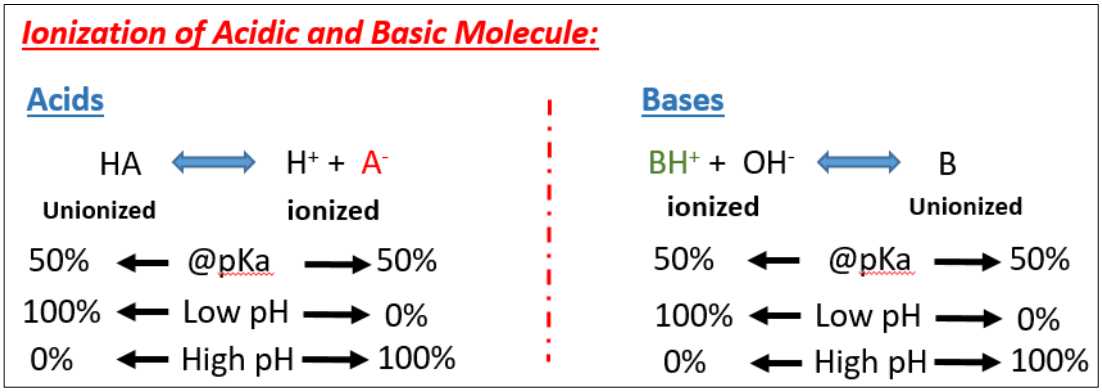


***Figure 4-1 Effect of pH in charge-state of acidic and basic molecules.***

Elution step optimisation experiments showed that the use of 70% acetonitrile in water as the eluting solution is optimal giving higher peak area yield without the need for a second elution cycle (figure 3.16 & 3.17). 0.2% FA was added to the eluting solution to provide a degree of retention orthogonality relative to the basic loading condition.

The inclusion of a protein precipitation/protein crash step in sample preparation was studied and a comparison between the recovery yield of hPTH (1-34) from a group of samples precipitated with acetonitrile (sample: ACN, 1:1) followed by dilution of supernatant with 1 mL 5%$NH_4OH$ with that from a group of samples have only been diluted by 0.5 mL 5% $NH_4OH$. The steps following sample pre-treatment were exactly the same for both groups. Figure 3-19 shows samples diluted with 0.5 mL $NH_4OH$ gave a 2-fold higher response yield compared to samples that underwent protein precipitation. This finding indicates that hPTH (1-34) may partially precipitated by acetonitrile or possibly adheres to vial surfaces during evaporation. This may explain the quadratic fit calibration curve obtained by Chambers *et al.* (136). The sample preparation method developed by Kay *et al.* (138) for extraction of PTH (1-34) from porcine plasma involves a protein precipitation, where 900 µL of solvent (75:25:0.1 ACN: $H_2O$: FA v/v) added to 150 µL of plasma followed by evaporation of the supernatant to dryness at 50 $^oC$, which I believe takes a long time to dry (138). The sample preparation method described herein is simple

and easy to be set up for automation on the Biotage® Extrahera™ automated plate processor, which is a big advantage when high throughput is required.

Before loading the eluent into the LC-MS/MS, it was diluted with water in order to lower the organic content (70%) to a reasonable value (≈35%) close to the organic ratio of LC gradient start (10%) and consequently efficient separation of the peptide in the LC column.

### 4.1.2 PTH (1-34) Method Validation

The calibration curve of the hPTH (1-34) assay demonstrated a good linearity over the range of 10 -2000 pg/mL. The LLoD and LLoQ of the assay were 2.1 pg/mL and 10.0 pg/mL respectively. The assessment of the precision and accuracy of the method showed the LC-MS/MS assay generated high-quality measurement data. The inter-assay precision was <9.8% and the inter-assay accuracy was <14.9%. While, the intra-assay precision and accuracy were <7.8% and <6.9% respectively. The mean recovery of hPTH (1-34) was 107.2% (range 98.6-112.9%), which indicates that the extraction method is able to efficiently extract hPTH (1-34) from human plasma. The assay was found to have an insignificant matrix effect of <6.1%, while ion-suppression assessment revealed that hPTH (1-34) and the IS do not co-elute with suppression and enhancement ions. The assay did not show cross-reactivity with hPTH (1-86), rat PTH(1-34), hPTH (13-34), hPTHrP (1-86) and hPTHrP (1-36) and was found to have high selectivity across all blank samples tested, where no peak at the elution time of hPTH (1-34) or IS were detected in all blank samples tested. Also the assay was not susceptible to carry-over contamination when samples with very high PTH (1-34) concentrations were analysed. One of the major advantages of this LC-MS/MS assay is its ability to measure oxidized forms of PTH (1-34) alongside non-oxidized PTH (1-34), which means that the assay measures the true bioactive form of the peptide-drug. This will have a positive impact on drug development studies and patient drug monitoring testing.

### 4.1.3 PTH (1-34) Methods Comparison

The validated LC-MS/MS assay was compared against a validated two-site PTH (1-34) IDS-iSYS immunoassay. Other immunoassays for PTH (1-34) measurement are also available and have been used in some published studies such as Immutopics (San Clemente, CA, USA) (53, 279). Comparison of hPTH (1-34) values of 390 samples measured using the validated LC-MS/MS assay with the IDS immunoassay

showed high correlation ($r^2$= 0.95) (figure 3-24). A concentration-dependent, negative bias of 35.5% was observed across the concentration range of 0-800 pg/mL. This finding is expected given the high selectivity of LC-MS/MS in comparison to the immunoassay which is subject to interferences. Several studies have reported similar finding when LC-MS/MS results compared with immunoassay results for several analytes. Tang *et* al. (280) demonstrated the same finding for urine free pyridinoline (PYD). The authors reported a negative bias (mean bias = -7.94 nmol/L), which is greater at higher concentrations for PYD values generated by LC-MS/MS in comparison to MicroVue immunoassay. Similarly, Farrell *et al.* (281) had the same observation when they compared two LC-MS/MS methods for Vitamin D against five automated immunoassays and an established RIA. Oe *et al.* (116) also reported higher Amyloid β peptide ($A\beta_{1-40}$) concentrations in CSF of Alzheimer's disease patients measured by ELISA compared to that measured by immunoaffinity purification and stable isotope dilution liquid chromatography negative electrospray tandem mass spectrometry assay. The two assays showed relatively poor correlation ($r^2$ = 0.644). The authors attributed this difference to the possibility of presence of post-translational modified forms of $A\beta_{1-40}$ or cross-reactivity of the assay's antibodies with truncated forms of $A\beta_{1-40}$.

There are several possible explanations for the observed correlation results between LC-MS/MS and IDS immunoassay hPTH (1-34) in this thesis. First, the immunoassay is prone to cross-reactivity to endogenous intact PTH (1-84) and other truncated PTH fragments compared to the high specificity of the LC-MS/MS assay. The LC-MS/MS assay has shown zero cross-reactivity with hPTH (1-84), rat PTH (1-34), hPTH (13-34), hPTHrP (1-86), and hPTHrP (1-36). In contrast, the IDS immunoassay showed mean (SD) 6.5% (0.3), 44.2% (0.8) cross-reactivity with hPTH (1-84) and rat PTH (1-34), respectively. Similarly, Satterwhite *et al.* (53) indicated severe cross-reactivity of their PTH (1-34) immunoassay to PTH (1-84) in addition to other smaller N- and C-terminus PTH fragments. The authors argued that endogenous PTH secretion was dramatically suppressed following teriparatide injection (53). However, endogenous PTH may be metabolised or truncated to smaller fragments that cross-react with immunoassays and a rebound of PTH (1-84) secretion has been observed following PTH (1-34) administration. The LC-MS/MS assay has been shown to be highly selective when blank plasma/serum from different

sources was analysed and no peak was detected at the elution time of hPTH (1-34) or the IS. Second, matrix type (plasma vs serum) has a severe effect on hPTH (1-34) results using the immunoassay, whereas matrix effect is negligible on LC-MS/MS. hPTH (1-34) values of calibration standards spiked in charcoal-stripped human plasma and in fetal bovine serum were similar using LC-MS/MS assay, whereas IDS Immunoassay showed higher concentrations of hPTH (1-34) spiked in charcoal-stripped human plasma compared to that spiked in bovine serum (figure 3-26 and 3-27). Moreover, when the known concentration standards provided with the IDS-immunoassay kit were analysed using LC-MS/MS method, true concentration values were obtained, which proves the LC-MS/MS method accurately measures hPTH (1-34). Third, data from this thesis have shown that the immunoassay is unable to differentiate oxidized from non-oxidized hPTH (1-34), which have different biological activity, whereas the LC-MS/MS assay is capable of measuring oxidized and non-oxidized PTH (1-34) separately. Therefore, it is likely that oxidized forms of PTH (1-34) are contributing to the total concentration of PTH (1-34) in the immunoassay. There might be an assay sensitivity-related issue with regards to the ability of the LC-MS/MS assay to pick up oxidized-PTH (1-34) as it is converted into several forms in little concentrations. This remains to be investigated in future.

Ursem *et al.* (282) studied whether oxidation of PTH occurs *in vivo*, or whether it is mainly an *in vitro* artefact. The authors provided evidence that PTH oxidation occurs mainly in biological systems and does not occur after venesection, which supports the value of the LC-MS/MS assay. The capability of LC-MS/MS assay to measure the true bioactive form of PTH (1-34) is of high importance for therapeutic peptide-drug development. Reliable pharmacokinetic (PK) and pharmacodynamic (PD) data is a prerequisite for successful PK/PD modelling and simulation in drug development (283). The LC-MS/MS assay would be helpful in optimizing dose and frequency of PTH (1-34) dosing in the treatment of hypoparathyroid patients.

### 4.1.4 PK analysis

PK analysis was conducted to assess the ability of our validated LC-MS/MS to conduct comparative PK analysis of the two oral PTH (1-34) doses and the standard Forsteo® injection. The assay was capable of detecting the change in PTH (1-34) concentrations of both oral and subcutaneous treatments.

Rapid absorption was observed upon oral administration of PTH (1-34) and subcutaneous injection of Forsteo® with maximum concentrations being observed around 20 min post dose. The complete elimination of PTH (1-34) from the circulation takes about 3 h following sc administration, whereas it takes less than 2 h after oral administration (figure 3.30). The slower elimination of sc injected PTH (1-34) compared to oral PTH (1-34) more likely to be due to continued slower absorption from muscle/subcutaneous tissue compared to more rapid absorption from the stomach (279). The pharmacokinetic data for sc Forsteo® administration are consistent with published data (53, 279). The data indicate that $C_{max}$ and $AUC_{0\text{-last}}$ values are proportional to oral PTH (1-34) doses. The two doses (0.69 mg and 2.07 mg) of oral PTH (1-34) brackets the Forsteo® PTH (1-34) $C_{max}$ indicating the relative bioavailability. Although, the 2.07 mg oral PTH (1-34) gives significantly higher (*p=0.009)* $C_{max}$ than Forsteo®, they both give statistically similar AUC (*p=0.871)*, which indicates similar overall exposure to PTH (1-34). The PK profile of the oral PTH (1-34) treatment showed a pulsatile peak with a periodicity less than 2 h, which is consistent with the requirement for optimal anabolic bone activity, and thus for osteoporosis treatment (47, 48, 56). Using a total daily dose of 80 µg/kg body weight of hPTH (1-34) is appropriate to treat osteoporosis, Dobing and Turner (56) demonstrated that the daily sc injection and 1 h/day infusion dramatically increased osteoblast number and bone formation in the proximal tibial metaphysis in rats, whereas longer infusion resulted in systemic side-effects, including up to a 10% loss in body weight, hypercalcemia, and histological changes in the proximal tibia resembling abnormalities observed in patients with chronic primary hyperparathyroidism, including peritrabecular marrow fibrosis and focal bone resorption. Infusion for as little as 2 h/day resulted in minor weight loss and changes in bone histology that were intermediate between sc and continuous administration. The results demonstrated that the therapeutic interval for hPTH exposure is brief but prolonged exposure can result in adverse effects. As it is shown in the PK profile (figure 3-31) for each treatment, both treatments remain above the typical basal endogenous PTH(1-84) concentration for postmenopausal women (>28 pg/mL) for less than 2 h, which may indicate appropriate drug exposure time for osteoporosis management.

A single high-amplitude pulse of PTH (1-34) that was demonstrated following a 2.07 mg oral PTH (1-34) dose may not provide acceptable treatment for chronic hypoparathyroidism patients as it does not mimic normal physiology, which involves frequent low-amplitude pulses superimposed on an underlying circadian rhythm. Frequent daily-doses of a low (e.g. 0.69 mg) oral PTH (1-34) or an intermediate dose given multiply during the day would be a better choice of treatment. However, safety and efficacy of oral PTH (1-34) treatment needs to be studied and dose adjustment based on individual pharmacokinetic assessment should be considered before starting oral PTH (1-34) therapy giving the large variability in $C_{max}$ and AUC between individuals. Oral formulations of PTH (1-34), will likely improve patient acceptance and compliance by providing a convenient and painless delivery route compared to current repeated sc therapy.

### 4.1.5 PTH (1-34) LC-MS/MS Method Applications

The data shows that the LC-MS/MS method is capable of performing PK analysis and monitoring the time-point response to various hPTH (1-34) doses and formulae. The high selectivity and sensitivity of the assay with its ability to detect oxidized and non-oxidized forms of PTH (1-34) qualify it to be a method of choice in drug development studies. As discussed previously, teriparatide has shown potential as a replacement therapy in hypoparathyroidism. Recently, the European Commission (EC) has granted conditional marketing authorization for Natpar® (rhPTH[1-84]), the first recombinant human protein with the full length 84-amino acid sequence of endogenous parathyroid hormone (PTH). Natpar® is the first and only approved hormone therapy for chronic hypoparathyroidism. It is available as a 25, 50, 75 and 100 micrograms once-daily injection as adjunctive treatment for adult patients with chronic hypoparathyroidism who cannot be adequately controlled with standard therapy alone. However, hypoparathyroidism is still the only classic endocrine deficiency disease for which the missing hormone, PTH, is not yet available as an oral replacement therapy (81). Our LC-MS/MS could play an important role in moving research into PTH (1-34) therapy forward. Once oral PTH (1-34) is approved as a replacement therapy for hypoparathyroidism, individual-based PTH (1-34) dose and frequency will need close monitoring before settling on a long-term treatment regimen. The LC-MS/MS method is capable of providing data to allow this type of personalised medicine approach.

Low-dose PTH (1-34) administered intermittently is proven to have an anabolic effect on the skeleton. It is used in treatment of osteoporosis and for accelerating bone fracture healing. PTH (1-34) is used as a stimulating agent to assess end organ resistance to PTH in pseudohypoparathyroidism and a reformat of the EHT, by adding measurement of plasma PTH (1-34) alongside urine and plasma cAMP and urinary phosphate can help improve the diagnostic value of this test. The addition of PTH (1-34) measurement allows confirmation that a suitable concentration of PTH (1-34) has been achieved that is required to stimulate a diagnostic plasma/urine cAMP and urine phosphate response. This format of the EHT should facilitate the study of disease to determine the appropriate administration dose of PTH (1-34) by SC injection and define the criteria of positive urinary and plasma cAMP excretion in healthy and diseased populations.

## 4.2 LC-MS/MS Method for quantification of Human PTHrP (1-36)

This study describes development and validation of a LC-MS/MS assay for quantification of hPTHrP (1-36) using the same platform employed for hPTH (1-34) described earlier in this thesis. Full MS scan spectra of hPTHrP (1-36) in aqueous solution has shown intense multi-charged ions with the 6+ molecule $[M+6H]^{6+}$, 7+ molecule $[M+7H]^{7+}$ and 5+ molecule $[M+5H]^{5+}$ under the positive ESI at *m/z* 711.1, 609.5 and 853.1, respectively, corresponding precisely to the molecular mass of hPTHrP (1-36). Surprisingly, only 7+ precursor molecules produced useful product ions with adequate intensity to be used in hPTHrP (1-36) measurement. Two product ions were obtained by collision-induced fragmentation of the 7+ precursor, namely at 682.7 and at 689.2. Precursor to product mass transitions 609.5>682.7 and 609.5>689.2 were designated as quantifier and qualifier transitions for hPTHrP (1-36) MS/MS monitoring, respectively.

The calibration curve of hPTHrP (1-36) assay shows a good linearity over a concentration range of 25-2000 pg/mL. The LLoD and LLoQ are 2.5 and 25 pg/mL, respectively. The inter- and intra-assay precision was <11.8 and <12.4%, respectively, while inter- and intra-assay accuracy were <9.1 and <10.7%, respectively at four QC concentrations (50, 100, 200, and 800 pg/mL). The assay

showed efficient recovery of hPTHrP (1-36) from plasma with an average recovery of 103.7% (range 96.7-113.7%) and no carry-over observed throughout the validation period of the assay. The calculated percentage matrix effect at the two concentrations used for testing for matrix effect on the assay (100 and 1000 pg/mL) were 14.4% and 1.7%, respectively. No ion suppression/enhancement affects the chromatography of hPTHrP (1-36) as PTHrP (1-36) does not co-elute with ion-suppression/enhancement species. The results of the validation study indicate that the extraction and LC method used with hPTH (1-34) is suitable to adequately extract and separate hPTHrP (1-36) from a complex biological matrix such as human plasma. The analytical sensitivity of the LC-MS/MS PTHrP (1-36) assay (25 pg/mL= 5.9 pmol/L) is sufficient for measurement of N-terminal PTHrP (1-36) in clinical setting of MAH as defined by RIAs for N-terminal PTHrP with affinity purification (167, 284-286).

Unlike hPTH (1-34), hPTHrP (1-36) does not contain methionine residues hence no oxidative effect was expected or detected after prolonged exposure with $H_2O_2$. Resistance to oxidation is an advantage for PTHrP (1-36) and PTHrP (1-34) analog drugs, such as abaloparatide, when used to treat metabolic bone disease and may result in enhanced drug stability and hence greater efficacy.

The LC-MS/MS assay for hPTHrP (1-36) may help in better understanding of the physiology and pathophysiology of PTHrP in human, animal models and even in cell culture extracts. The assay can be tuned/optimised for the quantification of PTHrP (1-34) analog (abaloparatide) given the significant homology between the native hPTHrP (1-36) and hPTHrP (1-34) analog, which will aid studies in the therapeutic use/efficacy of this osteoanabolic agent. It was recently reported that exogenous PTHrP (1-36) significantly enhances beta cell regeneration through increased beta cell proliferation and beta cell mass after partial pancreatectomy (219). This may indicate the potential therapeutic effectiveness of PTHrP (1-36) for diabetic-related pathophysiological conditions. Our assay for native hPTHrP (1-36) could be a good tool in future studies of the therapeutic use of PTHrP and its analogs. Although PTHrP was initially discovered as a PTH-like factor in context of hypercalcemia associated with malignancy and was first characterized in tumour tissues, subsequent studies showed that it is also expressed by various normal tissues (287). Because PTHrP was undetectable in the circulating blood of normal volunteers using high

sensitive immunoassays, a local paracrine/autocrine role was suggested in normal physiology outside the skeleton. It is now well-known that PTHrP is produced in a paracrine/autocrine fashion during fetal and adult life by a number of normal cells and tissues and likely plays an expanding number of physiological roles through these autocrine/paracrine pathways (287). PTHrP is also able to act through an intracrine pathway, which involves the translocation of the nascent protein into the nucleus via the NLS in its 88-107 region. PTHrP, signaling via the PTHR1, has been shown to be a critical regulator of chondrocyte differentiation during endochondral bone formation (193, 223, 288), to participate in epithelial- mesenchymal interactions during the formation of epithelial organs such as the skin (289), mammary glands (197-199) and teeth (212). The full-length PTHrP (1-39) and the N-terminal PTHrP (1-36) peptides also enhance beta cell function, proliferation and survival in mice (216, 219, 290, 291).

PTHrP also plays important role in carcinogenesis, tumour growth, differentiation and progression of breast cancer (244), prostate cancer (251), lung cancer (256), renal cancer (259), oral squamous cell carcinoma (260) and colorectal and gastric carcinoma (258). PTHrP or/and PTHR1 expression correlates significantly with tumour grade and its aggressiveness. PTHrP expression and localization in primary breast and prostate tumours is associated with increased incidence of bone metastases (249, 252).

It is widely accepted that the nascent PTHrP isoforms generated by alternative splicing of PTHrP gene are further processed by members of prohormone convertase to, at least, three fragments: N-terminal PTH-like PTHrP (1-36), a mid-region (38-94) and a C-terminal PTHrP (107-139). However, the lack of specific assays to detect the various isoforms of PTHrP and their products still limits the clear understanding of this complex molecule and our concept is about the circulating forms of PTHrP in plasma, so far, is based on various immunoassays using different region-specific antibodies produced by injecting synthetic fragments of PTHrP into different animal species. Several RIAs with region-specific antibodies directed against the N-terminus and C-terminus of PTHrP indicated that short truncated forms of PTHrP are likely to exist in the blood circulation of normal volunteers, renal failure patients and patients with malignancy-associated hypercalcemia (MAH) (166, 167) alongside longer peptide forms, e.g. PTHrP (1-86)

and PTHrP (1-74). For routine clinical practice, two-site IRMAs are the method of choice for measurement of PTHrP in MAH patients because of their clinical superiority to detect elevated PTHrP using direct methods without prior plasma extraction. LC-MS/MS should be the most appropriate alternative method for measurement of short PTHrP fragments like PTHrP (1-36) and PTHrP (109-136), that have molecular masses within the mass range and resolution capacity of MS. LC-MS/MS is superior in its ability to measure multiple PTHrP metabolites in a single run from the same sample. The assay developed in this thesis is a step towards producing a LC-MS/MS assay capable of measuring multiple forms of PTHrP. Recently, Kushnir *et al.* (171) reported a high sensitive LC-MS/MS method for quantification of PTHrP-specific digested peptide after PTHrP was enriched by extraction using a rabbit polyclonal antibody. The antigenic determinant/epitope portion of the polyclonal antibody used for immunoenrichment of PTHrP was not specified by the authors. Also the digested peptide selected as surrogate peptide for quantification of PTHrP was in the C-terminal of PTHrP and may not represent the bioactive peptide. Combination of immunoextraction with the assay developed in this thesis may offer an opportunity to improve detection of bioactive fragments of PTHrP acting via the PTHR1.

PTHrP blood concentrations have been examined in MAH patients using specific two-site IRMAs and it is estimated 50-80% of patients with solid tumours (166, 168, 285, 292), and 20-60% of patients with hematological malignancies (168, 292, 293), have high circulating concentrations of PTHrP. Elevated PTHrP is found to be strongly correlated with NcAMP in MAH patients (166, 168). It was demonstrated that the concentrations of circulating PTHrP decreased in some patients after the tumours were resected (166) and the chemotherapeutic intervention with concomitant reduction in tumour burden was associated with a reduction in circulating PTHrP and correction of hypercalcemia (285). PTHrP expression and localization in primary breast (245-248) and prostate (252, 292) tumours was associated with increased incidence of bone metastases and skeletal morbidity in patients. PTHrP maintains tumour burden within bone by activating bone turnover and hence the production of local cytokines by the bone microenvironment. These local growth factors then accelerate the tumour cell growth in a vicious cycle of mutually activating factors (292). PTHrP appears to be a prognostic indicator in

patients with MAH, where elevated PTHrP concentration is associated with a more advanced tumour state, a significant decrease in survival, poorer response to treatment and therefore poor prognosis (294, 295). PTHrP also seems to play an important role in treatment response with bone anti-resorptive agents such as bisphosphonates (294, 296, 297) and the proportion of recurrence of hypercalcemia following calcium normalization is higher in MAH patients with elevated PTHrP concentrations than in MAH patients with normal concentrations of PTHrP (296, 297). Onuma *et al.* (298) demonstrated that HHM refractory to osteoclastic bone resorption inhibitors such as bisphosphonates and calcitonin is caused by increased renal calcium reabsorption stimulated by high circulating PTHrP concentrations and the development of anti-osteoblastic bone resorption-refractory HHM can be reversed by a neutralizing antibodies against PTHrP.

PTHrP has clearly been identified as the major mediator of MAH in solid tumours and, at least in part, in a number of hematologic malignancies. It also may play an important role in controlling the metastatic process and can be a valid target in cancer therapy. PTHrP demonstrates multifunction and appears to acts systemically and locally in cancer and mostly locally in normal physiology. However, the lack of specific assays to detect the various isoforms of PTHrP and their products still limits our clear understanding to this complex molecules and may underestimate the expected benefits of its utility in tumour diagnosis and prognosis. This chapter of the thesis reports a LC-MS/MS assay for quantification of one of the widely reported PTHrP products, the PTHrP (1-36) fragment, whose measurement in future studies will undoubtedly contribute to the clarification of the common circulating forms of PTHrP in human plasma, tissue extracts and even in enriched culture-media extracts..

# 5. Conclusions

## 5.1 Summary

The main purpose of this thesis was to develop highly-sensitive LC-MS/MS assays for quantifying two human peptides: PTH (1-34) and PTHrP (1-36) which can achieve LLoQ at low picomolar concentrations. As part of the thesis, investigations were undertaken to develop a simple, yet highly selective and readily automatable sample preparation method using µElution 96-well SPE plates. The results of the LC-MS/MS assay validation experiments for both peptides show good reproducibility, specificity, sensitivity and recovery. The methods achieve a LLoQ of 10 pg/mL for hPTH (1-34) and 25 pg/mL for hPTHrP (1-36) using a 200 µL human plasma sample. The LC-MS/MS methods were evaluated for measurement of the analytes in human plasma. However, the assays are also suitable for analysis in animal plasma and aqueous solutions such as cell culture media. Importantly, the LC-MS/MS method for PTH (1-34) is able to differentiate non-oxidized PTH (1-34) and oxidized PTH (1-34) forms, which is, to the best of author knowledge, addressed for the first time. Measurement of non-oxidized and oxidized forms of PTH (1-34) may offer new insights into the physiology and pathophysiology of PTH and may aid in the therapeutic use/efficacy of PTH (1-34) as an osteoanabolic agent and facilitate the development of optimised therapy in many metabolic bone disease and combination therapy with other anti-resorptive/anti-remodeling agents. The study was unable to assess the true accuracy of endogenous PTH (1-34) and PTHrP (1-36) concentrations in humans due to the lack of reference standard material and external proficiency schemes available for PTH (1-34) and PTHrP (1-36). Data on LC-MS/MS precision and accuracy were based on assessment performed using in-house prepared calibration standards and quality control materials. Correlation and regression analysis revealed that hPTH (1-34) results from the validated LC-MS/MS assay and the IDS immunoassay were highly correlated with a concentration-dependent bias observed across the concentration range of 0 – 800 pg/mL. However, our data showed that the LC-MS/MS method gave the correct measurements for hPTH (1-34) and the immunoassay was positively biased. These results confirming that standardisation issues will need to be addressed in future for these analytes.

The PK analysis study has shown that the LC-MS/MS for PTH (1-34) is capable of detecting the change in hPTH (1-34) concentrations after oral and subcutaneous

administration. The PK analysis results show that the oral delivery technology used for hPTH (1-34) administration in this study enhances rapid peptide absorption from stomach and rapid elimination from the circulation, which produces sharp pulsatile peaks favouring an anabolic bone response of major value in the treatment of osteoporosis. This study was not designed to fully evaluate the pharmacodynamics of the oral hPTH (1-34) or to investigate correlates with adverse effects of the treatment on participants. Therefore, a conclusion with regard to the efficacy and safety of the oral drug cannot be provided in this thesis.

## 5.2 Limitations/Area of improvements

Here are some procedures that should be done to improve the quality of LC-MS/MS method validation results, which have been missed in this thesis:

- Matrix effect experiments should not have included internal standard.
- Water blank should be added in ion-suppression experiments.
- Six replicates of each sample should have tested for matrix and recovery experiments.

## 5.3 Future direction

Further experimental investigations are needed to estimate the amount of hPTH (1-34) that gets oxidized from the total amount which has been administered, and whether oral or subcutaneous hPTH (1-34) drugs are both vulnerable to the oxidation process during drug production and storage or during metabolism within the human body. This thesis has highlighted the tools and techniques for understanding, identifying and addressing the challenges associated with peptide analysis by LC-MS in routine bioanalytical laboratories. The combination of µElution SPE and high mass resolution ESI-MS/MS or ESI-Time of flight (TOF) MS may enable detection of several circulating PTH fragments. The analysis of intact PTH (1-84) is useful in the diagnosis of many bone and calcium disorders including hyper- and hypocalcemia, hyperparathyroidism, and in the prevention of bone mineral disorders in renal patients. The current immunoassays for PTH (1-84) can be susceptible to interference by cross-reacting PTH fragments, especially in renal failure patients with reduced renal clearance of C-terminal PTH fragments. So, the question is: can the lessons learnt from this thesis be applied to develop a sensitive and reliable LC-MS/MS for quantifying PTH (1-84) by cleaving it enzymatically into reasonable-size peptide fragments without the need of immunocapture antibody? High-specificity

chymotrypsin is the best enzyme candidate. Chymotrypsin is a proteolytic enzyme, which preferentially cleaves peptide at tryptophan (W), tyrosine (Y) and phenylalanine (F) in position P1 (High specificity) and to a lesser extent at leucine (L), Methionine (M) and histidine (H) at P1. Chymotrypsin-high specificity enzyme can cleave PTH (1-84) (SVSEIQLMHNLGKHLNSMERVEWLRKKLQDVHNFVALGAPLAPRDAGSQR PRKKEDNVLVESHEKSLGEADKADVNVLTKAKSQ) at two cleavage positions: amino acid 23 (W) and amino acid 34 (F) and produces fragments with peptide length of 23, 34, 11 and 50 amino acid and masses of 2738.1, 4117.8, 1397.6 and 5325.0 Da, respectively (https://web.expasy.org/cgi-bin/peptide_cutter). All chymotrypsin digestion fragments have masses within the detection range of either ESI-MS/MS or ESI-TOF MS. Any of the fragments that provides sufficient sensitivity and stability and are specific for human PTH can be used as a surrogate peptide for measurement of PTH (1-84). Designation of surrogate peptide will minimise the number of synthetic standard peptides for a calibration curve, which is necessary for accurate quantification. The use of isotopically-labelled PTH (1-84) as an internal standard and its incorporation with endogenous PTH (1-84) during the digestion process will empower the method and make the quantification more reliable.

The findings from PK analysis study of oral hPTH (1-34) also lead to several directions for further investigations into the possibility of using oral hPTH (1-34) as a replacement therapy for PHP. A more frequent daily regimen of low-dose oral hPTH (1-34) can give a response that will mimic the normal physiology of PTH and may provide more convenient and non-invasive way of treatment.

The PTHrP (1-36) LCMS/MS assay is an important initial step towards producing PTHrP fragment assays that could significantly expand our knowledge about PTHrP physiology and pathophysiology. The assay developed should readily be adapted to measure abaloparatide and help the development of this treatment in metabolic bone disease particularly osteoporosis. The current assay will now be utilised in the study of cancer biology, pregnancy related calcium homeostasis and chondrocyte biology contributing significantly to advances in knowledge in these areas of scientific investigation.

# References


1. Bellido T, Ali A, Gubrij I, Plotkin L, Fu Q, O'brien C, et al. Chronic elevation of parathyroid hormone in mice reduces expression of sclerostin by osteocytes: a novel mechanism for hormonal control of osteoblastogenesis. Endocrinology. 2005;146(11):4577-83.
2. Bilezikian JP, Marcus R, Levine MA, Marcocci C, Silverberg SJ, Potts Jr JT. The parathyroids: basic and clinical concepts: academic Press; 2014.
3. McCauley LK, Martin TJ. Twenty-five years of PTHrP progress: from cancer hormone to multifunctional cytokine. J Bone Miner Res. [Historical Article

Research Support, N.I.H., Extramural

Research Support, Non-U.S. Gov't

Review]. 2012 Jun;27(6):1231-9.
4. Karapl A. PTHrP Novel Roles in Skeletal Biology. Curr Pharm Des. 2001;7(8):655-70.
5. Habener JF, Rosenblatt M, Kemper B, Kronenberg HM, Rich A, Potts JT. Pre-proparathyroid hormone; amino acid sequence, chemical synthesis, and some biological studies of the precursor region. Proceedings of the National Academy of Sciences. 1978;75(6):2616-20.
6. Wiren KM, Ivashkiv L, Ma P, Freeman MW, Potts JT, Kronenberg HM. Mutations in signal sequence cleavage domain of preproparathyroid hormone alter protein translocation, signal sequence cleavage, and membrane-binding properties. Mol Endocrinol. 1989;3(2):240-50.
7. HABENER JF, KEMPER B, POTTS JT. Calcium-Dependent Intracellular Degradation of Parathyroid Hormone: A Possible Mechanism for the Regulation of Hormone Stores 1 2. Endocrinology. 1975;97(2):431-41.
8. Fraser R, Kronenberg H, Pang P, Harvey S. Parathyroid hormone messenger ribonucleic acid in the rat hypothalamus. Endocrinology. 1990;127(5):2517-22.
9. Nutley M, Parimi S, Harvey S. Sequence analysis of hypothalamic parathyroid hormone messenger ribonucleic acid. Endocrinology. 1995;136(12):5600-7.
10. Diehl M, Galich A, Pechín A, D'Alurzo M, Specterman S, Redal M, et al. Ectopic production of parathyroid hormone by a thymic carcinoma. Bone. 2007;40(3):S15-S6.
11. Gunther T, Zhou-Feng C, Kim J, Priemel M. Genetic ablation of parathyroid glands reveals another source of parathyroid hormone. Nature. 2000;406(6792):199.
12. Liu Z, Farley A, Chen L, Kirby BJ, Kovacs CS, Blackburn CC, et al. Thymus-associated parathyroid hormone has two cellular origins with distinct endocrine and immunological functions. PLoS genetics. 2010;6(12):e1001251.
13. Naveh-Many T, Silver J. Regulation of parathyroid hormone gene expression by hypocalcemia, hypercalcemia, and vitamin D in the rat. Journal of Clinical Investigation. 1990;86(4):1313.
14. Moallem E, Kilav R, Silver J, Naveh-Many T. RNA-protein binding and post-transcriptional regulation of parathyroid hormone gene expression by calcium and phosphate. Journal of Biological Chemistry. 1998;273(9):5253-9.
15. Kilav R, Silver J, Naveh-Many T. A conserved cis-acting element in the parathyroid hormone 3'-untranslated region is sufficient for regulation of RNA stability by calcium and phosphate. Journal of Biological Chemistry. 2001;276(12):8727-33.
16. Silver J, Russell J, Sherwood LM. Regulation by vitamin D metabolites of messenger ribonucleic acid for preproparathyroid hormone in isolated bovine parathyroid cells. Proceedings of the National Academy of Sciences. 1985;82(12):4270-3.

17. Okazaki T, Igarashi T, Kronenberg H. 5'-flanking region of the parathyroid hormone gene mediates negative regulation by 1, 25-(OH) 2 vitamin D3. Journal of Biological Chemistry. 1988;263(5):2203-8.
18. Kilav R, Silver J, Naveh-Many T. Parathyroid hormone gene expression in hypophosphatemic rats. Journal of Clinical Investigation. 1995;96(1):327.
19. Naveh-Many T, Rahamimov R, Livni N, Silver J. Parathyroid cell proliferation in normal and chronic renal failure rats. The effects of calcium, phosphate, and vitamin D. Journal of Clinical Investigation. 1995;96(4):1786.
20. Blau JE, Collins MT. The PTH-Vitamin D-FGF23 axis. Reviews in Endocrine and Metabolic Disorders. 2015;16(2):165-74.
21. Shimada T, Hasegawa H, Yamazaki Y, Muto T, Hino R, Takeuchi Y, et al. FGF-23 is a potent regulator of vitamin D metabolism and phosphate homeostasis. Journal of Bone and Mineral Research. 2004;19(3):429-35.
22. Shimada T, Kakitani M, Yamazaki Y, Hasegawa H, Takeuchi Y, Fujita T, et al. Targeted ablation of Fgf23 demonstrates an essential physiological role of FGF23 in phosphate and vitamin D metabolism. Journal of Clinical Investigation. 2004;113(4):561.
23. Imura A, Tsuji Y, Murata M, Maeda R, Kubota K, Iwano A, et al. α-Klotho as a regulator of calcium homeostasis. Science. 2007;316(5831):1615-8.
24. Chen G, Liu Y, Goetz R, Fu L, Jayaraman S, Hu M-C, et al. α-Klotho is a non-enzymatic molecular scaffold for FGF23 hormone signalling. Nature. 2018.
25. Erben RG. Update on FGF23 and Klotho signaling. Mol Cell Endocrinol. 2016;432:56-65.
26. Ben-Dov IZ, Galitzer H, Lavi-Moshayoff V, Goetz R, Kuro-o M, Mohammadi M, et al. The parathyroid is a target organ for FGF23 in rats. J Clin Invest. 2007;117(12):4003.
27. Krajisnik T, Björklund P, Marsell R, Ljunggren Ö, Åkerström G, Jonsson KB, et al. Fibroblast growth factor-23 regulates parathyroid hormone and 1α-hydroxylase expression in cultured bovine parathyroid cells. Journal of Endocrinology. 2007;195(1):125-31.
28. Lanske B, Razzaque MS. Molecular interactions of FGF23 and PTH in phosphate regulation. Kidney Int. 2014;86(6):1072.
29. Meir T, Durlacher K, Pan Z, Amir G, Richards WG, Silver J, et al. Parathyroid hormone activates the orphan nuclear receptor Nurr1 to induce FGF23 transcription. Kidney Int. 2014;86(6):1106-15.
30. Knab VM, Corbin B, Andrukhova O, Hum JM, Ni P, Rabadi S, et al. Acute parathyroid hormone injection increases C-terminal but not intact fibroblast growth factor 23 levels. Endocrinology. 2017;158(5):1130-9.
31. Brownstein CA, Adler F, Nelson-Williams C, Iijima J, Li P, Imura A, et al. A translocation causing increased α-Klotho level results in hypophosphatemic rickets and hyperparathyroidism. Proceedings of the National Academy of Sciences. 2008;105(9):3455-60.
32. Chong WH, Molinolo AA, Chen CC, Collins MT. Tumor-induced osteomalacia. Endocr Relat Cancer. 2011;18(3):R53-R77.
33. Juppner H, Freeman M. AG protein-linked receptor for parathyroid hormone and parathyroid hormone-related peptide. Science. 1991;254(5034):1024.
34. Singh A, Gilchrist A, Voyno-Yasenetskaya T, Radeff-Huang J, Stern P. Gα12/Gα13 subunits of heterotrimeric G proteins mediate parathyroid hormone activation of phospholipase D in UMR-106 osteoblastic cells. Endocrinology. 2005;146(5):2171-5.
35. Sneddon WB, Yang Y, Ba J, Harinstein LM, Friedman PA. Extracellular signal-regulated kinase activation by parathyroid hormone in distal tubule cells. American Journal of Physiology-Renal Physiology. 2007;292(3):F1028-F34.

36. Potts J, Tregear G, Keutmann H, Niall H, Sauer R, Deftos L, et al. Synthesis of a biologically active N-terminal tetratriacontapeptide of parathyroid hormone. Proceedings of the National Academy of Sciences. 1971;68(1):63-7.
37. TREGEAR GW, RIETSCHOTEN JV, GREENE E, KEUTMANN HT, NIALL HD, REIT B, et al. Bovine parathyroid hormone: minimum chain length of synthetic peptide required for biological activity. Endocrinology. 1973;93(6):1349-53.
38. Goltzmann D, Peytremann A, Callahan E, Tregear G, Potts J. Analysis of the requirements for parathyroid hormone action in renal membranes with the use of inhibiting analogues. Journal of Biological Chemistry. 1975;250(8):3199-203.
39. Rosenblatt M, Callahan EN, Mahaffey JE, Pont A, Potts J. Parathyroid hormone inhibitors. Design, synthesis, and biologic evaluation of hormone analogues. Journal of Biological Chemistry. 1977;252(16):5847-51.
40. Segre G, Rosenblatt M, Reiner B, Mahaffey J, Potts J. Characterization of parathyroid hormone receptors in canine renal cortical plasma membranes using a radioiodinated sulfur-free hormone analogue. Correlation of binding with adenylate cyclase activity. Journal of Biological Chemistry. 1979;254(15):6980-6.
41. Marx UC, Adermann K, Bayer P, Forssmann W-G, Rösch P. Solution structures of human parathyroid hormone fragments hPTH (1–34) and hPTH (1–39) and bovine parathyroid hormone fragment bPTH (1–37). Biochem Biophys Res Commun. 2000;267(1):213-20.
42. Marx UC, Adermann K, Bayer P, Meyer M, Forssmann W-G, Rösch P. Structure-activity relation of NH2-terminal human parathyroid hormone fragments. Journal of Biological Chemistry. 1998;273(8):4308-16.
43. Fraser WD, K. W. Colston and J. C. Stevenson (2013). Chapter 9.4 - Bone and Calcium Metabolism. The Immunoassay Handbook (Fourth Edition). D. Wild. Oxford, Elsevier: 705-720.
44. Kumar R, Thompson JR. The regulation of parathyroid hormone secretion and synthesis. Journal of the American Society of Nephrology. 2011;22(2):216-24.
45. Chen RA, Goodman WG. Role of the calcium-sensing receptor in parathyroid gland physiology. American Journal of Physiology-Renal Physiology. 2004;286(6):F1005-F11.
46. Mannstadt M, Bilezikian JP, Thakker RV, Hannan FM, Clarke BL, Rejnmark L, et al. Hypoparathyroidism. Nature Reviews Disease Primers. [Primer]. 2017 08/31/online;3:17055.
47. Girotra M, Rubin MR, Bilezikian JP. The use of parathyroid hormone in the treatment of osteoporosis. Reviews in Endocrine and Metabolic Disorders. 2006;7(1-2):113-21.
48. Neer RM, Arnaud CD, Zanchetta JR, Prince R, Gaich GA, Reginster J-Y, et al. Effect of parathyroid hormone (1-34) on fractures and bone mineral density in postmenopausal women with osteoporosis. New England journal of medicine. 2001;344(19):1434-41.
49. Greenspan SL, Bone HG, Ettinger MP, Hanley DA, Lindsay R, Zanchetta JR, et al. Effect of Recombinant Human Parathyroid Hormone (1-84) on Vertebral Fracture and Bone Mineral Density in Postmenopausal Women with OsteoporosisA Randomized TrialTreatment of Postmenopausal Osteoporotic Women with Parathyroid Hormone (1-84). Ann Intern Med. 2007;146(5):326-39.
50. Michalska D, Luchavova M, Zikan V, Raska Jr I, Kubena A, Stepan J. Effects of morning vs. evening teriparatide injection on bone mineral density and bone turnover markers in postmenopausal osteoporosis. Osteoporosis International. 2012;23(12):2885-91.
51. Nakajima A, Shimoji N, Shiomi K, Shimizu S, Moriya H, Einhorn TA, et al. Mechanisms for the enhancement of fracture healing in rats treated with intermittent low-

dose human parathyroid hormone (1–34). Journal of Bone and Mineral Research. 2002;17(11):2038-47.
52. Obermayer-Pietsch BM, Marin F, McCloskey EV, Hadji P, Farrerons J, Boonen S, et al. Effects of two years of daily teriparatide treatment on BMD in postmenopausal women with severe osteoporosis with and without prior antiresorptive treatment. Journal of bone and mineral research. 2008;23(10):1591-600.
53. Satterwhite J, Heathman M, Miller PD, Marín F, Glass EV, Dobnig H. Pharmacokinetics of teriparatide (rhPTH [1–34]) and calcium pharmacodynamics in postmenopausal women with osteoporosis. Calcif Tissue Int. 2010;87(6):485-92.
54. Sturmer A, Mehta N, Giacchi J, Cagatay T, Tavakkol R, Mitta S, et al. Pharmacokinetics of Oral Recombinant Human Parathyroid Hormone [rhPTH(1–31)NH2] in Postmenopausal Women with Osteoporosis. Clinical Pharmacokinetics. [journal article]. 2013;52(11):995-1004.
55. Takahata M, Schwarz EM, Chen T, O'Keefe RJ, Awad HA. Delayed short-course treatment with teriparatide (PTH1–34) improves femoral allograft healing by enhancing intramembranous bone formation at the graft–host junction. Journal of Bone and Mineral Research. 2012;27(1):26-37.
56. Dobnig H, Turner RT. The effects of programmed administration of human parathyroid hormone fragment (1–34) on bone histomorphometry and serum chemistry in rats. Endocrinology. 1997;138(11):4607-12.
57. Jiang Y, Zhao JJ, Mitlak BH, Wang O, Genant HK, Eriksen EF. Recombinant human parathyroid hormone (1–34)[teriparatide] improves both cortical and cancellous bone structure. Journal of Bone and Mineral Research. 2003;18(11):1932-41.
58. Ma YL, Zeng Q, Donley DW, Ste-Marie LG, Gallagher JC, Dalsky GP, et al. Teriparatide increases bone formation in modeling and remodeling osteons and enhances IGF-II immunoreactivity in postmenopausal women with osteoporosis. Journal of Bone and Mineral Research. 2006;21(6):855-64.
59. Jilka RL. Molecular and cellular mechanisms of the anabolic effect of intermittent PTH. Bone. 2007;40(6):1434-46.
60. Aslan D, Andersen MD, Gede LB, de Franca TK, Jørgensen SR, Schwarz P, et al. Mechanisms for the bone anabolic effect of parathyroid hormone treatment in humans. Scand J Clin Lab Invest. 2012;72(1):14-22.
61. https://www.researchgate.net/Simplified-depictions-of-members-of-the-RANK-RANKL-OPG-signalling-pathway-identified_fig1_229159844 [accessed 12 Apr, 2018] Goofg-wasAac-SFoRAf.
62. HABENER JF, SEGRE GV, POWELL D, MURRAY TM, POTTS JT. Immunoreactive parathyroid hormone in circulation of man. Nature. 1972;238(83):152-4.
63. Habener JF, Mayer G, Dee PC, Potts JT. Metabolism of amino-and carboxyl-sequence immunoreactive parathyroid hormone in the bovine: evidence for peripheral cleavage of hormone. Metabolism. 1976;25(4):385-95.
64. Roos B, Lindall A, Aron D, Orf J, Yoon M, Huber M, et al. Detection and characterization of small midregion parathyroid hormone fragment (s) in normal and hyperparathyroid glands and sera by immunoextraction and region-specific radioimmunoassays. The Journal of Clinical Endocrinology & Metabolism. 1981;53(4):709-21.
65. Flueck JA, Di Bella FP, Edis AJ, Kehrwald JM, Arnaud CD. Immunoheterogeneity of parathyroid hormone in venous effluent serum from hyperfunctioning parathyroid glands. Journal of Clinical Investigation. 1977;60(6):1367.
66. D'Amour P, Brossard J-H, Rousseau L, Nguyen-Yamamoto L, Nassif E, Lazure C, et al. Structure of non-(1-84) PTH fragments secreted by parathyroid glands in primary and secondary hyperparathyroidism. Kidney Int. 2005;68(3):998-1007.

67. Murray TM, Rao LG, Divieti P, Bringhurst FR. Parathyroid hormone secretion and action: evidence for discrete receptors for the carboxyl-terminal region and related biological actions of carboxyl-terminal ligands. Endocr Rev. 2005;26(1):78-113.
68. Hanley DA, Takatsuki K, Sultan JM, Schneider AB, Sherwood L. Direct release of parathyroid hormone fragments from functioning bovine parathyroid glands in vitro. Journal of Clinical Investigation. 1978;62(6):1247.
69. Segre GV, Perkins AS, Witters LA, Potts Jr JT. Metabolism of parathyroid hormone by isolated rat Kupffer cells and hepatocytes. Journal of Clinical Investigation. 1981;67(2):449.
70. Bringhurst FR, Segre GV, Lampman GW, Potts Jr JT. Metabolism of parathyroid hormone by Kupffer cells: analysis by reverse-phase high-performance liquid chromatography. Biochemistry. 1982;21(18):4252-8.
71. Pillai S, Zull J. Production of biologically active fragments of parathyroid hormone by isolated Kupffer cells. Journal of Biological Chemistry. 1986;261(32):14919-23.
72. Kau S, Maack T. Transport and catabolism of parathyroid hormone in isolated rat kidney. American Journal of Physiology-Renal Physiology. 1977;233(5):F445-F54.
73. Martin KJ, Hruska KA, Lewis J, Anderson C, Slatopolsky E. The renal handling of parathyroid hormone: role of peritubular uptake and glomerular filtration. Journal of Clinical Investigation. 1977;60(4):808.
74. Martin T, Melick R, De Luise M. The effect of nephrectomy on the metabolism of labelled parathyroid hormone. Clin Sci (Lond). 1969;37(1):137.
75. United Nations, Department of Economic and Social Affairs, Population Division (2015). World Population Ageing 2015 (ST/ESA/SERA/390). 2015.
76. health WHOAooatp, care level. Summary Report of a WHO Scientific Group. WHO G.
77. MacLean C, Newberry S, Maglione M, McMahon M, Ranganath V, Suttorp M, et al. Systematic review: comparative effectiveness of treatments to prevent fractures in men and women with low bone density or osteoporosis. Ann Intern Med. 2008;148(3):197-213.
78. Canalis E, Giustina A, Bilezikian JP. Mechanisms of anabolic therapies for osteoporosis. New England Journal of Medicine. 2007;357(9):905-16.
79. Dhillon RS, Schwarz EM. Teriparatide therapy as an adjuvant for tissue engineering and integration of biomaterials. Materials. 2011;4(6):1117-31.
80. Han SL, Wan SL. Effect of teriparatide on bone mineral density and fracture in postmenopausal osteoporosis: meta-analysis of randomised controlled trials. Int J Clin Pract. 2012;66(2):199-209.
81. Cusano NE, Rubin MR, Sliney J, Bilezikian JP. Mini-review: new therapeutic options in hypoparathyroidism. Endocrine. 2012;41(3):410-4.
82. Capriani C, Irani D, Bilezikian JP. Safety of osteoanabolic therapy: a decade of experience. Journal of Bone and Mineral Research. 2012;27(12):2419-28.
83. Winer KK, Zhang B, Shrader JA, Peterson D, Smith M, Albert PS, et al. Synthetic Human Parathyroid Hormone 1-34 Replacement Therapy: A Randomized Crossover Trial Comparing Pump Versus Injections in the Treatment of Chronic Hypoparathyroidism. J Clin Endocrinol Metab. 2012 11/16

06/29/received

10/18/accepted;97(2):391-9.
84. Winer KK, Yanovski JA, Cutler GB. Synthetic human parathyroid hormone 1-34 vs calcitriol and calcium in the treatment of hypoparathyroidism: Results of a short-term randomized crossover trial. Jama. 1996;276(8):631-6.
85. Winer KK, Yanovski JA, Sarani B, Cutler Jr GB. A randomized, cross-over trial of once-daily versus twice-daily parathyroid hormone 1–34 in treatment of

hypoparathyroidism. The Journal of Clinical Endocrinology & Metabolism. 1998;83(10):3480-6.
86. Winer KK, Ko CW, Reynolds JC, Dowdy K, Keil M, Peterson D, et al. Long-term treatment of hypoparathyroidism: a randomized controlled study comparing parathyroid hormone-(1–34) versus calcitriol and calcium. The Journal of Clinical Endocrinology & Metabolism. 2003;88(9):4214-20.
87. Winer KK, Sinaii N, Peterson D, Sainz Jr B, Cutler Jr GB. Effects of once versus twice-daily parathyroid hormone 1–34 therapy in children with hypoparathyroidism. The Journal of Clinical Endocrinology & Metabolism. 2008;93(9):3389-95.
88. Winer KK, Sinaii N, Reynolds J, Peterson D, Dowdy K, Cutler Jr GB. Long-term treatment of 12 children with chronic hypoparathyroidism: a randomized trial comparing synthetic human parathyroid hormone 1-34 versus calcitriol and calcium. The Journal of Clinical Endocrinology & Metabolism. 2010;95(6):2680-8.
89. De SA, De SS-J, Meeran K. The use of teriparatide to treat hypoparathyroidism following thyroidectomy; a case report. 2012.
90. Jahagirdar V, Stirling H, Sankar S. Continuous synthetic PTH1-34 replacement therapy in the treatment of autosomal dominant hypoparathyroidism type 1. 2016.
91. Aspenberg P, Genant HK, Johansson T, Nino AJ, See K, Krohn K, et al. Teriparatide for acceleration of fracture repair in humans: a prospective, randomized, double-blind study of 102 postmenopausal women with distal radial fractures. Journal of Bone and Mineral Research. 2010;25(2):404-14.
92. Aspenberg P, Johansson T. Teriparatide improves early callus formation in distal radial fractures: Analysis of a subgroup of patients within a randomized trial. Acta orthopaedica. 2010;81(2):234-6.
93. Warden SJ, Komatsu DE, Rydberg J, Bond JL, Hassett SM. Recombinant human parathyroid hormone (PTH 1-34) and low-intensity pulsed ultrasound have contrasting additive effects during fracture healing. Bone. 2009;44(3):485-94.
94. Ellegaard M, Kringelbach T, Syberg S, Petersen S, Beck Jensen JE, Brüel A, et al. The effect of PTH (1-34) on fracture healing during different loading conditions. Journal of Bone and Mineral Research. 2013;28(10):2145-55.
95. Liu F, Kohlmeier S, Wang C-Y. Wnt signaling and skeletal development. Cell Signal. 2008;20(6):999-1009.
96. Piters E, Boudin E, Van Hul W. Wnt signaling: a win for bone. Arch Biochem Biophys. 2008;473(2):112-6.
97. Holmen SL, Zylstra CR, Mukherjee A, Sigler RE, Faugere M-C, Bouxsein ML, et al. Essential role of β-catenin in postnatal bone acquisition. Journal of Biological Chemistry. 2005;280(22):21162-8.
98. Kramer I, Halleux C, Keller H, Pegurri M, Gooi JH, Weber PB, et al. Osteocyte Wnt/β-catenin signaling is required for normal bone homeostasis. Mol Cell Biol. 2010;30(12):3071-85.
99. Bellido T, Ali AA, Plotkin LI, Fu Q, Gubrij I, Roberson PK, et al. Proteasomal Degradation of Runx2 Shortens Parathyroid Hormone-induced Anti-apoptotic Signaling in Osteoblasts A PUTATIVE EXPLANATION FOR WHY INTERMITTENT ADMINISTRATION IS NEEDED FOR BONE ANABOLISM. Journal of Biological Chemistry. 2003;278(50):50259-72.
100. Jilka RL, Weinstein RS, Bellido T, Roberson P, Parfitt AM, Manolagas SC. Increased bone formation by prevention of osteoblast apoptosis with parathyroid hormone. Journal of Clinical Investigation. 1999;104(4):439.
101. Gazzerro E, Canalis E. Skeletal actions of insulin-like growth factors. Expert Review of Endocrinology & Metabolism. 2006;1(1):47-56.
102. Zhao G, Monier-Faugere M-C, Langub MC, Geng Z, Nakayama T, Pike JW, et al. Targeted overexpression of insulin-like growth factor I to osteoblasts of transgenic mice:

increased trabecular bone volume without increased osteoblast proliferation. Endocrinology. 2000;141(7):2674-82.
103. Ogata N, Chikazu D, Kubota N, Terauchi Y, Tobe K, Azuma Y, et al. Insulin receptor substrate-1 in osteoblast is indispensable for maintaining bone turnover. Journal of Clinical Investigation. 2000;105(7):935.
104. Zhang M, Xuan S, Bouxsein ML, von Stechow D, Akeno N, Faugere MC, et al. Osteoblast-specific knockout of the insulin-like growth factor (IGF) receptor gene reveals an essential role of IGF signaling in bone matrix mineralization. Journal of Biological Chemistry. 2002;277(46):44005-12.
105. Okazaki R. Differential diagnosis of hypoparathyroidism and the Ellsworth-Howard's test. Clin Calcium. 2007;17(8):1182-5.
106. Mantovani G. Pseudohypoparathyroidism: Diagnosis and Treatment. The Journal of Clinical Endocrinology & Metabolism. 2011;96(10):3020-30.
107. SOHN HE, FURUKAWA Y, YUMITA S, MIURA R, UNAKAMI H, YOSHINAGA K. Effect of Synthetic 1-34 Fragment of Human Parathyroid Hormone on Plasma Adenosine 3', 5'-Monophosphate Concentrations and the Diagnostic Criteria Based on the Plasma cAMP Response in Ellsworth-Howard Test. Endocrinol Jpn. 1984;31(1):33-40.
108. Mallette LE. Synthetic human parathyroid hormone 1-34 fragment for diagnostic testing. Ann Intern Med. 1988;109(10):800-4.
109. Tang J WC, Galitzer H, Hiemstra T, Meek C, Chipchase A, Fraser WD. The Ellsworth-Howard test revisited. Bone Abstracts. 2013;1 PP129., http://www.bone-abstracts.org/ba/0001/ba0001pp129.htm.
110. Fichorova RN, Richardson-Harman N, Alfano M, Belec L, Carbonneil C, Chen S, et al. Biological and technical variables affecting immunoassay recovery of cytokines from human serum and simulated vaginal fluid: a multicenter study. Anal Chem. 2008;80(12):4741-51.
111. Fritzler MJ, Wiik A, Tan EM, Smolen JS, McDougal JS, l Chan EK, et al. A critical evaluation of enzyme immunoassay kits for detection of antinuclear autoantibodies of defined specificities. III. Comparative performance characteristics of academic and manufacturers' laboratories. J Rheumatol. 2003;30(11):2374-81.
112. Massart C, Sapin R, Gibassier J, Agin A, d'Herbomez M. Intermethod variability in TSH-receptor antibody measurement: implication for the diagnosis of Graves disease and for the follow-up of Graves ophthalmopathy. Clin Chem. 2009;55(1):183-6.
113. Oe T, Ackermann BL, Inoue K, Berna MJ, Garner CO, Gelfanova V, et al. Quantitative analysis of amyloid β peptides in cerebrospinal fluid of Alzheimer's disease patients by immunoaffinity purification and stable isotope dilution liquid chromatography/negative electrospray ionization tandem mass spectrometry. Rapid communications in mass spectrometry. 2006;20(24):3723-35.
114. Rigo RB, Panyella MG, Bartolomé LR, Ramos PA, Soria PR, Navarro M-AM. Variations observed for insulin concentrations in an interlaboratory quality control program may be due to interferences between reagents and the matrix of the control materials. Clin Biochem. 2007;40(13):1088-91.
115. Cantor T, Yang Z, Caraiani N, Ilamathi E. Lack of comparability of intact parathyroid hormone measurements among commercial assays for end-stage renal disease patients: implication for treatment decisions. Clin Chem. 2006;52(9):1771-6.
116. Souberbielle J-C, Boutten A, Carlier M-C, Chevenne D, Coumaros G, Lawson-Body E, et al. Inter-method variability in PTH measurement: implication for the care of CKD patients. Kidney Int. 2006;70(2):345-50.
117. Ates F, Koken T, Demir S, Kahraman A, Dogan N. Comparison of three different immunoassay methods for the evaluation of intact parathyroid hormone levels in hemodialysis patients. Scand J Clin Lab Invest. 2011;71(3):227-31.

118. Kakuta T, Kato H, Komaba H, Akizawa T. Parathyroid Hormone Control Survey to Determine Inter-method and Inter-lab Variations in Japan. Therapeutic Apheresis and Dialysis. 2011;15(s1):50-5.
119. Sturgeon CM, Sprague SM, Metcalfe W. Variation in parathyroid hormone immunoassay results—a critical governance issue in the management of chronic kidney disease. Oxford University Press; 2011.
120. Almond A, Ellis AR, Walker SW. Current parathyroid hormone immunoassays do not adequately meet the needs of patients with chronic kidney disease. Ann Clin Biochem. 2012;49(1):63-7.
121. Ezan E, Dubois M, Becher F. Bioanalysis of recombinant proteins and antibodies by mass spectrometry. Analyst. 2009;134(5):825-34.
122. Bolstad N, Warren DJ, Nustad K. Heterophilic antibody interference in immunometric assays. Best Practice & Research Clinical Endocrinology & Metabolism. 2013;27(5):647-61.
123. Agarwal M, Das A, Singh AS. High-dose hook effect in prolactin macroadenomas: A diagnostic concern. J Hum Reprod Sci. 2010 Sep;3(3):160-1.
124. Tang J, Galitzer H, Washbourne C, Piec I, Wang N, Burshtien G, et al. First in Man Studies of Pharmacokinetic Profiles of a Novel Oral PTH (1-34). American Society of Bone and Mineral Research. 2014.
125. Cleland JL, Langer R. Formulation and Delivery of Proteins and Peptides. Formulation and Delivery of Proteins and Peptides: American Chemical Society; 1994. p. 1-19.
126. Chu J-W, Trout BL. On the mechanisms of oxidation of organic sulfides by H2O2 in aqueous solutions. Journal of the American Chemical Society. 2004;126(3):900-8.
127. Chu J-W, Yin J, Wang DI, Trout BL. Understanding Oxidative Instability of Protein Pharmaceuticals. 2004.
128. Davies Michael J. Protein oxidation and peroxidation. Biochemical Journal. 2016;473(7):805-25.
129. Li S, Schöneich C, Borchardt RT. Chemical instability of protein pharmaceuticals: Mechanisms of oxidation and strategies for stabilization. Biotechnology and Bioengineering. 1995;48(5):490-500.
130. Zull JE, Smith SK, Wiltshire R. Effect of methionine oxidation and deletion of amino-terminal residues on the conformation of parathyroid hormone. Circular dichroism studies. Journal of Biological Chemistry. 1990;265(10):5671-6.
131. Nabuchi Y, Fujiwara E, Ueno K, Kuboniwa H, Asoh Y, Ushio H. Oxidation of recombinant human parathyroid hormone: effect of oxidized position on the biological activity. Pharmaceutical research. 1995;12(12):2049-52.
132. Rane SS, Ajameri A, Mody R, Padmaja P. Development and validation of RP-HPLC and RP-UPLC methods for quantification of parathyroid hormones (1-34) in medicinal product formulated with meta-cresol. Journal of Pharmaceutical Analysis. 2012 4//;2(2):136-42.
133. GALCERAN T, LEWIS-FINCH J, MARTIN KJ, SLATOPOLSKY E. Absence of Biological Effects of Oxidized Parathyroid Hormone-(1–3 4) in Dogs and Rats. Endocrinology. 1984;115(6):2375-8.
134. Hocher B, Armbruster FP, Stoeva S, Reichetzeder C, Grön HJ, Lieker I, et al. Measuring parathyroid hormone (PTH) in patients with oxidative stress–do we need a fourth generation parathyroid hormone assay? PLoS One. 2012;7(7):e40242.
135. Vogt W. Oxidation of methionyl residues in proteins: tools, targets, and reversal. Free Radical Biology and Medicine. 1995;18(1):93-105.

136. Chambers EE, Lame ME, Bardsley J, Hannam S, Legido-Quigley C, Smith N, et al. High sensitivity LC–MS/MS method for direct quantification of human parathyroid 1–34 (teriparatide) in human plasma. Journal of Chromatography B. 2013;938:96-104.
137. MacNeill R, Stromeyer R, Urbanowicz B, Acharya V, Moussallie M. LC-MS/MS quantification of parathyroid hormone fragment 1-34 in human plasma. Bioanalysis. 2013;5(4):415-22.
138. Kay RG, Hands JT, Hawthorne G, Constable S, Grosvenor M, Sharman JA. Validation of an ultrasensitive LC-MS/MS method for PTH 1-34 in porcine plasma to support a solid dose PK study. Bioanalysis. 2015;7(12):1435-45.
139. Moseley JM, Kubota M, Diefenbach-Jagger H, Wettenhall R, Kemp B, Suva L, et al. Parathyroid hormone-related protein purified from a human lung cancer cell line. Proceedings of the National Academy of Sciences. 1987;84(14):5048-52.
140. Burtis WJ, Wu T, Bunch C, Wysolmerski JJ, Insogna KL, Weir EC, et al. Identification of a novel 17,000-dalton parathyroid hormone-like adenylate cyclase-stimulating protein from a tumor associated with humoral hypercalcemia of malignancy. Journal of Biological Chemistry. 1987;262(15):7151-6.
141. Stewler G, Stern P, Jacobs J. Parathyroid hormone-like protein from human renal carcinoma cells. J Clin Invest. 1987;80:1803-7.
142. Suva L, Winslow G, Wettenhall R, Hammonds R, Moseley J, Diefenbach-Jagger H, et al. A parathyroid hormone-related protein implicated in malignant hypercalcemia: cloning and expression. Science. 1987;237(4817):893-6.
143. Mangin M, Webb AC, Dreyer BE, Posillico JT, Ikeda K, Weir EC, et al. Identification of a cDNA encoding a parathyroid hormone-like peptide from a human tumor associated with humoral hypercalcemia of malignancy. Proceedings of the National Academy of Sciences. 1988;85(2):597-601.
144. Stewart AF, Wu T, Goumas D, Burtis WJ, Broadus AE. N-terminal amino acid sequence of two novel tumor-derived adenylate cyclase-stimulating proteins: identification of parathyroid hormone-like and parathyroid hormone-unlike domains. Biochem Biophys Res Commun. 1987;146(2):672-8.
145. Broadus A, Mangin M, Ikeda K, Insogna K, Weir E, Burtis W, et al. Humoral hypercalcemia of cancer. Identification of a novel parathyroid hormone-like peptide. N Engl J Med. 1988;319(9):556-63.
146. Wysolmerski JJ. Parathyroid hormone-related protein: an update. J Clin Endocrinol Metab. [Research Support, N.I.H., Extramural

Review]. 2012 Sep;97(9):2947-56.
147. Burtis WJ. Parathyroid hormone-related protein: structure, function, and measurement. Clin Chem. 1992;38(11):2171-83.
148. Martin TJ. Hypercalcemia of malignancy. Clinical Reviews in Bone and Mineral Metabolism. 2002;1(1):51-63.
149. Richard V, Rosol TJ, Foley J. PTHrP gene expression in cancer: do all paths lead to Ets? Critical Reviews™ in Eukaryotic Gene Expression. 2005;15(2).
150. Wysolmerski JJ, Broadus AE. Hypercalcemia of malignancy: the central role of parathyroid hormone-related protein. Annu Rev Med. 1994;45(1):189-200.
151. Mangin M, Ikeda K, Dreyer BE, Broadus AE. Isolation and characterization of the human parathyroid hormone-like peptide gene. Proceedings of the National Academy of Sciences. 1989;86(7):2408-12.
152. Yasuda T, Banville D, Hendy G, Goltzman D. Characterization of the human parathyroid hormone-like peptide gene. Functional and evolutionary aspects. Journal of Biological Chemistry. 1989;264(13):7720-5.

153. Soifer N, Dee K, Insogna K, Burtis W, Matovcik L, Wu T, et al. Parathyroid hormone-related protein. Evidence for secretion of a novel mid-region fragment by three different cell types. Journal of Biological Chemistry. 1992;267(25):18236-43.
154. Thiede MA, Rodan GA. Expression of a calcium-mobilizing parathyroid hormone-like peptide in lactating mammary tissue. Science. 1988;242(4876):278.
155. Yang KH, dePapp AE, Soifer NE, Dreyer BE, Wu TL, Porter SE, et al. Parathyroid hormone-related protein: evidence for isoform-and tissue-specific posttranslational processing. Biochemistry. 1994;33(23):7460-9.
156. Sourbier C, Massfelder T. Parathyroid hormone-related protein in human renal cell carcinoma. Cancer Lett. [Research Support, Non-U.S. Gov't

Review]. 2006 Aug 28;240(2):170-82.
157. Sharpe G, Dillon J, Durham B, Gallagher J, Fraser W. Human keratinocytes express transcripts for three isoforms of parathyroid hormone-related protein (PTHrP), but not for the parathyroid hormone/PTHrP receptor: effects of 1, 25 (OH) 2 vitamin D3. Br J Dermatol. 1998;138(6):944-51.
158. Philbrick W, Wysolmerski J, Galbraith S, Holt E, Orloff J, Yang K, et al. Defining the roles of parathyroid hormone-related protein in normal physiology. Physiol Rev. 1996;76(1):127-74.
159. Rabbani SA, Haq M, Goltzman D. Biosynthesis and processing of endogenous parathyroid hormone related peptide (PTHRP) by rat Leydig cell tumor H-500. Biochemistry. 1993;32(18):4931-7.
160. Juppner H, Abou-Samra A-B, Freeman M, Kong XF, Schipani E, Richards J, et al. AG protein-linked receptor for parathyroid hormone and parathyroid hormone-related peptide. Science. 1991;254(5034):1024-6.
161. Orloff JJ, Wu TL, Stewart AF. Parathyroid hormone-like proteins: biochemical responses and receptor interactions. Endocr Rev. 1989;10(4):476-95.
162. NICKOLS GA, NANA AD, NICKOLS MA, DiPETTE DJ, ASIMAKIS GK. Hypotension and Cardiac Stimulation due to the Parathyroid Hormone-Related Protein, Humoral Hypercalcemia of Malignancy Factor*. Endocrinology. 1989;125(2):834-41.
163. Jans DA, Thomas RJ, Gillespie MT. Parathyroid Hormone-Related Protein (PTHrP):: A Nucleocytoplasmic Shuttling Protein with Distinct Paracrine and Intracrine Roles. Vitamins & Hormones. 2003;66:345-84.
164. Kovacs CS, Lanske B, Hunzelman JL, Guo J, Karaplis AC, Kronenberg HM. Parathyroid hormone-related peptide (PTHrP) regulates fetal–placental calcium transport through a receptor distinct from the PTH/PTHrP receptor. Proceedings of the National Academy of Sciences. 1996;93(26):15233-8.
165. Portal-Núñez S, Lozano D, Fernández de Castro L, De Gortázar A, Nogués X, Esbrit P. Alterations of the Wnt/β-catenin pathway and its target genes for the N-and C-terminal domains of parathyroid hormone-related protein in bone from diabetic mice. FEBS Lett. 2010;584(14):3095-100.
166. Burtis WJ, Brady TG, Orloff JJ, Ersbak JB, Warrell Jr RP, Olson BR, et al. Immunochemical characterization of circulating parathyroid hormone–related protein in patients with humoral hypercalcemia of cancer. New England Journal of Medicine. 1990;322(16):1106-12.
167. Ratcliffe W, Norbury S, Stott R, Heath D, Ratcliffe J. Immunoreactivity of plasma parathyrin-related peptide: three region-specific radioimmunoassays and a two-site immunoradiometric assay compared. Clin Chem. 1991;37(10):1781-7.
168. Fraser WD, Robinson J, Lawton R, Durham B, Gallacher S, Boyle I, et al. Clinical and laboratory studies of a new immunoradiometric assay of parathyroid hormone-related protein. Clin Chem. 1993;39(3):414-9.

169. Lu CM, Burton DW, Fitzgerald RL, Deftos LJ, Buchholz BA, Vogel JS, et al. Mass spectrometric immunoassay for parathyroid hormone-related protein. Anal Chem. 2002;74(21):5507-12.
170. Washam CL, Byrum SD, Leitzel K, Ali SM, Tackett AJ, Gaddy D, et al. Identification of PTHrP(12-48) as a plasma biomarker associated with breast cancer bone metastasis. Cancer Epidemiol Biomarkers Prev. [Research Support, N.I.H., Extramural

Research Support, Non-U.S. Gov't]. 2013 May;22(5):972-83.
171. Kushnir MM, Rockwood AL, Strathmann FG, Frank EL, Straseski JA, Meikle AW. LC-MS/MS Measurement of Parathyroid Hormone–Related Peptide. Clin Chem. 2016;62(1):218-26.
172. Henderson JE, Amizuka N, Warshawsky H, Biasotto D, Lanske B, Goltzman D, et al. Nucleolar localization of parathyroid hormone-related peptide enhances survival of chondrocytes under conditions that promote apoptotic cell death. Mol Cell Biol. 1995;15(8):4064-75.
173. Goltzman D. Interactions of PTH and PTHrP with the PTH/PTHrP receptor and with downstream signaling pathways: exceptions that provide the rules. J Bone Miner Res. [Comment

Editorial

Review]. 1999 Feb;14(2):173-7.
174. Swarthout JT, D'Alonzo RC, Selvamurugan N, Partridge NC. Parathyroid hormone-dependent signaling pathways regulating genes in bone cells. Gene. 2002;282(1):1-17.
175. Gensure RC, Gardella TJ, Juppner H. Parathyroid hormone and parathyroid hormone-related peptide, and their receptors. Biochem Biophys Res Commun. [Review]. 2005 Mar 18;328(3):666-78.
176. Mannstadt M, Jüppner H, Gardella TJ. Receptors for PTH and PTHrP: their biological importance and functional properties. American Journal of Physiology-Renal Physiology. 1999;277(5):F665-F75.
177. Iida-Klein A, Guo J, Xie LY, Jüppner H, Potts JT, Kronenberg HM, et al. Truncation of the carboxyl-terminal region of the rat parathyroid hormone (PTH)/PTH-related peptide receptor enhances PTH stimulation of adenylyl cyclase but not phospholipase C. Journal of Biological Chemistry. 1995;270(15):8458-65.
178. Schwindinger WF, Fredericks J, Watkins L, Robinson H, Bathon JM, Pines M, et al. Coupling of the PTH/PTHrP receptor to multiple G-proteins. Endocrine. 1998;8(2):201-9.
179. Fiaschi-Taesch NM, Stewart AF. Minireview: parathyroid hormone-related protein as an intracrine factor—trafficking mechanisms and functional consequences. Endocrinology. 2003;144(2):407-11.
180. Lam MH, Briggs LJ, Hu W, Martin TJ, Gillespie MT, Jans DA. Importin β recognizes parathyroid hormone-related protein with high affinity and mediates its nuclear import in the absence of importin α. Journal of Biological Chemistry. 1999;274(11):7391-8.
181. Massfelder T, Dann P, Wu TL, Vasavada R, Helwig J-J, Stewart AF. Opposing mitogenic and anti-mitogenic actions of parathyroid hormone-related protein in vascular smooth muscle cells: a critical role for nuclear targeting. Proceedings of the National Academy of Sciences. 1997;94(25):13630-5.
182. Tovar Sepulveda VA, Shen X, Falzon M. Intracrine PTHrP protects against serum starvation-induced apoptosis and regulates the cell cycle in MCF-7 breast cancer cells. Endocrinology. 2002;143(2):596-606.
183. De Miguel F, Fiaschi-Taesch N, Lopez-Talavera J, Takane K, Massfelder T, Helwig J-J, et al. The C-terminal region of PTHrP, in addition to the nuclear localization signal, is essential for the intracrine stimulation of proliferation in vascular smooth muscle cells. Endocrinology. 2001;142(9):4096-105.

184. Kumari R, Robertson JF, Watson SA. Nuclear targeting of a midregion PTHrP fragment is necessary for stimulating growth in breast cancer cells. International journal of cancer. 2006;119(1):49-59.
185. Sirchia R, Priulla M, Sciandrello G, Caradonna F, Barbata G, Luparello C. Mid-region parathyroid hormone-related protein (PTHrP) binds chromatin of MDA-MB231 breast cancer cells and isolated oligonucleotides "in vitro". Breast Cancer Res Treat. [Research Support, Non-U.S. Gov't]. 2007 Sep;105(1):105-16.
186. Kronenberg HM. Developmental regulation of the growth plate. Nature. 2003;423(6937):332.
187. Karsenty G, Kronenberg HM, Settembre C. Genetic control of bone formation. Annual Review of Cell and Developmental. 2009;25:629-48.
188. Long F. Building strong bones: molecular regulation of the osteoblast lineage. Nature reviews Molecular cell biology. 2011;13(1):nrm3254.
189. Lanske B, Karaplis AC, Lee K, Luz A, Vortkamp A, Pirro A, et al. PTH/PTHrP receptor in early development and Indian hedgehog--regulated bone growth. Science. 1996;273(5275):663-6.
190. Vortkamp A, Lee K, Lanske B, Segre GV, Kronenberg HM, Tabin CJ. Regulation of rate of cartilage differentiation by Indian hedgehog and PTH-related protein. Science. 1996;273(5275):613-22.
191. Kronenberg HM. PTHrP and skeletal development. Ann N Y Acad Sci. 2006;1068(1):1-13.
192. Silve C, Jüppner H. Ollier disease. Orphanet J Rare Dis. 2006;1(1):37.
193. Amizuka N, Warshawsky H, Henderson JE, Goltzman D, Karaplis AC. Parathyroid hormone-related peptide-depleted mice show abnormal epiphyseal cartilage development and altered endochondral bone formation. J Cell Biol. 1994;126(6):1611-23.
194. Lanske B, Karaplis AC, Lee K, Luz A, Vortkamp A, Pirro A, et al. PTH/PTHrP receptor in early development and Indian hedgehog-regulated bone growth. SCIENCE-NEW YORK THEN WASHINGTON-. 1996:663-5.
195. Schipani E, Langman C, Hunzelman J, Le Merrer M, Loke K, Dillon M, et al. A novel parathyroid hormone (PTH)/PTH-related peptide receptor mutation in Jansen's metaphyseal chondrodysplasia. The Journal of Clinical Endocrinology & Metabolism. 1999;84(9):3052-7.
196. Karperien M, van der Harten HJ, van Schooten R, Farih-Sips H, den Hollander NS, Kneppers SL, et al. A frame-shift mutation in the type I parathyroid hormone (PTH)/PTH-related peptide receptor causing Blomstrand lethal osteochondrodysplasia. The Journal of Clinical Endocrinology & Metabolism. 1999;84(10):3713-20.
197. Wysolmerski JJ, Philbrick WM, Dunbar ME, Lanske B, Kronenberg H, Broadus A. Rescue of the parathyroid hormone-related protein knockout mouse demonstrates that parathyroid hormone-related protein is essential for mammary gland development. Development. 1998;125(7):1285-94.
198. Foley J, Dann P, Hong J, Cosgrove J, Dreyer B, Rimm D, et al. Parathyroid hormone-related protein maintains mammary epithelial fate and triggers nipple skin differentiation during embryonic breast development. Development. 2001;128(4):513-25.
199. Dunbar ME, Dann PR, Robinson GW, Hennighausen L, Zhang J-P, Wysolmerski JJ. Parathyroid hormone-related protein signaling is necessary for sexual dimorphism during embryonic mammary development. Development. 1999;126(16):3485-93.
200. VanHouten J, Dann P, McGeoch G, Brown EM, Krapcho K, Neville M, et al. The calcium-sensing receptor regulates mammary gland parathyroid hormone–related protein production and calcium transport. Journal of Clinical Investigation. 2004;113(4):598.

201. Ardeshirpour L, Dann P, Pollak M, Wysolmerski J, VanHouten J. The calcium-sensing receptor regulates PTHrP production and calcium transport in the lactating mammary gland. Bone. 2006;38(6):787-93.
202. Germain A, Attaroglu H, MacDonald P, Casey M. Parathyroid hormone-related protein mRNA in avascular human amnion. The Journal of Clinical Endocrinology & Metabolism. 1992;75(4):1173-5.
203. Hellman P, Ridefelt P, Juhlin C, Åkerström G, Rastad J, Gylfe E. Parathyroid-like regulation of parathyroid-hormone-related protein release and cytoplasmic calcium in cytotrophoblast cells of human placenta. Arch Biochem Biophys. 1992;293(1):174-80.
204. Bowden S, Emly J, Hughes S, Powell G, Ahmed A, Whittle M, et al. Parathyroid hormone-related protein in human term placenta and membranes. Journal of Endocrinology. 1994;142(2):217-24.
205. Urena P, Kong X, Abou-Samra A-B, Jüppner H, Kronenberg HM, Potts Jr JT, et al. Parathyroid hormone (PTH)/PTH-related peptide receptor messenger ribonucleic acids are widely distributed in rat tissues. Endocrinology. 1993;133(2):617-23.
206. Kovacs CS, Chafe LL, Woodland ML, McDonald KR, Fudge NJ, Wookey PJ. Calcitropic gene expression suggests a role for the intraplacental yolk sac in maternal-fetal calcium exchange. American Journal of Physiology-Endocrinology and Metabolism. 2002;282(3):E721-E32.
207. Curtis N, King R, Moseley J, Ho P, Rice G, Wlodekd M. Intrauterine expression of parathyroid hormone-related protein in normal and pre-eclamptic pregnancies. Placenta. 1998;19(8):595-601.
208. Simmonds CS, Kovacs CS. Role of parathyroid hormone (PTH) and PTH-related protein (PTHrP) in regulating mineral homeostasis during fetal development. Critical Reviews™ in Eukaryotic Gene Expression. 2010;20(3).
209. Dilworth M, Sibley C. Transport across the placenta of mice and women. Placenta. 2013;34:S34-S9.
210. Care A, Abbas S, Pickard D, Barri M, Drinkhill M, Findlay J, et al. Stimulation of ovine placental transport of calcium and magnesium by mid-molecule fragments of human parathyroid hormone-related protein. Exp Physiol. 1990;75(4):605-8.
211. Philbrick WM, Dreyer BE, Nakchbandi IA, Karaplis AC. Parathyroid hormone-related protein is required for tooth eruption. Proc Natl Acad Sci U S A. [Research Support, U.S. Gov't, P.H.S.]. 1998 Sep 29;95(20):11846-51.
212. Philbrick WM, Dreyer BE, Nakchbandi IA, Karaplis AC. Parathyroid hormone-related protein is required for tooth eruption. Proceedings of the National Academy of Sciences. 1998;95(20):11846-51.
213. Vasavada RC, Cavaliere C, D'Ercole AJ, Dann P, Burtis WJ, Madlener AL, et al. Overexpression of parathyroid hormone-related protein in the pancreatic islets of transgenic mice causes islet hyperplasia, hyperinsulinemia, and hypoglycemia. Journal of Biological Chemistry. 1996;271(2):1200-8.
214. Zhang B, Hosaka M, Sawada Y, Torii S, Mizutani S, Ogata M, et al. Parathyroid Hormone–Related Protein Induces Insulin Expression Through Activation of MAP Kinase–Specific Phosphatase-1 That Dephosphorylates c-Jun NH2-Terminal Kinase in Pancreatic β-Cells. Diabetes. 2003;52(11):2720-30.
215. Vasavada RC, Wang L, Fujinaka Y, Takane KK, Rosa TC, Mellado-Gil JM, et al. Protein Kinase C-ζ Activation Markedly Enhances β-Cell Proliferation: An Essential Role in Growth Factor–Mediated β-Cell Mitogenesis. Diabetes. 2007;56(11):2732-43.
216. Guthalu KN, Joshi-Gokhale S, Harb G, Williams K, Zhang XY, Takane KK, et al. Parathyroid hormone-related protein enhances human ß-cell proliferation and function with associated induction of cyclin-dependent kinase 2 and cyclin E expression. Diabetes. 2010;59(12):3131.

217. Porter SE, Sorenson RL, Dann P, Garcia-Ocana A, Stewart AF, Vasavada RC. Progressive pancreatic islet hyperplasia in the islet-targeted, parathyroid hormone-related protein-overexpressing mouse. Endocrinology. 1998;139(9):3743-51.
218. Guthalu KN, Joshi-Gokhale S, Harb G, Williams K, Zhang XY, Takane KK, et al. Parathyroid hormone-related protein enhances human ß-cell proliferation and function with associated induction of cyclin-dependent kinase 2 and cyclin E expression. Diabetes. 2010;59(12):3131-8.
219. Mozar A, Lin H, Williams K, Chin C, Li R, Kondegowda NG, et al. Parathyroid Hormone-Related Peptide (1-36) Enhances Beta Cell Regeneration and Increases Beta Cell Mass in a Mouse Model of Partial Pancreatectomy. PLoS One. 2016;11(7):e0158414.
220. Merendino J, Insogna K, Milstone L, Broadus A, Stewart A. Cultured human keratinocytes produce a parathyroid hormone-like protein. Science. 1986;231(4736):388-90.
221. Foley J, Wysolmerski JJ, Dreyer BE, Broadus AE, Philbrick WM, Longely BJ. PTHrP regulates epidermal differentiation in adult mice. Journal of investigative dermatology. 1998;111(6):1122-8.
222. Karaplis AC, Luz A, Glowacki J, Bronson RT, Tybulewicz V, Kronenberg HM, et al. Lethal skeletal dysplasia from targeted disruption of the parathyroid hormone-related peptide gene. Genes Dev. 1994;8(3):277-89.
223. Weir EC, Philbrick WM, Amling M, Neff LA, Baron R, Broadus AE. Targeted overexpression of parathyroid hormone-related peptide in chondrocytes causes chondrodysplasia and delayed endochondral bone formation. Proceedings of the National Academy of Sciences. 1996;93(19):10240-5.
224. Miao D, Su H, He B, Gao J, Xia Q, Zhu M, et al. Severe growth retardation and early lethality in mice lacking the nuclear localization sequence and C-terminus of PTH-related protein. Proceedings of the National Academy of Sciences. 2008:pnas. 0805690105.
225. Toribio RE, Brown HA, Novince CM, Marlow B, Hernon K, Lanigan LG, et al. The midregion, nuclear localization sequence, and C terminus of PTHrP regulate skeletal development, hematopoiesis, and survival in mice. The FASEB Journal. 2010;24(6):1947-57.
226. Wysolmerski JJ, Broadus AE, Zhou J, Fuchs E, Milstone LM, Philbrick WM. Overexpression of parathyroid hormone-related protein in the skin of transgenic mice interferes with hair follicle development. Proceedings of the National Academy of Sciences. 1994;91(3):1133-7.
227. Hens JR, Dann P, Zhang J-P, Harris S, Robinson GW, Wysolmerski J. BMP4 and PTHrP interact to stimulate ductal outgrowth during embryonic mammary development and to inhibit hair follicle induction. Development. 2007;134(6):1221-30.
228. Hiremath M, Dann P, Fischer J, Butterworth D, Boras-Granic K, Hens J, et al. Parathyroid hormone-related protein activates Wnt signaling to specify the embryonic mammary mesenchyme. Development. 2012:dev. 080671.
229. Safer JD, Ray S, Holick MF. A topical parathyroid hormone/parathyroid hormone-related peptide receptor antagonist stimulates hair growth in mice. Endocrinology. 2007;148(3):1167-70.
230. Schilli MB, Ray S, Paus R, Obi-Tabot E, Holick MF. Control of hair growth with parathyroid hormone (7-34). Journal of Investigative Dermatology. 1997;108(6).
231. Diamond AG, Gonterman RM, Anderson AL, Menon K, Offutt CD, Weaver CH, et al. Parathyroid hormone hormone-related protein and the PTH receptor regulate angiogenesis of the skin. Journal of Investigative Dermatology. 2006;126(9):2127-34.
232. Nakayama T, Ohtsuru A, Enomoto H, Namba H, Ozeki S-i, Shibata Y, et al. Coronary atherosclerotic smooth muscle cells overexpress human parathyroid hormone-related peptides. Biochem Biophys Res Commun. 1994;200(2):1028-35.

233. Ozeki S-i, Ohtsuru A, Seto S, Takeshita S, Yano H, Nakayama T, et al. Evidence That Implicates the Parathyroid Hormone–Related Peptide in Vascular Stenosis: Increased Gene Expression in the Intima of Injured Rat Carotid Arteries and Human Restenotic Coronary Lesions. Arterioscler Thromb Vasc Biol. 1996;16(4):565-75.
234. Philbrick W, Wysolmerski J, Galbraith S, Holt E, Orloff J, Yang K, et al. Defining the roles of parathyroid hormone-related protein in normal physiology. Physiol Rev. 1996;76(1):127-73.
235. Fiaschi-Taesch N, Takane KK, Masters S, Lopez-Talavera JC, Stewart AF. Parathyroid Hormone–Related Protein as a Regulator of pRb and the Cell Cycle in Arterial Smooth Muscle. Circulation. 2004;110(2):177-85.
236. Fiaschi-Taesch N, Sicari BM, Ubriani K, Bigatel T, Takane KK, Cozar-Castellano I, et al. Cellular Mechanism Through Which Parathyroid Hormone–Related Protein Induces Proliferation in Arterial Smooth Muscle Cells: Definition of an Arterial Smooth Muscle PTHrP/p27kip1 Pathway. Circ Res. 2006;99(9):933-42.
237. Sicari BM, Troxell R, Salim F, Tanwir M, Takane KK, Fiaschi-Taesch N. c-myc and skp2 Coordinate p27 Degradation, Vascular Smooth Muscle Proliferation, and Neointima Formation Induced by the Parathyroid Hormone-Related Protein. Endocrinology. 2012;153(2):861-72.
238. Ogino K, Burkhoff D, Bilezikian JP. The hemodynamic basis for the cardiac effects of parathyroid hormone (PTH) and PTH-related protein. Endocrinology. 1995;136(7):3024-30.
239. Schlüter K-D, Katzer C, Frischkopf K, Wenzel S, Taimor G, Piper H. Expression, Release, and Biological Activity of Parathyroid Hormone–Related Peptide From Coronary Endothelial Cells. Circ Res. 2000;86(9):946-51.
240. Lütteke D, Ross G, Abdallah Y, Schäfer C, Piper HM, Schlüter K-D. Parathyroid hormone–related peptide improves contractile responsiveness of adult rat cardiomyocytes with depressed cell function irrespectively of oxidative inhibition. Basic Res Cardiol. 2005;100(4):320-7.
241. Pirola CJ, Wang HM, Strgacich MI, Kamyar A, Cercek B, Forrester JS, et al. Mechanical stimuli induce vascular parathyroid hormone-related protein gene expression in vivo and in vitro. Endocrinology. 1994;134(5):2230-6.
242. Noda M, Katoh T, Takuwa N, Kumada M, Kurokawa K, Takuwa Y. Synergistic stimulation of parathyroid hormone-related peptide gene expression by mechanical stretch and angiotensin II in rat aortic smooth muscle cells. Journal of Biological Chemistry. 1994;269(27):17911-7.
243. Noonan WT, Qian J, Stuart WD, Clemens TL, Lorenz JN. Altered renal hemodynamics in mice overexpressing the parathyroid hormone (PTH)/PTH-related peptide type 1 receptor in smooth muscle. Endocrinology. 2003;144(11):4931-8.
244. Linforth R, Anderson N, Hoey R, Nolan T, Downey S, Brady G, et al. Coexpression of parathyroid hormone related protein and its receptor in early breast cancer predicts poor patient survival. Clinical cancer research. 2002;8(10):3172-7.
245. Powell GJ, Southby J, Danks JA, Stillwell RG, Hayman JA, Henderson MA, et al. Localization of parathyroid hormone-related protein in breast cancer metastases: increased incidence in bone compared with other sites. Cancer Res. 1991;51(11):3059-61.
246. Bundred N, Morrison J, Ratcliffe W, Ratcliffe J, Warwick J, Walker R. Parathyroid hormone related protein and skeletal morbidity in breast cancer. Eur J Cancer. 1992;28(2):690-2.
247. Bouizar Z, Spyratos F, Deytieux S, de Vernejoul M-C, Jullienne A. Polymerase chain reaction analysis of parathyroid hormone-related protein gene expression in breast cancer patients and occurrence of bone metastases. Cancer Res. 1993;53(21):5076-8.

248. Guise TA, Yin JJ, Taylor S, Kumagai Y, Dallas M, Boyce B, et al. Evidence for a causal role of parathyroid hormone-related protein in the pathogenesis of human breast cancer-mediated osteolysis. Journal of Clinical Investigation. 1996;98(7):1544.
249. Ghoussaini M, Fletcher O, Michailidou K, Turnbull C, Schmidt MK, Dicks E, et al. Genome-wide association analysis identifies three new breast cancer susceptibility loci. Nat Genet. 2012;44(3):312-8.
250. Iwamura M, di Sant'Agnese PA, Wu G, Benning CM, Cockett AT, Deftos LJ, et al. Immunohistochemical localization of parathyroid hormone-related protein in human prostate cancer. Cancer Res. 1993;53(8):1724-6.
251. Asadi F, Farraj M, Sharifi R, Malakouti S, Antar S, Kukreja S. Enhanced expression of parathyroid hormone-related protein in prostate cancer as compared with benign prostatic hyperplasia. Hum Pathol. 1996;27(12):1319-23.
252. Bryden AA, Islam S, Freemont AJ, Shanks JH, George NJ, Clarke NW. Parathyroid hormone-related peptide: expression in prostate cancer bone metastases. Prostate Cancer Prostatic Dis. [Research Support, Non-U.S. Gov't]. 2002;5(1):59-62.
253. BRANDT DW, BURTON DW, GAZDAR AF, OIE HE, DEFTOS LJ. All Major Lung Cancer Cell Types Produce Parathyroid Hormone-Like Protein: Heterogeneity Assessed by High Performance Liquid Chromatography*. Endocrinology. 1991;129(5):2466-70.
254. Kitazawa S, Takenaka A, Gotoh A, Maeda S, Fukase M, Kitazawa R, et al. Immunohistologic evaluation of parathyroid hormone-related protein in human lung cancer and normal tissue with newly developed monoclonal antibody. Cancer. 1991;67(4):984-9.
255. Davidson L, Black M, Carey F, Logue F, McNicol A. Lung tumours immunoreactive for parathyroid hormone related peptide: analysis of serum calcium levels and tumour type. Journal of pathology. 1996;178(4):398-401.
256. Iguchi H, Tanaka S, Ozawa Y, Kashiwakuma T, Kimura T, Hiraga T, et al. An experimental model of bone metastasis by human lung cancer cells: the role of parathyroid hormone-related protein in bone metastasis. Cancer Res. 1996;56(17):4040-3.
257. Nishihara M, Ito M, Tomioka T, Ohtsuru A, Taguchi T, Kanematsu T. Clinicopathological implications of parathyroid hormone-related protein in human colorectal tumours. J Pathol. 1999;187(2):217-22.
258. Nishihara M, Kanematsu T, Taguchi T, Razzaque MS. PTHrP and tumorigenesis: is there a role in prognosis? Ann N Y Acad Sci. [Review]. 2007 Nov;1117:385-92.
259. Iwamura M, Wu W, Muramoto M, Ohori M, Egawa S, Uchida T, et al. Parathyroid hormone-related protein is an independent prognostic factor for renal cell carcinoma. Cancer. 1999;86(6):1028-34.
260. Lv Z, Wu X, Cao W, Shen Z, Wang L, Xie F, et al. Parathyroid hormone-related protein serves as a prognostic indicator in oral squamous cell carcinoma. J Exp Clin Cancer Res. 2014;33:100.
261. de Castro LF, Lozano D, Portal-Núñez S, Maycas M, De la Fuente M, Caeiro JR, et al. Comparison of the skeletal effects induced by daily administration of PTHrP (1–36) and PTHrP (107–139) to ovariectomized mice. J Cell Physiol. 2012;227(4):1752-60.
262. Horwitz MJ, Augustine M, Kahn L, Martin E, Oakley CC, Carneiro RM, et al. A comparison of parathyroid hormone-related protein (1-36) and parathyroid hormone (1-34) on markers of bone turnover and bone density in postmenopausal women: The PrOP study. Journal of Bone and Mineral Research. 2013;28(11):2266-76.
263. Horwitz MJ, Tedesco MB, Gundberg C, Garcia-Ocana A, Stewart AF. Short-term, high-dose parathyroid hormone-related protein as a skeletal anabolic agent for the treatment of postmenopausal osteoporosis. The Journal of Clinical Endocrinology & Metabolism. 2003;88(2):569-75.
264. Horwitz MJ, Tedesco MB, Garcia-Ocaña A, Sereika SM, Prebehala L, Bisello A, et al. Parathyroid hormone-related protein for the treatment of postmenopausal osteoporosis:

defining the maximal tolerable dose. The Journal of Clinical Endocrinology & Metabolism. 2010;95(3):1279-87.
265. Gonnelli S, Caffarelli C. Abaloparatide. Clinical Cases in Mineral and Bone Metabolism. 2016 May-Aug

10/05;13(2):106-9.
266. Hattersley G, Dean T, Corbin BA, Bahar H, Gardella TJ. Binding Selectivity of Abaloparatide for PTH-Type-1-Receptor Conformations and Effects on Downstream Signaling. Endocrinology. 2016;157(1):141-9.
267. Leder BZ, O'dea LSL, Zanchetta JR, Kumar P, Banks K, McKay K, et al. Effects of abaloparatide, a human parathyroid hormone-related peptide analog, on bone mineral density in postmenopausal women with osteoporosis. The Journal of Clinical Endocrinology & Metabolism. 2014;100(2):697-706.
268. Chew CK, Clarke BL. Abaloparatide: Recombinant human PTHrP (1–34) anabolic therapy for osteoporosis. Maturitas. 2017;97:53-60.
269. Miller PD, Hattersley G, Riis B, et al. Effect of abaloparatide vs placebo on new vertebral fractures in postmenopausal women with osteoporosis: A randomized clinical trial. Jama. 2016;316(7):722-33.
270. Kadavil J. Guidance for Industry Bioanalytical Method Validation. US Department of Health and Human Services Food and Drug Administration, 2013 Draft Guidance Revision 1. 2013.
271. Guideline on Bioanalytical Method Validation. European Medicine Agency Committee for Medicine Products for Human Use (CHMP), London, UK. 2012.
272. Gu H, Liu G, Wang J, Aubry A-F, Arnold ME. Selecting the Correct Weighting Factors for Linear and Quadratic Calibration Curves with Least-Squares Regression Algorithm in Bioanalytical LC-MS/MS Assays and Impacts of Using Incorrect Weighting Factors on Curve Stability, Data Quality, and Assay Performance. Anal Chem. 2014 2014/09/16;86(18):8959-66.
273. Hocher B, Oberthür D, Slowinski T, Querfeld U, Schaefer F, Doyon A, et al. Modeling of oxidized PTH (oxPTH) and non-oxidized PTH (n-oxPTH) receptor binding and relationship of oxidized to non-oxidized PTH in children with chronic renal failure, adult patients on hemodialysis and kidney transplant recipients. Kidney and Blood Pressure Research. 2013;37(4-5):240-51.
274. Frelinger Ad, Zull JE. Oxidized forms of parathyroid hormone with biological activity. Separation and characterization of hormone forms oxidized at methionine 8 and methionine 18. Journal of Biological Chemistry. 1984;259(9):5507-13.
275. Frelinger AL, Zull JE. The role of the methionine residues in the structure and function of parathyroid hormone. Arch Biochem Biophys. 1986;244(2):641-9.
276. Chu J-W, Yin J, Wang DI, Trout BL. A structural and mechanistic study of the oxidation of methionine residues in hPTH (1− 34) via experiments and simulations. Biochemistry. 2004;43(44):14139-48.
277. Kastner M. Protein liquid chromatography. First Edition ed: Elsevier; 1999.
278. Chambers EE, Lame ME, Bardsley J, Hannam S, Legido-Quigley C, Smith N, et al. High sensitivity LC-MS/MS method for direct quantification of human parathyroid 1-34 (teriparatide) in human plasma. J Chromatogr B Analyt Technol Biomed Life Sci. 2013 Nov 1;938:96-104.
279. Hämmerle SP, Mindeholm L, Launonen A, Kiese B, Loeffler R, Harfst E, et al. The single dose pharmacokinetic profile of a novel oral human parathyroid hormone formulation in healthy postmenopausal women. Bone. 2012;50(4):965-73.
280. Tang JC, Dutton JJ, Piec I, Green D, Fisher E, Washbourne CJ, et al. LC–MS/MS application for urine free pyridinoline and free deoxypyridinoline: Urine markers of collagen and bone degradation. Clinical Mass Spectrometry. 2016;1:11-8.

281. Farrell C-JL, Martin S, McWhinney B, Straub I, Williams P, Herrmann M. State-of-the-art vitamin D assays: a comparison of automated immunoassays with liquid chromatography–tandem mass spectrometry methods. Clin Chem. 2012:clinchem. 2011.172155.
282. Ursem S, Vervloet, M., Hillebrand, J., et al. (2017). Oxidation of PTH: in vivo feature or effect of preanalytical conditions?. Clinical Chemistry and Laboratory Medicine (CCLM), 0(0), pp. -. Retrieved 11 Oct. 2017. doi:10.1515/cclm-2017-0313.
283. Schwickart M, Vainshtein I, Lee R, Schneider A, Liang M. Interference in immunoassays to support therapeutic antibody development in preclinical and clinical studies. 2014.
284. Grill V, Ho P, Body J-J, Johanson N, Lee S, Kukreja S, et al. Parathyroid hormone-related protein: elevated levels in both humoral hypercalcemia of malignancy and hypercalcemia complicating metastatic breast cancer. The Journal of Clinical Endocrinology & Metabolism. 1991;73(6):1309-15.
285. Henderson JE, Shustik C, Kremer R, Rabbani SA, Hendy GN, Goltzman D, et al. Circulating concentrations of parathyroid hormone-like peptide in malignancy and in hyperparathyroidism. Journal of Bone and Mineral Research. 1990;5(2):105-13.
286. KAO PC, Klee GG, TAYLOR RL, HEATH H, editors. Parathyroid hormone-related peptide in plasma of patients with hypercalcemia and malignant lesions. Mayo Clin Proc; 1990: Elsevier.
287. Clemens TL, Cormier S, Eichinger A, Endlich K, Fiaschi-Taesch N, Fischer E, et al. Parathyroid hormone-related protein and its receptors: nuclear functions and roles in the renal and cardiovascular systems, the placental trophoblasts and the pancreatic islets. Br J Pharmacol. 2001;134(6):1113-36.
288. Amizuka N, Karaplis AC, Henderson JE, Warshawsky H, Lipman ML, Matsuki Y, et al. Haploinsufficiency of parathyroid hormone-related peptide (PTHrP) results in abnormal postnatal bone development. Dev Biol. 1996;175(1):166-76.
289. Cho YM, Woodard GL, Dunbar M, Gocken T, Jimènez JA, Foley J. Hair-cycle-dependent expression of parathyroid hormone-related protein and its type I receptor: evidence for regulation at the anagen to catagen transition. Journal of investigative dermatology. 2003;120(5):715-27.
290. Villanueva-Penacarrillo M, Cancelas J, De Miguel F, Redondo A, Valin A, Valverde I, et al. Parathyroid hormone-related peptide stimulates DNA synthesis and insulin secretion in pancreatic islets. Journal of Endocrinology. 1999;163(3):403-8.
291. Williams K, Abanquah D, Joshi-Gokhale S, Otero A, Lin H, Guthalu N, et al. Systemic and acute administration of parathyroid hormone-related peptide (1–36) stimulates endogenous beta cell proliferation while preserving function in adult mice. Diabetologia. 2011;54(11):2867.
292. Rabbani SA, Gladu J, Harakidas P, Jamison B, Goltzman D. Over-production of parathyroid hormone–related peptide results in increased osteolytic skeletal metastasis by prostate cancer cells In vivo. International journal of cancer. 1999;80(2):257-64.
293. Kremer R, Shustik C, Tabak T, Papavasiliou V, Goltzman D. Parathyroid-hormone-related peptide in hematologic malignancies. Am J Med. 1996;100(4):406-11.
294. Pecherstorfer M, Schilling T, Blind E, Zimmer-Roth I, Baumgartner G, Ziegler R, et al. Parathyroid hormone-related protein and life expectancy in hypercalcemic cancer patients. The Journal of Clinical Endocrinology & Metabolism. 1994;78(5):1268-70.
295. Truong U, Papavasiliou V, Goltzman D, Kremer R, editors. Parathyroid hormone related peptide (PTHRP) is a prognostic indicator in hypercalcemic cancer patients with skeletal or extra skeletal metastasis. JOURNAL OF BONE AND MINERAL RESEARCH; 1999: AMER SOC BONE & MINERAL RES PO BOX 2759, DURHAM, NC 27715-2759 USA.

296. Wimalawansa SJ. Significance of plasma PTH-rp in patients with hypercalcemia of malignancy treated with bisphosphonate. Cancer. 1994;73(8):2223-30.
297. Grill V, Murray R, Ho P, Santamaria J, Pitt P, Potts C, et al. Circulating PTH and PTHrP levels before and after treatment of tumor induced hypercalcemia with pamidronate disodium (APD). The Journal of Clinical Endocrinology & Metabolism. 1992;74(6):1468-70.
298. Onuma E, Azuma Y, Saito H, Tsunenari T, Watanabe T, Hirabayashi M, et al. Increased Renal Calcium Reabsorption by Parathyroid Hormone–Related Protein Is a Causative Factor in the Development of Humoral Hypercalcemia of Malignancy Refractory to Osteoclastic Bone Resorption Inhibitors. Clinical cancer research. 2005;11(11):4198-203.